SUBSTITUTED *m*-TERPHENYL LIGANDS IN MAIN GROUP AND TRANSITION METAL CHEMISTRY

by

Diane Amanda Dickie
B.Sc. (Hons.), Mount Allison University, 2001

THESIS SUBMITTED IN PARTIAL FULFILLMENT OF
THE REQUIREMENTS FOR THE DEGREE OF

DOCTOR OF PHILOSOPHY

In the
Department
of
Chemistry

SIMON FRASER UNIVERSITY

Fall 2006

APPROVAL

Name: Diane Dickie

Degree: Doctor of Philosophy

Title of Thesis: Substituted *m*-Terphenyl Ligands in Main Group and Transition Metal Chemistry

Examining Committee:

Chair: Dr. D.J. Vocadlo (Assistant Professor)

Dr. J.A.C. Clyburne (Associate Professor)
Senior Supervisor

Dr. R.H. Hill (Professor)
Committee Member

Dr. D.B. Leznoff (Associate Professor)
Committee Member

Dr. R.A. Britton (Assistant Professor)
Internal Examiner

Dr. D.P. Gates (Associate Professor)
External Examiner
Department of Chemistry
University of British Columbia

Date Approved: September 14, 2006

ABSTRACT

m-Terphenyls are bowl-shaped molecules that have been shown to be effective ligands for main group and transition metal complexes with unusual coordination environments. Many *m*-terphenyl complexes are formed via direct element-carbon bonds, but the chemistry of *substituted m*-terphenyls, in which the primary interaction is through a functional group, is relatively unexplored. The introduction of functional groups allows for more varied coordination modes, and therefore, more varied structures. To explore this chemistry, a series of 13 *m*-terphenyl molecules in which the aryl group was either phenyl or 2,4,6-trimethylphenyl were prepared and substituted in the *m*-terphenyl pocket with oxygen containing donors including carboxylic and boronic acids, aldehydes, Schiff bases, amides, and alcohols.

A survey of their coordination chemistry was performed, and, in most cases, the new molecules were characterized by standard spectroscopic methods, and when possible, single crystal X-ray diffraction. The protonolysis reactions of the carboxylic acid, Schiff base and alcohol ligands with main group elements [$AlMe_3$, $Sn[N(SiMe_3)_2]_2$, $Ge[N(SiMe_3)_2]_2$, and $Si(NMe_2)_4$] and transition metals [$Ti(NMe_2)_4$ and $ZnEt_2$] produced nearly 20 new complexes. Particularly notable results of this study include an aluminium Schiff base complex TPIP·$AlMe_2$·$AlMe_3$ [TPIP = *N*-(2',4',6'-triphenylbenzylidene)2-iminophenol] that acts as an initiator in the ring-opening polymerization of ε-caprolactone, and the first structurally characterized mixed aryloxy/amido germanium (II) complex [$(Mes_2C_6H_3O)Ge(N\{SiMe_3\}_2)$]. Most exciting is the serendipitous discovery of

a Sn_2N_2 analogue of 1,3-cyclobutadienide, namely $[(Mes_2C_6H_3CO_2)Sn(\mu\text{-}NSiMe_3)]_2$, produced by the oxidation of $[(Me_3Si)_2NSn(\mu\text{-}O_2CC_6H_3Mes_2)]_2$ with AgOCN.

The chemistry of *m*-terphenyls was also extended beyond discrete molecular complexes with the synthesis of two bifunctional ligands 2,6-diphenylterephthalic acid and 4-mercaptomethyl-2,6-diphenylbenzoic acid. The latter was used in a collaborative project to form a low-surface density self-assembled monolayer on gold that adsorbed adenine, a model compound for biological macromolecules. The former was used to prepare six 1-D metal-organic chains and 2-D networks from nitrate salts of zinc, copper, cobalt and silver.

DEDICATION

To everyone who helped make this possible.

ACKNOWLEDGEMENTS

So many people have helped and supported me during the five years I spent on this research project. I will try to thank all of them here, but it is almost inevitable that I will forget someone, so if you are that someone, please remember that it was not intentional and I truly appreciate everything you did for me. First, I need to thank my mentors from my undergraduate and graduate studies, Dr. Steve Westcott (Mount Allison University) and Dr. Jason Clyburne. Steve convinced me to stick with chemistry when I was thinking of switching to a different program during my sophomore year. During the middle of the final exam for my first inorganic chemistry course, he asked me if I would like to work in his lab the following semester. The timing seemed a bit strange back then – most people probably would have waited until the end of the exam in order not to distract the student – but I said yes and now can't imagine where I would be if he hadn't done that.

Steve is also the person who introduced me to Jason when I was looking for graduate schools. Jason has given so much to me that I can't even begin to describe it here. He always believed in me and let me take on responsibilities that most students do not experience until much later in their careers. He supported my extensive extra-curricular activities, demonstrating through both his words and his actions how important it is to maintain a healthy work-life balance, and created at lab that was truly a fun place to be. Even when he moved to Saint Mary's University, four time zones away a few

months before I completed my Ph.D., he was always available when I needed him. THANK YOU!

I would also like to thank Drs. Danny Leznoff and Ross Hill, the members of my supervisory committee who spent a lot more time with me than would normally be expected of committee members because of Jason being away. On a related note, thanks are due to Drs. Rob Britton and Charles Walsby and their students, for putting up with me keeping a desk and fumehood in their new lab and office space during my final semester. I'll be out of your way in just a few more days!

I said earlier that I was allowed to take on many responsibilities in the lab, and one of those was training and working with undergraduate students. Nearly two dozen passed through the lab during my time at SFU, and while they all made a difference, I'd especially like to thank those whose projects were closely related to my own: Sherry Li, Rahul Samant, Karina Shi, Sarah Khoo, Shamola Labeodan, Julia Heinonen, Michelle Hauser, Daisuke Ino and Hanifa Jalali. Most of the others worked with Madhvi Ramnial, who I also thank for being a friend and sharing the load.

I want to thank my friends Marissa Bender and Ivan Hemeon for proof-reading large parts of this thesis. Hanifa Jalali and Dr. Hogan Yu are thanked for their guidance on the surface chemistry discussed in Chapter 4. Most of the work in this thesis would not have been possible without the help of three crystallographers who guided me when I began learning to solve my own structures and did the work themselves before I knew how: Dr. Gabriele Schatte (Saskatchewan Structural Sciences Centre), Dr. Hilary Jenkins (Saint Mary's University) and Dr. Michael Jennings (University of Western Ontario). All the technicians and support staff at Simon Fraser University were also essential to my

research, especially Dr. Andrew Lewis who was relentless in his pursuit of the elusive ^{119}Sn NMR spectra of a few of my compounds, and Susie Smith who helped get all the pre- and post-defense paperwork in order.

I'd like to thank my family for supporting me even when they didn't really understand what I was doing. I also thank the children in the Brownie units I've lead for the last several years for providing me with something totally unrelated to research to focus on at least once a week. The many women I've met and become friends with in the Girl Guide organization also played a large role in keeping balance in my life. My future post-doctoral advisor, Dr. Rick Kemp, deserves recognition for his patience while I finished my work at SFU. Finally, one more blanket thanks to everyone that I haven't been able to mention by name here. I couldn't have done it without you.

TABLE OF CONTENTS

Approval ii

Abstract iii

Dedication v

Acknowledgements vi

Table of Contents ix

List of Figures xi

List of Schemes xv

List of Tables xvii

List of Abbreviations xix

1 Introduction 1

1.1 Classes of bulky ligands 4
1.2 *m*-Terphenyl ligands 7
1.2.1 Definition and synthesis 7
1.2.2 Applications to synthetic materials 10
1.2.3 *m*-Terphenyls as ligands 15
1.3 Thesis report 20

2 *m*-Terphenyl carboxylate complexes of transition metals and main group elements 23

2.1 Dimeric group 12, 13 and 14 complexes with a common $M_2O_4C_2$ core 25
2.2 Oxidation of tin (II) complexes 35
2.3 Tetravalent group 4 and 14 *m*-terphenyl carboxylate complexes 45
2.4 Summary and conclusions 50
2.5 Future work 52
2.6 Experimental 54
2.6.1 General experimental 54
2.6.2 Crystallographic studies 56
2.6.3 Synthesis of carboxylate ligands 57
2.6.4 Synthesis of metal complexes 59

3 *m*-Terphenyls in metal-organic chains and networks 65

3.1 Applications of metal-organic frameworks 66
3.2 Frameworks based upon a bifunctional *m*-terphenyl carboxylate ligand 68
3.2.1 Organic chains 69
3.2.2 1-D metal-organic chains 75
3.2.3 2-D hydrogen bonded metal-organic networks 78

3.2.4 2-D covalent metal-organic networks 83
3.3 Summary and conclusions 89
3.4 Future work 90
3.5 Experimental 91
3.5.1 Synthesis of organic molecules 91
3.5.2 Synthesis of metal chains and networks 93

4 Gold-thiol self-assembled monolayers 96

4.1 Traditional SAMs 96
4.1.1 Problems with surface density of traditional SAMs 97
4.2 *m*-Terphenyls in SAMs 98
4.2.1 Ligand synthesis and characterization 98
4.2.2 Surface characterization by FTIR spectroscopy 101
4.2.3 Surface characterization by contact angle measurement 104
4.3 Summary and conclusions 105
4.4 Future work 106
4.5 Experimental 107

5 New bidentate *m*-terphenyl compounds 109

5.1 Schiff bases, amides and boronic acids in coordination chemistry 109
5.2 *m*-Terphenyl Schiff base ligands 112
5.3 Main group *m*-terphenyl Schiff base complexes 115
5.3.1 Ring-opening polymerization of ε-caprolactone 122
5.4 *m*-Terphenyl amides and boronic acids 123
5.5 Summary and conclusions 128
5.6 Future work 130
5.7 Experimental 133
5.7.1 Synthesis of ligands and precursors 133
5.7.2 Synthesis of metal Schiff base complexes 137
5.7.3 Polymerization reactions 139

6 Main group and transition metal complexes of *m*-terphenyl phenols and benzyl alcohols 140

6.1 Ligand synthesis 142
6.2 Main group *m*-terphenyl phenol complexes 150
6.3 Transition metal *m*-terphenyl phenol and benzyl alcohol complexes 157
6.4 Summary and conclusions 162
6.5 Future work 163
6.6 Experimental 165
6.6.1 Synthesis of ligands and precursors 165
6.6.2 Synthesis of main group complexes 168
6.6.3 Synthesis of transition metal complexes 169

7 Global conclusions 171

Appendix 1: Crystallographic data 173

Appendix 2: Atomic coordinates 178

Reference List 197

LIST OF FIGURES

Figure 1.1 Examples of intermolecular (left) and intramolecular (right) base stabilization of a monomeric aluminium hydride. 2

Figure 1.2 Electronic stabilization of a carbene through both the σ (left) and π (right) framework. 2

Figure 1.3 Diagram of relative strain energies for the cyclodimerization of substituted ethylenes. 2

Figure 1.4 Method for measuring cone angles of phosphine and cyclopentadienyl ligands. 5

Figure 1.5 Generic β-diketiminate (nacnac) (left) and *N*-heterocyclic carbene (NHC) (right) 6

Figure 1.6 Method for measuring $\%V_{bur}$ using the NHC 1,3-bis(2,4,6-trimethylphenyl)imidazol-2-ylidene (IMes) 7

Figure 1.7 The pocket formed by the *m*-terphenyl 2,6-bis(2,4,6-trimethylphenyl)benzene is shown in the space-filling diagram. 8

Figure 1.8 Example of a *m*-terphenyl rotaxane 11

Figure 1.9 Example of a *m*-terphenyl cyclophane (left), stilbenophane (centre) and azobenzenophane (right).. 11

Figure 1.10 Example of a *m*-terphenyl liquid crystal mesogen. 11

Figure 1.11 Example of a *m*-terphenyl capped dendrimer 12

Figure 1.12 Examples of *m*-terphenyls in acetylenes (left) and phosphaalkenes (right) 13

Figure 1.13 Examples of PPV polymers incorporating *m*-terphenyls. 13

Figure 1.14 Examples of non-traditional *m*-terphenyl coordination 15

Figure 1.15 The first complexes of substituted (left) and unsubstituted *m*-terphenyl ligands. 16

Figure 1.16 Structure of $[(Dipp_2C_6H_3)Cr]_2$, the first chromium-chromium five-fold bond.. 17

Figure 1.17 Indium(I) complex of 2,6-bis(2,4,6-triisopropylphenyl)phenyl. 18

Figure 1.18 Cationic gallium(III) complex of 2,6-bis(2,4,6-trimethylphenyl)phenyl. 19

Figure 2.1 Carboxylate coordination modes. 23

Figure 2.2 Isoelectronic *m*-terphenyl carboxylate, dithiocarboxylate and amidinate. 24

Figure 2.3 Structure of $[Me_2Al(\mu\text{-}O_2CC_6H_2(Ph_3)]_2$ **2**.. 26

Figure 2.4 Structure of [EtZn(μ-$O_2CC_6H_3Mes_2$)] **4**.....29
Figure 2.5 Structure of [$(Me_3Si)_2NSn(\mu\text{-}O_2CC_6H_2Ph_3)]_2$ **6**. 32
Figure 2.6 Structure of [$(Me_3Si)_2NSn(\mu\text{-}O_2CC_6H_3Mes_2)]_2$ **7**.....33
Figure 2.7 Structure of [$(Me_3Si)_2NSn(\mu\text{-}O_2CC_6H_2Mes_2Me)]_2$ **8**.. 33
Figure 2.8 Structure of [$(Mes_2C_6H_3CO_2)Sn(\mu\text{-}NSiMe_3)]_2$ **9**, obtained from reaction with $H_2O{\cdot}B(C_6F_5)$.. 37
Figure 2.9 Tin-chlorine interactions in Lappert's Sn_2N_2 complex. 37
Figure 2.10 Lewis diagrams of alternative bonding descriptions of a P_2C_2 heterocycle. Mes* = 2,4,6-tri-*t*-butylphenyl.....40
Figure 2.11 Isoelectronic group 14 M_2N_2 heterocycles. 42
Figure 2.12 Structure of $(CH_2Cl)(Cl)Sn[N(SiMe_3)_2]_2$ **11**. 44
Figure 2.13 Structure of [$(Mes_2C_6H_3CO_2)Si(NMe_2)_3$] **12**. 48
Figure 2.14 Structure of the [$(Mes_2C_6H_3CO_2)Ti(NMe_2)_3$] **13**.. 49
Figure 2.15 Structure of the[$(Mes_2C_6H_3CO_2)_2Ti(NMe_2)_2$] **13a**.. 49
Figure 3.1 Structure of ligand **15H$_2$**.. 70
Figure 3.2 Packing diagrams of **15H$_2$** along the crystallographic *a* and *c* axes. 72
Figure 3.3 Structure of [**15**·bipy] **16**. 73
Figure 3.4 Strong [O-H···N] hydrogen bonds along chains and weaker [C-H···O] interactions between chains produces a 2-D network along the crystallographic *b* axis of **16**. 74
Figure 3.5 Structure of [**15**·Zn·$(py)_2$·MeOH] **17**.....76
Figure 3.6 Structure of [**15**·Co·$(py)_2$·MeOH] **18**.. 76
Figure 3.7 Extended structure of [15·Zn·$(py)_2$·MeOH] **17**. The same motif is present in [**15**·Co·$(py)_2$·MeOH] **18**.....77
Figure 3.8 Structure of [(**15**H)$_2$·Cu·$(py)_2$] **19**.....78
Figure 3.9 Short [O-H···O] hydrogen bonds and long [Cu···O] interactions connecting a 2-D network in **19**. 80
Figure 3.10 Structure of [$(15H)_2$·Cu·$(py)_4$·$(H_2O)_2$] **20**.....80
Figure 3.11 The carboxylate oxygen not bound to copper forms hydrogen bonds with water to give this 2-D network in **20**.....82
Figure 3.12 [C-H···O] Bonds in **20**. 83
Figure 3.13 Structure of [**15**·Ag_2] **21**.. 84
Figure 3.14 Extended structure of **21**, showing the network formed by Ag-Ag bonds and bridging carboxylates. 85
Figure 3.15 π-Stacking interactions in **21** viewed along the crystallographic *b* and *c* axes, respectively. 85
Figure 3.16 Structure of [**15**·Zn·$(EtOH)_2$] **22**.. 86
Figure 3.17 Rectangular grid formed by **22**, shown in crystal structure and schematically. 87
Figure 3.18 Hydrogen bonds in[**15**·Zn·$(EtOH)_2$] **22**. 88

Figure 3.19 Thermogravimetric analysis of [**15**·Zn·$(EtOH)_2$] **22**. 89
Figure 4.1 Structure of 4-methyl-2,6-diphenylbenzoic acid **14**. 100
Figure 4.2 Estimated surface coverage of *m*-terphenyl thiols, as shown by the shadow cast on a surface by the solid-state space-filling model of **14**. The grid size is 0.5 Å. 101
Figure 4.3 Schematic representation of SAM of m-terphenyl thiol 24 after reaction with adenine 102
Figure 4.4 FTIR spectra of m-terphenyl SAMs formed from the adsorption of 24 on gold (A) and after further reaction with adenine/THF solution (B). 103
Figure 4.5 Schematic representation of contact angle measurements at high (left) and low (right) pH. 104
Figure 4.6 Contact angle titration curve of *m*-terphenyl SAMs prepared from the adsorption of **24** on gold, measured using a nonreactive spreading protocol. 104
Figure 5.1 Carboxylic acids (A) are isoelectronic with Schiff bases (B) and amides (C), and isostructural with boronic acids (D). 109
Figure 5.2 Structure of TPIP **26**. 114
Figure 5.3 Structure of TPAP **27**. 115
Figure 5.4 Structure of Sn·TPIP **28**.. 117
Figure 5.5 Solid state dimer formed through Sn-O dative bonds in Sn·TPIP **28**. 118
Figure 5.6 Complexes showing similar aluminium coordination to TPIP·$AlMe_2$·$AlMe_3$ **29**. 119
Figure 5.7 Structure of TPIP·$AlMe_2$·$AlMe_3$ **29**.. 120
Figure 5.8 Structure of 2,6-bis(2,4,6-trimethylphenyl)phenylboronic acid **33**. 126
Figure 5.9 [O-H···O] hydrogen bonds in **33**, viewed along the crystallographic *a* axis. 126
Figure 6.1 Two of Yamamoto's "designer" catalysts, methylaluminium bis(2,6-di-t-butyl-4-methylphenoxide (left) and aluminium tris(2,6-diphenylphenoxide) (right). 140
Figure 6.2 Known *m*-terphenyl phenols, from least to most bulky. 143
Figure 6.3 Structure of 2,6-bis(2,4,6-trimethylphenyl)phenol **34**. 144
Figure 6.4 Structure of 2,4,6-triphenylbenzyl alcohol **36**. 148
Figure 6.5 Structure of 2,6-bis(2,4,6-trimethylphenyl)benzyl alcohol **37** 148
Figure 6.6 [O-H···O] hydrogen bonds in 2,4,6-triphenylbenzyl alcohol **36** form a solid-state tetramer. 149
Figure 6.7 Structure of [$Sn(OC_6H_3Mes_2)_2$] **38**, showing Sn-π interactions. 152
Figure 6.8 Structure of [$(Me_3Si)_2NGe(OC_6H_3Mes_2)$] **39**. 154
Figure 6.9 Structure of [$Me_2Al(\mu\text{-}OC_6H_3Mes_2)]_2$ **40**. 155

Figure 6.10 Rothwell's 2,6-diphenylphenol aluminium complex (left) and Power's 2,6-bis(2,4,6-triisopropylphenyl) phenol aluminium complex (right). 156
Figure 6.11 Structure of $[(Me_2N)_2Ti(OC_6H_3Mes_2)_2]$ **41**. 158
Figure 6.12 Structure of $[EtZn(\mu\text{-}OCH_2C_6H_2Ph_3)]_2$ **42**. 161

LIST OF SCHEMES

Scheme 1.1 The sterics of the Mes* ligand favour addition of I_2 to selenium. 3
Scheme 1.2 Synthesis of a halogenated *m*-terphenyl by the Hart aryne route. 9
Scheme 1.3 Synthesis of *m*-terphenyls by the modified Hart route 9
Scheme 1.4 Synthesis of *m*-terphenyls by the cyclization route. 10
Scheme 1.5 Addition of hydrogen to a digermyne 18
Scheme 1.6 Example of C-H activation in a *m*-terphenyl to form 9-phospha- or 9-arsafluorenes. 20
Scheme 2.1 Synthesis of $[(CH_3)_2Al(\mu\text{-}O_2CC_6H_2Ph_3)]_2$ **2**. 25
Scheme 2.2 Synthesis of $[EtZn(\mu\text{-}O_2CC_6H_3Mes_2)]$ **4**. 28
Scheme 2.3 Synthesis of tin(II) carboxylate complexes $[(Me_3Si)_2NSn(\mu\text{-}O_2CAr)]$ **6-8**. 31
Scheme 2.4 Reaction of $H_2O{\cdot}B(C_6F_5)$ with an alkylaluminium nacnac. 36
Scheme 2.5 Proposed reaction of **7** with $H_2O{\cdot}B(C_6F_5)$. 36
Scheme 2.6 Rational synthesis of $[(Mes_2C_6H_3CO_2)Sn(\mu\text{-}NSiMe_3)]_2$ **9** using silver cyanate. 38
Scheme 2.7 Oxidative addition of CH_2Cl_2 to $Sn[N(SiMe_3)_2]_2$. 43
Scheme 2.8 Synthesis of $[(Mes_2C_6H_3CO_2)Si(NMe_2)_3]$ **12**. 47
Scheme 2.9 Synthesis of $[(Mes_2C_6H_3CO_2)Ti(NMe_2)_3]$ **13** and $[(Mes_2C_6H_3CO_2)_2Ti(NMe_2)_2]$ **13a**. 47
Scheme 3.1 Synthesis of 2,6-diphenylterephthalic acid **15H$_2$**. 70
Scheme 4.1 Syntheses of 4-bromomethyl-2,6-diphenyl benzoic acid **22** and 4-mercaptomethyl-2,6-diphenylbenzoic acid **23**. 99
Scheme 5.1 General synthesis of Salen molecules. 110
Scheme 5.2 Synthesis of 2,4,6-triphenylbenzaldehyde **25**. 112
Scheme 5.3 Synthesis of TPIP **26** and TPAP **27**. 113
Scheme 5.4 Synthesis of Sn·TPIP complex **28**. 116
Scheme 5.5 Synthesis of $TPIP{\cdot}AlMe_2{\cdot}AlMe_3$ **29**. 119
Scheme 5.6 Synthesis of $TPAP{\cdot}AlMe_2$ **30**. 121
Scheme 5.7 Ring-opening polymerization of ε-caprolactone (top) and propylene oxide (bottom). 123
Scheme 5.8 Synthesis of the *m*-terphenyl amide **30**. 123
Scheme 5.9 Synthesis of boronic acids **32** and **33**. 125
Scheme 6.1 Synthesis of 2,6-bis(2,4,6-trimethylphenyl)phenol **34**. 143

Scheme 6.2 Synthesis of 2,4,6-triphenylbenzylalcohol **36** and 2,6-bis(2,4,6-trimethylphenyl)benzyl alcohol **37**.....146
Scheme 6.3 Synthesis of [$Sn(OC_6H_3Mes_2)_2$] **38**.....151
Scheme 6.4 Synthesis of [$(Me_3Si)_2NGe$ ($OC_6H_3Mes_2$)] **39**.....153
Scheme 6.5 Synthesis of [$Ge(OC_6H_3Mes_2)_2$] **39a**.....153
Scheme 6.6 Synthesis of [$Me_2Al(\mu\text{-}OC_6H_3Mes_2)]_2$ **40**.....155
Scheme 6.7 Synthesis of [$(Me_2N)_2Ti(OC_6H_3Mes_2)_2$] **41**.....157
Scheme 6.8 Synthesis of [$EtZn(\mu\text{-}OCH_2C_6H_2Ph_3)]_2$ **42**.....160

LIST OF TABLES

Table 2.1 Selected structural data for $[Me_2Al(\mu\text{-}O_2CC_6H_2(Ph_3)]_2$ **2**. 27

Table 2.2 Selected structural data for$[EtZn(\mu\text{-}O_2CC_6H_3Mes_2)]$ **4**. 30

Table 2.3 Selected structural data for tin complexes $[(Me_3Si)_2NSn(\mu\text{-}O_2CAr)]$ **6-8**. 34

Table 2.4 Selected structural data for $[(Mes_2C_6H_3CO_2)Sn(\mu\text{-}NSiMe_3)]_2$ **9**. 39

Table 2.5 Selected structural data for $(CH_2Cl)(Cl)Sn[N(SiMe_3)_2]_2$ **11**. 44

Table 2.6 Selected structural data for $[(Mes_2C_6H_3CO_2)Si(NMe_2)_3]$ **12**, $[(Mes_2C_6H_3CO_2)Ti(NMe_2)_3]$ **13** and $[(Mes_2C_6H_3CO_2)_2Ti(NMe_2)_2]$ **13a**. 50

Table 3.1 Selected structural data for bifunctional *m*-terphenyl carboxylate **15H$_2$**. 71

Table 3.2 Selected structural data for [**15**·bipy] **16**. 73

Table 3.3: Selected structural data for [**15**·Zn·$(py)_2$·MeOH] **17** and[**15**·Co·$(py)_2$·MeOH] **18**. 77

Table 3.4 Selected structural data for [(**15H**)$_2$·Cu·$(py)_2$] **19**. 79

Table 3.5 Selected structural data for [(**15H**)$_2$·Cu·$(py)_4$·$(H_2O)_2$] **20**. 82

Table 3.6 [O-H···O] Hydrogen bond lengths and angles in [(**15H**)$_2$·Cu·$(py)_4$·$(H_2O)_2$] **20**. 82

Table 3.7 Selected structural data for [**15**·Ag_2] **21**. 85

Table 3.8 Selected structural data for[**15**·Zn·$(EtOH)_2$] **22**. 87

Table 3.9 [O-H···O] Hydrogen bond lengths and angles of [**15**·Zn·$(EtOH)_2$] **22**. 88

Table 4.1 Selected structural data for 4-methyl-2,6-diphenylbenzoic acid **14**. 100

Table 5.1 Selected structural data for TPIP 26 and TPAP **27**. 115

Table 5.2 Selected structural data for Sn·TPIP **28**. 117

Table 5.3 Selected structural data for TPIP·$AlMe_2$·$AlMe_3$ **29**. 121

Table 5.4 Selected structural data for 2,6-bis(2,4,6-trimethylphenyl)phenylboronic acid **33**. 127

Table 6.1 Selected structural data for 2,6-bis(2,4,6-trimethylphenyl)phenol **34**. 145

Table 6.2 Selected structural parameters of 2,4,6-triphenylbenzylalcohol **36** and2,6-bis(2,4,6-trimethylphenyl)benzyl alcohol **37**. 148

Table 6.3 [O-H···O] hydrogen bond lengths and angles in 2,4,6-triphenylbenzyl alcohol **36**. 150

Table 6.4 Selected structural data for $[Sn(OC_6H_3Mes_2)_2]$ **38**. 152

Table 6.5 Selected structural data for $[(Me_3Si)_2NGe\ (OC_6H_3Mes_2)]$ **39**. 154

Table 6.6 Selected structural data for $[Me_2Al(\mu\text{-}OC_6H_3Mes_2)]_2$ **40**.....156
Table 6.7 Selected structural data for $[(Me_2N)_2Ti(OC_6H_3Mes_2)_2]$ **41**.....159
Table 6.8 Selected structural data for $[EtZn(\mu\text{-}OCH_2C_6H_2Ph_3)]_2$ **42**.....161

LIST OF ABBREVIATIONS

Ar	aryl
br	broad
Bu	butyl, C_4H_9
COF	covalent organic framework
Cp	cyclopentadienyl, $[C_5H_5]$
d	doublet
DFT	density functional theory
DMF	*N,N*-dimethyl formamide
DMSO	dimethyl sulfoxide
DNA	Deoxyribonucleic acid
Dipp	2,6-diisopropylphenyl
Et	ethyl, C_2H_5
FT	Fourier transform
GPC	gel permeation chromatography
h	hour
HOMO	highest occupied molecular orbital
IMes	1,3-bis(2,4,6-trimethylphenyl)imidazol-2-ylidene
IR	infrared
LUMO	lowest unoccupied molecular orbital
m	medium (infrared absorption)

m	*meta*
m	multiplet
MALDI-TOF	matrix-assisted laser desorption ionization time-of-flight
MAO	methylaluminoxane
Me	methyl, CH_3
Mes	mesityl, 2,4,6-trimethylphenyl
Mes*	supermesityl, 2,4,6-tri-*t*-butylphenyl
MOCN	metal-organic coordination network
mp	melting point
nacnac	R'N=C(R)CH=C(R)(HNR')
NBS	*N*-bromosuccinimide
NHC	*N*-heterocyclic carbene
NLO	non-linear optic
NMR	nuclear magnetic resonance
Ph	phenyl, C_6H_5
ppm	parts per million
PPV	poly(phenylene vinylene)
Pr	propyl, C_3H_7
r.t.	room temperature
ROP	ring-opening polymerization
s	singlet
s	strong (infrared absorption)
SAM	self-assembled monolayer

SOHIO	Standard Oil of Ohio company
SOMO	singly occupied molecular orbital
t	triplet
TGA	thermogravimetric analysis
THF	tetrahydrofuran
TMS	trimethylsilyl [$Si(CH_3)_3$]
TPAP	*N*-(2',4',6'-Triphenylbenzyl)-2-aminophenol
TPIP	*N*-(2',4',6'-triphenylbenzylidene)-2-iminophenol
vs	very strong (infrared absorption)
w	weak (infrared absorption)

1 INTRODUCTION

The goal of synthetic chemists in any discipline is to design and prepare molecules with specific sets of characteristics. The motivation for such research could perhaps be to make molecules for use in a specific application, or for the sheer challenge of trying to stretch the limits of what current theories predict is or is not possible. Organic chemists often take their inspiration from nature, mimicking the complex architecture of natural products. Inorganic chemists, particularly bioinorganic chemists, sometimes follow a similar pathway. More often than not, however, inorganic chemists take the opposite approach.[1] They aim to prepare compounds with *unnatural* coordination environments around one or more metal centres so that they can explore the unusual reactivity that often results. Unnatural coordination could mean metals with higher than normal coordination numbers. More typically, though, it means metals with unusually low coordination numbers or metals exhibiting multiple bonds between two or more centres.

Since ligands, defined as an atom or group of atoms attached to the central atom of a coordination complex,[2] generally dictate the reactivity of that central atom, several ligand-based techniques have been developed for the synthesis of compounds with unusual coordination environments. One method is base stabilization[3,4] (Figure 1.1), in which a Lewis base donates a lone pair of electrons to an electron deficient metal. Another approach is electronic stabilization.[5] The example in Figure 1.2 shows how the electrophilicity of the carbene is diminished by electron donation into the empty carbon

p-orbital by the formal lone pairs on the nitrogen atoms, while at the same time the nucleophilicity is reduced by electron withdrawal through the σ-bonds by the more electronegative nitrogen atoms.

Figure 1.1 **Examples of intermolecular (left) and intramolecular (right) base stabilization of a monomeric aluminium hydride.**

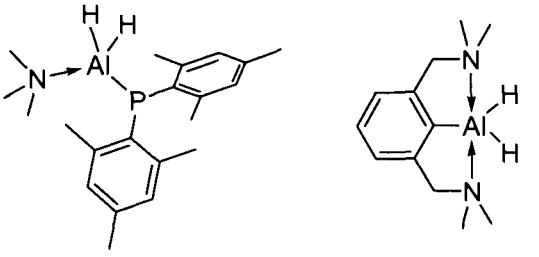

Figure 1.2 **Electronic stabilization of a carbene through both the σ (left) and π (right) framework.**

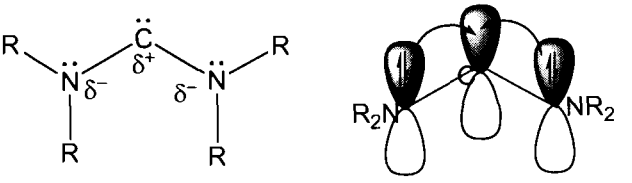

Figure 1.3 **Diagram of relative strain energies for the cyclodimerization of substituted ethylenes.**

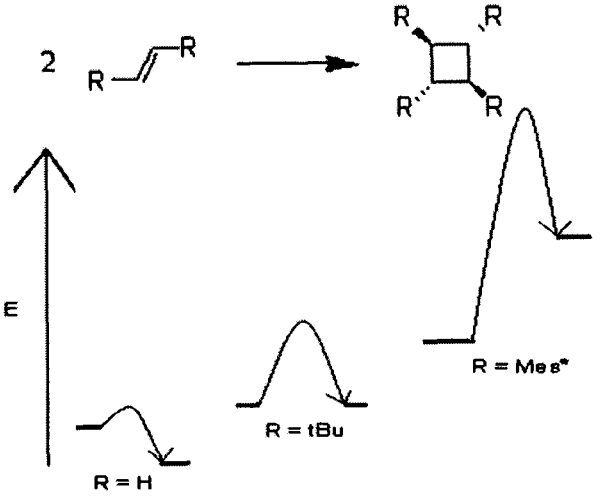

An alternative to electronic stabilization is, of course, steric stabilization. Bulky ligands are often used for the preparation of reactive organometallic molecules because

they can provide both kinetic and thermodynamic stability to the complexes. They can hinder the approach of reactive molecules (kinetic stability) or increase strain energy with respect to oligomerization (thermodynamic stability),[6] both of which may be an advantage or disadvantage depending on the desired application.[7] An example of thermodynamic stability is shown in Figure 1.3. The energy of cyclization of an unsubstituted ethylene is clearly exothermic, with a calculated value of -85 kJ/mol, but when the substituents are changed to the bulky 2,4,6-tri-t-butylphenyl (Mes*), the reaction is endothermic ($E_{cyclodimerization}$ = 395 kJ/mol).[6] This effect is also demonstrated experimentally (Scheme 1.1) in the addition of I_2 to Mes*Se-SeMes* which has an equilibrium constant, K_{eq}, of 10^2. Covalent bonds between selenium and iodine are generally considered unstable with respect to homoatomic Se-Se and I-I bonds, but their formation is favoured in this case by the steric demands of the Mes* ligand.[6]

Scheme 1.1 The sterics of the Mes* ligand favour addition of I_2 to selenium.

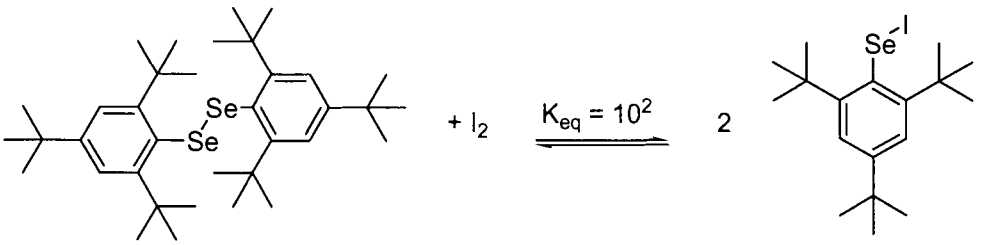

In principle, the choice of ligand is limited only by the imagination of the chemist; however, in practice ligands tend to fall into a number of well-defined molecular families.[8] All ligands, bulky or not, are either cationic, anionic, or neutral. Not surprisingly, cationic ligands are the least common.[9] This class includes, but is by no means limited to, such ions as nitrosyl[10] (NO^+), phosphenium[11] (PR_2^+), triazolium[12] ($C_2N_3R_4^+$), and tropylium[13] ($C_7H_7^+$) that coordinate to metals in a variety of ways.

Neutral and anionic ligands are more common and typically feature group 15 or 16 elements donating a formal lone pair to an empty metal d-orbital. Alternatively, unsaturated cyclic carbon-based molecules such as cyclooctadiene (neutral) or cyclopentadienyl (anionic) can coordinate through cation-π interactions. Although there are many other examples of small neutral or anionic ligands, further discussion will be limited to those typically classified as bulky ligands.

1.1 Classes of bulky ligands

Tertiary phosphine (PR_3, R = alkyl or aryl) and cyclopentadienyl (Cp^-) ($C_5R_5^-$, R = H, alkyl) molecules are classic bulky ligands. Phosphines are neutral donors with pyramidal geometry. Unlike analogous amines, they do not readily undergo inversion at room temperature, so their stereochemistry, if present, is maintained.[14] They coordinate to transition metals through the phosphorus lone pair, although secondary metal-π interactions or cyclometallation reactions are not unknown.[15] Cyclopentadienyl ligands, on the other hand, are monoanionic and can coordinate in a variety of ways, although η^5 coordination, found in sandwich-type complexes, and η^1 coordination are by far the most common.[16] Both the steric and electronic properties of these ligands can be tuned by varying the nature of the alkyl or aryl substituents. The importance of quantifying these two properties has been extensively investigated for phosphine[15,17] and cyclopentadienyl[18] transition metal complexes.

It is possible to measure the steric effects of phosphine ligands at both the phosphorus centre and the metal centre. At phosphorus, this is done by finding the sum of bond angles around phosphorus, $\Sigma\{\angle CPC\}$.[19] The classic method for determining the

steric properties of phosphines at the metal centre is the Tolman cone angle[20] (Figure 1.4). In simple terms, this is defined as the angle, θ, subtended by a cone with its apex placed 2.28 Å from the centre of the phosphorus atom (an idealized M-P bond length) and the edges just touching the van der Waals radii of the ligand substituents. From Figure 1.4, it should be clear that the larger the value of θ, the closer the substituents will be to the metal centre, and therefore the ligand will be more sterically demanding. Over the years, the Tolman theory has been refined to account for things like variable M-P bond lengths as well as intermeshing of ligands.[21] In a similar manner, the sterics of cyclopentadienyl ligands are generally described by cone angles measured from either the metal apex or the ring centroid[18a] (Figure 1.4).

Figure 1.4 Method for measuring cone angles of phosphine and cyclopentadienyl ligands.

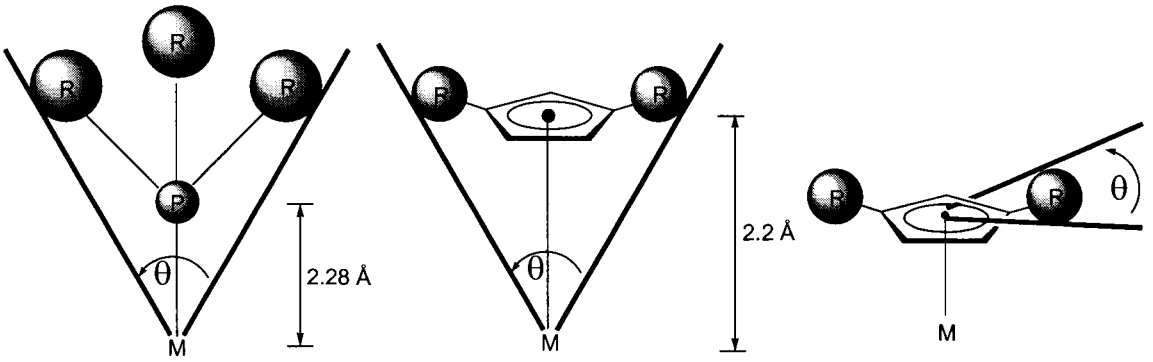

Recently, two other types of bulky ligands have become increasingly prominent. These are the *N*-heterocyclic carbenes (NHC) and the β-diketimines (Figure 1.5). β-Diketimines are nitrogen derivatives of β-diketonates, whose common name "acetylacetonato" is often abbreviated "acac". By analogy, the term "nacnac" was coined by Theopold in 1998 to describe β-diketimines.[22] Nacnac derivatives are monoanionic ligands that primarily form chelate complexes, although a variety of other bonding modes

are known.[23] Their steric properties are easily tuneable by varying the R groups on the nitrogen atoms as well as on the carbon backbone. Their use as ligands ranges across the entire periodic table,[23] from main group elements,[24] to early[25] and late[26] transition metals, and even lanthanides[27] and actinides.[28]

Figure 1.5 Generic β-diketiminate (nacnac) (left) and *N*-heterocyclic carbene (NHC) (right).

Like phosphines, NHCs are neutral two-electron donors,[29] and initially, they were treated as phosphine analogues. Studies have shown, however, that the analogy is not particularly valid.[30] For example, the difference between 1st and 2nd generation Grubbs catalysts is the simple substitution of a phosphine (1st generation) by a carbene (2nd generation), but their activities are very dissimilar.[31] Besides being better electron donors than phosphines, the sterics of carbenes are quite different. NHCs are more accurately described as "fan-shaped"[30b], not cones like phosphines. In addition, while the alkyl and/or aryl substituents on phosphine ligands point away from the metal centre, those on carbenes point towards the metal, thereby allowing more possible metal-ligand interactions.[30b]

Because of these differences, an alternative method to the Tolman cone angle for quantifying steric demands was recently developed by Nolan to enable a direct comparison of phosphines and NHCs.[32] His method, based on experimental measurements of CO stretches and Ni-CO bond dissociation energies in a series of $Ni(CO)_3(NHC)$ and $Ni(CO)_3(PR_3)$ compounds, involves calculating the percentage of the

volume of a metal-centred sphere with a radius of 3 Å that overlaps with space occupied by the ligand (Figure 1.6). The metal-ligand distance was set at 2 Å for NHC ligands and 2.28 Å for phosphine, the same M-P distance used in Tolman calculations. The resulting values for $\%V_{bur}$ ranged from 17-30% for common phosphines, with the benchmark phosphine PPh_3 at 22%. The NHC values ranged from 23-38%, with the most common NHC 1,3-bis(2,4,6-trimethylphenyl)imidazol-2-ylidene (IMes) at 26%. Since aryl-substituted NHCs such as IMes have an isosteric relationship to both the nacnac and *m*-terphenyl ligand classes, this measurement provides a good estimate for the steric demands of the bulky ligands that are the focus of this thesis.

Figure 1.6 Method for measuring $\%V_{bur}$ using the NHC 1,3-bis(2,4,6-trimethylphenyl)imidazol-2-ylidene (IMes).

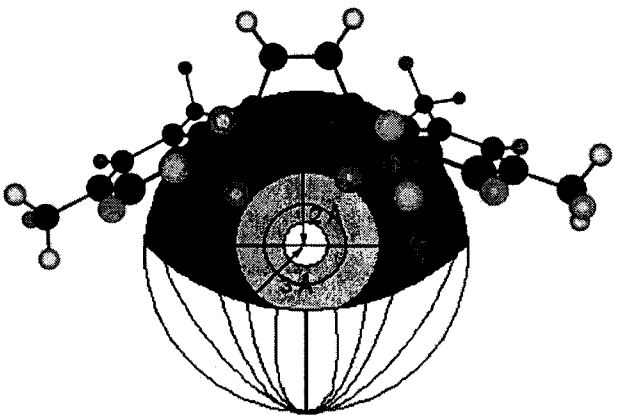

1.2 *m*-Terphenyl ligands

1.2.1 Definition and synthesis

m-Terphenyls are defined as molecules with two aryl substituents arranged *meta* to one another on a central phenyl ring. As shown in Figure 1.7, the aryl groups twist out of the plane of the central ring to form a bowl-shaped pocket with a diameter of approximately 12 Å. This pocket acts as a steric shield for reactive species found within

it. The steric protection provided by the *m*-terphenyl can be easily tuned by varying the nature of the aryl substituents. Common groups include phenyl, 2,4,6-trimethylphenyl (mesityl), and 2,6-diisopropylphenyl (Dipp). Throughout this thesis, metals and/or functional groups attached to the central ring at the position between the two aryl substituents will be referred to as being in the pocket, while those bound at the opposite end of the ring will be called *para*.

Figure 1.7 The pocket formed by the *m*-terphenyl 2,6-bis(2,4,6-trimethylphenyl)benzene is shown in the space-filling diagram.

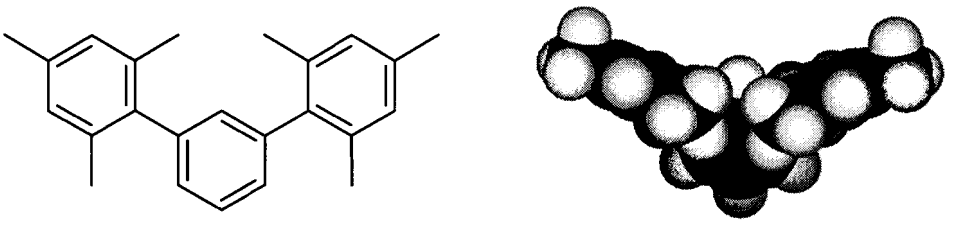

The most common and versatile synthetic route for *m*-terphenyls is the aryne method developed by Hart and co-workers[33] (Scheme 1.2). In this reaction, three equivalents of an aryl Grignard reagent are added to an ethereal solution containing a 1,2,3-trihalobenzene. This reaction can be quenched with water, to give an unsubstituted *m*-terphenyl, or iodine, to give a halogenated *m*-terphenyl. Direct addition of other electrophiles is possible, but the presence of excess aryl Grignard reagent in the reaction mixture can lead to the formation of unwanted and often hard-to-separate by-products.[33] Further functionalization of the *m*-terphenyls is typically done by lithiation of the isolated halogenated product. This route was used to prepare all the diaryl-substituted *m*-terphenyls described in this report; however, it is of limited use for extremely bulky aryl substituents including Mes* (2,4,6-tri-*t*-$Bu_3C_6H_2$).[34]

Scheme 1.2 Synthesis of a halogenated *m*-terphenyl by the Hart aryne route.

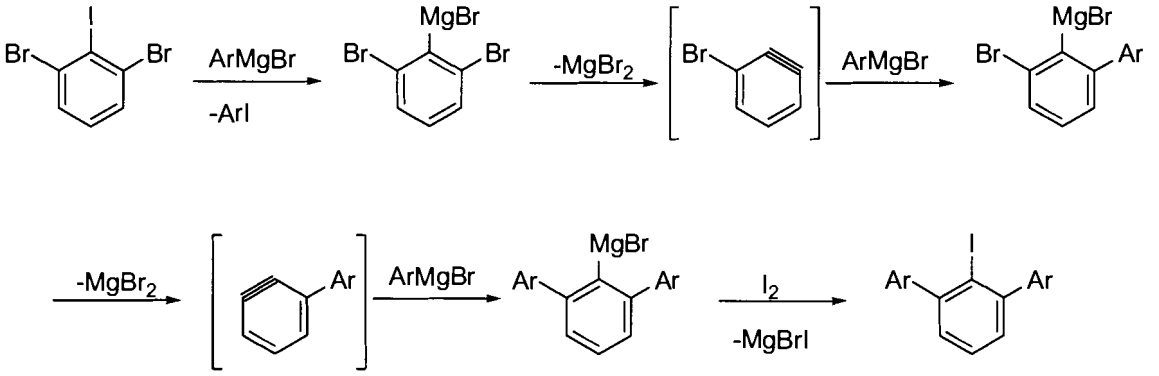

Hart has also developed a variation[35] on this synthesis, which has been refined by Power and co-workers.[36] It involves the lithiation of 1,3-dichlorobenzene, followed by the addition of the Grignard reagents (Scheme 1.3). Its advantage lays in the use of the more affordable dihalobenzene and requires only two equivalents of Grignard reagents. However, if the temperature is allowed to rise above -78 °C, it is potentially explosive, unlike the original aryne synthesis that can be safely done at room temperature.

Scheme 1.3 Synthesis of *m*-terphenyls by the modified Hart route

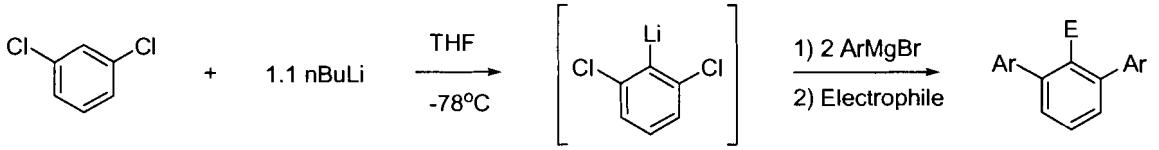

A further route to functionalized *m*-terphenyls is the homocondensation of aromatic ketones in ethanol.[37] This cyclization reaction occurs in the presence of Lewis acids like silicon tetrachloride and typically proceeds cleanly and in high yields (Scheme 1.4). The resulting 1,3,5-triarylbenzene can undergo direct electrophilic aromatic substitution reactions with molecular bromine.[38] This route was used to prepare all the triaryl-substituted *m*-terphenyls described in this report.

Scheme 1.4 Synthesis of *m*-terphenyls by the cyclization route.

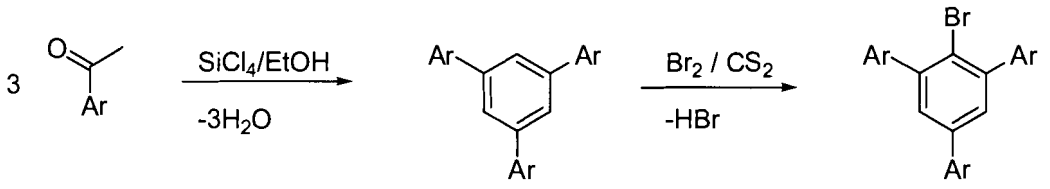

1.2.2 Applications to synthetic materials

Although *m*-terphenyl frameworks have been found in a small number of natural products,[39] it is primarily in synthetic chemistry that they are used. In recent years, *m*-terphenyls have made an impact in many areas of chemistry. In organic materials synthesis, the group of Rajakumar has been particularly active. They have used the bulk and rigidity of the *m*-terphenyl as stoppers for rotaxanes (Figure 1.8) made by both threading and clipping methods.[40] The inherent π-donating ability of the *m*-terphenyl was implicated in the improvement of relative yield by clipping compared to threading, and the hydrophobicity of the molecule was found to affect its electrochemical behaviour. The same group, along with the group of Guan, has also explored *m*-terphenyls as the basis for intra-annularly functionalized cyclophanes,[41] stilbenophanes,[42] and photochemically active azobenzenophane host-guest systems[43] (Figure 1.9). Tschierske saw a different application for the rigid *m*-terphenyl core, and used them as a basis for his "banana-shaped" liquid crystals[44] (Figure 1.10).

Figure 1.8 **Example of a *m*-terphenyl rotaxane. The *m*-terphenyl fragments are highlighted in bold.**

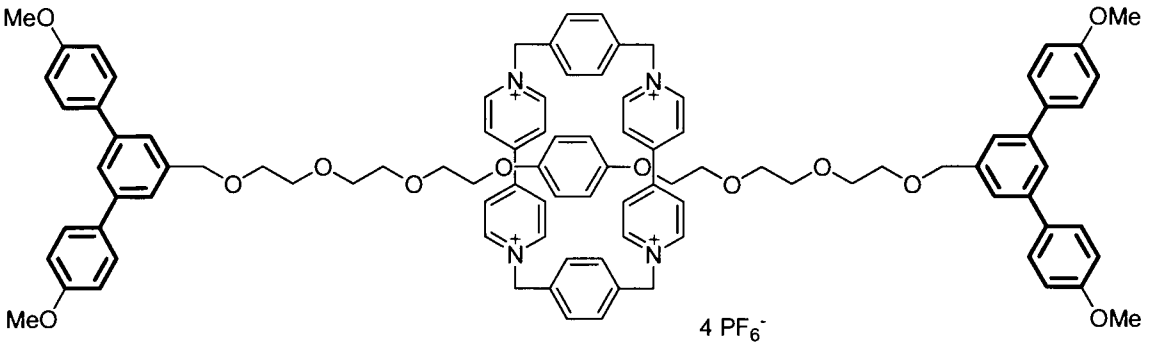

Figure 1.9 **Example of a *m*-terphenyl cyclophane (left), stilbenophane (centre) and azobenzenophane (right). The *m*-terphenyl fragments are highlighted in bold.**

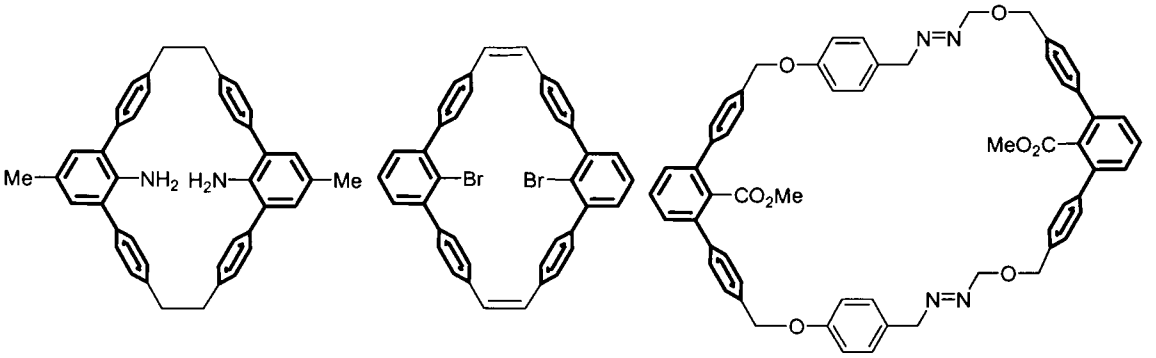

Figure 1.10 **Example of a *m*-terphenyl liquid crystal mesogen. The *m*-terphenyl fragment is highlighted in bold.**

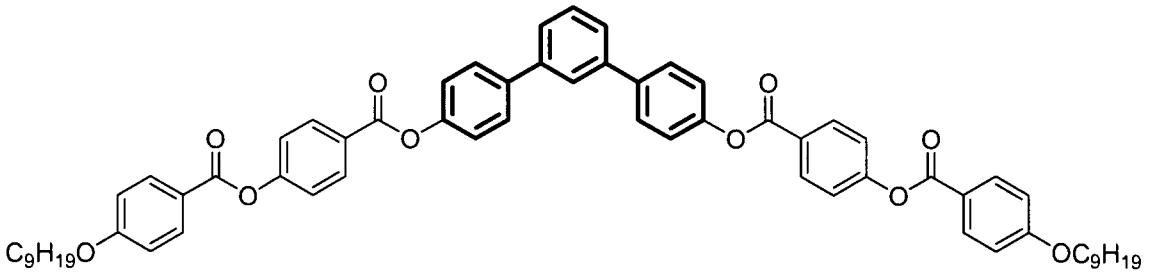

In addition, Rajakumar and co-workers have designed a series of chiral[45] and achiral[46] dendrimers (Figure 1.11) in which it was hoped that the peripheral *m*-terphenyl pockets would provide binding sites for molecular recognition applications. He has also explored the antibacterial activity of *m*-terphenyl dendrimers,[47] and their use as

fluorescence sensors.[48] Goto et al. have taken a different approach to the bulky pockets of *m*-terphenyl dendrimers, using them to stabilize reactive organic molecules.[49]

Figure 1.11 Example of a *m*-terphenyl capped dendrimer. The *m*-terphenyl fragments are highlighted in bold.

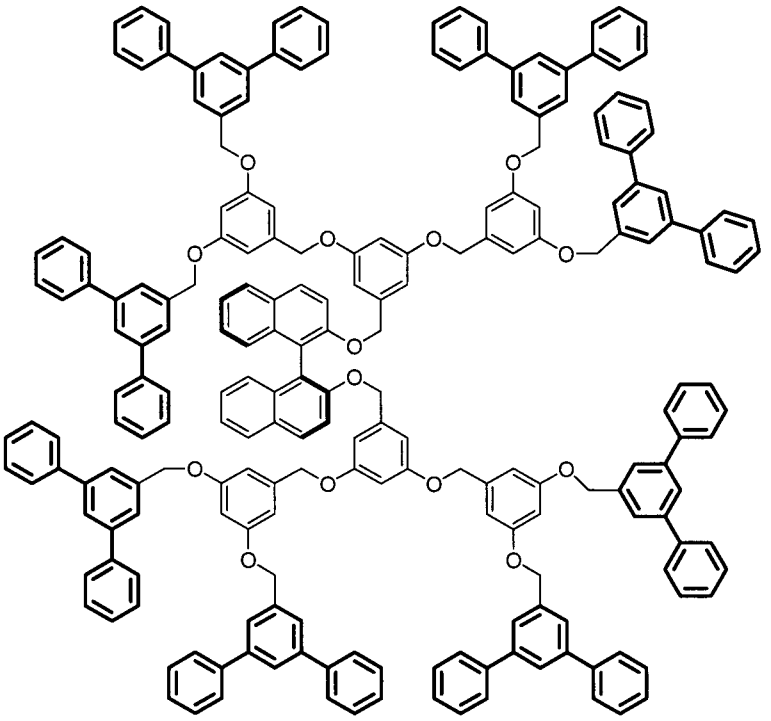

The *m*-terphenyl pocket was also the property exploited by Lee and colleagues to develop biconcave molecules for incorporation into non-porous solids.[50] They fused three *m*-terphenyls around a common organic core, causing the individual pockets to converge to form the biconcave cavities. Internal concerted rotation of the *m*-terphenyl "wings" allowed the cavities to open and close, releasing guest solvent molecules in a remarkable crystal-to-crystal transformation. The steric demands of the *m*-terphenyls have also been exploited to induce restricted rotation in acetylenic bonds,[51] to control and study the photoisomerization of phosphaalkenes[52] (Figure 1.12), and for stereoselective protonation reactions of allyl and cyclohexyl anions.[53]

Figure 1.12 **Examples of *m*-terphenyls in acetylenes (left) and phosphaalkenes (right). The *m*-terphenyl fragments are highlighted in bold.**

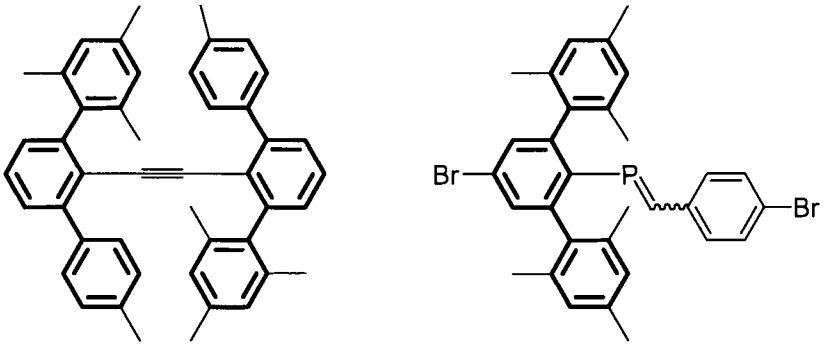

Figure 1.13 **Examples of PPV polymers incorporating *m*-terphenyls. The *m*-terphenyl fragments are highlighted in bold.**

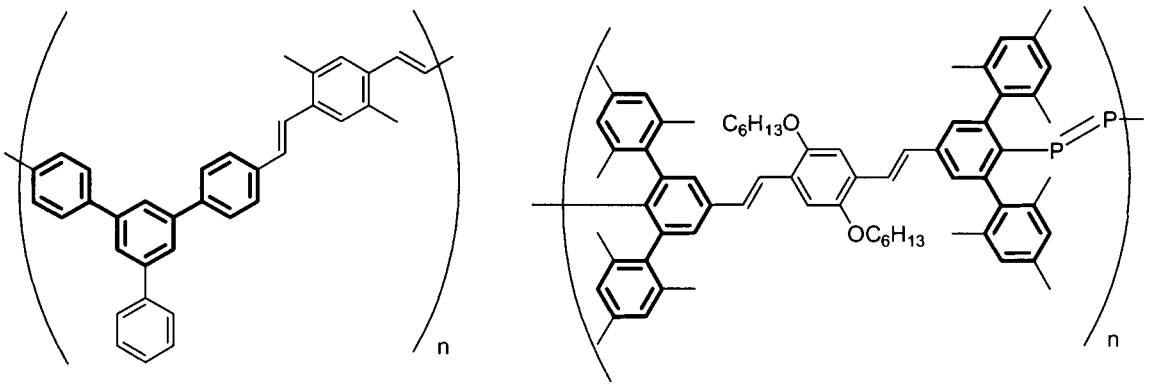

m-Terphenyls have recently appeared in polymer chemistry as well. Spiliopoulos incorporated them into the main chain of luminescent organic poly(*p*-phenylene vinylene) (PPV) polymers (Figure 1.13) used as organic light-emitting diodes and laser materials.[54] The purpose of the *m*-terphenyl was to introduce a kink into the polymer chain, thereby reducing conjugation and lowering the emission wavelength. In that case, the polymer was linked through the aryl substituents of the *m*-terphenyl. Protasiewicz, on the other hand, used a linkage through the central phenyl ring to incorporate *m*-terphenyls into diphosphene-PPV oligomers[55] and polymers[56] (Figure 1.13). The low-coordinate phosphorus was protected by the steric bulk of the *m*-terphenyl pocket, providing the first example of a P=P double bond in a polymer backbone. Among other things, this changes

the HOMO-LUMO gap of the conjugated polymers, opening up exciting possibilities for the future of hybrid inorganic-organic conjugated systems. Protasiewicz is also investigating *m*-terphenyl protected P=P complexes as redox active molecular switches.[57]

These phosphorus applications relate directly to the most common and traditional use of *m*-terphenyls, which is highlighted throughout this thesis: their use as ligands for main group[58] and transition metal complexes. Complexes in which the metal is bound at the *para* position of the *m*-terphenyl will not be discussed in detail, although they do have interesting applications as non-coordinating ions[59] (Figure 1.14a, b), substituents on chelating[60] (Figure 1.14c) or extremely bulky[61] phosphines, germanols and silanols[62] (Figure 1.14d) and ligands for nitrogen-fixing molybdenum and tungsten catalysts[63] (Figure 1.14e). Complexes in which the metal is bound primarily η^6 through one of the flanking aryls will also not be discussed[64] (Figure 1.14f). The focus will be on those complexes in which the metal is bound in the *m*-terphenyl pocket.

Figure 1.14 Examples of non-traditional *m*-terphenyl coordination. The *m*-terphenyl fragments are highlighted in bold.

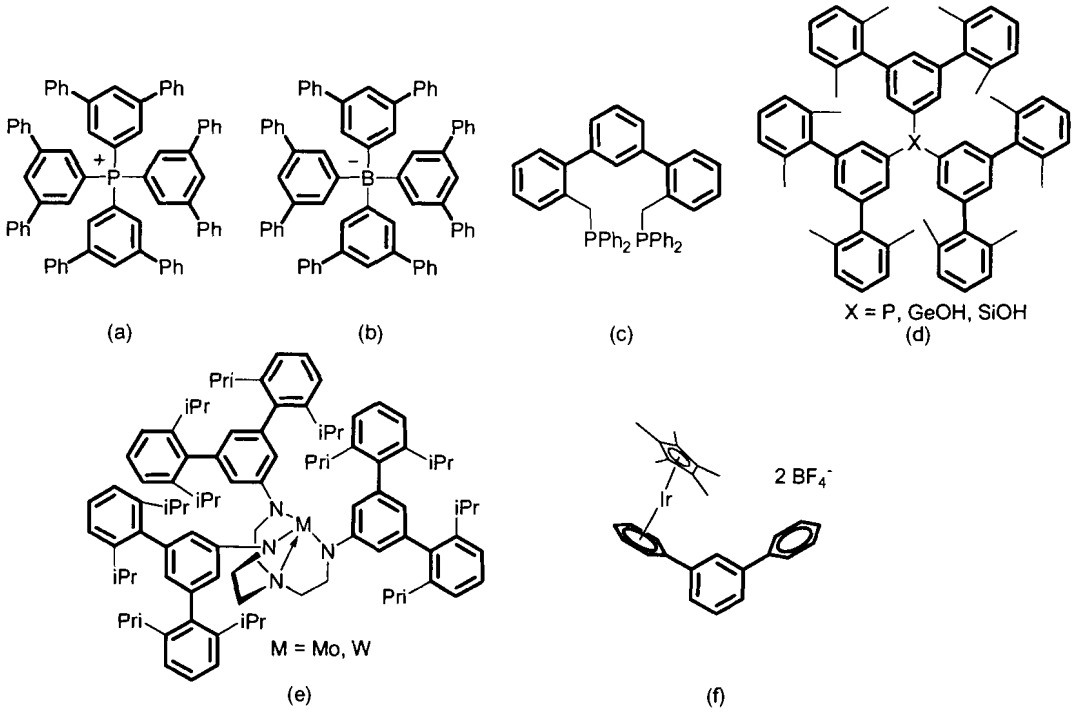

1.2.3 *m*-Terphenyls as ligands

The first use of substituted *m*-terphenyls as ligands came in 1985,[65] with reports of 2,6-diphenylphenol with tungsten (Figure 1.15) and 2,6-diphenylthiophenol with molybdenum. A direct metal-carbon bond through a *m*-terphenyl was reported in 1988,[66] but this has since been discredited.[67] This was only a temporary setback, as the *m*-terphenyl 2,4,6-triphenylbenzene was the ligand used on gallium in Power's 1991 report of a cyclic Ga_3P_3 complex, the first benzene analogue composed exclusively of heavy main group elements.[68]

Figure 1.15 The first complexes of substituted (left) and unsubstituted *m*-terphenyl ligands.

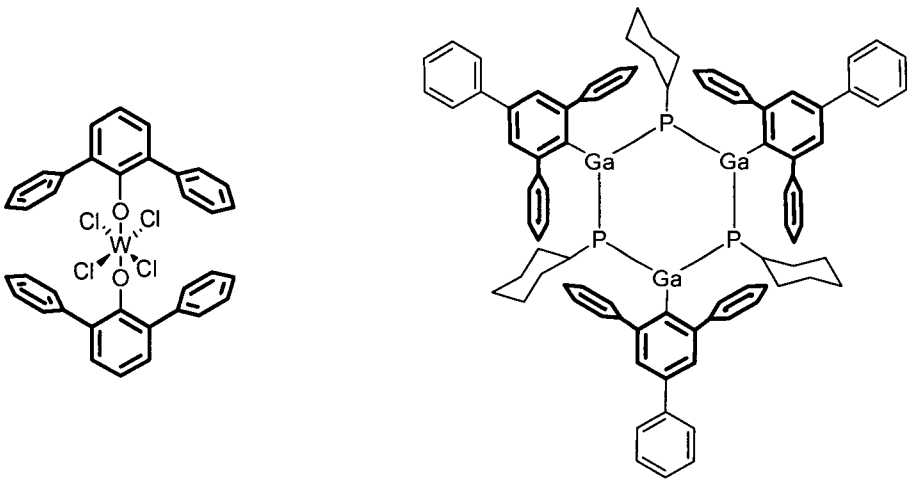

According to a recent report in *Chemical and Engineering News*,[69] one of the top developments in inorganic chemistry in 2005 was the isolation by Power and co-workers of the first *five-fold* bond between two metal centres, namely Cr(I)[70] (Figure 1.16). This remarkable synthetic feat, achieved more than 40 years after the isolation of the first metal-metal quadruple bond was reported by Cotton,[71] was made possible by the *m*-terphenyl ligand 2,6-bis(2,6-diisopropylphenyl)phenyl (Dipp). Chosen for its ability to prevent the formation of lower bond order metal oligomers or clusters while formally occupying only a single coordination site on each metal, the ligand left five orbitals available for chromium-chromium bonds. Calculations suggest that while there is not a true "quintuple" bond, there is significant orbital overlap that can be identified as five σ, π and δ bonds.[70,72]

Figure 1.16 Structure of $[(Dipp_2C_6H_3)Cr]_2$, the first chromium-chromium five-fold bond. Thermal ellipsoids are shown at 50% probability and all hydrogen atoms have been removed for clarity.

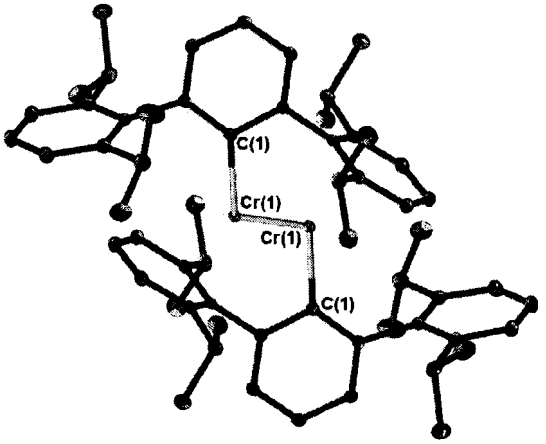

Although the second row elements of carbon, nitrogen and oxygen readily form double and triple bonds to themselves and other elements, this is not the case as one moves deeper into the periodic table.[73] By 1999, fewer than five examples each of possible homoatomic double bonds between group 13-13 or 14-14 elements (other than carbon) had been reported, and heteroatomic 13-14 or 14-15 were almost as rare.[74] Triple bonds were just as elusive, with only 23 examples from all possible combinations of group 13 to 16 elements. Certain combinations, such as 14-14 triple bonds, which are directly analogous to alkynes, were completely unknown.[74]

Since then, much has changed. *m*-Terphenyl supported triple bonds between heavy main group elements and transition metals have been reported.[75] Power et al. have used *m*-terphenyls to prepare and characterize alkyne analogues of germanium, tin and lead,[76] and they have done extensive reactivity studies on these molecules.[77] The digermyne and the distannyne showed different reactivity from alkynes and from one another. Most striking was the addition of hydrogen across the formally triple bond of the digermyne (Scheme 1.5) to give the digermene, digermane and/or germane, depending on the number of equivalents of hydrogen gas used.[78] Similar reactions with

unsaturated carbon compounds (i.e. alkenes and alkynes) are not possible without the use of hydrogenation catalysts.[79] In fact, molecular fluorine (F_2) is the only other main group compound known to react directly with dihydrogen.[78]

Scheme 1.5 Addition of hydrogen to a digermyne

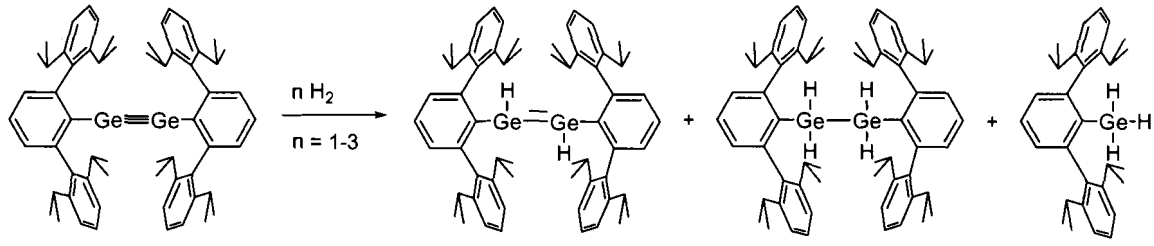

In the examples described so far, the metal or main group element is bound to a *m*-terphenyl ligand and itself. Power and co-workers realized that it should be possible to prevent the metal-metal bonding and prepare monomeric, *monocoordinate* main group complexes of the general form ArM. By using the slightly bulkier 2,6-bis(2,4,6-triisopropylphenyl)phenyl ligand, they prepared a cationic monocoordinate lead(II) complex,[80] which shows an additional weak metal-π interaction with a molecule of toluene solvent. The same ligand was featured in the neutral group 13 ArM complexes of indium(I)[81] (Figure 1.17), thallium(I)[82] and most surprisingly gallium(I).[83]

Figure 1.17 Indium(I) complex of 2,6-bis(2,4,6-triisopropylphenyl)phenyl. Thermal ellipsoids are shown at 50% probability and hydrogen atoms have been removed for clarity.

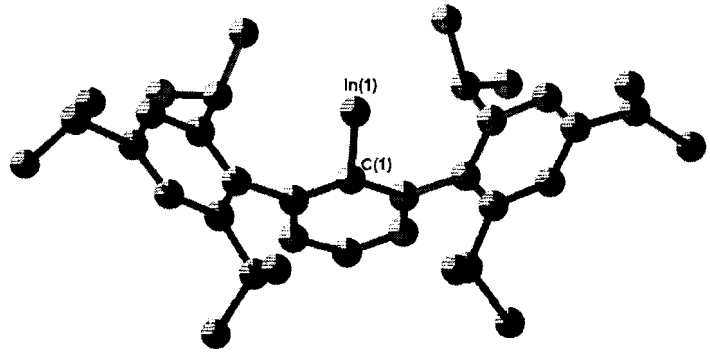

When the steric bulk was slightly reduced to the *m*-terphenyl ligand 2,6-bis(2,4,6-trimethylphenyl)phenyl, Power obtained indium(I) clusters with the formula In_8Ar_4 instead of monomers.[84] With the same ligand, Wehmschulte's group was able to prepare dicoordinate aluminium(III)[85] and gallium(III)[86] (Figure 1.18) complexes. The cationic aluminium(III) atom is bound to two *m*-terphenyl ligands, and like Power's lead(II) complex, shows weak metal-π interactions, this time with the flanking aryls of the ligand.

Figure 1.18 Cationic gallium(III) complex of 2,6-bis(2,4,6-trimethylphenyl)phenyl. Thermal ellipsoids are shown at 50% probability. Hydrogen atoms and the non-coordinating anion have been removed for clarity.

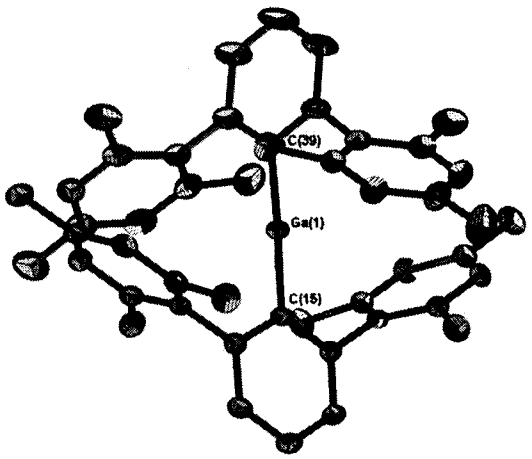

Despite their many advantages, *m*-terphenyls, like most ligands, are not always inert towards further reactivity. One of the known side reactions of *m*-terphenyls is C-H activation of one of the flanking phenyls to form a cyclometallated product.[87] This pathway can be reduced or eliminated by, for example, introducing additional bulky substituents at the 3- and 5-positions of the central phenyl ring, thus preventing the aryl groups at the 2- and 6-positions from becoming co-planar and undergoing cyclometallation.[88] More positively, cyclometallation can be a route to otherwise inaccessible molecules, as was recently established by Wehmschulte's synthesis of

unsymmetrically substituted 9-phosphafluorenes and 9-arsafluorenes, which can themselves be used as new ligands for transition metals.[89]

Scheme 1.6 Example of C-H activation in a *m*-terphenyl to form 9-phospha- or 9-arsafluorenes.

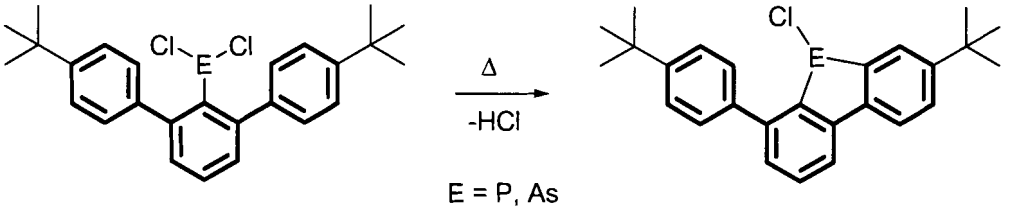

One common feature in all the examples described in this section is a direct element-carbon bond through the *m*-terphenyl ligand. With direct carbon-element bonds, we are limited to a monodentate,[90] monoanionic ligand. The introduction of an organic functional group into the *m*-terphenyl pocket allows variation of the charge and coordination modes, leading to even more structural diversity than what has been already described. The chemistry of these substituted *m*-terphenyls will be discussed in the remaining chapters of this thesis.

1.3 Thesis report

The work discussed in this thesis is a *survey* of substituted *m*-terphenyl ligands and their coordination chemistry with main group elements and transition metals. The goal of this research was to build upon the unusual steric control provided by *m*-terphenyl ligands by expanding into previously *unexplored* or *under-explored* metal-ligand combinations. Of particular interest were those metals with the potential to be catalytically active. This study would provide the knowledge necessary to enable the introduction of *m*-terphenyls into systems beyond simple molecules, such as extended networks with low-coordinate metal site, and functionalized surfaces. The intent was to

chart many different areas in which these ligands may be useful, so that they could later be used as the basis for several in-depth studies.

The chemistry of *m*-terphenyl carboxylates is described in Chapters 2-4 of this thesis. Chapter 2 focuses on *molecular* carboxylate complexes of titanium, zinc, aluminium, silicon and tin. Their syntheses, and spectroscopic and crystallographic characterization, are described. In addition, some unusual reactions of a tin(II) complex are discussed. Chapter 3 broadens the chemistry of the carboxylate complexes from small molecules into extended networks, using a new bifunctional *m*-terphenyl ligand with a carboxylic acid group in both the pocket and *para* positions. Six metal-organic coordination networks based upon this carboxylate ligand with four different metals (copper, zinc, silver and cobalt) were prepared. In Chapter 4, another new bifunctional carboxylic acid is discussed. This ligand has a mercaptomethyl group *para* to the carboxylic acid. Its use in the preparation of gold-thiol self-assembled monolayers is described.

In Chapters 5 and 6, the focus returns to molecular compounds with non-carboxylate ligands. Chapter 5 describes potentially bidentate ligands such as Schiff bases, boronic acids and amides, while Chapter 6 is devoted to the monodentate phenols and benzyl alcohols. The preparation of a *m*-terphenyl Schiff base aluminium and its activity as a ring-opening polymerization catalyst is discussed in Chapter 5, along with the synthesis of two other Schiff base complexes. This chapter also includes a discussion of the unusual hydrogen bonding observed in *m*-terphenyl boronic acids. The solid-state structures of a *m*-terphenyl phenol and two *m*-terphenyl benzyl alcohols, and their

reactions tin, germanium, aluminium, zinc, phosphorus and titanium are described in Chapter 6.

The final chapter of this thesis, Chapter 7, brings together the results discussed in each of the experimental chapters, and places into context the conclusions drawn from those results. A description of the relevant experimental work is found at the end of each chapter, along with proposals for future studies. The general experimental section and a description of X-ray crystallographic procedures are included in Chapter 2 and not repeated in the subsequent chapters. Experimental details of all crystallographic studies are tabulated in Appendix 1, while atomic coordinates are listed in Appendix 2. All references are found at the end of the thesis.

2 *m*-TERPHENYL CARBOXYLATE COMPLEXES OF TRANSITION METALS AND MAIN GROUP ELEMENTS*

Carboxylate anions are among the most versatile ligands available for transition metals and main group elements. This is a result of their varied coordination modes (Figure 2.1), the most common of which are the monodentate (a), chelating (b) and bridging (c) modes. The formal lone pairs on the oxygen atoms can also form additional dative bonds with metals. Differentiating between monodentate and bidentate binding is relatively easy with infrared spectroscopy because there is typically much greater difference between the asymmetric and symmetric C-O stretches in monodentate modes compared to the free anion than there is in bidentate modes.[91] The difference between bridging and chelating modes is much harder to identify, so in most cases, single crystal X-ray diffraction is now used when definitive statements about bonding are made.

Figure 2.1 Carboxylate coordination modes.

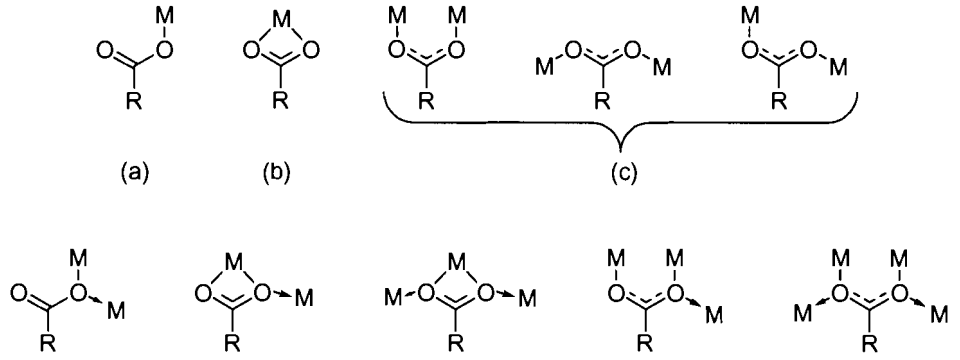

* Portions of this chapter are reproduced in part, with permission, from the following journal articles: Dickie, D. A.; Choytun, D. D.; Jennings, M. C.; Jenkins, H. A.; Clyburne, J. A. C. *J. Organomet. Chem.* **2004**, *689*, 2186-2191 (Copyright 2004 Elsevier); and Dickie, D. A.; Jennings, M. C.; Jenkins, H. A.; Clyburne, J. A. C. *Inorg. Chem.* **2005**, *44*, 828-830 (Copyright 2005 American Chemical Society).

It is important to note that the bonding modes are not necessarily static. In the early 1990s, Lippard coined the term "carboxylate shift" to denote the transition from monodentate bridging to bidentate bridging,[92] which is particularly relevant in bioinorganic systems, especially the modelling of enzyme active sites. In 1998, the groups of Lippard and Tolman recognized almost simultaneously that *m-terphenyl carboxylates* were ideal ligands for the preparation of model compounds of the enzyme active site of non-heme diiron enzymes.[93] Both realized that the steric bulk provided by these ligands would lead to the formation of the desired coordinatively unsaturated binuclear complexes, while at the same time providing a rigid, hydrophobic pocket reminiscent of natural enzymes. This has since been lauded as a significant breakthrough in the field,[94] and these ligands are now extensively studied for diiron enzymes[95] as well as copper[96] and manganese enzymes.[97] Hagadorn has even prepared the related dithiocarboxylate complexes with a *m*-terphenyl backbone (Figure 2.2) in order to model sulphur-based metalloproteins.[98]

Figure 2.2 Isoelectronic *m*-terphenyl carboxylate, dithiocarboxylate and amidinate.

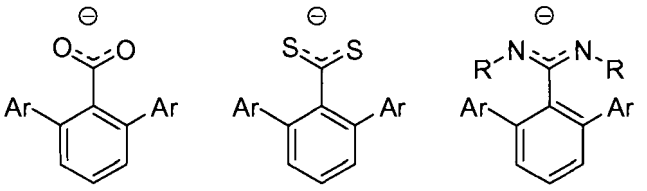

Since enzymes are nature's catalysts, it is not surprising that carboxylates[99] and the isoelectronic amidinates[100] (Figure 2.2) have been explored as ligands for metal catalysts. Specifically, Arnold[101] and Clyburne[102] have used *m*-terphenyl amidinates to prepare a variety of catalytic aluminium and transition metal complexes.[103] Previous work on main group complexes with bulky amidinate ligands focused primarily on

sterically crowding nitrogen substituents[104] rather than the carbon, as is the case for the *m*-terphenyl derivatives.[105] Since studies have shown that the bulk and placement of the substituents can have dramatic effects on catalytic activity,[106] the use of *m*-terphenyl ligands should be beneficial in these complexes.

2.1 Dimeric group 12, 13 and 14 complexes with a common $M_2O_4C_2$ core

Compared to the general carboxylate chemistry of transition metal complexes, the structural chemistry of aluminium carboxylates is relatively unexplored[107] despite the fact that aluminium salts of long-chain alkyl carboxylates (fatty acids) have a long history in industrial and even military applications.[108] Building on previous work in the Clyburne lab with aluminium amidinate complexes[102] based on the 2,4,6-triphenylbenzene *m*-terphenyl backbone, the isoelectronic 2,4,6-triphenylbenzoic acid[38a,109] **1** was prepared as described in the literature and combined in dichloromethane with one equivalent of a toluene solution of trimethylaluminium. Slow evaporation of the solvent and/or cooling to -30 °C gave colourless crystals **2** that were characterized using ^1H and ^{13}C NMR spectroscopy, IR spectroscopy and X-ray crystallography. The byproduct of this standard group 13 protonolysis reaction is CH_4,[110] but no attempts were made here to isolate it.

Scheme 2.1 Synthesis of $[(CH_3)_2Al(\mu\text{-}O_2CC_6H_2Ph_3)]_2$ 2.

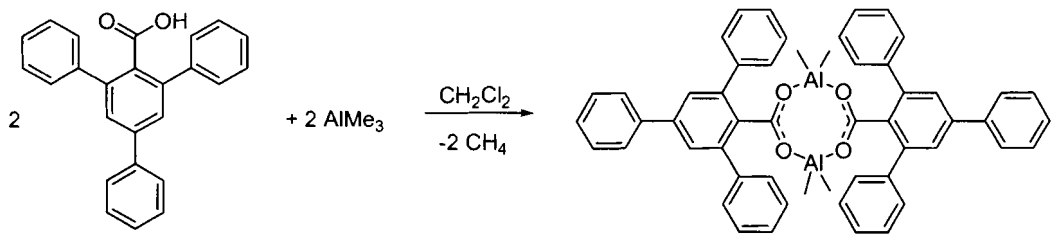

1 **2**

The ^{1}H NMR spectrum of **2** shows a distinctive singlet at –1.51 ppm attributed to the aluminium methyl groups. The aromatic protons of the flanking phenyls appear as a multiplet ranging from 7.37-7.49 ppm, while the two protons of the central phenyl appear as a sharp singlet at 7.61 ppm. In the infrared spectrum, a diagnostic shift of ν (C=O) from 1696 cm^{-1} in the free ligand to 1624 cm^{-1} in the complex was observed, as well as the disappearance of ν (O-H) at 3438 cm^{-1} in the free ligand.

X-ray crystallographic studies* revealed that **2** exists as a symmetrical dimer in the solid state. An eight-membered $Al_2O_4C_2$ heterocyclic core is formed by the carboxylate ligands bridging two aluminium centres. This is in contrast to the analogous aluminium amidinates that showed chelation through the nitrogen atoms to give monomeric compounds. Although there are, to date, no structurally characterized dialkylaluminium carboxylate chelates in the literature, it is somewhat surprising that **2** formed a bridging dimer, given that the steric demands were so similar to known *m*-terphenyl amidinate complexes.[102]

Figure 2.3 Structure of $[Me_2Al(\mu\text{-}O_2CC_6H_2(Ph_3)]_2$ 2. Thermal ellipsoids are shown at 50% probability and hydrogen atoms have been removed for clarity.

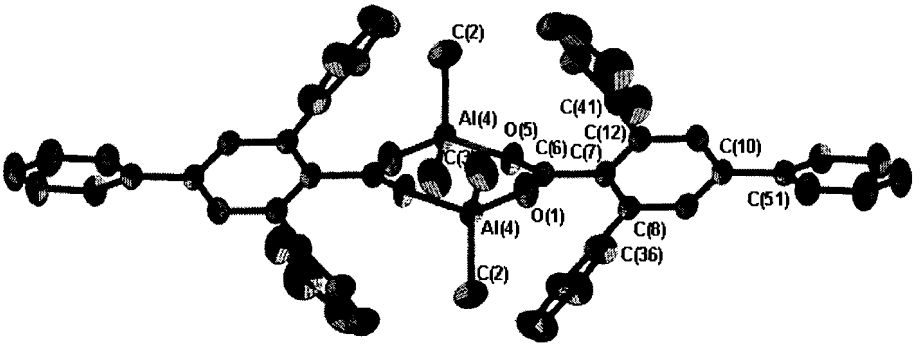

Reproduced with permission from Dickie, D. A.; Choytun, D. D.; Jennings, M. C.; Jenkins, H. A.; Clyburne, J. A. C. *J. Organomet. Chem.* **2004**, *689*, 2186-2191. Copyright 2004 Elsevier.

* Structure solved by Dr. Michael Jennings, University of Western Ontario.

The C-O bonds of the carboxylate group are equivalent within experimental error [C(6)-O(1) = 1.248(2) Å , C(6)-O(5) = 1.250(2) Å], suggesting delocalization around the $Al_2O_4C_2$ core. Complex **2** has an Al···Al distance of 4.320 Å and Al(4)-O(1) and Al(4)-O(5) bond lengths of 1.810(1) and 1.809(1) Å, respectively, which all fall within the range of the handful of previously characterized dialkylaluminium carboxylate dimers (Al···Al = 4.202-4.330 Å, Al-O = 1.767-1.840 Å).[111]

Table 2.1 Selected structural data for $[Me_2Al(\mu\text{-}O_2CC_6H_2(Ph_3)]_2$ 2.

Bond lengths (Å)			
Al(4)-O(1)	1.8095(11)	Al(4)-O(5)	1.8090(11)
O(1)-C(6)#1	1.2482(18)	O(5)-C(6)	1.2502(17)
Al(4)-C(2)	1.9449(19)	Al(4)-C(3)	1.9255(19)
Bond angles (°)			
O(5)-Al(4)-O(1)	107.89(6)	C(3)-Al(4)-C(2)	123.84(11)
O(1)-C(6)-O(5)	124.20(13)		

The $Al_2O_4C_2$ ring of **2** is nearly flat, with a maximum deviation from the heterocyclic plane of ±0.066 Å for O(5). Due to the steric constraints imposed by the *ortho*-phenyls of the ligand, the heterocyclic core of **2** is twisted out of the plane of the central phenyl by about 65°. Barron et al. reported a similar effect, with a twist angle of 42.6 °, in a gallium-carboxylate complex based on *ortho*-toluic acid.[111b] This contrasts with his aluminium complexes, all but one of which show chair-like conformations. He explained this based on steric interactions between the carboxylate ligand and the alkyls of the aluminium: the more bulk in the ligands, the more planar was the ring.[111a] The structural parameters of **2** are in accord with this explanation.

Scheme 2.2 Synthesis of [EtZn(μ-$O_2CC_6H_3Mes_2$)] 4.

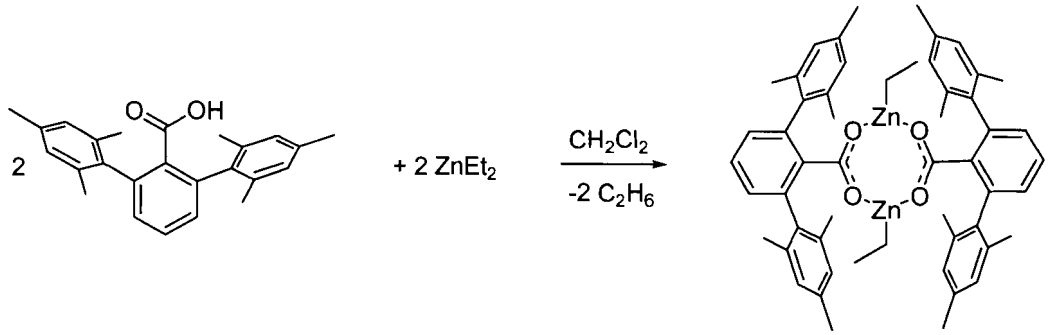

3 **4**

Moving up the bulkiness scale slightly from 2,4,6-triphenylbenzoic acid **1** to 2,6-bis(2,4,6-trimethylphenyl)benzoic acid **3**, a similar reaction* was performed with diethylzinc to give the zinc carboxylate **4** as colourless crystals. The ^{1}H NMR spectrum showed a triplet and a quartet at 1.27 and 0.08 ppm respectively, due to the ethyl group attached to zinc. Singlets at 2.32 and 2.15 ppm were assigned, respectively, to the *para* and *ortho* methyl groups of the *m*-terphenyl ligand. The IR spectrum showed strong ν C=O absorptions at 1586 and 1551 cm^{-1}, significantly different from the corresponding absorptions in the free acid **3** (1733 and 1704 cm^{-1}).

* In order to make a more direct comparison, the reactions of **1** with $ZnEt_2$ and **3** with $AlMe_3$ were both attempted, however crystalline products were not obtained and IR studies were inconclusive.

Figure 2.4 Structure of [EtZn(μ-$O_2CC_6H_3Mes_2$)] 4. Thermal ellipsoids are shown at 50% probability and hydrogen atoms have been removed for clarity.

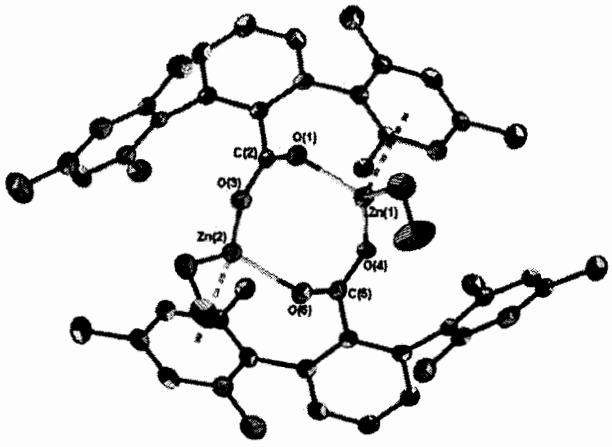

Reproduced with permission from Dickie, D. A.; Jennings, M. C.; Jenkins, H. A.; Clyburne, J. A. C. *Inorg. Chem.* **2005**, *44*, 828-830. Copyright 2005 American Chemical Society.

In order to confirm the structure of **4**, X-ray crystallographic studies* were performed (Figure 2.4). The carboxylate groups bridge two zinc atoms, forming an eight-membered $Zn_2O_4C_2$ ring in which the metal centres are separated by 3.5769(6) Å. The zinc atoms exhibit trigonal planar geometry ($\Sigma\angle$ Zn(1) = 358.92°; Zn(2) = 359.04°), and their coordination sphere is completed by an ethyl ligand. This was exciting, as there are relatively few examples of structurally characterized[112] tri-coordinate zinc complexes, compared to the more common four or six coordinate states,[113] despite the fact that such coordinatively unsaturated zinc centres have long been implicated as important species in a variety of applications, particularly catalysis.[114]

*Structure solved by Dr. Michael Jennings, University of Western Ontario.

Table 2.2 Selected structural data for[EtZn(μ-$O_2CC_6H_3Mes_2$)] 4.

Bond lengths (Å)			
Zn(1)-O(1)	1.998(2)	Zn(2)-O(6)	2.007(2)
Zn(1)-O(4)	1.971(2)	Zn(2)-O(3)	1.960(2)
Zn(1)-C(7)	1.950(4)	Zn(2)-C(9)	1.949(4)
O(1)-C(2)	1.268(4)	O(4)-C(5)	1.258(4)
O(3)-C(2)	1.265(4)	O(6)-C(5)	1.264(4)
Zn(1)···Zn(2)	3.5769(6)		
Bond angles (°)			
C(7)-Zn(1)-O(4)	135.28(14)	C(9)-Zn(2)-O(3)	139.48(13)
C(7)-Zn(1)-O(1)	120.48(15)	C(9)-Zn(2)-O(6)	118.03(14)
O(4)-Zn(1)-O(1)	103.16(10)	O(3)-Zn(2)-O(6)	101.53(10)

Each zinc atom also shows a weak metal-π interaction (dotted line in Figure 2.4) with one of the flanking aryls of the *m*-terphenyl ligand (Zn(1)···centroid = 3.083; Zn(2)···centroid =3.154 Å). The sum of the van der Waals radii of zinc and benzene is 3.16 Å.[115] This is most likely the reason for the conformation of the $Zn_2O_4C_2$ core. Unlike the aluminium heterocycle in **2**, which was planar, the core of **4** is puckered into a boat-like conformation to maximize the metal-aryl contacts. Consequently, both *m*-terphenyl ligands are found on the same face of the molecule forming a hydrophobic pocket, leaving the remaining ethyl group on each zinc exposed on the opposite face.

Building on the successful use of a *m*-terphenyl carboxylate in the synthesis of a *low coordinate* metal complex, the same idea was applied to the synthesis of *low valent* metal complexes. As one moves down the periodic table, the relative stability of group 14 oxidation states changes dramatically. Carbon is almost exclusively tetravalent (with the notable exception of carbenes), while lead is mostly found as Pb(II). Tin is equally likely to be found as either +2 or +4 oxidation states.[118c,128] Tin(II), in the form of the amido stannylene $Sn[N(SiMe_3)_2]_2$ was chosen for the carboxylate studies, as it was expected to be susceptible to the same sort of protonolysis reactions as the previously studied aluminium and zinc alkyl complexes.

Surprisingly, despite the fact that stannylenes ($:SnR_2$) were first isolated[116] more than a decade before the analogous carbenes[117] (see Chapter 1) and are commercially available, stannylene chemistry has been much less explored relative to carbenes. This investigation was further motivated by observation that although tin (II) carboxylates have long been studied,[118] and are implicated in a variety of catalytic processes,[119] commercial resins,[120] and even food safety,[121] structural data is relatively rare and composed mainly, though not exclusively,[121,122] of oxalate[123] and acetate[118b,124] complexes. This is in contrast to Sn(IV) carboxylate complexes, which are extremely well characterized.[125]

Scheme 2.3 Synthesis of tin(II) carboxylate complexes $[(Me_3Si)_2NSn(\mu\text{-}O_2CAr)]$ 6-8.

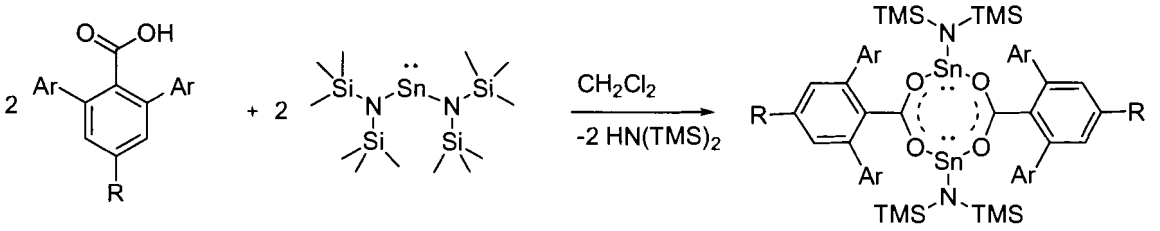

1 Ar = R = Ph
3 Ar = Mes, R = H
5 Ar = Mes, R = Me

6 Ar = R = Ph
7 Ar = Mes, R = H
8 Ar = Mes, R = Me

The *m*-terphenyl carboxylates **1** and **3**, along with a third ligand 4-methyl-2,6-bis(2,4,6-trimethylphenyl) benzoic acid **5** were treated with bis[bis(trimethylsilyl)amido] tin(II) in dichloromethane to give the tin(II) carboxylates **6-8** as colourless crystals. The ^1H NMR spectra showed a singlet at 0.09 ppm (**7**) or 0.00 (**6**, **8**) that was assigned to the 18 hydrogens of the amido trimethylsilyl groups. The distinctive singlets of the methyl groups in *m*-terphenyl ligand **7** appeared at 2.27 ppm (*para* CH_3) and 2.17 ppm (*ortho* CH_3) and showed a 1:1 ratio with the amido ligand. In **8**, the *ortho* methyls were

downfield of the *para* methyls, at 2.21 and 2.20 ppm respectively. An additional singlet for the methyl on the central ring of **8** was found at 1.98 ppm.

^{119}Sn NMR spectroscopy, which has a chemical shift range from approximately +4000 to -2500 ppm (0 ppm = $SnMe_4$), is also a useful tool for compound characterization, as the chemical shift is sensitive to the oxidation state of the tin centre, its coordination number and the type of ligands present.[126] Attempts were made, therefore, to obtain the ^{119}Sn NMR spectra of **6-8**, with mixed results. The two mesityl derivatives, **7** and **8**, showed peaks at 74 and 76 ppm respectively, but under identical conditions, no signal was observed for **6**. The absence of a signal for **6** is likely due chemical exchange caused by a rapid shift in the carboxylate bonding modes in solution.[127] The strongest absorption in the infrared spectra of the three compounds was the C=O stretch at 1544 (**6**), 1538 (**7**) or 1536 (**8**) cm^{-1}.

Figure 2.5 **Structure of $[(Me_3Si)_2NSn(\mu\text{-}O_2CC_6H_2Ph_3)]_2$ 6. Thermal ellipsoids are shown at 50% probability and hydrogen atoms and solvent molecule have been removed for clarity.**

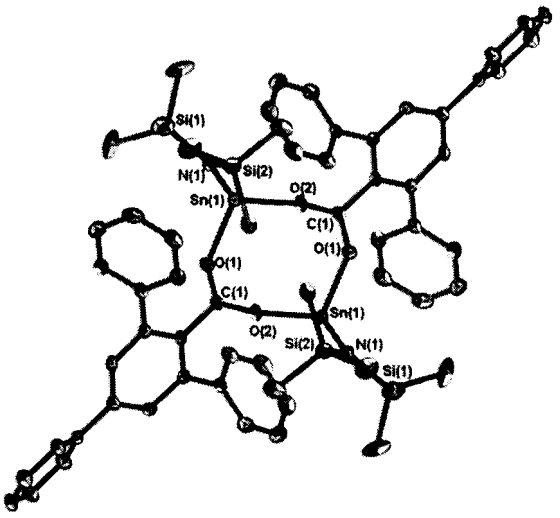

X-ray crystallographic studies* were performed on the tin complexes **6-8**, and it was found that each had the general formula $[(Me_3Si)_2NSn(\mu\text{-}O_2CAr)]\cdot CH_2Cl_2$. In **7**, the two halves of the dimer are crystallographically distinct, while in **6** and **8**, the second half is symmetry-generated. None of the tin complexes showed any significant interactions with the CH_2Cl_2 solvent of crystallization.

Figure 2.6 **Structure of $[(Me_3Si)_2NSn(\mu\text{-}O_2CC_6H_3Mes_2)]_2$ 7. Thermal ellipsoids are shown at 50% probability and hydrogen atoms and solvent molecule have been removed for clarity.**

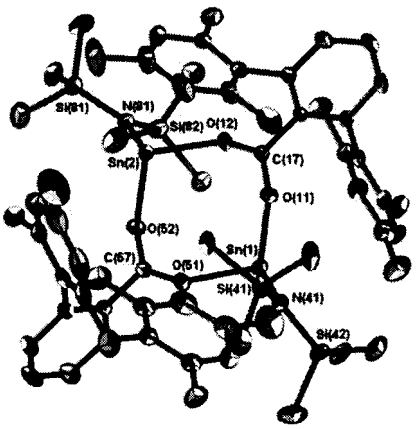

Figure 2.7 **Structure of $[(Me_3Si)_2NSn(\mu\text{-}O_2CC_6H_2Mes_2Me)]_2$ 8. Thermal ellipsoids are shown at 50% probability and hydrogen atoms and solvent molecule have been removed for clarity.**

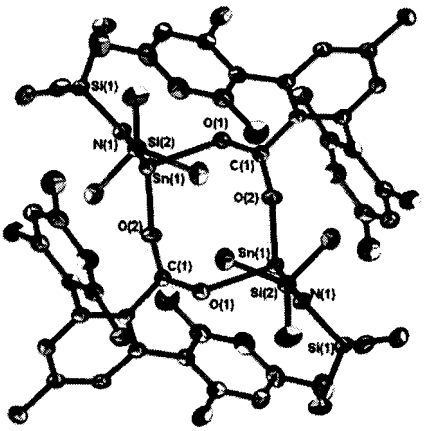

* Structures of **6** and **8** solved by Diane Dickie, structure of **7** solved by Dr. Gabriele Schatte, Saskatchewan Structural Sciences Centre.

Table 2.3 Selected structural data for tin complexes [$(Me_3Si)_2NSn(\mu\text{-}O_2CAr)$] 6-8.

Selected bond lengths (Å)					
6 (Ar = R = Ph)		**7** (Ar = Mes, R = H)		**8** (Ar = Mes, R = Me)	
Sn(1)-O(1)	2.243(2)	Sn(1)-O(11)	2.2175(16)	Sn(1)-O(1)	2.240(4)
		Sn(1)-O(51)	2.2194(18)		
Sn(1)-O(2)	2.199(2)	Sn(2)-O(12)	2.2222(17)	Sn(1)-O(2)	2.208(4)
		Sn(2)-O(52)	2.2407(16)		
O(1)-C(1)	1.262(3)	O(11)-C(17)	1.267(3)	O(1)-C(1)	1.257(7)
		O(12)-C(17)	1.264(3)		
O(2)-C(1)	1.259(4)	O(51)-C(57)	1.258(3)	O(2)-C(1)	1.259(7)
		O(52)-C(57)	1.263(3)		
Sn(1)-N(1)	2.072(2)	Sn(1)-N(41)	2.090(2)	Sn(1)-N(1)	2.093(5)
		Sn(2)-N(81)	2.087(2)		
Si(1)-N(1)	1.734(3)	Si(41)-N(41)	1.738(2)	Si(1)-N(1)	1.729(5)
		Si(42)-N(41)	1.733(2)		
Si(2)-N(2)	1.727(3)	Si(81)-N(81)	1.735(2)	Si(2)-N(2)	1.737(5)
		Si(82)-N(81)	1.742(2)		
Sn(1)···Sn(1)	4.397	Sn(1)···Sn(2)	4.411	Sn(1)···Sn(1)	4.557
Bond Angles (°)					
O(1)-Sn(1)-O(2)	96.63(8)	O(11)-Sn(1)-O(51)	100.44(7)	O(1)-Sn(1)-O(2)	98.15(15)
		O(12)-Sn(2)-O(52)	99.91(6)		
N(1)-Sn(1)-O(1)	90.97(9)	N(41)-Sn(1)-O(11)	90.63(7)	N(1)-Sn(1)-O(1)	91.53(17)
		N(41)-Sn(1)-O(51)	89.79(8)		
N(1)-Sn(1)-O(2)	90.08(9)	N(81)-Sn(2)-O(12)	91.90(7)	N(1)-Sn(1)-O(2)	89.53(17)
		N(81)-Sn(2)-O(52)	90.42(7)		
Si(1)-N(1)-Si(2)	122.61(15)	Si(41)-N(41)-Si(42)	121.48(12)	Si(1)-N(1)-Si(2)	120.3(3)
Si(1)-N(1)-Sn(1)	113.18(13)	Si(41)-N(41)-Sn(1)	123.94(11)	Si(1)-N(1)-Sn(1)	116.1(3)
Si(2)-N(1)-Sn(1)	123.93(14)	Si(42)-N(41)-Sn(1)	114.58(12)	Si(2)-N(1)-Sn(1)	123.3(3)
		Si(81)-N(81)-Si(82)	120.14(12)		
		Si(81)-N(81)-Sn(2)	115.14(12)		
		Si(82)-N(81)-Sn(2)	124.72(11)		

In **6-8**, all the tin atoms are tri-coordinate with a stereochemically active lone pair of electrons. The tin atoms exhibit trigonal pyramidal geometry, with the N-Sn-O bond angles ranging from 89.53(17)-91.90(7)°, while the O-Sn-O angles of the bridging carboxylate are 96.63(8)-100.44(7)°. This is the most common geometry for divalent tin, and the angles observed here are consistent with literature values.[128] The nitrogen atoms, on the other hand, are trigonal planar, with $\Sigma\angle$ N = 359.72° (**6**), 360.00° (**7**) and 359.7° (**8**). These observations are consistent with silylamines in general,[129] and Sn(II) complexes of $N(SiMe_3)_2$ specifically.[130]

As with the aluminium (**2**) and zinc (**4**) complexes, the *m*-terphenyl carboxylate ligand bridges the tin atoms in **6-8** forming a central eight-membered heterocyclic

$Sn_2O_4C_2$ core. The C-O bonds of the carboxylate group are delocalized, with the C-O bond lengths ranging from 1.257(7) to 1.267(3) Å. The Sn-O bond lengths vary from 2.2194(18) to 2.243(2) Å. Although the $Sn_2O_4C_2$ core has not been previously observed for Sn(II) compounds, these Sn-O values fall at the shorter end of the range [2.241(7) to 2.349(7) Å] reported for Sn(IV) carboxylates (excluding clusters) showing the same $Sn_2O_4C_2$ structural motif.[131] All of these dimeric Sn(IV) carboxylate complexes had a planar $Sn_2O_4C_2$ core, similar to the $Al_2O_4C_2$ core of **2**. In contrast, the Sn(II) heterocycles **6-8** showed a chair-like conformation, presumably due to the stereochemically active lone pair on the tin atoms. In each complex, the tin atoms are separated by a Sn···Sn distance of more than 4.3 Å, much more than the 2.7 Å average of the Sn(IV) complexes.[131]

2.2 Oxidation of tin (II) complexes

To probe the reactivity of the *m*-terphenyl tin(II) carboxylates **6-8**, removal of the amido ligand was attempted. Perfluoroarylboranes [$B(C_6F_5)$] are well known for their ability to abstract alkyl groups from metals,[132] including tin,[133] and recent studies[134] have shown that $B(C_6F_5)_3 \cdot H_2O$ is an excellent Brønsted acid, with a pK_a of 8.4 in acetonitrile. For comparison, the pK_a values of HCl and H_2SO_4 in acetonitrile are 8.4 and 7.4, respectively.[134] Green[135] used this reagent in the oxidation of chromium, iron and cobalt, while Roesky[136] used this reagent to produce the first monoalumoxane from an alkylaluminium nacnac derivative (Scheme 2.4). This unusual molecule features both intramolecular Lewis base coordination, at aluminium, and intermolecular Lewis acid stabilization at oxygen. It seemed, therefore, that $B(C_6F_5)_3 \cdot H_2O$ would be an interesting

test reagent for the tin complexes, as either the water or the perfluoroarylborane fragment could potentially remove the amido ligand.

Scheme 2.4 Reaction of $H_2O{\cdot}B(C_6F_5)$ with an alkylaluminium nacnac.

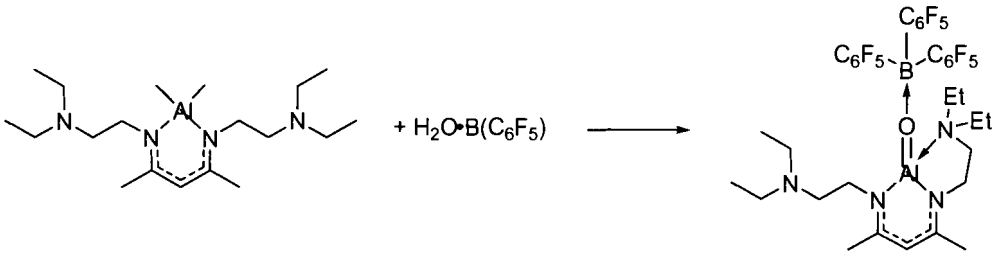

Scheme 2.5 Proposed reaction of 7 with $H_2O{\cdot}B(C_6F_5)$.

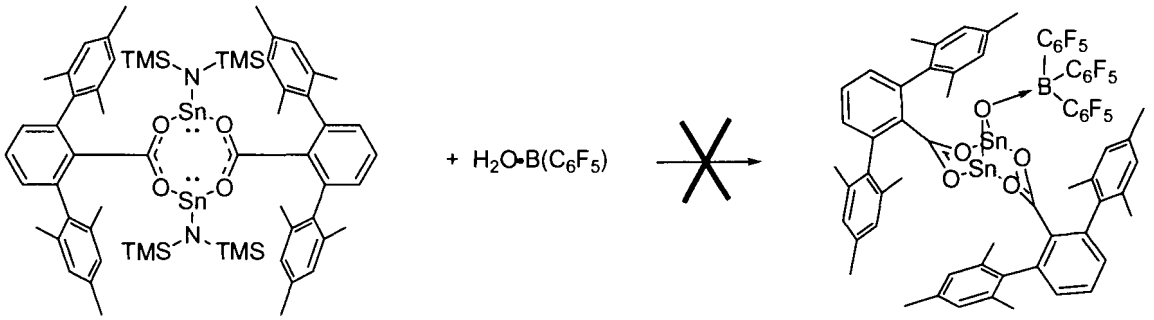

7

Addition of **7** to $H_2O{\cdot}B(C_6F_5)$ in dichloromethane followed by cooling to -30 °C led to the isolation of colourless crystals **9**. It was anticipated that the oxygen from the water would be transferred to the tin; however, this product was not obtained (Scheme 2.5).* X-ray crystallographic studies† of **9** (Figure 2.8) showed that one trimethylsilyl group from each nitrogen ligand had been lost, allowing the amido groups to act as bridging ligands between the two tin atoms. The formation of this Sn_2N_2 heterocyclic

* The nature of the byproducts of this reaction, including the fate of the $B(C_6F_5)_3$ was not determined.
† Structure of $\mathbf{9}{\cdot}CH_2Cl_2$ solved by Diane Dickie, with the assistance of Dr. Hilary Jenkins, Saint Mary's University.

core caused the *m*-terphenyl carboxylate ligands to shift from a bridging bidentate to a terminal monodentate coordination mode.

Figure 2.8 **Structure of $[(Mes_2C_6H_3CO_2)Sn(\mu\text{-}NSiMe_3)]_2$ 9, obtained from reaction with $H_2O{\cdot}B(C_6F_5)$. Thermal ellipsoids are shown at 50% probability and hydrogen atoms and solvent of crystallization have been removed for clarity.**

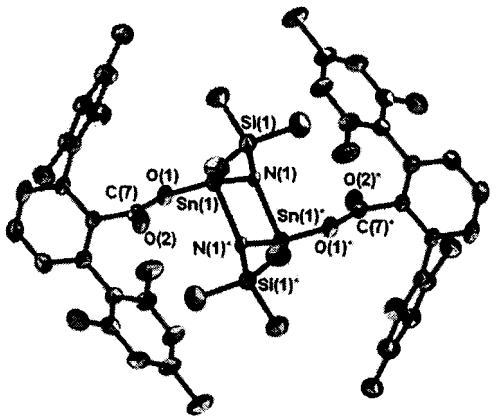

The nitrogen atoms in **9** are almost trigonal planar, with $\Sigma\angle N$ = 355.73° ($\mathbf{9}{\cdot}CH_2Cl_2$) or 354.11° ($\mathbf{9}{\cdot}Et_2O$), similar to the geometry in **7**. The tin atoms again show trigonal pyramidal geometry, however the angles in **9** are much more acute, ranging from 75.94(9) to 93.17(8)°, than they were in **7** [89.79(8) to 100.44(7)°]. These values, as well as the Sn-N and Si-N bond lengths, compare very well with those reported recently by Lappert[137] for the related Sn_2N_2 heterocycle **10a**. It featured a chloride ligand in place of the bulky *m*-terphenyl carboxylate (Figure 2.9).

Figure 2.9 **Tin-chlorine interactions in Lappert's Sn_2N_2 complex.**

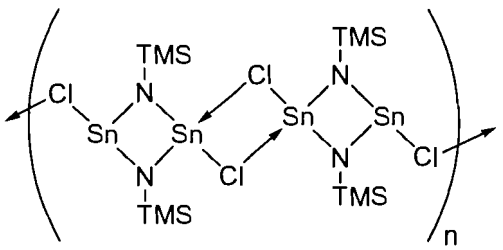

10a

The work of Lappert provided the basis for a rational synthetic route to **9**. The overnight reaction, in the absence of light, of **7** with two equivalents of silver cyanate in either anhydrous diethyl ether or dichloromethane provides **9** in good yield. The nine hydrogens of the trimethylsilyl group were assigned to the singlet at 0.11 ppm in the ^{1}H NMR spectrum, while the *ortho* and *para* methyl groups of the *m*-terphenyl ligand appeared as singlets at 2.01 and 2.27 ppm, respectively.

Scheme 2.6 Rational synthesis of $[(Mes_2C_6H_3CO_2)Sn(\mu\text{-}NSiMe_3)]_2$ 9 using silver cyanate.

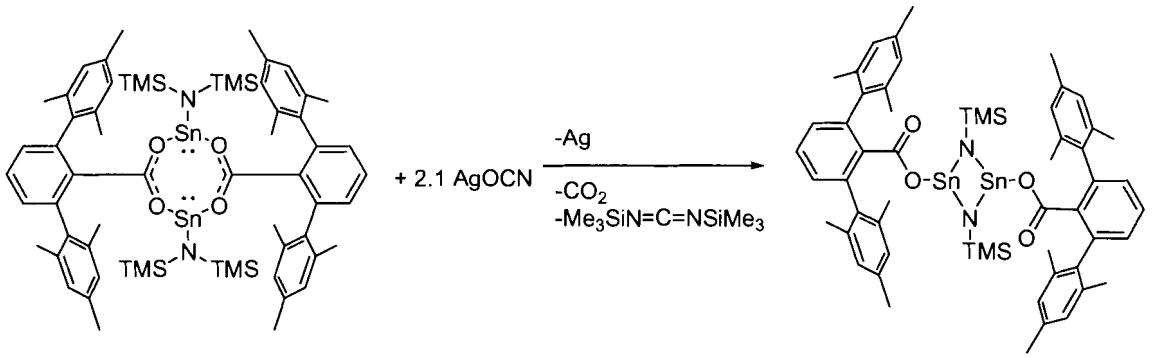

7 **9**

Numerous attempts were made to obtain the solution-state ^{119}Sn NMR spectrum of **9** but all were unsuccessful. As in **6**, this was attributed to a rapid solution-state carboxylate shift. The solid-state ^{119}Sn NMR spectrum of **9** was acquired by Dr. Guy Bernard at University of Alberta and showed the isotropic peak at -100 ppm, albeit with poor signal to noise ratio. This is somewhat different from the value of -17 ppm reported for isotropic peak in the solid state ^{119}Sn spectrum of **10a**, but within the range of values he found for the solvent-dependent solution-state ^{119}Sn chemical shifts of that molecule [-87 in C_6D_6 to -285 in C_6D_6/PhMe/$(Me_3P)_2NH$].[137] This solvent dependence is likely caused by a combination of two factors. First, **10a** shows extended Sn-Cl coordination

interactions forming infinite one-dimensional chains (Figure 2.9), which could be disrupted by solvent interactions. Since the bulky *m*-terphenyl carboxylate ligands of **9** allow it to exist as discrete molecules, this is not an issue. Second, the tin(II) centre in **10a** could be coordinating to the solvents. To confirm whether the *m*-terphenyl could also shield the tin atoms from coordinating solvents, **9** was crystallized as both the diethyl ether* and dichloromethane solvate. No interaction with the solvent was observed in the solid-state structures.

Table 2.4 Selected structural data for $[(Mes_2C_6H_3CO_2)Sn(\mu\text{-}NSiMe_3)]_2$ 9.

Bond lengths (Å)			
	9·CH_2Cl_2		**9**·Et_2O
Sn(1)-N(1)	2.194(3)	Sn(1)-N(1)	2.198(2)
Sn(1)-N(1)*	2.116(3)	Sn(1)-N(1)*	2.119(2)
Sn(1)-O(1)	2.149(3)	Sn(1)-O(1)	2.169(2)
Sn(1)···O(2)	2.628(3)	Sn(1)···O(2)	2.573(2)
N(1)-Si(1)	1.677(3)	N(1)-Si(1)	1.674(2)
O(1)-C(7)	1.286(5)	O(1)-C(7)	1.286(4)
O(2)-C(7)	1.231(5)	O(2)-C(7)	1.234(4)
Sn(1)···Sn(1)*	3.3896(5)	Sn(1)···Sn(1)*	3.404(4)
Bond angles (°)			
N(1)-Sn(1)-N(1)*	76.28(11)	N(1)-Sn(1)-N(1)*	75.94(9)
O(1)-Sn(1)-N(1)*	92.72(11)	O(1)-Sn(1)-N(1)*	93.17(8)
O(1)-Sn(1)-N(1)	81.98(10)	O(1)-Sn(1)-N(1)	81.77(8)
Sn(1)-N(1)-Sn(1)*	103.72(11)	Sn(1)-N(1)-Sn(1)*	104.06(9)
Sn(1)-N(1)-Si(1)	123.99(15)	Sn(1)-N(1)-Si(1)	123.05(12)
Sn(1)*-N(1)-Si(1)	128.02(16)	Sn(1)*-N(1)-Si(1)	127.00(12)

Symmetry transformations used to generate equivalent atoms: * -x,-y,-z+1

Much more interesting than the structural parameters of **9** is its electronic environment. With the loss of one trimethylsilyl group, the nitrogen ligand has a formal charge[138] of -2. To balance that, the tin becomes formally +3, a unusual oxidation state for group 14 atoms which usually adopt either +2 or +4 oxidation states. The result is that **9** is formally a neutral isoelectronic Sn_2N_2 analogue of a cyclobuta-1,3-dienediide anion.[139] The first such analogue to be isolated and fully characterized by spectroscopic

* Structure of **9**·Et_2O solved by Dr. Gabriele Schatte, Saskatchewan Structural Science Centre.

and X-ray crystallographic methods was a dark red P_2C_2 heterocycle reported by Niecke in 1995.[140] Several possible descriptions of the bonding in that heterocycle were proposed, and are summarized in Figure 2.10. Subsequent theoretical studies, whose details are beyond the scope of this thesis, suggest that the P_2C_2 heterocycle can not be described only as a delocalized four-centred six-π electron system **A**, but also incorporates a contribution from an open-shell singlet biradical **C**.[141] This is significant as singlet biradicals are invoked as models of bond-forming and bond-breaking processes.[142]

Figure 2.10 Lewis diagrams of alternative bonding descriptions of a P_2C_2 heterocycle. Mes* = 2,4,6-tri-*t*-butylphenyl.

A **B** **C** **D**

Biradicals or diradicals are currently defined as even-electron molecules "that have one bond less than the number permitted by the standard rules of valence",[143] "with two radical centres that act nearly independently of each other and ... normally display quite high reactivity",[144] with "a narrow separation between their highest occupied and lowest unoccupied molecular orbitals."[145] Perhaps the most simple definition is molecules "with two unpaired electrons, each of which is occupying two degenerate or nearly degenerate molecular orbitals."[146] Depending on whether the spin states of the unpaired electrons are parallel or anti-parallel, the biradicals are classified as either triplet

or singlet. Triplet states are generally more stable than singlet states, but with appropriate substituents, this preference can be reversed.[147]

Not surprisingly, given the possibility of more traditional bonding descriptions, the exact nature of nominally six-π electron, four-centered heterocylic singlet species is controversial.[145,148] Calculations and experimental results from systems isoelectronic with the P_2C_2 heterocycle, such as E_2N_2 (E = S, Se, Te),[149] B_2P_2,[143,150] or C_2P_2,[144] suggest that the biradical contribution should not be ignored. Returning to the bonding description of **9**, we must take into account the following observations on this compound: 1) obersvation of typical NMR spectroscopic studies, including solid state ^{119}Sn NMR spectroscopy; 2) lack of EPR signals; 3) its colourless nature. Taken together, this data points to a singlet ground state for **9**.

The only previous reports of group 14/15 M_2N_2 heterocycles similar to **9** came in late 2004 from Lappert[137] (M = Sn) **10a** and Power[151] (M = Ge) **10b** (Figure 2.11). Like **9**, compound **10a** produced normal multinuclear NMR spectra, was colourless and diamagnetic. It was therefore reported to best fit a delocalized pseudo six-π electron model rather than a biradical description.[137] This is contrast to what was reported for the previously described isoelectronic systems, and also what was reported for Ge_2N_2 compound **10b**. This compound was NMR active and EPR silent but other experimental evidence, such as its colour and reactivity led the authors to suggest that **10b** has germanium-centred biradicals character.[151] Extensive theoretical investigations have subsequently shown that the biradical character of **10b** is present.[152]

Figure 2.11 Isoelectronic group 14 M_2N_2 heterocycles.

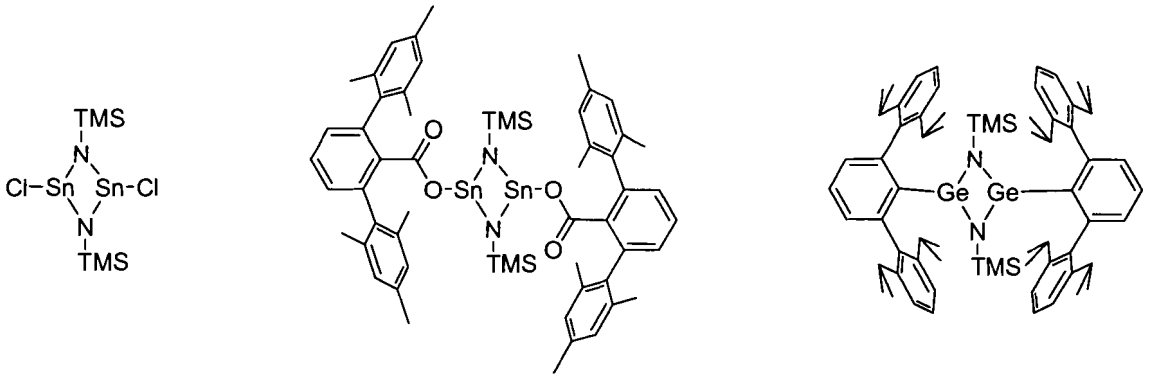

10a **9** **10b**

Preliminary B3LYP/LANL2DZ DFT calculations* using Gaussian98[153] on a model compound of **9**, with formate in place of the bulky *m*-terphenyl carboxylate ligand, have not provided a complete description of the bonding in **9**. We note that the experimental data is more consistent with the ground state singlet **10a** than the apparent biradical **10b**. It is tempting to suggest that a standard four-centred six-π electron system is at play in **9**, but this clearly oversimplifies the situation given the well-recognized poor 5p-π 2p-π overlap that would be required between the atoms.[74a] The planarity of the Sn_2N_2 core could be naively taken as evidence for extensive four-centre six-π electron delocalization within the ring, but the low inversion barrier for nitrogen as well as the steric strain imparted by the bulky ligands can easily enforce this. Additionally, planarity at nitrogen is common place for trimethylsilyl-substituted amines.[129,130] In light of this, further theoretical and experimental work is required before a definitive statement can be made about the nature of **9**, and such research is currently in progress.

During the study of the tin(II) carboxylate complexes, a second oxidation product was serendipitously encountered. Since compounds **6-9** were synthesized in and

* All calculations were done by Dr. Noham Weinberg, Simon Fraser University and University College of the Fraser Valley. Non-hydrogen atoms were restricted to their experimentally determined geometry.

recrystallized from dichloromethane, it appeared that the solvent was unreactive towards the starting tin compound, $Sn[N(SiMe_3)_2]_2$. This was in contrast to reports by Lappert and Power,[154] who used spectroscopic techniques to follow the oxidative addition of organic halides to Sn(II) amides. They found that while CH_2Cl_2 does react as shown in Scheme 2.7 to give **11**, it does so much more slowly that the bromo or iodo compounds, and also more slowly than $CHCl_3$ or CCl_4. During one synthesis of **7**, however, an excess of $Sn[N(SiMe_3)_2]_2$ was used, and oxidation product **11** was indeed isolated.

Scheme 2.7 Oxidative addition of CH_2Cl_2 to $Sn[N(SiMe_3)_2]_2$.

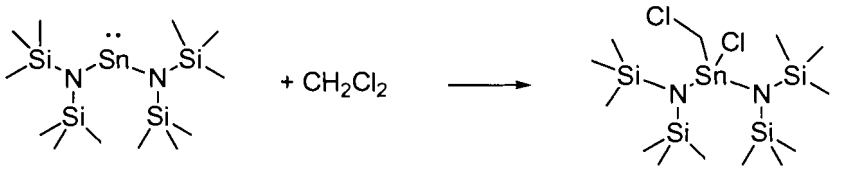

11

The identity of **11** was confirmed crystallographically and its formation was also observed during the course of ^{119}Sn NMR experiments on the *m*-terphenyl tin(II) complexes. A sample of $Sn[N(SiMe_3)_2]_2$ was dissolved in CD_2Cl_2 as a test compound for the spectroscopic studies, and was found to have a ^{119}Sn chemical shift of 763 ppm, very close to the reported value of 766 in C_6D_6.[155] As the experiment progressed, a second signal was observed growing in at -83 ppm and the solution faded from orange to colourless. This signal was assigned to **11** based on its proximity to the reported value of -82 ppm in C_6D_6.[154]

Figure 2.12 Structure of $(CH_2Cl)(Cl)Sn[N(SiMe_3)_2]_2$ 11. Thermal ellipsoids are shown at 50% probability and hydrogen atoms have been removed for clarity.

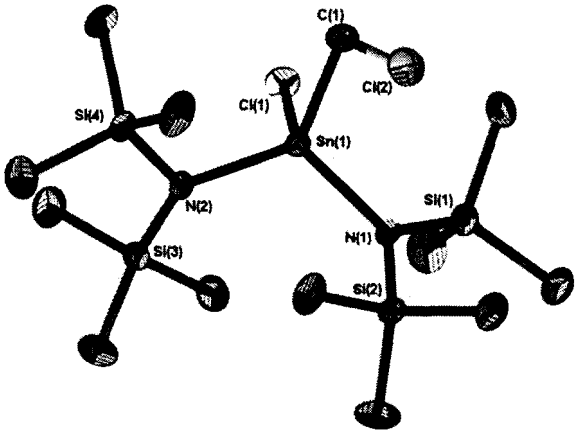

X-ray crystallographic studies,* which had not been previously reported for **11**, showed oxidative insertion of the tin atom into one of the C-Cl bonds. The geometry around tin was approximately tetrahedral, with angles ranging from 99.94(6)° [C(1)-Sn(1)-Cl(1)] to 117.81(8)° [C(1)-Sn(1)-N(2)]. There was very little change in the Sn-N or N-Si bonds of **11** compared to the tin(II) compounds **6-9**. The Sn-Cl, Sn-C and C-Cl bonds were also similar to the related $Cl_2Sn(CHCl)_2$.[156]

Table 2.5 Selected structural data for $(CH_2Cl)(Cl)Sn[N(SiMe_3)_2]_2$ 11.

Bond lengths (Å)			
Sn(1)-N(1)	2.0318(16)	N(1)-Si(1)	1.7530(17)
Sn(1)-N(2)	2.0270(17)	N(1)-Si(2)	1.7516(17)
Sn(1)-C(1)	2.160(2)	N(2)-Si(3)	1.7508(19)
Sn(1)-Cl(1)	2.3689(5)	N(2)-Si(4)	1.7574(18)
C(1)-Cl(2)	1.782(2)		
Bond angles (°)			
N(1)-Sn(1)-N(2)	116.50(7)	N(2)-Sn(1)-C(1)	117.81(8)
N(1)-Sn(1)-Cl(1)	108.49(5)	N(2)-Sn(1)-Cl(2)	102.34(5)
N(1)-Sn(1)-C(1)	109.66(8)	Cl(1)-Sn(1)-C(1)	99.94(6)

* Structure solved by Diane Dickie with the assistance of Dr. Gabriele Schatte, Saskatchewan Structural Sciences Centre.

2.3 Tetravalent group 4 and 14 *m*-terphenyl carboxylate complexes

After the unexpected results of the reactions of tin(II) with *m*-terphenyl carboxylates, these ligands were next combined with another group 14 element – silicon. Like carbon, silicon is usually tetravalent. Unlike carbon, however, silicon has a tendency to form hypervalent complexes (five or more bonds). Hypervalent disilanes are thought to possess unique electronic and optical properties, and bridging ligands like carboxylates are expected to help in the isolation of such molecules.[157] Carboxylate ligands have also been used to probe the effect of axial substitution of hypervalent silicon phthalocyanines for improving their quantum yields in optical applications.[158] Other uses for hypervalent silicon carboxylates include the study of zwitterionic silicates,[159] and as linkers in biologically active silatranes.[160] They are also used as transition state models.[161] Not all silicon carboxylates are hypervalent, of course. Standard tetravalent compounds are known, primarily in the form of silyl ester protecting groups.[162]

The hypervalent tendencies of silicon were reminiscent of transition metals, so the reaction of titanium with *m*-terphenyl carboxylates was also explored. Previous interest in titanium carboxylates has been focused on their environmental and physiological properties,[163] and as their use as alternatives to alkoxide ligands in catalysts, as they impart greater hydrolytic stability.[164] Carboxylates have long been used in commercial processes for the production of barium titanate powders[165] and other materials like thin films for optical sensors,[166] or semiconductor processing.[167] Benzoate ligands specifically are used in titanium cluster formation[168] and host-guest materials.[169] All of these applications make use of pre-formed carboxylate ligands, but titanium carboxylate

complexes have also been generated in situ by addition of carbon dioxide to alkyltitanium complexes.[170] Bifunctional carboxylates have been used as linkers for magnetic exchange between titanium(III) centres.[171]

Just as isoelectronic amidinates served as inspiration for the aluminium carboxylate study, a survey of the titanium counterparts also proved interesting. Amidinate ligands have been used to prepare alternatives to cyclopentadienyl titanium catalysts,[172] or as supporting ligands for titanium-ligand multiple bonds.[173]

The *m*-terphenyl carboxylate **3** was added to a dichloromethane solution of tetrakis(dimethylamino)silane or tetrakis(dimethylamino)titanium. Recrystallization in hexanes of the crude products of the silicon reaction gave colourless crystals **12**. In contrast, it was possible to obtain two different titanium products **13** and **13a**, both orange-red crystals, by slightly varying the reaction conditions. The ^{1}H NMR spectrum of **12** showed the expected 3:1 ratio of dimethylamino ligands to *m*-terphenyl ligands, based on a singlet of 18 hydrogens at 1.92 ppm (NMe_2) and singlets for the six *para* and 12 *ortho* methyl protons of the *m*-terphenyl at 2.15 and 1.95 ppm, respectively. This data is consistent with the formation of the desired mono-carboxylate silicon complex. The ^{1}H NMR spectrum of **13** showed the same ratios, but the signal at 2.79 ppm attributed to the dimethylamino protons was downfield of those assigned to the *para* and *ortho* *m*-terphenyl methyls at 2.26 and 2.04 ppm respectively. Titanium complex **13a**, however, showed a 1:1 ratio between the NMe_2 protons at 2.35 ppm and the *m*-terphenyl methyl groups at 2.20 (*para*) and 1.89 (*ortho*) ppm, indicating a bis(carboxylate) complex.

Scheme 2.8 Synthesis of $[(Mes_2C_6H_3CO_2)Si(NMe_2)_3]$ 12.

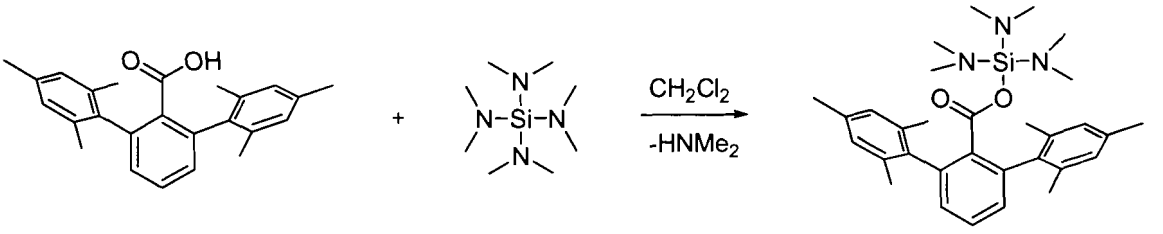

3 **12**

Scheme 2.9 Synthesis of $[(Mes_2C_6H_3CO_2)Ti(NMe_2)_3]$ 13 and $[(Mes_2C_6H_3CO_2)_2Ti(NMe_2)_2]$ 13a.

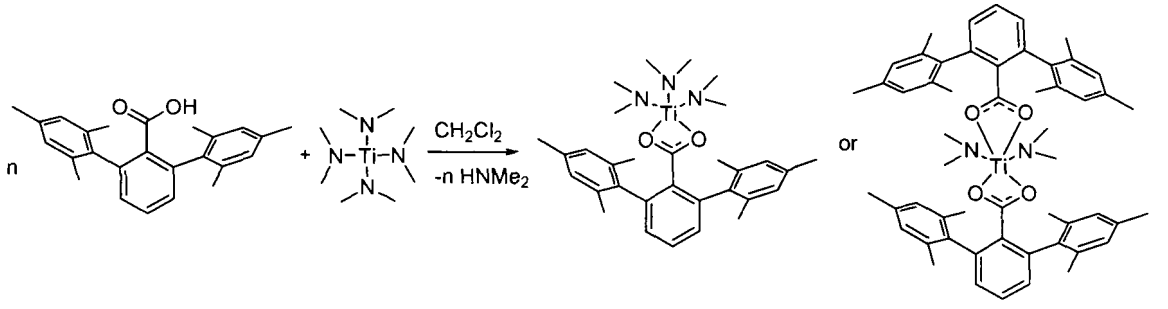

3 **13** (n = 1) **13a** (n = 2)

Further differences between the three compounds were noted in their IR spectra. There was a strong C=O stretch at 1717 cm^{-1} in the spectrum of silicon complex **12**, indicative of terminal monodentate binding by the carboxylate. The spectrum of the mono-carboxylate **13**, which might be expected to be similar to **12** based on the ligand stoichiometry, instead showed only a very weak C=O stretch at 1731 cm^{-1}. The major absorption was at 1520 cm^{-1}, suggesting chelation rather than monodentate carboxylate coordination. The IR spectrum of **13a** was very similar, with the strongest absorption at 1521 cm^{-1}.

Figure 2.13 Structure of $[(Mes_2C_6H_3CO_2)Si(NMe_2)_3]$ 12. Thermal ellipsoids are shown at 50% probability and hydrogen atoms have been removed for clarity.

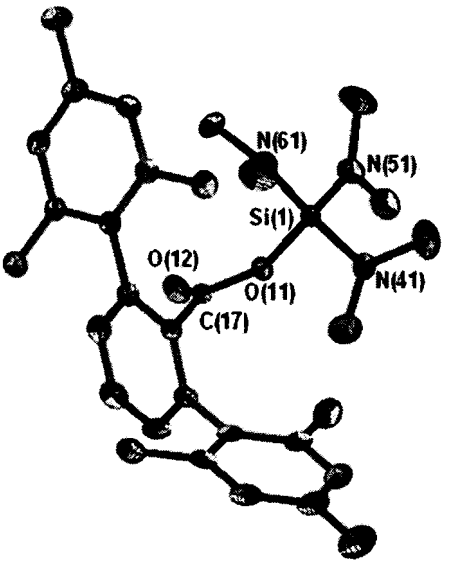

To confirm that the carboxylate binding in **12** and **13** was different despite the similarities in their formulae, and that the coordination was the same in **13** and **13a** with very different compositions, X-ray crystallographic studies were performed* and found to be in excellent agreement with the infrared data. There are distinct C-O and C=O bonds [1.341(3) and 1.188(3) Å, respectively] in the silicon complex **12** (Figure 2.13). The Si(1)-O(1) bond measures 1.6946(19) Å, while the second oxygen is separated from the silicon atom by nearly twice that distance, 3.096 Å. While this is within the sum of the van der Waals radii of silicon and oxygen (3.62 Å), it seems unlikely that any realistic bonding interaction is present. Neither the oxygen nor the silicon interacted with neighbouring molecules, likely due to steric constraints.

* Silicon structure **12** solved by Dr. Gabriele Schatte, Saskatchewan Structural Sciences Centre. Titanium structures **13** and **13a** solved by Diane Dickie.

Figure 2.14 Structure of the $[(Mes_2C_6H_3CO_2)Ti(NMe_2)_3]$ 13. Thermal ellipsoids are shown at 50% probability and hydrogen atoms have been removed for clarity.

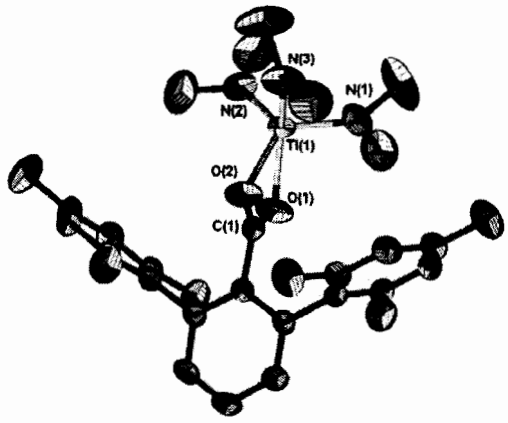

Evidence of carboxylate chelation in **13** (Figure 2.14) is given by the equal C-O bond lengths of 1.244 Å, and similar Ti-O distances of 2.138(3) and 2.198(3) Å. The situation is more mixed in **13a** (Figure 2.15). The C-O bonds range from 1.257(4) to 1.285(4) Å, all somewhat longer than in **13**, but certainly not different enough from one another to be considered distinct C-O and C=O bonds. The Ti-O bonds in **13a** indicate a more asymmetric chelation than in **13**. One pair has Ti-O distances of 2.202(2) and 2.066(2) Å [O(1) and O(2)] while the other measures 2.084(3) and 2.182(2) Å. The longer Ti-O bonds in each pair correlate with the shorter C-O bonds.

Figure 2.15 Structure of the$[(Mes_2C_6H_3CO_2)_2Ti(NMe_2)_2]$ 13a. Thermal ellipsoids are shown at 50% probability and hydrogen atoms and solvent molecule have been removed for clarity.

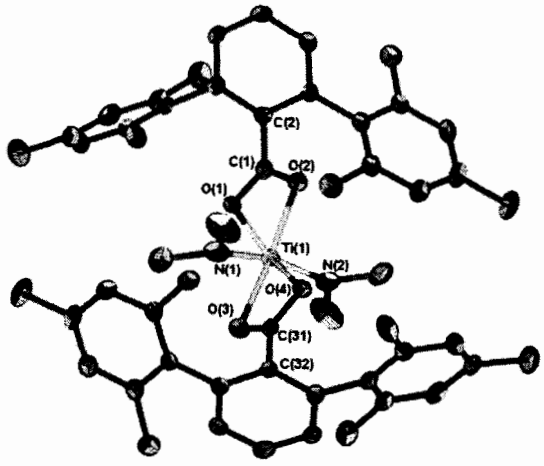

Within experimental error, the three Si-N bonds of **12** were all equal, with an average value of 1.69 Å that falls in between the values for the Si-N bonds in the $Sn_2O_4C_4$ heterocycles **6-8** and the Sn_2N_2 complex **9**. The Ti-N bonds of **13a** are also the same within experimental error, at 1.866(3) and 1.869(3) Å. The bonds in **13** show more variability, but all are within the range of literature values for titanium complexes with at least two dimethylamino ligands [1.838(2)[174] to 2.19(3)[175] Å].

Table 2.6 Selected structural data for $[(Mes_2C_6H_3CO_2)Si(NMe_2)_3]$ 12, $[(Mes_2C_6H_3CO_2)Ti(NMe_2)_3]$ 13 and $[(Mes_2C_6H_3CO_2)_2Ti(NMe_2)_2]$ 13a.

Bond lengths (Å)					
$[(Mes_2C_6H_3CO_2)Si(NMe_2)_3]$ 12		**$[(Mes_2C_6H_3CO_2)Ti(NMe_2)_3]$ 13**		**$[(Mes_2C_6H_3CO_2)_2Ti(NMe_2)_2]$ 13a**	
Si(1)-N(41)	1.695(3)	Ti(1)-N(1)	1.912(4)	Ti(1)-N(1)	1.866(3)
Si(1)-N(51)	1.692(3)	Ti(1)-N(2)	1.868(4)	Ti(1)-N(2)	1.869(3)
Si(1)-N(61)	1.690(2)	Ti(1)-N(3)	1.871(4)	Ti(1)-O(1)	2.202(2)
Si(1)-O(11)	1.6946(19)	Ti(1)-O(1)	2.138(3)	Ti(1)-O(2)	2.066(2)
Si(1)···O(12)	3.096	Ti(1)-O(2)	2.198(3)	Ti(1)-O(3)	2.084(3)
O(11)-C(17)	1.341(3)	O(1)-C(1)	1.245(4)	Ti(1)-O(4)	2.182(2)
O(12)-C(17)	1.188(3)	O(2)-C(1)	1.243(4)	O(1)-C(1)	1.265(4)
				O(2)-C(1)	1.283(4)
				O(3)-C(31)	1.285(4)
				O(4)-C(31)	1.257(4)
Bond angles (°)					
N(41)-Si(1)-N(51)	111.71(14)	N(1)-Ti(1)-N(2)	105.39(18)	N(1)-Ti(1)-N(2)	104.77(16)
N(41)-Si(1)-N(61)	113.99(14)	N(1)-Ti(1)-N(3)	99.1(2)	N(1)-Ti(1)-O(1)	93.39(13)
N(51)-Si(1)-N(61)	109.31(13)	N(2)-Ti(1)-N(3)	104.24(19)	N(1)-Ti(1)-O(2)	102.33(13)
O(11)-Si(1)-N(41)	104.97(12)	O(1)-Ti(1)-N(1)	92.41(16)	N(1)-Ti(1)-O(3)	92.06(13)
O(11)-Si(1)-N(51)	103.52(11)	O(1)-Ti(1)-N(2)	99.11(15)	N(1)-Ti(1)-O(4)	150.99(13)
O(11)-Si(1)-N(61)	112.82(11)	O(1)-Ti(1)-N(3)	150.09(16)	N(2)-Ti(1)-O(1)	152.80(13)
		O(2)-Ti(1)-N(1)	128.52(16)	N(2)-Ti(1)-O(2)	94.45(12)
		O(2)-Ti(1)-N(2)	119.84(16)	N(2)-Ti(1)-O(3)	101.90(13)
		O(2)-Ti(1)-N(3)	92.78(17)	N(2)-Ti(1)-O(4)	92.44(13)
				O(1)-Ti(1)-O(2)	61.48(9)
				O(1)-Ti(1)-O(3)	97.41(10)
				O(1)-Ti(1)-O(4)	80.25(9)
				O(2)-Ti(1)-O(3)	154.74(10)
				O(2)-Ti(1)-O(4)	99.35(10)
				O(3)-Ti(1)-O(4)	61.19(9)

2.4 Summary and conclusions

m-Terphenyl carboxylates were found to be versatile ligands for both transition metals and main group elements, as exemplified by the eight complexes described in this

chapter. At least one example of each of the three common coordination modes for carboxylate ligands was observed, namely bridging bidentate (**2, 4, 6, 7, 8**), terminal monodentate (**9, 12**) and chelate (**13** and **13a**). Tin complexes **7** and **9** showed that it was possible to switch from one mode to the other during the course of a redox reaction, a trait that bodes well for eventual catalytic applications. Tin complex **11** also showed that not all solvents are innocent and can react in undesired ways, an important point for future synthetic studies of low-valent compounds.

The series of tin(II) complexes **6-8** demonstrated that small variations in the steric demands of the *m*-terphenyl ligands do not have an effect on the metal coordination mode. The nature of the metal has a much bigger effect. Despite the fact that they have identical ligand sets of one *m*-terphenyl carboxylate **3** and three NMe_2 groups, silicon complex **12** and titanium complex **13** show different coordination modes (Si = monodentate, Ti = chelate). Both titanium complexes **13** and **13a** show the same mode with different ligand sets. The effect of the metal is also evident in the different conformations of the $M_2O_4C_2$ core in **2** (Al, planar), **4** (Zn, boat) and **6-8** (Sn, chair), although direct comparisons are not as valid, as only **2** and **6**, and **4** and **7** had the same *m*-terphenyl ligand. The ancillary ligands also varied from aluminium (Me) to zinc (Et) to tin ($NTMS_2$).

Additionally, work in this chapter provides support to the hypothesis that *m*-terphenyl carboxylates are able to support unusual metal coordination environments. Specifically, the zinc complex **4** was a rare example of a tri-coordinate zinc centre. In the solid state, the low-coordinate metal is supported by an additional Zn-π interaction with one flanking aryl of the *m*-terphenyl ligand, but the ^{1}H and ^{13}C NMR spectra provide no

evidence for the persistence of this interaction in solution. The other, more striking example of unusual coordination was provided by the Sn_2N_2 heterocycle **9**. This molecule, in which the tin had a formal oxidation state of +3, raised many questions about the nature of the bonding in this potentially biradicaloid species, most of which have not yet been answered.

2.5 Future work

Each of the metal complexes described in this chapter could provide the basis for a variety of new studies. Jordan's work on dialkylaluminium complexes of monoanionic, bidentate nitrogen ligands[176] suggests that the aluminium complex **2** should be tested for its catalytic potential. Upon methyl abstraction to give a cationic aluminium complex, they found very different reactivity patterns towards ethylene monomers depending upon the nature of the ligand, so the behaviour of **2** and its related derivatives with the *m*-terphenyl carboxylate ligands **3** and **5**, if prepared, is not readily predictable.

Similarly, Coates et al. found that zinc-nacnac complexes were generally quite active towards the copolymerization of epoxides and carbon dioxides, but that this activity was sensitive to the steric demands of the nacnac ligands.[177] The zinc carboxylate complex **4** and its possible derivatives with ligands **1** and **5**, should be tested to see if a similar pattern is observed. Studies by Bochmann[178] have shown that alkylzinc complexes can undergo ligand exchange reactions, β-hydride abstraction and ion-pair formation upon reaction with $B(C_6F_5)_3$ or its salts, so if this is chosen as the activator for the polymerization studies, it should be tested with **4** beforehand to see how it behaves. Alternatively, attempts could be made to replace the ethyl group of **4** with a more air and moisture stable ligand in order to explore the possibility of using it as a model

compounds for zinc enzymes. There are a variety of reports describing enzyme active sites currently of interest in the literature that feature two bridged zinc atoms separated by 3.0 to 3.5 Å combined with carboxylate ligands.[179]

Metal-amide bonds are generally susceptible to CO_2 insertion reactions,[180] and the groups of Sita[181] and Kemp[182] have studied Sn(II) amides specifically. Since CO_2 is presumed to be one of the by-products generated during the formation of tin complex **9** and no insertion reaction was observed, this raises questions about the reactivity of the tin-amide bonds in **6-9** that should be further explored. Attempts should also be made to identify the mechanism of formation of **9** from both the intentional AgOCN and serendipitous $H_2O{\cdot}B(C_6F_5)_3$ reactions. Further redox reactions of the $Sn_2O_4C_2$ heterocycles **6-8** should be examined to see if it is possible to generate other Sn(III) or even Sn(IV) carboxylates from the Sn(II) precursors. Radical-type reactions of **9** should be studied to see if this Sn_2N_2 can address the question of whether it is accurately described as biradicaloid despite its apparent diamagnetic nature. Variable temperature ^{119}Sn NMR studies should be performed to obtain a better understanding of the solution state bonding in **6-9**. Mössbauer spectroscopy would also be informative in that regard.

The most attractive possibility for the silicon carboxylate **12** is that it could produce a stable silylium cation upon abstraction of one of the dimethylamino ligands, perhaps upon reaction with $B(C_6F_5)_3$. Isolated silylium cations were first identified in 2002 but have been the subject of intense interest for much longer.[183] The *m*-terphenyl carboxylate ligands should be bulky enough to prevent ion-pairing interactions, and the ability of the carboxylate group to shift from the monodentate coordination found in **12** to chelate coordination similar to **13** could help stabilize the positive charge on the silicon.

Silanones ($R_2Si=O$) are another class of silicon compounds that have proven difficult if not impossible to isolate experimentally despite their proposed existence from theoretical calculations.[184] If the reaction of **13** with $H_2O{\cdot}B(C_6F_5)_3$ were to proceed analogously to Roesky's alumoxane,[136] this ephemeral molecule might finally be readily accessible.

Future studies proposed for the titanium complexes **13** and **13a** are related to those already described for **2**, **4**, and **6-9**. First, the work of Schafer[185] on sterically restricted titanium amidate complexes suggests that **13/13a** should be tested as hydroamination catalysts. Alternatively, Cotton, Cummins and Murillo[186] have recently found that exposing sterically hindered titanium amide complexes to CO_2 results in the expected insertion into the Ti-N bonds, but with unexpected magnetic properties and unprecedented structures. Since the *m*-terphenyl ligand of **13** changes the placement of the steric demands, locating it further from the metal than in Cotton's compounds, it could cause the complex to behave quite differently. The two *m*-terphenyls on **13a** would be expected to have an even greater effect on its reactivity.

2.6 Experimental

2.6.1 General experimental

A nitrogen-atmosphere MBraun UL-99-245 dry box and standard Schlenk techniques on a double manifold vacuum line were used in the manipulation of air and moisture sensitive compounds. Solution-state NMR spectra were recorded in five millimetre tubes at Simon Fraser University on a Bruker AMX 400 or 600 MHz spectrometers or Varian AS 400 or 500 MHz spectrometers, or at Dalhousie University by Dr. Mike Lumsden on a Bruker Avance 500 MHz spectrometer. Chemical shifts are

reported in parts per million (ppm) downfield from $SiMe_4$ (^1H and ^{13}C), $BF_3 \cdot Et_2O$ (^{11}B) or $SnMe_4$ (^{119}Sn). ^1H and ^{13}C spectra are calibrated to the residual signal of the solvent. ^{11}B and ^{119}Sn spectra are calibrated to the external $BF_3 \cdot Et_2O$ or $SnMe_4$ standard. Solid-state ^{119}Sn NMR spectra were recorded by Dr. Guy Bernard at University of Alberta on a Bruker Avance 500 NMR spectrometer, operating at a frequency of 186.6 MHz for ^{119}Sn with ramped CP/MAS (cross-polarization, with magic angle spinning) and TPPM (two-pulse phase modulated) decoupling. The MAS frequencies were 6 and 11 kHz, the contact time was 7 ms, the recycle delay was 3 s and 29168 transients were co-added.

Infrared spectra were obtained using a Bomem MB spectrometer with the % transmittance values reported in cm^{-1}. Melting points were measured using a Mel-Temp apparatus and are uncorrected. Elemental analyses were obtained at Simon Fraser University by Mr. M. K. Yang on a Carlo Erba Model 1106 CHN analyzer. High-resolution mass spectra were obtained at University of Victoria by Dr. David McGillivray on a Kratos Concept IH mass spectrometer with EI ionization and were referenced to perfluorokerosene. Thermogravimetric analyses were obtained from a Shimadzu TGA-50 instrument under ambient conditions at a heating rate of 3 °C/minute.

Anhydrous solvents were obtained from an MBraun Solvent Purification system, or were purchased from Aldrich and used without further purification. All other reagents and solvents were purchased from commercial sources including Aldrich, Strem and Gelest, and used without further purification, except deuterated solvents for NMR experiments on air- and/or moisture-sensitive compounds, which were dried over P_2O_5 and distilled prior to use.

2.6.2 Crystallographic studies

Data for all X-ray crystallographic studies was collected by either Dr. Michael C. Jennings at the University of Western Ontario, Dr. Gabriele Schatte at the Saskatchewan Structural Science Centre, or Dr. Hilary A. Jenkins at Saint Mary's University. The structures were solved by the people indicated in the appendix tables and the footnotes in the thesis text. All figures were generated using X-SEED.[187]

University of Western Ontario X-ray data collection: The crystal was mounted on a glass fibre. Data were collected at the temperature indicated in the appendix on a Nonius Kappa-CCD diffractometer with COLLECT.[188] The unit cell parameters were calculated and refined from the full data set. Crystal cell refinement and data reduction were carried out using DENZO.[189] The data were scaled using SCALEPACK.[189] The SHELXTL-NT V6.1 suite of programs[190] was used to solve the structure by direct methods. Subsequent difference Fourier transformations allowed the remaining atoms to be located. All of the non-hydrogen atoms were refined with anisotropic thermal parameters. The hydrogen atom positions were calculated geometrically and were included as riding on their respective heavy atoms, unless otherwise indicated in the text.

Saskatchewan Structural Sciences Centre X-ray data collection: The crystal was coated with oil (Paratone 8277, Exxon), was collected on top of the nylon fibre of a CryoLoop™ (diameter of the nylon fibre: 10 microns; loop diameter 0.2-0.3 mm; Hampton Research, USA) that had previously been attached using epoxy to a metallic pin. All measurements were made on a Nonius Kappa CCD 4-Circle Kappa FR540C diffractometer using monochromated Mo K_α radiation (λ = 0.71073 Å) at the temperature

indicated in the appendix. Cell parameters were initially retrieved using the COLLECT[188] software, and refined with the HKL DENZO and SCALEPACK software,[189] that was also used for data reduction. The structure was solved using direct methods using SIR-97[191] and refined by full-matrix least-squares method on F^2 with SHELXL97-2.[192] The non-hydrogen atoms were refined anisotropically. Hydrogen atoms were included at geometrically idealized positions and were not refined, unless otherwise indicated in the text. The isotropic thermal parameters of the hydrogen atoms were fixed at 1.2 times that of the preceding carbon atom.

Saint Mary's University X-ray data collection: The crystal was mounted on a glass fibre and centred on a Siemens 1K SMART/CCD diffractometer. Data were collected at the temperature indicated in the appendix using Mo(Kα) radiation. Lorentz and polarization corrections were applied and data were corrected for absorption using redundant data and the SADABS program. Direct methods and Fourier techniques were used to solve the crystal structures. Refinement was conducted using full-matrix least-squares calculations and SHELX-TL PC V 5.03. All non-hydrogen atoms were refined with anisotropic displacement parameters. Hydrogen atoms were treated as riding models and were updated after each refinement.

2.6.3 Synthesis of carboxylate ligands

2,4,6-Triphenylbenzoic acid (1): Prepared according to a variation of literature procedures.[38a,109] Under an inert atmosphere, *n*-BuLi (20 mL, 1.6M in hexanes) was added dropwise to a suspension of 2,4,6-triphenylbromobenzene (10.0 g, 26.0 mmol) in ca. 100 mL anhydrous Et_2O. The mixture was allowed to stir for 3.5 h and then CO_2 was bubbled through the solution for 1.5 h. The reaction was quenched with H_2O and dilute

(ca. 1 M) HCl, then extracted with Et_2O. The combined organic fractions were dried over $MgSO_4$ and the solvent was removed under vacuum to give a yellow powder that was recrystallized from CH_2Cl_2. Slow evaporation of the CH_2Cl_2 solution resulted in a white powder. Yield: 6.07 g (67%), mp = 259-260 °C (lit. 253-255 °C). ^1H NMR (CD_2Cl_2, 499.768 MHz) δ 7.70 (d, J = 7 Hz, 2H), 7.66 (s, 2H), 7.40-7.51 (m, 13H). IR (nujol mull) ν 1696 (vs), 1597 (m), 1575 (w), 1561 (w), 1493 (m), 1445 (m), 1399 (w), 1293 (s), 1133 (w), 1076 (w), 886 (w), 777 (s), 765 (m), 699 (vs).

2,6-bis(2,4,6-Trimethylphenyl)benzoic acid[193] (3): Prepared according to the same procedure as **1**, beginning with 2,6-bis(2,4,6-trimethylphenyl)iodobenzene (5.0 g, 11.4 mmol). The crude product was recrystallized from Et_2O to give a white powder. Yield: 3.17 g (78%), mp = 292-295 °C. ^1H NMR ($CDCl_3$, 400.136 MHz) δ 7.47 (t, J = 7.5 Hz, 1H), 7.08 (d, J = 7.5 Hz, 2 H), 6.97 (s, 4H), 2.36 (s, 6 H), 1.99 (s, 12 H). $^{13}C\{^1H\}$ ($CDCl_3$, 125.680 MHz) δ 136.7, 128.5, 128.0, 31.2, 20.6 (quaternary carbons not observed). IR (nujol mull) ν 3208 (br), 1733 (vs), 1705 (s), 1611 (m), 1577 (m), 1365 (s), 1216 (vs), 1127 (m), 844 (m), 820 (m), 799 (m), 791 (m), 688 (m). Anal Calcd for $C_{25}H_{26}O_2$: C, 83.76; H, 7.31. Found: C, 83.41; H, 7.57.

4-Methyl-2,6-bis(2,4,6-trimethylphenyl)benzoic acid (5): Prepared according to the same procedure as **1**, beginning with 4-methyl-2,6-bis(2,4,6-trimethylphenyl) iodobenzene (3.00 g, 6.61 mmol). The crude product was recrystallized from hexanes to give a white powder. Yield = 0.90 g (37 %), mp = 257-259 °C. ^1H NMR (C_6D_6, 499.767 MHz) δ 6.86 (s, 4H), 6.73 (s, 2H), 2.20 (s, 12H), 2.19 (s, 6H), 2.03 (s, 3H). $^{13}C\{^1H\}$ ($CDCl_3$, 125.679 MHz) δ 169.5, 140.4, 139.6, 137.0, 136.9, 136.5, 130.0, 129.2, 127.9, 21.4, 20.7, 20.6. IR (nujol mull) ν 3208 (br), 1731 (vs), 1699 (m), 1613 (m), 1597 (w),

1573 (w), 1224 (vs), 1186 (m), 1160 (m), 1110 (s), 864 (m), 844 (s), 831 (m), 768 (m). Anal Calcd for $C_{26}H_{28}O_2$: C, 83.83; H, 7.58. Found: C, 83.67; H, 7.49.

2.6.4 Synthesis of metal complexes

$[Me_2Al(\mu\text{-}O_2CC_6H_2(Ph_3)]_2$ (2): Under an inert atmosphere, $AlMe_3$ (0.34 mL, 2.0 M in toluene) was added to a suspension of 2,4,6-triphenylbenzoic acid **1** (0.20 g, 0.57 mmol) in 10 mL anhydrous CH_2Cl_2. Colourless crystals formed upon slow evaporation of the solvent. Additional crystals formed upon cooling the solution to –30 °C. Yield = 0.15 g (64%), mp 265-266 °C. ^1H NMR (CD_2Cl_2, 499.771 MHz) δ 7.61 (s, 2 H), 7.37-7.49 (m, 15 H), -1.51 (s, 6 H); $^{13}C\{^1H\}$ NMR (CD_2Cl_2, 125.679 MHz) δ 174.7, 142.9, 141.8, 140.5, 139.7, 131.7, 129.2, 128.9, 128.5, 128.4, 128.3, 128.1, 127.4, -12.4. IR (nujol mull) v 1624 (vs), 1598 (vs), 1503 (s), 1418 (s), 1262 (w), 1200 (s), 1192 (s), 1030 (m), 892 (s), 805 (m), 756 (s), 698 (vs). Anal. Calcd. for $C_{54}H_{48}Al_2O_4$: C, 79.59; H, 5.94. Found: C, 79.44; H, 5.71.

$[EtZn(\mu\text{-}O_2CC_6H_3Mes_2)]_2$ (4): Under an inert atmosphere, 2,6-bis(2,4,6-trimethylphenyl)benzoic acid **3** (1.00 g, 2.8 mmol) was suspended in 25 mL anhydrous CH_2Cl_2. To this unstirred solution, $ZnEt_2$ (3.3 mL, 1.0M in hexanes) was added dropwise. Once the evolution of gas had ceased, the reaction was left to sit at r.t. for 1 h to allow a small amount of insoluble white powder to settle. The clear solution was decanted and concentrated to ca. 5 mL. Colourless block-like crystals formed upon cooling to -30 °C. Yield = 0.68 g (54%), mp >350 °C. ^1H NMR (C_6D_6, 400.136 MHz) δ 7.14 (t, J = 7 Hz, 1H), 6.90 (d, J = 7 Hz, 2H), 6.89 (s, 4H), 2.32 (s, 6H), 2.15 (s, 12H), 1.28 (t, J = 8 Hz, 3H), 0.07 (q, J = 8 Hz, 2H). $^{13}C\{^1H\}$ (C_6D_6, 125.680 MHz) δ 180.5,

142.9, 140.3, 137.5, 136.5, 131.7, 130.3, 129.6, 129.2, 22.3, 21.9, 13.0, 0.001. IR (nujol mull) ν 1612 (w), 1586 (m), 1551 (s), 1521 (w), 1276 (w), 852 (m), 786 (w), 743 (w), 710 (w). Anal. Calcd for $C_{54}H_{62}O_4Zn_2$: C, 71.60; H, 6.90. Found: C, 71.43; H, 6.63.

$[(Me_3Si)_2NSn(\mu\text{-}O_2CC_6H_2Ph_3)]_2$ (6): Under an inert atmosphere, a solution of $Sn[N(SiMe_3)_2]_2$ (1.38 g, 3.14 mmol) in 5 mL anhydrous CH_2Cl_2 was added dropwise to a stirring suspension of 2,4,6-triphenylbenzoic acid **1** (1.00 g, 2.85 mmol). After 1.5 h, the solution was decanted from a brown precipitate that was recrystallized from warm hexanes to give colourless crystals. Yield = 0.59 g (32%), mp = 242-247 °C (dec.). ^1H NMR (CD_2Cl_2, 499.767 MHz) δ 7.69 (d, J = 7.6 Hz, 2H), 7.57 (s, 2H), 7.39-7.49 (m, 13H), 0.00 (s, 18H). ^{13}C NMR{^1H} (CD_2Cl_2, 125.678 MHz) δ 141.0, 139.9, 129.2, 128.9, 128.8, 127.9, 127.7, 127.2, 5.3 (quaternary carbons not observed). IR (nujol mull) ν 3083 (w), 3058 (w), 3034 (w), 1595 (s), 1583 (m), 1567 (vs), 1544 (vs), 1503 (s), 1496 (s), 1439 (s), 1346 (m), 1262 (m), 1252 (m), 1241 (s), 1194 (w), 1150 (m), 1073 (w), 1056 (w), 1030 (w), 936 (vs), 869 (vs), 849 (s), 833 (s), 790 (m), 778 (m), 759 (s), 740 (w), 698 (s), 687 (m), 670 (m). Anal Calcd for $C_{31}H_{35}NO_2Si_2Sn$: C, 59.24; H, 5.61; N, 2.23. Found: C, 58.91; H, 5.43; N, 2.41.

$[(Me_3Si)_2NSn(\mu\text{-}O_2CC_6H_3Mes_2)]_2$ (7): Under an inert atmosphere, a solution of $Sn[N(SiMe_3)_2]_2$ (1.35 g, 3.07 mmol) in 5 mL anhydrous CH_2Cl_2 was added dropwise to a stirring suspension of 2,6-bis(2,4,6-trimethylphenyl)benzoic acid **3** (1.00 g, 2.79 mmol) in 15 mL anhydrous CH_2Cl_2. Over the course of 5.5 h, the solution faded from bright orange to very pale yellow. It was then concentrated under vacuum and cooled to -30 °C to give colourless crystals. Yield = 1.47 g (83%) mp = 168-169 °C. ^1H NMR (C_6D_6, 499.767 MHz) δ 6.92 (d, J = 7 Hz, 2H), 6.89 (s, 4H), 6.87 (br, 1H), 2.27 (s, 6H), 2.17 (s,

12H), 0.09 (s, 18H). $^{13}C\{^1H\}$ (CD_2Cl_2, 125.678 MHz) δ 137.2, 136.8, 128.6, 128.0, 21.0, 20.8, 2.32 (quaternary carbons not observed). ^{119}Sn (C_6D_6, 223.867 MHz) δ 74.43. IR (nujol mull) ν 1613 (m), 1580 (m), 1538 (vs), 1442 (s), 1257 (m), 1245 (s), 1183 (w), 1146 (w), 1065 (w), 1033 (w), 926 (vs), 866 (vs), 849 (vs), 833 (s), 790 (m), 780 (m), 755 (m), 740 (m), 710 (w), 699 (w), 670 (m). Anal Calcd for $C_{62}H_{86}N_2O_4Si_4Sn_2$: C, 58.49; H, 6.81; N, 2.20. Found C, 57.99; H, 6.63; N, 2.27.

$[(Me_3Si)_2NSn(\mu\text{-}O_2CC_6H_2Mes_2Me)]_2$ (8): Prepared according to the same procedure as **7**, beginning with 4-methyl-2,6-bis(2,4,6-trimethylphenyl)benzoic acid **5** (0.45 g, 1.21 mmol). Yield = 0.47 g (60%), mp = 151-155 °C. ^1H NMR (C_6D_6, 499.767 MHz) δ 6.85 (s, 4H), 6.69 (s, 2H), 2.21 (s, 12H), 2.20 (s, 6H), 1.98 (s, 3H), 0.00 (s, 18H). $^{13}C\{^1H\}$ NMR (CD_2Cl_2, 125.678 MHz) δ 137.8, 137.6, 136.6, 136.4, 136.2, 129.2, 128.8, 127.9, 21.3, 21.0, 20.8, 5.2. ^{119}Sn (C_6D_6, 223.867 MHz) δ 75.86. IR (nujol mull) ν 1715 (w), 1612 (m), 1597 (m), 1573 (m), 1536 (vs), 1486 (m), 1246 (s), 1164 (w), 1121 (w), 1102 (w), 1033 (w), 921 (s), 865 (vs), 849 (vs), 834 (s), 790 (m), 757 (w), 709 (w), 669 (m), 608 (s). Anal Calcd for $C_{64}H_{90}N_2O_4Si_4Sn_2$: C, 59.08; H, 6.97; N, 2.15. Found: C, 58.78; H, 6.68; N, 2.01.

$[(Mes_2C_6H_3CO_2)Sn(\mu\text{-}NSiMe_3)]_2$ (9) – Method 1: Under an inert atmosphere, $[(Me_3Si)_2NSn(\mu\text{-}O_2CC_6H_3Mes_2)]_2$ **7** (0.30 g, 0.23 mmol) was added to a suspension of $H_2O{\cdot}B(C_6F_5)_3$ (0.25 g, 0.47 mmol) in ca. 5 mL anhydrous CH_2Cl_2. The colourless solution stirred for 30 min at r.t. then placed in a -30 °C freezer. After one week, the solution was decanted from colourless crystals. Yield = 0.13 g (49%), mp = 168-170 °C.

$[(Mes_2C_6H_3CO_2)Sn(\mu\text{-}NSiMe_3)]_2$ (9) – Method 2: Under an inert atmosphere, silver cyanate (0.12 g, 0.80 mmol) was added to a solution of $[(Me_3Si)_2NSn(\mu\text{-}O_2CC_6H_3Mes_2)]_2$ **7** (0.46 g, 0.36 mmol) in 15 mL anhydrous Et_2O. The beige suspension was stirred overnight in the dark, then filtered through glass wool and Celite and cooled to -30 °C to give colourless crystals. Yield = 0.23 g (57%), mp = 170 °C (dec). ^1H NMR (CD_2Cl_2, 500.132 MHz) δ 7.48 (t, J = 7.5 Hz, 1H), 7.08 (d, J = 7.5 Hz, 2H), 6.83 (s, 4H), 2.27 (s, 6 H), 2.01 (s, 12 H), 0.11 (s, 9H). $^{13}C\{^1H\}$ NMR (CD_2Cl_2, 125.772 MHz) δ 138.0, 137.2, 136.9, 136.6, 128.9, 127.7, 127.5, 20.9, 20.1, 1.6. ^{119}Sn (186.6 MHz, CP/MAS) δ -100. IR (nujol mull) ν 2729 (w), 1715 (w), 1610 (m), 1588 (m), 1574 (s), 1556 (s), 1519 (s), 1484 (m), 1461 (vs), 1359 (vs), 1309 (w), 1259 (s), 1249 (s), 1180 (w), 1140 (m), 1101 (m), 1088 (m), 1060 (m), 1032 (m), 938 (w), 847 (vs), 810 (m), 785 (s), 771 (m), 752 (m), 737 (m), 709 (s), 667 (w). Anal Calcd for $C_{56}H_{68}N_2O_4Si_2Sn_2$: C, 59.69; H, 6.08; N, 2.49. Found: C, 59.90; H, 5.97; N, 2.67.

$[(Mes_2C_6H_3CO_2)Si(NMe_2)_3]$ (12): Under an inert atmosphere, 2,6-bis(2,4,6-trimethylphenyl)benzoic acid **3** (1.00 g, 2.79 mmol) was added to a solution of $Si(NMe_2)_4$ (0.57 g, 2.79 mmol) in 10 mL anhydrous CH_2Cl_2. The white suspension was stirred at r.t. for 24 h, and then the solvent was removed under vacuum to give a white powder. The crude product was suspended in ca. 25 mL warm hexanes, and then filtered to remove insoluble solids. The hexanes solution was concentrated and cooled to -30 °C to give colourless crystals. Yield = 0.37 g (26%), mp = 122 °C. ^1H NMR (C_6D_6, 499.767 MHz) δ 7.33 (t, 1H, J=7.5Hz), 6.96 (d, 2H, J=7.5 Hz), 6.74 (s, 4H), 2.15 (s, 6H), 1.95 (s, 12H), 1.92 (s, 18H). $^{13}C\{^1H\}$ (CD_2Cl_2, 125.678 MHz) δ 167.4, 137.9, 137.0, 136.9, 136.8, 136.7, 128.8, 128.3, 127.8, 36.6, 20.9, 20.5. IR (nujol mull) ν 1717 (s), 1611 (m), 1482

(m), 1298 (s), 1272 (vs), 1178 (s), 1120 (s), 1072 (m), 1058 (m), 998 (vs), 849 (m), 799 (m), 778 (m), 748 (m), 738 (m), 709 (m), 697 (m). Anal Calcd for $C_{31}H_{43}N_3O_2Si$: C, 71.91; H, 8.37; N, 8.12. Found: C, 71.73; H, 8.17; N, 8.26.

[($Mes_2C_6H_3CO_2$)Ti(NMe_2)$_3$] (13): Under an inert atmosphere, a solution of $Ti(NMe_2)_4$ (0.38 g, 1.67 mmol) in 5 mL anhydrous CH_2Cl_2 was added dropwise to a stirring suspension of 2,6-bis(2,4,6-trimethylphenyl)benzoic acid **3** (0.60 g, 1.67 mmol) in 15 mL CH_2Cl_2. After 3 h, the solvent was removed to give an orange powder that was recrystallized from hexanes to give orange crystals. Yield = 0.28 g (31%), mp = 143-146 °C. ^{1}H NMR (CD_2Cl_2, 499.768 MHz) δ 7.48 (t, J = 7.6 Hz, 1H), 7.11 (d, J = 7.6 Hz, 2H), 6.45 (s, 4H), 2.79 (s, 18H), 2.26 (s, 6H), 2.04 (s, 12H). $^{13}C\{^1H\}$ (CD_2Cl_2, 125.680 MHz) δ 184.9, 138.2, 137.1, 136.8, 136.7, 129.2, 127.9, 127.6, 44.2, 20.9, 20.5. IR (nujol mull) ν 2767 (m), 1731 (w), 1613 (m), 1578 (m), 1520 (s), 1487 (s), 1413 (m), 1246 (m), 1181 (w), 1141 (m), 1118 (w), 1093 (w), 1051 (m), 1032 (m), 1014 (m), 961 (m), 942 (s), 906 (w), 867 (s), 848 (s), 801 (m), 768 (w), 737 (m), 718 (m), 590 (s). Elemental analysis not obtained.

[($Mes_2C_6H_3CO_2$)$_2$Ti(NMe_2)$_2$] (13a): Under an inert atmosphere, a solution $Ti(NMe_2)_4$ (0.10 g, 0.45 mmol) in 2 mL CH_2Cl_2 was added dropwise to a stirring suspension of 2,6-bis(2,4,6-trimethylphenyl)benzoic acid **3** (0.15 g, 0.42 mmol) in 10 mL anhydrous CH_2Cl_2. After 1.5 h, the solution was concentrated to ca. 5 mL and then cooled to -30 °C to give orange crystals. Yield = 0.12 g (67%), mp = 200 °C (dec). ^{1}H NMR (CD_2Cl_2, 499.768 MHz) δ 7.46 (t, J = 7.6 Hz, 1H), 7.02 (d, J = 7.6 Hz, 2H), 6.82 (s, 4H), 2.43 (s, 6H), 2.28 (s, 6H), 1.96 (s, 12H). $^{13}C\{^1H\}$ (CD_2Cl_2,125.678 MHz) δ 140.0, 137.9, 136.1, 136.0, 129.9, 128.7, 127.6, 43.9, 21.1, 20.6. IR (nujol mull) ν 3054

(w), 2770 (w), 1612 (m), 1580 (m), 1521 (vs), 1486 (m), 1417 (m), 1248 (w), 1183 (w), 1144 (w), 1052 (w), 1032 (w), 946 (m), 865 (s), 847 (m), 826 (w), 803 (w), 782 (m), 592 (s). Elemental analysis not obtained.

3 *m*-TERPHENYLS IN METAL-ORGANIC CHAINS AND NETWORKS*

Metal-organic coordination networks (MOCNs), are a class of coordination compounds composed of metal atoms or clusters with well-defined coordination geometry coordinated to multidentate organic spacer ligands through donor atoms such as nitrogen or oxygen to give extended one-, two-, or three-dimensional frameworks. Networks based upon phosphonate,[194] sulfonate,[195] cyanate, azide and other such ligands have been extensively reported in the literature; however, they properly belong to a separate class of organic-inorganic hybrid materials[196] and will not be further discussed here. The ability of MOCNs to form rare or unique supramolecular structures makes them interesting from a fundamental standpoint. It is the ability to design and tune various properties of the MOCNs, though, which has driven their development for applied chemistry.

In order to give a degree of structural rigidity to the networks, the organic spacers are almost exclusively composed of aromatic backbones, although the use of more flexible ligands is increasing.[197] Nitrogen donor ligands are typically based on neutral pyridyl[198] or imidazole[199] groups. These types of ligands have the advantage of a single coordination mode, giving more control over the final morphology of the network. Their neutrality, however, can be a disadvantage, as the counteranions of the metal will often

* Portions of this chapter are reproduced in part, with permission, from the following journal articles: Dickie, D. A.; Jennings, M. C.; Jenkins, H. A.; Clyburne, J. A. C. *Inorg. Chem.* **2005**, *44*, 828-830 (Copyright 2005 American Chemical Society); and Dickie, D. A.; Schatte, G.; Jennings, M. C.; Jenkins, H. A.; Khoo, S. Y. L.; Clyburne, J. A. C. *Inorg. Chem.*, **2006**, *45*, 1646-1655 (Copyright 2006 American Chemical Society).

occupy any pores in the resultant network. This can be avoided by using negatively charged spacer ligands to balance the cationic metal, and the most common of these are carboxylates.[200] This is not surprising, given that the same diversity of coordination modes described for molecular carboxylates in Chapter 2 is found in the extended structures of metal organic frameworks.

3.1 Applications of metal-organic frameworks

The year-end review in the science magazine *Chemical and Engineering News* chose an application of metal-organic frameworks as its top materials chemistry story of 2005.[69] Kitagawa and co-workers[201] developed a copper-based network that was able to adsorb and release acetylene, allowing it to be stored at a density 200 times greater than what would be safe for the compressed gas alone. Their network was also able to bind selectively to acetylene in the presence of carbon dioxide. As these are both rod shaped molecules of similar size, the authors concluded that the difference in binding ability was due to interactions between the acidic hydrogen of the acetylene with free carboxylate oxygen from the network ligand backbone.

Similar gas sorption applications are the most widespread use of MOCNs. From early studies using nitrogen and carbon dioxide adsorption as measures of network porosity,[202] to sorption of small-molecule organic vapours,[203] the focus has shifted towards networks designed specifically for methane[204] and hydrogen storage[205] for fuel applications. These studies have progressed to the point where it is now possible to characterize molecular dihydrogen binding sites within the networks.[206] Of course, guest exchange is not limited to the gas phase. Liquid phase uptake, where an insoluble network is soaked in a solution or neat sample of organic guest molecules, has also been

studied.[207] Recently, MOCNs were even proven capable of separating hydrocarbons based on size and shape.[208]

The sorption properties of MOCNs lead to them often being described as porous, based on either gas sorption methods or computational results.[209] As with many buzzwords, the term "porous" has been subject to a fair amount of abuse in the literature. An excellent recent article by Barbour discussing the phenomenon of porosity divides it into three distinct categories: virtual porosity, porosity without pores, and conventional porosity.[210] Conventional porosity is the hardest to achieve, and refers to solids with permanent, interconnected channels that are able to absorb and exchange guest molecules with no significant change to the network. This type of porosity is found in zeolites, the inspiration for much MOCN synthesis.

Virtual porosity is also rarely reported, a good thing since it is the most suspect, as it exists only *in silico* rather than *in situ*. Counterions or solvent molecules that fill what might otherwise be called pores or channels within the network are deleted by computer so that the subsequently generated space-filling diagrams show large, empty voids. Since the actual removal of these guests would cause the framework to collapse, they should not be considered truly porous. Porosity without pores describes the ability of certain crystals with internal voids that are not connected into channels to nevertheless absorb and release guest molecules over time without significant changes to their structural coordinates. Barbour admits that the mechanism for such a crystal-to-crystal transformation is not yet understood but it likely involves a cooperative dynamic process within the solid that creates temporary channels for exchange.

Related to their sorption applications is the use of MOCNs as heterogeneous catalysts.[211] Kitagawa recently reported that a copper-based network with carboxylate-functionalized pores could catalyze the polymerization of monosubstituted acetylenes in a stereoselective manner.[212] The dangling carboxylate groups within the pores form hydrogen bonds to the acetylene monomer while the size restrictions of the network pore permit formation of only the desired *trans* polymers. Monomers without hydrogen-bonding capabilities are not held in the pores, and thus the network acts as a monomer-selective catalyst. Nguyen and Hupp recently published a very different example of active sites along a pore rather than at one of the network vertices.[213] They modified an existing manganese complex and incorporated, with retention of its catalytic activity, as a supporting strut in a three-dimensional zinc-carboxylate MOCN.

A number of non-sorption and non-catalytic applications for MOCNs have also been studied. Molecule-based magnets[214] are the motivation for many networks, particularly those based on cobalt,[215] copper,[215a, 216] nickel,[215c, 217] managenese,[215c, 218] and iron.[219] Copper and cadmium are the materials of choice for ferroelectric MOCNs.[220] Optical properties including non-linear optics (NLO),[221] luminescence[222] and fluorescence[223] have also been investigated.

3.2 Frameworks based upon a bifunctional *m*-terphenyl carboxylate ligand

The ability to enforce coordinative unsaturation at a metal site within MOCNs was identified early on as one of the major challenges in their development.[224] Coordinative unsaturation would lead to greater Lewis acidity and potentially improved binding of guest molecules. *m*-Terphenyl ligands are known for their ability to shield

metals and prevent aggregation while still allowing for small molecule reactivity, exactly what would be required in a MOCN. In fact, *m*-terphenyl derivatives have already been designed for use in similar crystal engineering applications; however, in that case, the functional groups were placed on the flanking aryls, rather than on the central ring.[225]

An additional advantage of using *m*-terphenyl ligands in network synthesis is that the hydrophobic pocket formed around the metal site could influence the guest selectivity. The steric bulk provided by the backbone would likely also reduce network interpenetration, thereby increasing the chances of obtaining a network with permanent porosity. Additionally, placing the steric bulk directly next to the metal could affect the dimensionality of the framework by controlling the availability of coordination sites. Finally, the 2,6-substitution pattern on the ligand would be unique among structural characterized 1,4-benzenedicarboxylic acids,[226] and would perhaps lead to different reactivity at the two ends of the molecule.

3.2.1 Organic chains

The preparation of coordination networks based on bifunctional *m*-terphenyl carboxylic acids began with the potassium permanganate oxidation in water of 2,6-diphenyl-4-methylbenzoic acid **14** to give the bifunctional molecule 2,6-diphenylterephthalic acid **15H$_2$**. Because this reaction is done in water, the addition of a surfactant greatly improves the product yield by helping to solubilise the starting material. Sodium dodecylsulfate works well, however commercial laundry detergents such as Tide® were found to give comparable results and are often more readily available and affordable.[227]

Scheme 3.1 Synthesis of 2,6-diphenylterephthalic acid $15H_2$.

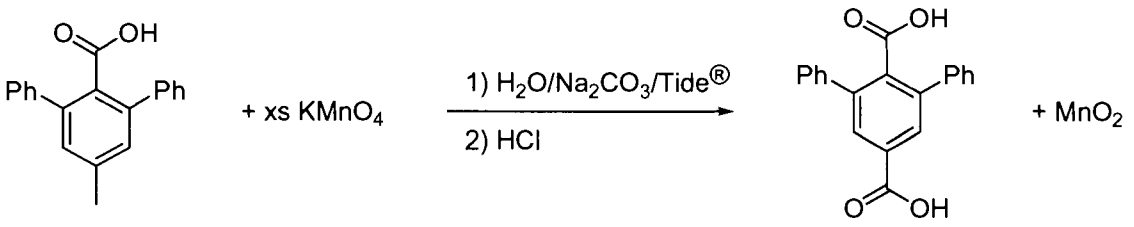

14 **$15H_2$**

Distinctive peaks in the ^{1}H NMR spectrum of **$15H_2$** include the very broad signal at 13.1 ppm due to the hydrogen bonded OH groups, and a sharp singlet at 7.87 ppm from the hydrogens on the central phenyl ring. The peaks at 167.1 and 170.2 ppm in the ^{13}C NMR spectrum were assigned to the two carboxylate carbons. The IR spectrum shows a strong ν C=O absorption at 1692 cm^{-1}. Recrystallization from diethyl ether afforded colourless needles suitable for X-ray diffraction.

Figure 3.1 Structure of ligand $15H_2$. Thermal ellipsoids are shown at the 50% probability level. For clarity, hydrogen atoms on the aromatic rings are not shown.

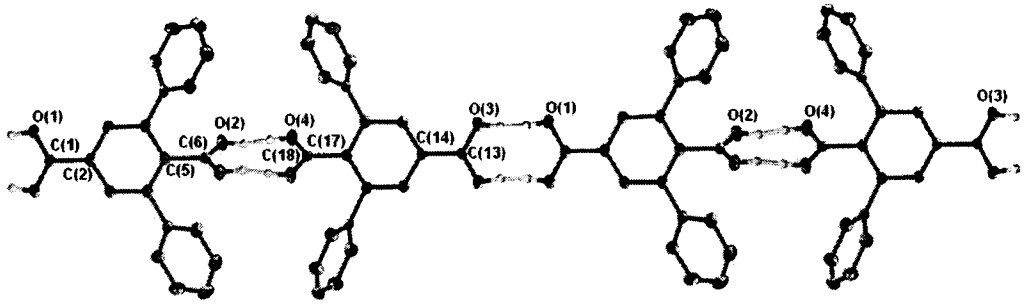

Reproduced with permission from Dickie, D. A.; Schatte, G.; Jennings, M. C.; Jenkins, H. A.; Khoo, S. Y. L.; Clyburne, J. A. C. *Inorg. Chem.*, **2006**, *45*, 1646-1655. Copyright 2006 American Chemical Society.

Not surprisingly, the crystallographic studies of **$15H_2$** revealed an infinite one-dimensional hydrogen-bonded chain (Figure 3.1). There is a plane of symmetry running along the centre of each of the two crystallographically distinct molecules, from C(1)-C(6) and C(13)-C(18). Consequently, the C-O bond lengths within each carboxylate are

identical, with an average length of 1.264 Å, and the hydrogen atom could not be accurately located. The intermolecular hydrogen bonding is strong and shows average [O···O] distances for neutral carboxylic acid chains,[228] at 2.648(3) Å for the less hindered *para*-carboxylate and 2.637(3) Å for the more crowded pocket carboxylate.

Table 3.1 Selected structural data for bifunctional *m*-terphenyl carboxylate $15H_2$.

Bond lengths (Å)			
O(1)-C(1)	1.2642(16)	O(3)-C(13)	1.2663(17)
O(2)-C(6)	1.2633(16)	O(4)-C(18)	1.2614(16)
O(1)···O(3)	2.648	O(2)···O(4)	2.637
Bond angles (°)			
O(1)-C(1)-O(1)	123.3(2)	O(3)-C(13)-O(3)	123.5(2)
O(2)-C(6)-O(2)	124.7(2)	O(4)-C(18)-O(4)	124.2(2)

Based on sterics alone, it might be expected that the molecules would align in a head-to-tail fashion, keeping the bulky substituents are far apart as possible. Examination of the structure shows instead a head-to-head alignment of the *m*-terphenyls. This can be explained by examining the angle between the carboxylates and the central phenyl rings. Studies have shown that although the optimal conformation for unsubstituted benzoic acids is co-planarity between the aromatic ring and the CO_2H fragments, the energy required to rotate from 0 to 90° is only 20-40 kcal/mol.[229] The presence of other favourable crystal packing interactions, such as hydrogen bonds, can therefore have a significant impact on the twist angle. Since this angle has also been shown to be dependent on the nature of the *ortho* substituents,[230] it is not surprising that the steric demands imposed by the phenyl substituents in **$15H_2$** have a significant impact on the geometry of the ligand.

The pocket carboxylates twist significantly out of the plane (46.88° and 68.45° in the two molecules), while the *para*-carboxylates are nearly co-planar (10.04° and 9.89°

respectively). Complementarity demands, therefore, that the two twisted fragments align to give essentially flat chains that are oriented anti-parallel to neighbouring chains and perpendicular to chains above and below it (Figure 3.2). This is in contrast to terephthalic acid which has all chains parallel with an inter-layer spacing of 3.333-3.403 Å.[231] Although the central rings of the *m*-terphenyls in each chain of **15H$_2$** are aligned in a face-to-face fashion, the bulk of the substituents pushes them too far apart (centroid···centroid = 4.414 Å) to be considered a π-stacking interaction.[232]

Figure 3.2 Packing diagrams of 15H$_2$ along the crystallographic *a* and *c* axes. For clarity, aryl hydrogen atoms have been removed in both, as were the flanking phenyls in *c*.

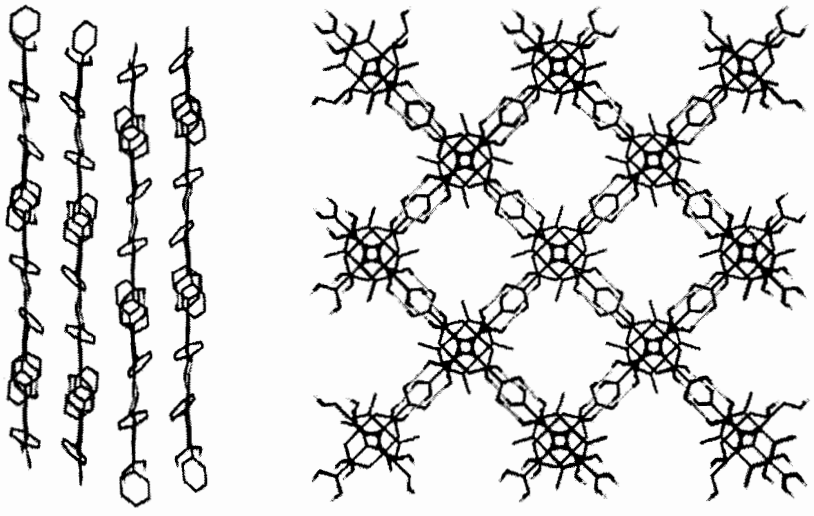

Reproduced with permission from Dickie, D. A.; Schatte, G.; Jennings, M. C.; Jenkins, H. A.; Khoo, S. Y. L.; Clyburne, J. A. C. *Inorg. Chem.*, **2006**, *45*, 1646-1655. Copyright 2006 American Chemical Society.

A second organic hydrogen-bonded chain **16** was prepared by the reaction of equimolar amounts of **15H$_2$** and 4,4'-dipyridyl in ethanol. The solution ^{1}H NMR spectrum of the resulting solid showed the expected 1:1 ratio; however, the carboxylic hydrogen was not observed. Crystals were grown from ethanol and X-ray crystallography showed an alternating hydrogen-bonded chain **16** in the solid state

(Figure 3.3). The CO_2H hydrogen atoms in both the *para* and pocket positions were located in the Fourier difference map and their coordinates were allowed to refine freely.

Figure 3.3 Structure of [15·bipy] 16. Thermal ellipsoids are shown at the 50% probability level. For clarity, hydrogen atoms on the aromatic rings are not shown.

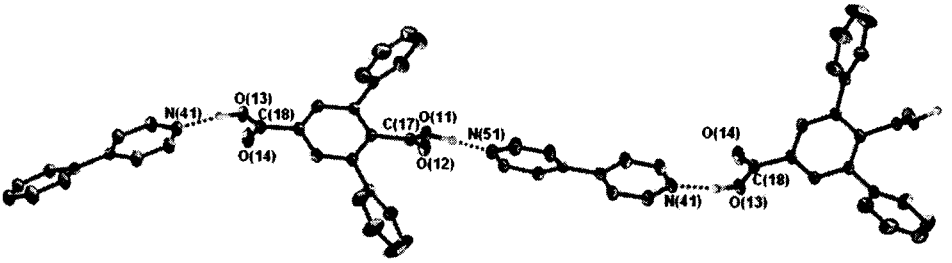

Reproduced with permission from Dickie, D. A.; Schatte, G.; Jennings, M. C.; Jenkins, H. A.; Khoo, S. Y. L.; Clyburne, J. A. C. *Inorg. Chem.*, **2006**, *45*, 1646-1655. Copyright 2006 American Chemical Society.

Table 3.2 Selected structural data for [15·bipy] 16.

Bond lengths (Å)			
O(11)-C(17)	1.314(2)	O(13)-C(18)	1.299(2)
O(12)-C(17)	1.210(2)	O(14)-C(18)	1.216(2)
H(1)···N(51)	1.589	H(3)···N(41)	1.728
O(11)···N(51)	2.631	O(13)···N(41)	2.641
Bond angles (°)			
O(12)-C(17)-O(11)	125.14(16)	O(14)-C(18)-O(13)	124.55(17)
O(11)-H(1)···N(51)	176.21	O(13)-H(3)···N(41)	170.64

The presence of a single acceptor group at each end of the dipyridyl fragment breaks the plane of symmetry of **15H$_2$**, resulting in distinct C=O and C-O bonds of 1.210(2) and 1.314(2) Å in the pocket and 1.216(2) and 1.299(2) Å at the *para* position. The out-of-plane twisting of the *para*-carboxylate is more pronounced, with an angle of 28.95°, compared to ca. 10° in **15H$_2$**, while pocket carboxylate of **15** has a similar orientation (66.45°). Combined with the twist in the planes of the 4,4'-dipyridyl (13.29°), this give the chains of **16** a wavy appearance, unlike the flat chains of **15H$_2$**.

Figure 3.4 **Strong [O-H···N] hydrogen bonds along chains and weaker [C-H···O] interactions between chains produces a 2-D network along the crystallographic *b* axis of 16.**

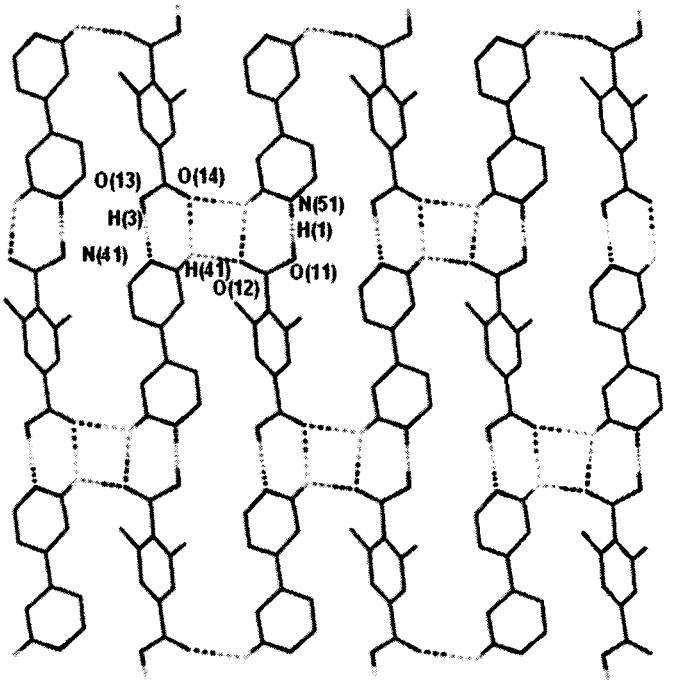

Reproduced with permission from Dickie, D. A.; Schatte, G.; Jennings, M. C.; Jenkins, H. A.; Khoo, S. Y. L.; Clyburne, J. A. C. *Inorg. Chem.*, **2006**, *45*, 1646-1655. Copyright 2006 American Chemical Society.

As in **15H$_2$**, the hydrogen bond in the *m*-terphenyl pocket of **15** is slightly shorter, O(11)···N(51) = 2.631 Å, than in the *para* position, O(13)···N(41) = 2.641 Å. Both hydrogen bonds are also very close to linear ([O-H···N] = 176.21° and 170.64° for the pocket and *para*, respectively), and within the ranges[233,234] of typical carboxylic acid-dipyridyl co-crystals.[235] In addition to the expected [O-H···N] hydrogen bonding, there is also extensive [C-H···O] hydrogen bonding[236] (Figure 3.4). By twisting significantly out of the plane of the central phenyl, the carboxylate is able to engage in the maximum number of interactions.[229] Each C=O acts as an acceptor to distinct C-H donors from two neighbouring pyridyl fragments. The shortest bond for each carbonyl is to the hydrogen *ortho* to the pyridine nitrogen within the same chain. The distance for the pocket C=O is O(12)···C(51) = 3.265 Å, while the *para* C=O is again shorter at O(14)···C(41) = 3.092 Å,

close to the range of values reported between 4,4'-dipyridyl and other bifunctional acids (3.111-3.446 Å).[233]

The interactions with the *ortho* hydrogen of the pyridyl in the adjacent chain measure O(12)···C(41) = 3.261 Å in the pocket and O(14)···C(51) = 3.147 Å in the *para* position. When these interactions are taken into account, the 1-D chain becomes a 2-D network. Organic hydrogen-bonded 2-D networks based upon trimesic or trimelletic acid with *N,N*-dibenzylamine are known to absorb a wide variety of aromatic guest molecules,[237] however, this has not yet been tested for **16**.

3.2.2 1-D metal-organic chains

Attempts to use **16** or other combinations of **15H$_2$** and 4,4'-dipyridyl to prepare single-crystal networks have to date proven unsuccessful, giving insoluble precipitates that were not characterized. Instead, the reaction of **15H$_2$** with either cobalt (II) nitrate or zinc (II) nitrate was done in methanol in the presence of excess pyridine. The pyridine deprotonates both carboxylates to give 1-D chains **17** (M = Zn) and **18** (M = Co) with the general formula **15**·M·(py)$_2$·MeOH, as determined by single crystal X-ray diffraction. Elemental analysis was consistent with this formula for **18**, but results for **17** were off by nearly two percent for carbon.

X-ray crystallographic studies revealed that in both **17** (Figure 3.5) and **18** (Figure 3.6), the metal ion is bound to two pyridine molecules that are oriented *cis* to one another. A single oxygen of the pocket carboxylate is coordinated to the metal centre and one equivalent of methanol is bound trans to a pyridine. This type of solvent coordination is found in similar cobalt complexes.[238,239] This methanol, whose O*H* hydrogen was

located in the Fourier difference map, is further held in place through a hydrogen bond to the C=O of the pocket carboxylate. Examination of the extended structure shows that the distorted octahedron of the metal coordination sphere is completed by chelation of the *para* carboxylate, forming a 1-D chain.

Figure 3.5 **Structure of [15·Zn·(py)$_2$·MeOH] 17. Thermal ellipsoids are shown at 50% probability and for clarity, all hydrogen atoms except the methanolic proton have been removed.**

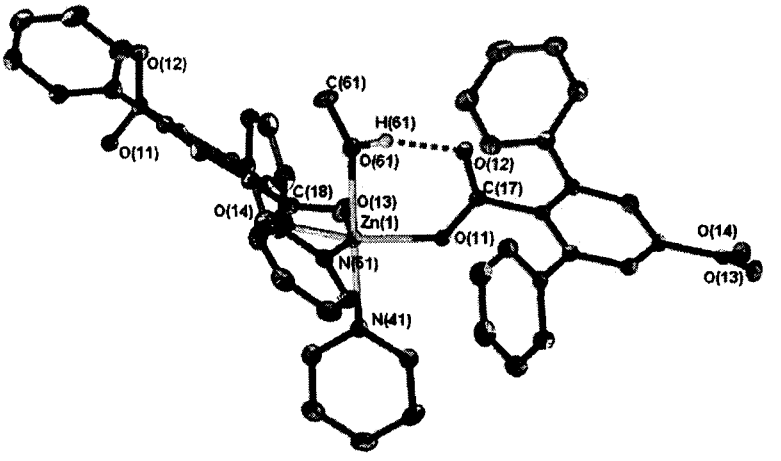

Figure 3.6 **Structure of [15·Co·(py)$_2$·MeOH] 18. Thermal ellipsoids are shown at 50% probability and for clarity, all hydrogen atoms except the methanolic proton have been removed.**

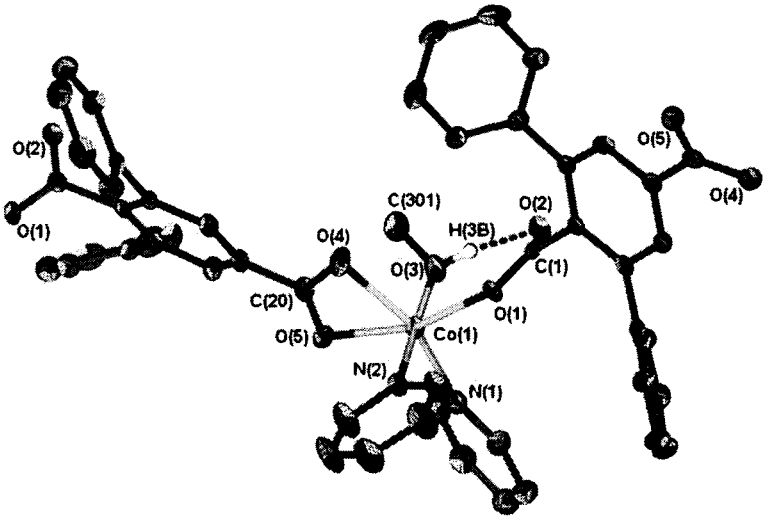

Figure 3.7 **Extended structure of [15·Zn·(py)$_2$·MeOH] 17. The same motif is present in [15·Co·(py)$_2$·MeOH] 18.**

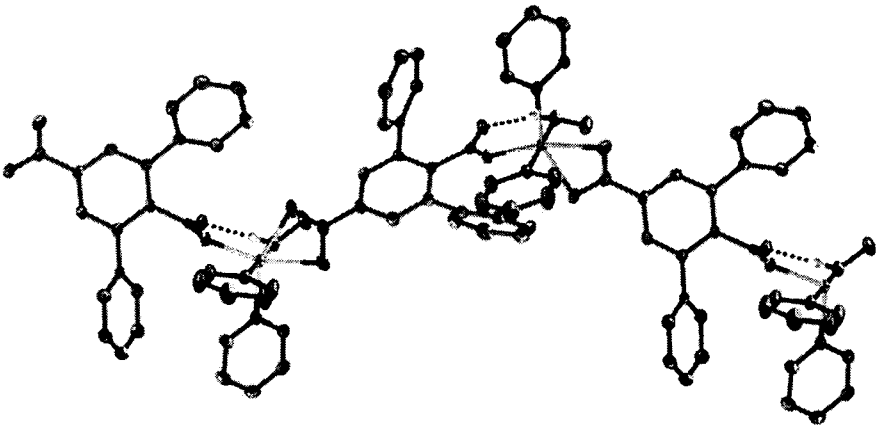

Table 3.3: **Selected structural data for [15·Zn·(py)$_2$·MeOH] 17 and[15·Co·(py)$_2$·MeOH] 18.**

Bond lengths (Å)			
[15·Zn·(py)$_2$·MeOH] **17**		[15·Co·(py)$_2$·MeOH] **18**	
Zn(1)-N(41)	2.162(2)	Co(1)-N(2)	2.102(3)
Zn(1)- N(51)	2.092(3)	Co(1)-N(1)	2.102(3)
Zn(1)-O(11)	2.037(2)	Co(1)-O(1)	2.0544(19)
Zn(1)- O(13)	2.209(2)	Co(1)-O(4)	2.183(2)
Zn(1)- O(14)	2.187(2)	Co(1)-O(5)	2.151(2)
Zn(1)- O(61)	2.177(2)	Co(1)-O(3)	2.128(2)
O(11)- C(17)	1.273(3)	O(1)-C(1)	1.272(3)
O(12)- C(17)	1.243(3)	O(2)-C(1)	1.242(3)
O(13)-C(18)	1.259(4)	O(4)-C(20)	1.271(3)
O(14)-C(18)	1.262(4)	O(5)-C(20)	1.253(3)
O(12)···H(61)	1.822	O(2)···H(3b)	1.841
O(12)···O(61)	2.626	O(2)···O(3)	2.625
Bond angles (°)			
O(12)···H(61)-O(61)	156.72	O(2)···H(3b)-O(3)	157.04
N(51)-Zn(1)-N(41)	93.31(9)	N(1)-Co(1)-N(2)	92.05(10)
N(41)-Zn(1)-O(61)	178.51(9)	N(2)-Co(1)-O(3)	177.78(9)
O(14)-Zn(1)-O(13)	59.97(9)	O(5)-Co(1)-O(4)	60.90(8)

While the zinc (**17**) and cobalt (**18**) chains have the same connectivity, there are slight differences in their structural parameters. The M-O_{MeOH} bond and the M-O_{para} bonds are all slightly longer in **17** than in **18**, but the pocket carboxylate has a shorter M-O bond. The pyridine M-N bonds are the same in both chains, within experimental error. The out-of-plane twist of the *para*-carboxylate was virtually identical in **16**, **17**, and **18** (ca. 28°), in order to maximize secondary [C-H···O] interactions between neighbouring chains.[234]

3.2.3 2-D hydrogen bonded metal-organic networks

The reaction of **15H$_2$** with copper (II) nitrate in ethanol with pyridine, although analogous to preparation of **17**, gives complex **19** with the significantly different formula (**15H**)$_2$·Cu·(py)$_2$ (Figure 3.8). No solvent is present in the final product, and only one of the two carboxylic acid groups has been deprotonated, necessitating a 2:1 metal:ligand ratio in the neutral compound. The hydrogen atom of the protonated carboxylate was located in the Fourier difference map and allowed to refine freely. As in **17** and **18**, two pyridines are again present, but examination of the crystal structure showed that they are bound in *trans* conformation across a crystallographic mirror plane. The deprotonated pocket carboxylates are also trans and bound to the copper ions through a single oxygen, giving the metal square planar geometry with O-Cu-N angles of 92.37(6)and 87.63(6)°.

Figure 3.8 **Structure of [(15H)$_2$·Cu·(py)$_2$] 19. Thermal ellipsoids are shown at 50% probability and for clarity, only the O-H hydrogen is shown.**

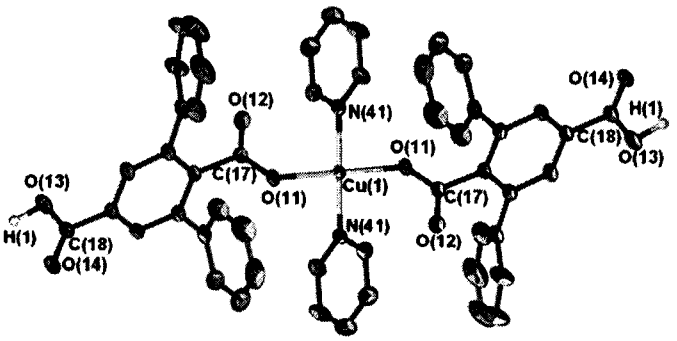

Reproduced with permission from Dickie, D. A.; Schatte, G.; Jennings, M. C.; Jenkins, H. A.; Khoo, S. Y. L.; Clyburne, J. A. C. *Inorg. Chem.*, **2006**, *45*, 1646-1655. Copyright 2006 American Chemical Society.

The Cu-O and Cu-N bond lengths of 1.9771(13) and 1.9948(18) Å, respectively, are significantly shorter than the metal-ligand bonds in **17** and **18**. They are also on the short end of the average reported for recent copper-based MOCNs (Cu-O = 1.945 – 2.159 Å, Cu-N = 1.924 – 2.286 Å).[239,240] The difference of at least 0.05 Å for the M-O bond

and 0.08 Å for the M-N bond may be caused by the increased demand for electron density from the solvent-free metal in **19**. It may also be due to the reduced steric hindrance around the four-coordinate copper compared to the six-coordinate zinc or cobalt in **17** and **18**.

Table 3.4 Selected structural data for [(15H)$_2$·Cu·(py)$_2$] 19.

Bond lengths (Å)			
Cu(1)-O(11)	1.9771(13)	Cu(1)-N(41)	1.9948(18)
O(11)-C(17)	1.252(2)	Cu(1)···O(14)	2.517
O(12)-C(17)	1.246(2)	O(12)···H(1)	1.466
O(13)-C(18)	1.319(3)	O(12)···O(13)	2.497
O(14)-C(18)	1.211(2)		
Bond angles (°)			
O(11)-Cu(1)-O(11)*	179.997(1)	O(11)-Cu(1)-N(41)*	87.63(6)
O(11)-Cu(1)-N(41)	92.37(6)	N(41)-Cu(1)-N(41)*	180.0
O(12)···H(1)-O(13)	159.71		

Symmetry transformation used to generate equivalent atoms: * -x + 1, -y + 1, -z

The C-O bonds in the pocket (1.252(2) and 1.246(2) Å, respectively) are delocalized while those in the protonated *para*-carboxylic acid can still be considered distinct single and double bonds (1.319(3) and 1.211(2) Å). In the pocket of the *m*-terphenyl ligand, the oxygen that is not bound to the metal is instead engaged in a very short[228] hydrogen bond (H···O = 1.466 Å, O···O = 2.495 Å, O-H···O = 159.71°) to the O-H of a neighbouring *para*-carboxylic acid. This brings the remaining C=O from the *para* group close enough to interact with the copper, transforming it from square planar to a Jahn-Teller[239] distorted octahedral geometry (Figure 3.9). This secondary Cu-O interaction measures 2.517 Å, nearly 0.5 Å less than the sum of the van der Waals radii of Cu (II) and O (2.92 Å), and is undoubtedly a significant interaction. The hydrogen bond and Cu-O interaction form a "figure eight" around the metal centre, resulting in the formation of a 2-D network

Figure 3.9 Short [O-H···O] hydrogen bonds and long [Cu···O] interactions connecting a 2-D network in 19. Phenyls removed for clarity

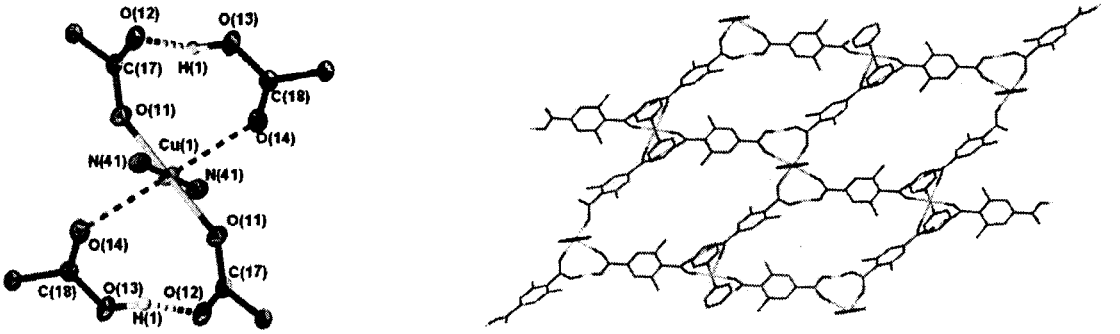

Reproduced with permission from Dickie, D. A.; Schatte, G.; Jennings, M. C.; Jenkins, H. A.; Khoo, S. Y. L.; Clyburne, J. A. C. *Inorg. Chem.*, **2006**, *45*, 1646-1655. Copyright 2006 American Chemical Society.

To demonstrate how changes in reaction conditions can effect MOCN formation, it is interesting to compare **19** with another complex formed by the reaction of two equivalents of $\mathbf{15H_2}$ with copper (II) nitrate in methanol with excess pyridine. This variation in solvent (from ethanol to methanol), pyridine concentration and reaction stoichiometry gave complex **20** with a formula of $(\mathbf{15H})_2{\cdot}Cu{\cdot}(py)_4{\cdot}(H_2O)_2$ (Figure 3.10). As with **19**, compound **20** has a 2:1 ligand:metal ratio and a singly deprotonated carboxylate, but it has incorporated twice as many pyridine molecules.

Figure 3.10 Structure of $[(15H)_2{\cdot}Cu{\cdot}(py)_4{\cdot}(H_2O)_2]$ 20. Thermal ellipsoids are shown at 50% probability and for clarity, all hydrogens except the O-H have been removed. Two molecules of water are also not shown.

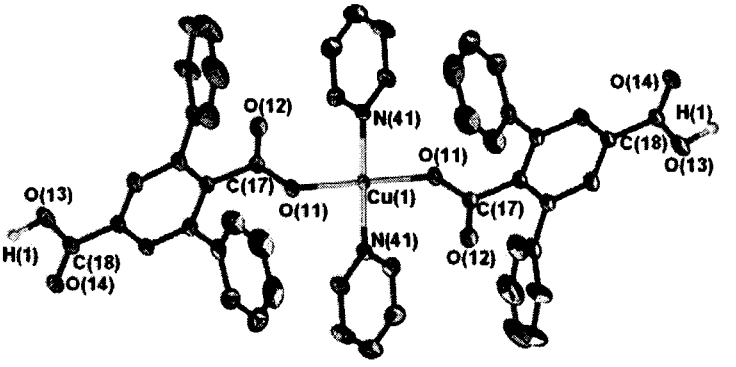

Reproduced with permission from Dickie, D. A.; Schatte, G.; Jennings, M. C.; Jenkins, H. A.; Khoo, S. Y. L.; Clyburne, J. A. C. *Inorg. Chem.*, **2006**, *45*, 1646-1655. Copyright 2006 American Chemical Society.

The four Cu-N bonds in **20** range from 2.025(2) to 2.040(2) Å, somewhat longer than those measured in **19**. The Cu-O bonds are also significantly longer, measuring 2.377(2) and 2.517(2) Å, compared to 1.9771(13) in **19**. In fact, the longer Cu(1)-O(5) bond is the same length as the secondary Cu-O in **19**. As with **19**, the C-O bond lengths in the pocket are indistinguishable, averaging 1.252 Å, indicating delocalization around the carboxylate fragment, despite the fact that the copper is clearly bound to only one of the two oxygen atoms (non-bonded Cu(1)-O(2) = 3.802 Å and Cu(1)-O(6) = 3.945 Å). The protonated *para* position has distinct C=O and C-O bonds averaging 1.216 and 1.315 Å, respectively.

Given that the *para* and pocket carboxylates formed very strong hydrogen bonds to one another in **19**, a similar but perhaps weaker interaction might be expected in **20**. Examination of the extended structure (Figure 3.11), however, shows instead that hydrogen bonding through the two waters of crystallization gives rise to a 2-D network made up of three distinct ring systems. The protonated *para*-carboxylates of each *m*-terphenyl ligand bridge an oxygen and hydrogen from two water molecules to form the smallest ring. The remaining hydrogen atom from each water molecule forms a hydrogen bond to the unbound oxygen of the pocket carboxylate, completing the two other rings.

Figure 3.11 The carboxylate oxygen not bound to copper forms hydrogen bonds with water to give this 2-D network in 20. For clarity, only the ipso carbon atoms of the phenyls and the nitrogen of the pyridines are shown.

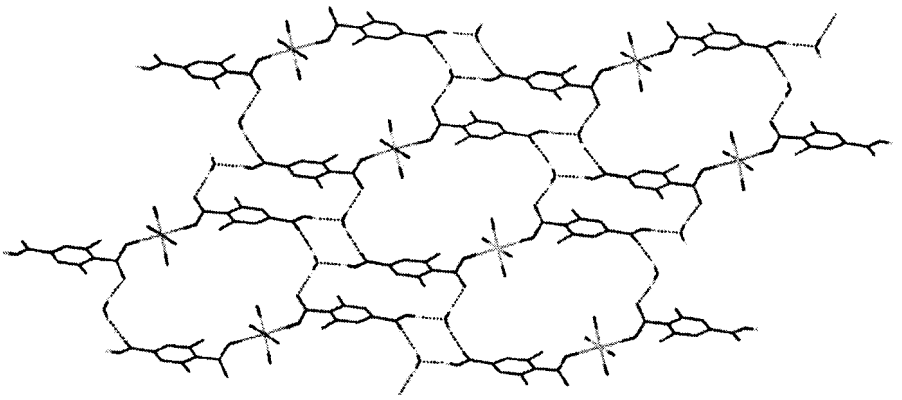

Reproduced with permission from Dickie, D. A.; Schatte, G.; Jennings, M. C.; Jenkins, H. A.; Khoo, S. Y. L.; Clyburne, J. A. C. *Inorg. Chem.*, **2006**, *45*, 1646-1655. Copyright 2006 American Chemical Society.

Table 3.5 Selected structural data for $[(15H)_2{\cdot}Cu{\cdot}(py)_4{\cdot}(H_2O)_2]$ 20.

Bond lengths (Å)			
Cu(1)-N(1)	2.0377(18)	Cu(1)-N(3)	2.0400(19)
Cu(1)-N(2)	2.0253(19)	Cu(1)-N(4)	2.0285(19)
Cu(1)-O(1)	2.3770(16)	Cu(1)-O(5)	2.5167(15)
O(1)-C(7)	1.252(3)	O(5)-C(27)	1.248(3)
O(2)-C(7)	1.252(3)	O(6)-C(27)	1.258(3)
O(3)-C(8)	1.215(3)	O(7)-C(28)	1.217(3)
O(4)-C(8)	1.316(3)	O(8)-C(28)	1.314(2)
Bond angles (°)			
N(1)-Cu(1)-N(2)	89.81(7)	N(2)-Cu(1)-N(3)	91.56(8)
N(1)-Cu(1)-N(3)	178.20(8)	N(2)-Cu(1)-N(4)	174.77(8)
N(1)-Cu(1)-N(4)	88.37(7)	N(3)-Cu(1)-N(4)	90.17(7)
O(1)-Cu(1)-O(5)	178.23(6)		

Table 3.6 [O-H···O] Hydrogen bond lengths and angles in $[(15H)_2{\cdot}Cu{\cdot}(py)_4{\cdot}(H_2O)_2]$ 20.

Hydrogen bond lengths (Å)			
H(4A)···O(9)#1	1.69	O(4)···O(9)#1	2.504(2)
H(8A)···O(10)#2	1.69	O(8)···O(10)#2	2.518(2)
H(9A)···O(3)#3	1.950(17)	O(9)···O(3)#3	2.796(2)
H(9B)···O(2)#4	1.787(16)	O(9)···O(2)#4	2.657(2)
H(7A)···O(7)#5	1.931(17)	O(10)···O(7)#5	2.772(2)
H(7B)···O(6)#6	1.772(16)	O(10)···O(6)#6	2.629(2)
Hydrogen bond angles (°)			
O(4)-H(4A)...O(9)#1	168.3	O(9)-H(9B)...O(2)#4	177(3)
O(8)-H(8A)...O(10)#2	171.1	O(10)-H(7A)...O(7)#5	165(2)
O(9)-H(9A)...O(3)#3	170(3)	O(10)-H(7B)...O(6)#6	170(2)

Symmetry transformations used to generate equivalent atoms: #1 x-1,y,z; #2 x+1,y-1,z; #3 -x,-y+1,-z; #4 -x+1,-y+1,-z; #5 -x+2,-y,-z+1; #6 -x+1,-y,-z+1.

The shortest hydrogen bonds are between water and the O-H of the *para*-carboxylate, while the C=O of the *para* groups form the longest and the C-O of the pocket are intermediate. All of the bonds are of moderate to strong strength.[228] This network is further stabilized by extensive [C-H···O] hydrogen bonding between the pocket carboxylate and the *ortho* hydrogens of the coordinated pyridines (Figure 3.12). The free pocket oxygens each form a single short [C-H···O] bond of 2.332 and 2.292 Å for O(2) and O(6), respectively. The two copper-coordinated oxygen atoms each engage in two [C-H···O] bonds, ranging from 2.413-2.522 Å. This results in two pyridines using both *ortho* hydrogens to interact with opposite carboxylates and two pyridines using only a single *ortho* hydrogen atom.

Figure 3.12 [C-H···O] Bonds in 20. Phenyl groups, water, and non-hydrogen bonded hydrogens have been removed for clarity.

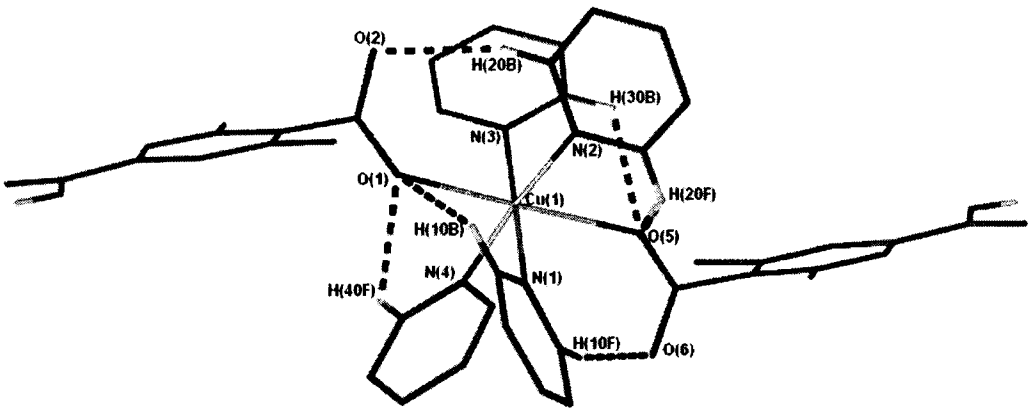

Reproduced with permission from Dickie, D. A.; Schatte, G.; Jennings, M. C.; Jenkins, H. A.; Khoo, S. Y. L.; Clyburne, J. A. C. *Inorg. Chem.*, **2006**, *45*, 1646-1655. Copyright 2006 American Chemical Society.

3.2.4 2-D covalent metal-organic networks

In compounds **17-20**, the coordinated pyridine molecules are occupying at least two metal coordination sites, limiting the dimensionality of the resulting complex. In an attempt to prepare a pyridine-free complex based solely on metal-ligand interactions

rather than hydrogen-bonding, silver nitrate was reacted with the dipotassium salt of **15** in methanol and water. The resulting 2-D network **21** (Figure 3.13) is the only one in this series to be free of both solvent and base, with a formula of **15**·Ag_2. The X-ray crystal structure shows that there is a plane of symmetry down the centre of the molecule, as there was in $\mathbf{15H_2}$.

The *para*-carboxylate bridges two silver atoms, with an Ag-O bond length of 2.178(3) Å, and there is an argentophilic Ag-Ag bond of 2.8689(7) Å. This compares well with the Ag-Ag bond length in metallic silver of 2.889 Å and is at the very low end of the range of silver-silver interactions in coordination networks reported recently.[241] Examination of the extended structure (Figure 3.14) shows that the silver atoms are also coordinated to the pocket carboxylate at an Ag-O bond length of 2.242(3) Å, forming a twisted eight-membered $Ag_2C_2O_4$ ring. Each oxygen of the pocket also bridges a silver from a neighbouring chain, Ag-O = 2.430(3) Å, forming a planar four-membered Ag_2O_2 heterocycle.

Figure 3.13 Structure of [15·Ag_2] 21. Thermal ellipsoids are shown at 50% probability and all hydrogen atoms have been removed for clarity.

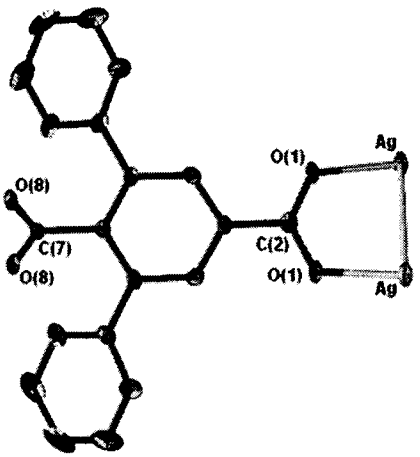

Figure 3.14 Extended structure of 21, showing the network formed by Ag-Ag bonds and bridging carboxylates. Phenyl substituents have been omitted for clarity.

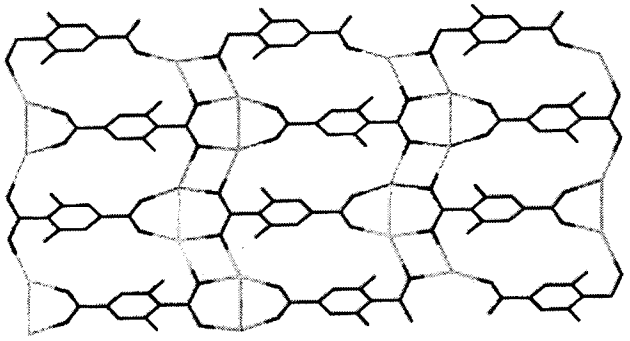

Reproduced with permission from Dickie, D. A.; Schatte, G.; Jennings, M. C.; Jenkins, H. A.; Khoo, S. Y. L.; Clyburne, J. A. C. *Inorg. Chem.*, **2006**, *45*, 1646-1655. Copyright 2006 American Chemical Society.

Table 3.7 Selected structural data for [15·Ag_2] 21.

		Bond lengths (Å)	
Ag-O(1)	2.178(3)	C(2-)O(1)	1.266(4)
Ag-O(8)#1	2.242(3)	C(2)-O(1)#3	1.266(5)
Ag-O(8)#2	2.430(3)	C(7)-O(8)	1.256(4)
Ag-Ag#3	2.8689(7)	C(7)-O(8)#3	1.256(4)
		Bond angles (°)	
O(1)-Ag-O(8)#1	156.62(12)	O(1)-Ag-Ag#3	77.43(9)
O(1)-Ag-O(8)#2	128.42(12)	O(8)#1-Ag-Ag#3	79.87(8)
O(8)#1-Ag-O(8)#2	74.33(12)	O(8)#2-Ag-Ag#3	154.14(8)

Symmetry operations used to generate equivalent atoms: #1 x, y+1, z; #2 -x+1, -y+1, -z; #3 -x+1, y, -z+1/2

Figure 3.15 π-Stacking interactions in 21 viewed along the crystallographic *b* and *c* axes, respectively.

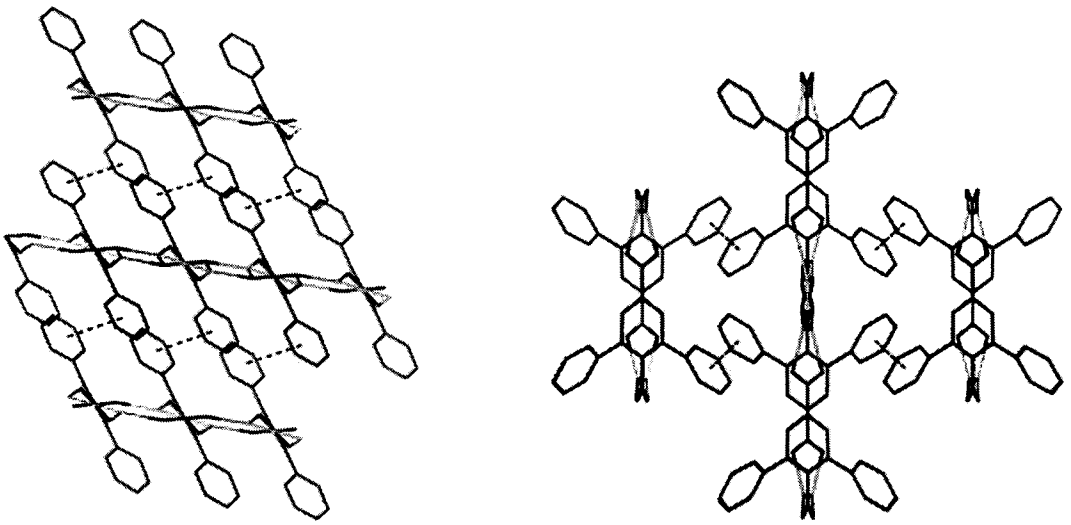

Reproduced with permission from Dickie, D. A.; Schatte, G.; Jennings, M. C.; Jenkins, H. A.; Khoo, S. Y. L.; Clyburne, J. A. C. *Inorg. Chem.*, **2006**, *45*, 1646-1655. Copyright 2006 American Chemical Society.

The *m*-terphenyl ligands are arranged so that the phenyl substituents lie above and below the plane of the 2-D sheet-like network (Figure 3.15). This allows the phenyls to engage in face-to-face π-stacks with the layers above and below. The interaction, which has a centroid···centroid distance of 3.823 Å, is longer than benzene-benzene stacks (3.77 Å),[232] but in the absence of other interactions, the shear number of them surely contributes substantially to the structure of the network.

Finally, in another attempt to prepare a low-coordinate, pyridine-free network, **15H$_2$** was combined with zinc nitrate in ethanol. Triethylamine was chosen as the deprotonating agent because of its poor metal-coordination properties compared to pyridine. The base was allowed to slowly diffuse into the reaction mixture as a vapour, leading to the formation of **22** (Figure 3.16), with a crystallographically determined formula of **15**·Zn·(EtOH)$_2$, although elemental analysis results were off by nearly one and half percent for carbon. Both ends of the bifunctional ligand were deprotonated, and two molecules of solvent were incorporated into the structure.

Figure 3.16 Structure of [15·Zn·(EtOH)$_2$] 22. Thermal ellipsoids are shown at 50% probability and all hydrogen atoms except O-H, and one of two disordered ethanol molecules have been removed for clarity. The ethanols were refined isotropically and are shown as sticks.

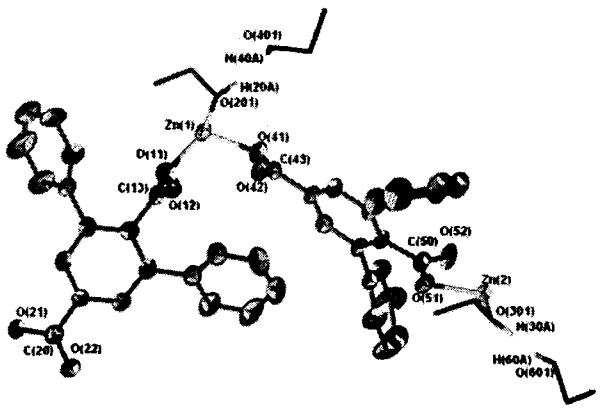

Reproduced with permission from Dickie, D. A.; Schatte, G.; Jennings, M. C.; Jenkins, H. A.; Khoo, S. Y. L.; Clyburne, J. A. C. *Inorg. Chem.*, **2006**, *45*, 1646-1655. Copyright 2006 American Chemical Society.

The X-ray structure shows two crystallographically distinct molecules. The *para*-carboxylates bridge two symmetry-related zinc atoms to form an eight-membered $Zn_2C_2O_4$ heterocycle that makes up the corner of each repeat unit in the rectangular 2-D network of the extended structure (Figure 3.17). The zinc ions are further coordinated to one oxygen from the pocket carboxylate and one ethanolic oxygen.

Figure 3.17 Rectangular grid formed by 22, shown in crystal structure and schematically.[242]

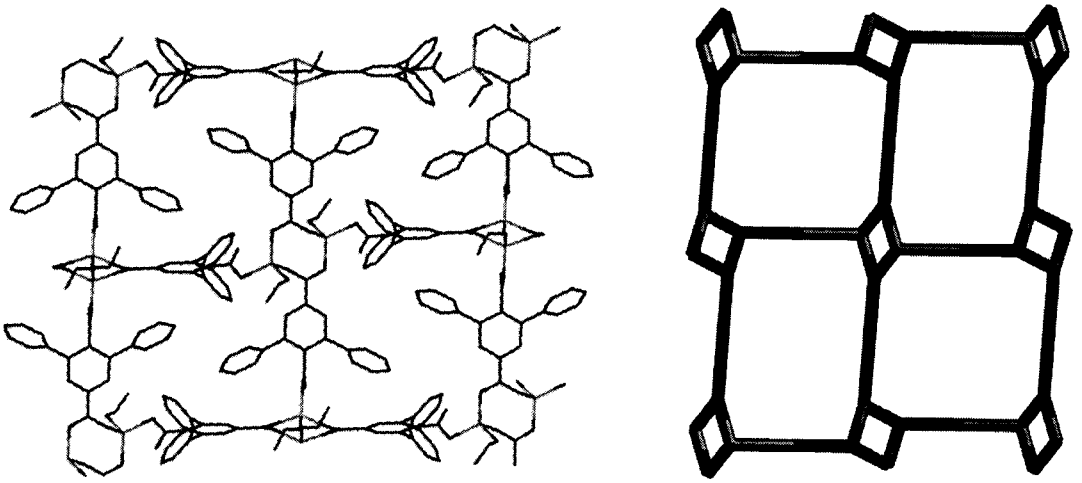

Reproduced with permission from Dickie, D. A.; Schatte, G.; Jennings, M. C.; Jenkins, H. A.; Khoo, S. Y. L.; Clyburne, J. A. C. *Inorg. Chem.*, **2006**, *45*, 1646-1655. Copyright 2006 American Chemical Society.

Table 3.8 Selected structural data for[15·Zn·(EtOH)$_2$] 22.

Bond lengths (Å)			
Zn(1) – O(41)	1.943(4)	Zn(2) – O(22)#2	1.943(4)
Zn(1) – O(42)#1	1.936(4)	Zn(2) – O(21)#3	1.953(4)
Zn(1) – O(11)	1.973(4)	Zn(2) – O(51)	1.948(4)
Zn(1) – O(201)	2.008(4)	Zn(2) – O(301)	1.980(5)
O(11)-C(13)	1.265(7)	C(50)-O(52)	1.218(7)
O(12)-C(13)	1.242(7)	C(50)-O(51)	1.271(7)
O(41)-C(43)	1.258(7)	C(20)-O(21)	1.256(7)
O(42)-C(43)	1.269(6)	C(20)-O(22)	1.261(6)
Bond angles			
O(41)-Zn(1)-O(42)#1	129.81(17)	O(22)#2-Zn(2)-O(21)#3	111.93(18)
O(41)-Zn(1)-O(11)	112.67(17)	O(22)#2-Zn(2)-O(51)	115.21(16)
O(42)#1-Zn(1)-O(11)	112.17(17)	O(21)#3-Zn(2)-O(51)	116.18(16)

Symmetry transformations used to generate equivalent atoms: #1 -x, -y, -z+3; #2 -x, -y, -z+2; #3 x+1, y+1, z; #4 x-1, y-1, z

For each zinc ion, a second equivalent of ethanol is held in place by hydrogen bonds to the metal-bound ethanol and the extra pocket-carboxylate oxygen (Figure 3.18). Both molecules of ethanol are intercalated into the space between the layers of the 2-D network, suggesting that they could be removed without affecting the structural integrity of the network. Thermogravimetic analysis (TGA) showed a 20% weight loss, consistent with two molecules of ethanol, up to 225 °C with no further drop until 350 °C.

Table 3.9 [O-H···O] Hydrogen bond lengths and angles of [15·Zn·(EtOH)$_2$] 22.

Hydrogen bond lengths (Å)			
H(20A)···O(401)	1.80	O(201)···O(401)	2.604(10)
H(30A)···O(501)	1.88	O(301) ···O(501)	2.635(11)
H(30A)···O(601)	1.76	O(301) ···O(601)	2.580(13)
H(40A)···O(12)#1	1.88	O(401))···O(12)#1	2.698(9)
H(50A)···O(52)#5	2.04	O(501) ···O(52)#5	2.794(11)
H(60A)···O(301)	2.10	O(601) ···O(301)	2.580(13)
Hydrogen bond angles (°)			
O(201)-H(20A)···O(401)	168.7	O(401)-H(40A)···O(12)#1	176.0
O(301)-H(30A)···O(501)	152.2	O(501)-H(50A)···O(52)#5	152.7
O(301)-H(30A)···O(601)	176.2	O(601)-H(60A)···O(301)	117.4

Symmetry operations used to generate equivalent atoms: #1 -x, -y, -z+3; #5 -x+1, -y+1, -z+2

Figure 3.18 Hydrogen bonds in[15·Zn·(EtOH)$_2$] 22.

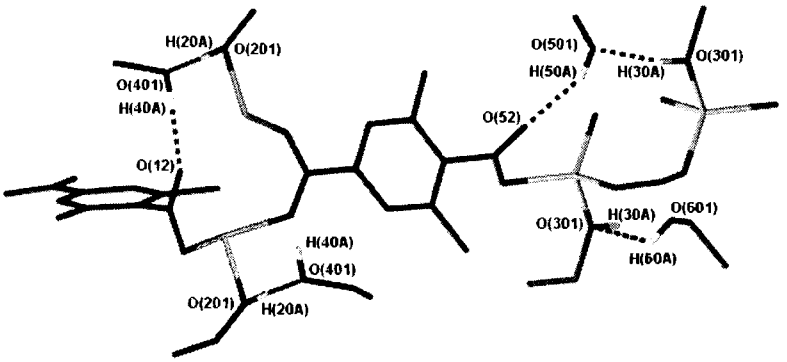

Reproduced with permission from Dickie, D. A.; Schatte, G.; Jennings, M. C.; Jenkins, H. A.; Khoo, S. Y. L.; Clyburne, J. A. C. *Inorg. Chem.*, **2006**, *45*, 1646-1655. Copyright 2006 American Chemical Society.

Figure 3.19 Thermogravimetric analysis of [15·Zn·(EtOH)$_2$] 22.

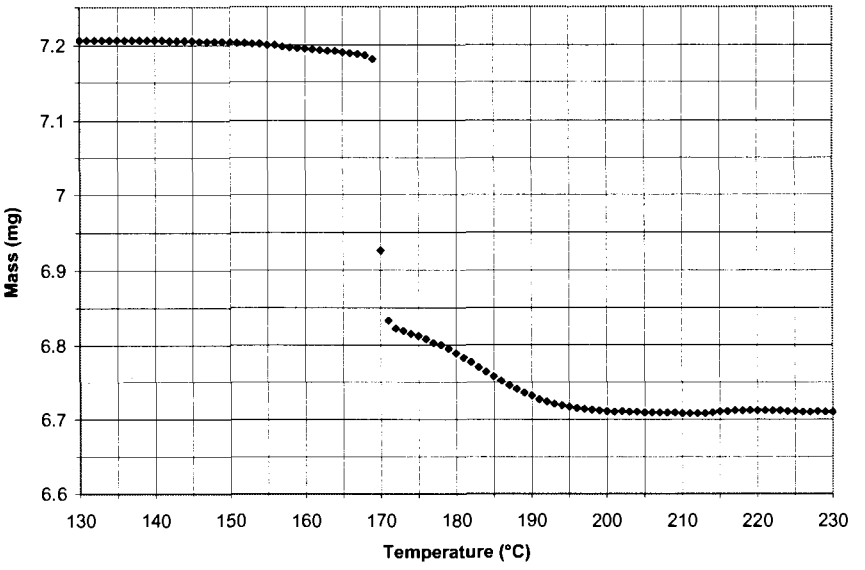

3.3 Summary and conclusions

Less than 15 years ago, playwright, poet and Nobel prize-winning chemist Roald Hoffmann stated that

> ... in two or three dimensions, it's a synthetic wasteland. The methodology for exercising control so that one can make unstable but persistent extended structures on demand is nearly absent. Or to put it in a positive way – this is a certain growth point of the chemistry of the future.[243]

Much progress has certainly been made since this was written, but scientists are still not at the point of being able to predict absolutely the structure of most MOCNs based on a particular ligand and metal salt. The two copper compounds, **19** and **20**, demonstrated how very different topologies could result from the same starting materials, while the one-dimensional chains **17** and **18** had the same structure despite using different metals. Taken together, the compounds **17-22** show that the sterically demanding ligand **15H$_2$** is able to shield metal sites from aggregation and network interpenetration, while still allowing for small molecules (pyridine or solvent) to

coordinate. This bodes well for eventual applications in gas sorption and/or catalysis, even though a three-dimensional network with permanent porosity based on **15H$_2$** has not yet been prepared. In most cases presented here, hydrogen-bonding or other supramolecular interactions play an important role in determining the overall topology of the networks or chains. The choice of base, solvent and reaction stoichiometry also influence product formation, but the structures are dominated, for the most part, by the bulky *m*-terphenyl ligand that effectively limits the dimensionality of the networks to two.

3.4 Future work

Now that an initial synthetic survey of MOCNs based on the bifunctional *m*-terphenyl ligand 2,6-diphenylterephthalic acid **15H$_2$** has been completed, an in-depth study of the properties of the most promising complexes should be undertaken. Although space-filling diagrams the complexes suggest that they lack permanent porosity, they should nevertheless be tested[209] for their ability to absorb and release guest molecules. Compound **22**, which appears to release ethanol upon heating, is the most likely to exhibit this "porosity without pores"[210] and should be the first complex to be tested for its ability to exchange guest molecules in both liquid and vapour phases.

The best test molecules would be small organic molecules with heteroatoms able to act as Lewis bases towards the unsaturated Zn centre, and to engage in hydrogen bonds with the free carboxylate oxygen of the *m*-terphenyl ligand. Ideally, the crystallinity of the network would be retained throughout the guest exchange, allowing for characterization via single crystal X-ray diffraction, but data from IR spectroscopy and thermogravimetric analysis would also be informative. Preliminary results of powder

diffraction studies suggest that while some long-range order is present in desolvated **22**, it does not retain its single-crystal character. This work should be followed up in order to clarify the nature of the desolvated material

The difference in reaction conditions between the one-dimensional zinc **17** and cobalt **18** chains resulted in no change between their structures, while a similar difference in the preparation of the copper networks **19** and **20** gave two remarkably different outcomes. Careful studies of solvent, concentration, and pH dependence are necessary in order to understand better the factors influencing the network formation. TGA studies of the two copper compounds would also be interesting, to see if it is possible to remove some or all of the pyridine molecules with disrupting the hydrogen bonds holding the networks together. If that proves possible, then these compounds should be investigated for guest-exchange in a similar manner to **22**. Finally, someone with suitable expertise should examine the magnetic properties of **18-20** (cobalt and copper), and the luminescence of the silver network **21**.

3.5 Experimental

3.5.1 Synthesis of organic molecules

4-Methyl-2,6-diphenylbenzoic acid (14): Under an inert atmosphere, phenylmagnesium bromide (165 mL, 1.0 M in THF) was added dropwise to a stirred solution of 2,6-dibromo-1-iodo-4-methylbenzene (20.0 g, 253.2 mmol) in 30 mL anhydrous THF. After 3.5 h, dry CO_2 was bubbled through the reaction mixture for 2.5 h. The reaction was quenched with H_2O and dilute (ca. 1 M) HCl, then extracted with Et_2O. The combined organic fractions were dried over $MgSO_4$ and the solvent was

removed under vacuum to give a yellow-orange solid that was recrystallized from hexanes to give colourless crystals. Yield = 10.7 g (70%), mp = 242-243 °C. ^{1}H NMR ($CDCl_3$, 500 MHz) δ 7.35-7.43 (m, 10H), 7.19 (s, 2H), 2.45 (s, 3H). $^{13}C\{^{1}H\}$ NMR ($CDCl_3$, 125 MHz) δ 173.4, 140.7, 140.6, 139.9, 130.4, 129.9, 129.1, 128.9, 128.6, 128.5, 127.7, 21.5. IR (nujol, cm^{-1}) ν 1683 (s), 1598 (m), 1495 (m), 1299 (s), 1189 (w), 1115 (w), 951 (w), 871 (w), 784 (w), 773 (m), 699 (s). HR-MS (*m/z*): [M^+] calculated for $C_{20}H_{16}O_2$, 288.1150; Found, 288.1145.

2,6-Diphenylterephthalic acid (15H$_2$): Potassium permanganate (4.11 g, 26.0 mmol) and sodium carbonate (3.00 g, 28.3 mmol) were dissolved in 100 mL water. To this solution 4-methyl-2,6-diphenylbenzoic acid **14** (3.00 g, 10.4 mmol) and Tide® laundry detergent (0.30 g) were added. The mixture was heated to reflux for 2 h then cooled to r.t. Sodium bisulfite was added in small solid portions until the solution was colourless, and then the brown precipitate was removed by filtration through Celite. The solution was cooled to 0 °C and concentrated HCl (12 mL) was added dropwise, resulting in the formation of a white precipitate. The mixture was extracted with Et_2O and the combined organic fractions were dried over $MgSO_4$. Slow evaporation of the solvent gave colourless crystals. Yield = 2.59 g (82%), mp = 325-327 °C. ^{1}H NMR (DMSO-d_6, 499.770 MHz) δ 13.1 (br s, O*H*), 7.87 (s, 2H), 7.39-7.49 (m, 10H). $^{13}C\{^{1}H\}$ (DMSO-d_6, 125.680 MHz) δ 170.2, 167.1, 140.0, 139.9, 138.2, 133.5, 131.9, 130.1, 129.9, 129.2, 129.0, 128.6. IR (nujol) ν 1692 (s), 1568 (w), 1496 (w), 1337 (w), 1267 (m), 1098 (w), 787 (w), 700 (w). Anal. Calcd for $C_{20}H_{14}O_4$: C, 75.46; H, 4.43. Found: C, 75.57; H, 4.48.

15·bipy (16): 4,4′-Bipyridyl (0.12 g, 0.78 mmol) was dissolved in 5 mL ethanol and added dropwise to a solution of 2,6-diphenylterephthalic acid **15H$_2$** (0.25 g, 0.78 mmol) in 5 mL ethanol. Slow evaporation at r.t. over three days gave large, colourless crystals. Yield: 0.27 g (73%), mp = 225 °C. ^{1}H NMR (DMSO-d$_6$, 400.136 MHz) δ 8.72 (d, J = 4.6 Hz, 4H), 7.87 (s, 2H), 7.83 (d, J = 4.7 Hz, 4H), 7.43-7.49 (m, 10H). IR (nujol) ν 1704(s), 1599 (s), 1405 (m), 1283 (m), 1260 (s), 1214 (s), 1137 (w), 1057 (m), 1050 (m), 903 (w), 807 (s), 782 (s), 759 (s), 720 (m), 697(s), 628 (s). Anal. Calcd for $C_{30}H_{22}N_2O_4$: C, 75.94; H, 4.67; N, 5.90. Found: C, 75.62; H, 4.81; N, 5.71.

3.5.2 Synthesis of metal chains and networks

1-D zinc chain [15·Zn·(py)$_2$·MeOH] (17): 2,6-Diphenylterephthalic acid **15H$_2$** (0.25 g, 0.78 mmol) and $Zn(NO_3)_2·6H_2O$ (0.23 g, 0.78 mmol) were combined and dissolved in 8 mL warm methanol. This solution was layered onto a solution of 0.1 mL pyridine in 8 mL benzene. After one week, the solution was carefully decanted from a white precipitate and allowed to evaporate slowly to give white crystals. Yield = 0.25 g (56%, based on Zn), mp >350 °C. IR (nujol) ν 3447 (br), 1693 (m), 1632 (w), 1606 (m), 1585 (m), 1573 (m), 1546 (m), 1447 (s), 1310 (m), 1153 (m), 1071 (m), 1042 (m), 913 (m), 796 (m), 753 (m), 698 (s). Anal Calcd for $C_{31}H_{26}N_2O_5Zn$: C, 65.10; H, 4.58; N, 4.90. Found: C, 63.18; H, 4.61; N, 5.74.

1-D cobalt chain [15·Co·(py)$_2$·MeOH] (18): A solution of $Co(NO_3)_2·6H_2O$ (0.15 g, 0.51 mmol) in 5 mL methanol was added to a solution of 2,6-diphenylterephthalic acid **15H$_2$** (0.35 g, 1.10 mmol) in 15 mL methanol and 1 mL pyridine. Slow evaporation of the solvent at r.t. gave dark pink crystals within hours. Yield = 0.25 g (87%, based on

Co), mp >320 °C (dec.) IR (nujol) ν 1601 (s), 1574 (s), 1538 (s), 1493 (m), 1486 (m), 1444 (vs), 1369 (vs), 1275 (w), 1216 (w), 1151 (w), 1070 (w), 1040 (s), 912 (m), 809 (m), 795 (s), 781 (m), 752 (s), 698 (vs). Anal Calcd for $C_{31}H_{26}CoN_2O_5$: C, 65.84; H, 4.63; N, 4.95. Found: C, 65.52; H, 4.94; N, 4.99.

2-D copper network [(15H)$_2$·Cu·(py)$_2$] (19): 2,6-Diphenylterephthalic acid **15H$_2$** (0.25 g, 0.78 mmol) and $Cu(NO_3)_2 \cdot 2.5H_2O$ (0.18 g, 0.78 mmol) were dissolved in 8 mL ethanol. This solution was layered onto a solution of 0.1 mL pyridine in 8 mL benzene. After one week, the solution was carefully decanted from a blue precipitate and allowed to evaporate slowly to give blue crystals. Yield = 0.26 g (39%, based on Cu), mp = 270-272 °C. IR (nujol) ν 1867 (br), 1682 (vs), 1612 (m), 1580 (s), 1557 (s), 1455 (vs), 1331 (m), 1240 (s), 1219 (s), 1154 (m), 1106 (m), 1075 (m) 1049 (m), 912 (m), 822 (s), 695 (vs). Anal Calcd for $C_{50}H_{36}N_2O_8Cu$: C, 70.13; H, 4.24; N, 3.27. Found: C, 70.05; H, 4.34; N, 3.34.

2-D copper network [(15H)$_2$·Cu·(py)$_4$·(H$_2$O)$_2$] (20): A solution of $Cu(NO_3)_2 \cdot 2.5H_2O$ (0.12 g, 0.51 mmol) in 5 mL methanol was added to a solution of 2,6-diphenylterephthalic acid **15H$_2$** (0.35 g, 1.10 mmol) in 5 mL methanol and 1 mL pyridine. Slow evaporation of the solvent at r.t. gave dark blue crystals within hours. Yield = 0.33 g (62% based on Cu), mp = 93-98 °C (dec). IR (nujol) ν 3464 (s), 3063 (w), 3024 (w), 1964 (br), 1693 (m), 1605 (s), 1581 (s), 1564 (s), 1557 (s), 1493 (s), 1448 (vs), 1337 (s), 1283 (s), 1269 (vs), 1235 (w), 1218 (w), 1154 (m), 1103 (w), 1068 (s), 1042 (m), 905 (m), 818 (s), 788 (w), 777 (s), 757 (vs), 720 (s), 698 (vs). Anal Calcd for $C_{60}H_{50}CuN_4O_{10}$: C, 68.59; H, 4.80; N, 5.33. Found: C, 68.38; H, 4.80; 5.43.

2-D silver network [15·Ag_2] (21): A solution of the dipotassium salt of 2,6-diphenylterephthalate **15** (10 mL, 0.1M in H_2O) was isolated from the synthesis of **$15H_2$** prior to acidification and placed in a test tube. A solution of 2:1 MeOH/H_2O (6 mL) was carefully layered onto the potassium solution. Silver nitrate (0.17 g, 1.0 mmol) was dissolved in 8 mL warm methanol and layered onto the mixed solvent. The test tube was kept in the dark for one week, and then the solution was decanted off to leave needle-like crystals. Yield = 0.04 g (7.5% based on Ag), mp >350 °C. IR (nujol) 1611 (w), 1583 (vs), 1544 (m), 1536 (m), 1509 (m), 1492 (s), 1318 (m), 1156 (m), 1073 (m), 1029 (m), 914 (w), 880 (m), 832 (s), 805 (m), 766 (m), 750 (s), 722 (m), 701 (vs). Elemental analysis not performed due to low yield.

2-D zinc network [15·Zn·$(EtOH)_2$] (22): A solution of $Zn(NO_3)_2·6H_2O$ (0.47 g, 1.57 mmol) in 10 mL ethanol was added to a solution of 2,6-diphenylterephthalic acid **$15H_2$** (0.50 g, 1.57 mmol) in 10 mL ethanol. Triethylamine (0.5 mL) was allowed to vapour diffuse into the reaction mixture. After one week, colourless crystals were isolated. Yield = 0.26 g (35%), mp >350 °C. IR (nujol) 3367 (br), 1604 (s), 1557 (s), 1495 (w), 1318 (w), 1051 (m), 700 (m), 668 (w). Anal Calcd for $C_{24}H_{24}O_6Zn$: C, 60.84; H, 5.11. Found: C, 59.36; H, 5.40.

4 GOLD-THIOL SELF-ASSEMBLED MONOLAYERS*

In 1983, Nuzzo and Allara reported the first example of self-assembled monolayer (SAM) formation by the adsorption of disulfides on a gold surface.[244] Since that time, the chemisorption of organosulfur compounds such as thiols, sulfides and disulfides on gold surfaces has become quite widespread, surpassing other chemisorbed SAM systems including carboxylic acids on metal oxides or silanes on glass.[245] Part of the popularity of gold-thiol SAMs stems from the fact that they are generally stable with respect to hydrolysis, and can be prepared from either gas phase or solution phase reactions.[246] The structurally well-defined surfaces of SAMs have found a variety of applications including, but not limited to, templates for semiconductor crystal growth,[247] sensor development,[248] polymer supports,[249] electrochemistry[250] and nanomaterials.[251] This type of SAM is also commonly used for immobilising proteins or other biological macromolecules for analysis[252] or even catalysis.[253]

4.1 Traditional SAMs

The most common organosulfur compounds used in SAM formation are ω-functionalized alkylthiols.[254] Occasionally, instead of flexible alkyl chains, rigid thioaromatic molecules[255] such as *p*-terphenyls are used due to their potential for electrical conductivity.[256] The typical thiol adsorbate is divided into three distinct regions: the sulphur atom that binds to the gold with an average bond energy of 50

* Portions of this chapter are reproduced in part, with permission, from the following journal article: Dickie, D. A.; Chan, A. Y. C.; Jalali, H.; Jenkins, H. A.; Yu, H.-Z.; Clyburne, J. A. C. *Chem. Commun.* **2004**, 2432-2433 (Copyright 2004, Royal Society of Chemistry).

kcal/mol, the alkyl linker fragment whose hydrophobic interactions contribute 1-2 kcal/mol of stabilization energy per methylene, and the all important ω-terminal head group,[246] the most common of which is the carboxylic acid.[257] While this portion of the molecule has limited impact on the self-assembly process, it is the primary point of interaction with solution-phase analyte molecules.

4.1.1 Problems with surface density of traditional SAMs

Both alkyl and aryl thiols form well-organized, closely-packed monolayers. While this close-packing is often desirable, for example in the SAM-mediated synthesis of molecular wires,[258] certain applications require lower density surfaces. In many applications involving biological macromolecules or other large analytes, it is advantageous to have a low-density surface in which the ω-terminal functionality is isolated from its neighbours to prevent aggregation and undesired steric restrictions.[252a] A common approach for achieving this goal is to shorten the immersion time of the substrate in the deposition solution.[259] This method offers very little control over the arrangement of and the environment around the ω-terminal functional groups on the SAM. Since studies have shown that the chemical and physical properties of surfaces are dependent on structure,[260] such imprecision may be detrimental to many applications.

Recently, two groups have developed new routes to prepare low-density monolayers. Langer et al. designed alkanethiols with bulky head groups[261] while Liu used substituted alkanethiols wrapped with cyclodextrins.[262] Both of these approaches make use of protecting groups. The low-density surfaces are achieved by removal, after SAM

formation, of either the head group or cyclodextrin to leave isolated ω-carboxyl terminated alkyl chains.

4.2 *m*-Terphenyls in SAMs

The need for removable protecting groups is not a particularly atom-economical route to low-density functionalized surfaces. A logical alternative would be permanent steric control through the organic adsorbate. The rigid and bulky nature of *m*-terphenyl molecules make them appealing targets for the formation of SAMs with inherently low density ($<1.4\times10^{-10}$ mol/cm^2). In addition, because each carboxylic acid group is isolated within an individual hydrophobic pocket, a high acid-dissociation (pK_a) on the surface would be expected, *i.e.* the carboxyl group would be in the protonated form over a large pH range.[263] This is desirable because many biological macromolecules attach to the surface *via* amide or hydrogen bond formation. We therefore aimed to prepare a bifunctional *m*-terphenyl with a carboxylic acid group in the pocket and a mercaptomethyl group in the *para* position.

4.2.1 Ligand synthesis and characterization

No precedent for *m*-terphenyl gold-thiol SAMs is known, but they have been featured in Langmuir monolayers,[264] and structurally related pyrylium ions have been attached to polymer surfaces for use as colorimetric sensors.[265] The first step in the preparation of a *m*-terphenyl decorated SAM, therefore, was the development of a bifunctional ligand similar to that used in the networks of Chapter 3, but with a thiol substituent in place of the *para* carboxylate. The radical bromination of 4-methyl-2,6-diphenylbenzoic acid **14** with *N*-bromosuccinimide in benzene is initiated with benzoyl

peroxide. This synthetic route was based on the conversion of *p*-toluic acid to the brominated derivative.[266] After heating to reflux for several hours, a white powder characterized as 4-bromomethyl-2,6-diphenylbenzoic acid **23** was isolated.

Scheme 4.1 Syntheses of 4-bromomethyl-2,6-diphenyl benzoic acid 22 and 4-mercaptomethyl-2,6-diphenylbenzoic acid 23.

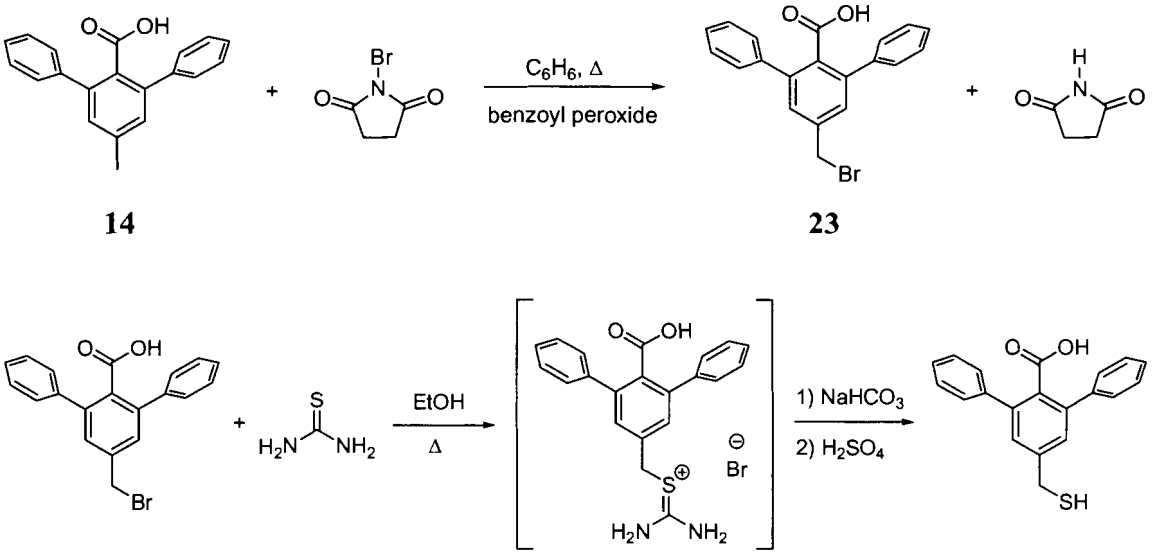

Following procedures developed for the synthesis of 4-mercaptomethylbenzoic acid,[267] **23** can be combined with thiourea in ethanol to give a salt that is then transformed by saponification and acidification into the thiol-substituted *m*-terphenyl 4-mercaptomethyl-2,6-diphenylbenzoic acid **24**. The ^{1}H NMR spectrum of **24** shows a triplet at 3.08 ppm and a doublet at 3.81 ppm due to the S*H* and CH_2 respectively. The IR spectrum shows a strong ν C=O absorption at 1693 cm^{-1}. Neither **22** nor **24** formed crystals suitable X-ray crystallographic analysis; however, a crystal structure of **14** was obtained, which allowed us to assess the steric hindrance at the binding site.*

* Structure of **14** solved by Dr. Hilary Jenkins, Saint Mary's University.

Figure 4.1 Structure of 4-methyl-2,6-diphenylbenzoic acid 14.

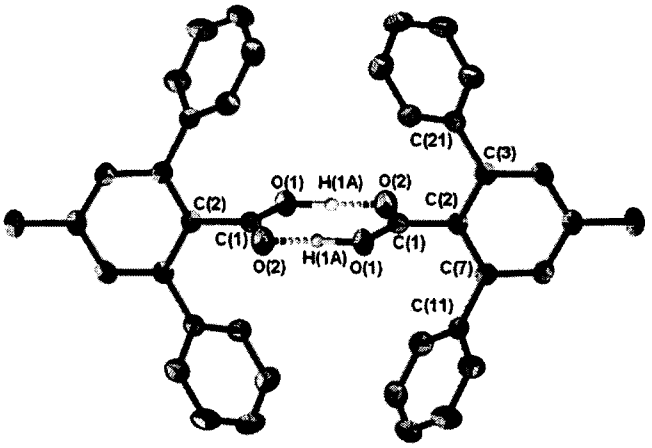

Table 4.1 Selected structural data for 4-methyl-2,6-diphenylbenzoic acid 14.

Bond lengths (Å)			
O(1)-C(1)	1.269(2)	O(1)···O(2)#1	2.6234(18)
O(2)-C(1)	1.261(2)	H(1A)···O(2)#1	1.40(2)
Bond angles (°)			
O(1)-C(1)-O(2)	124.04(16)	O(1)-H(1A)···O(2)#1	173.7(18)

Symmetry transformations used to generate equivalent atoms: #1 -x,-y,-z

Analysis of the X-ray crystal structure shows that **14** (Figure 4.1) exists in the solid state as a hydrogen-bonded dimer. The ring formed by the carboxylate groups is twisted approximately 65° out of the plane of the central phenyl ring, while the flanking phenyls are found at angles of 45° [C(21) ring] and 51° [C(11) ring]. The C-O bonds are equal within experimental error, indicating delocalization within the carboxylate framework. These bonds lengths, as well as the [O(1)-H(1A)···O(2)] hydrogen bond, are indistinguishable from those found in the pocket of the bifunctional *m*-terphenyl **15H$_2$**. From the structural parameters of **14**, it was possible to estimate the surface coverage of **24**. As shown in Figure 4.2,* each molecule in the upright position occupies an area of

* Figure prepared with the assistance of Dr. Len Barbour, University of Stellenbosch, from the X-ray crystallographic data of **14** using modified X-Seed software.

ca. 112 $Å^2$. This corresponds to a surface coverage of 1.48×10^{-10} mol/cm^2, comparable to the density of cyclodextrin-modified surfaces (0.99 to 2.08×10^{-10} mol/cm^2).[262]

Figure 4.2 **Estimated surface coverage of *m*-terphenyl thiols, as shown by the shadow cast on a surface by the solid-state space-filling model of 14. The grid size is 0.5 Å.**

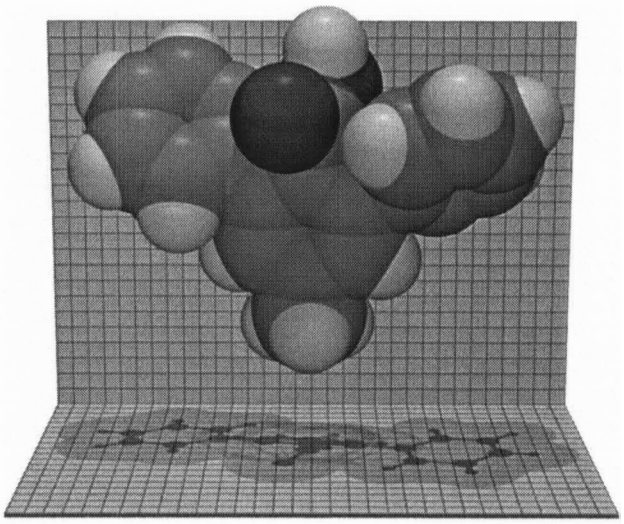

Reproduced with permission from Dickie, D. A.; Chan, A. Y. C.; Jalali, H.; Jenkins, H. A.; Yu, H.-Z.; Clyburne, J. A. C. *Chem. Commun.* **2004**, 2432-2433. Copyright 2004 Royal Society of Chemistry.

4.2.2 Surface characterization by FTIR spectroscopy

All work related to the *m*-terphenyl SAM formation and characterization was done by undergraduate students Hanifa Jalali and Andy Chan in collaboration with Dr. Hogan Yu at Simon Fraser University.* The *m*-terphenyl SAMs were formed by the immersion of clean gold substrates for 24 hours in deoxygenated 1.0 mM 9:1 ethanol-acetic acid solutions of **24**. The addition of acetic acid is essential as it decreases the hydrogen-bonded dimerization of **24** in solution.[254,268] Finally, the modified gold substrate was washed sequentially with solvent mixture and deionized water to remove any unbound molecules.

* Experimental details can be found in: Dickie, D. A.; Chan, A. Y. C.; Jalali, H.; Jenkins, H. A.; Yu, H.-Z.; Clyburne, J. A. C. *Chem. Commun.* **2004**, 2432-2433.

The FTIR (Figure 4.4a) of the modified gold surfaces shows peaks that are consistent with the formation of a monolayer of **24**. Most importantly, the ν C=O absorption at 1671 cm^{-1} confirms the presence of the carboxylate functionality on the surface. Additional peaks for ν C-O are present at 1148 and 1092 cm^{-1} and C=C aromatic stretches from the *m*-terphenyl appear at 1594 and 1466 cm^{-1}. In contrast to long chain *n*-alkanethiolate SAMs, the bands in the region of 2700-3200 cm^{-1} corresponding to CH_2 stretches are rather weak because only one methylene group is present in the *m*-terphenyl thiol **24**. The low-density packing of the molecules in the SAM also reduces the signal intensity. Further evidence supporting monolayer formation was provided by collecting the FTIR spectrum of the modified surface under both p-polarized and s-polarized light. Surface selection rules indicate that FTIR absorptions will be observed only under p-polarization if a monolayer is present, but both s- and p-polarization will provide spectra for a bilayer or greater.[269] In the case of gold surfaces modified with **24**, the FTIR spectrum was visible only under p-polarized light.

Figure 4.3 Schematic representation of SAM of *m*-terphenyl thiol 24 after reaction with adenine.

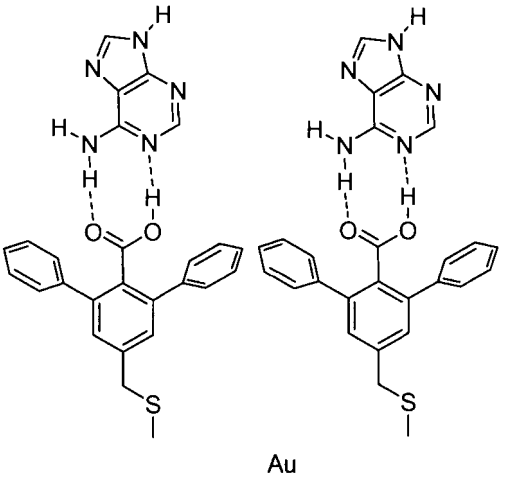

Figure 4.4 **FTIR spectra of *m*-terphenyl SAMs formed from the adsorption of 24 on gold (A) and after further reaction with adenine/THF solution (B).**

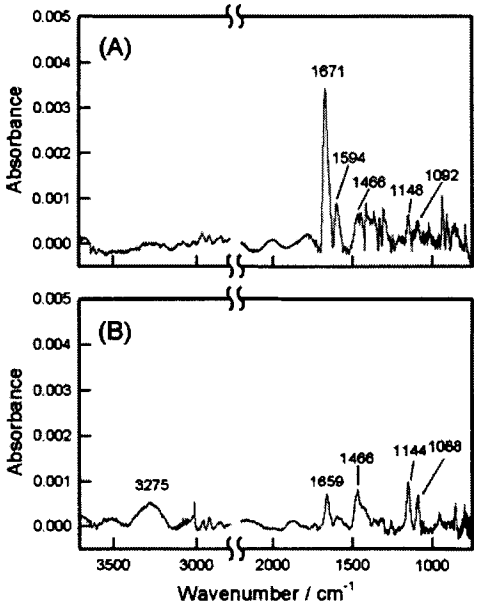

Reproduced with permission from Dickie, D. A.; Chan, A. Y. C.; Jalali, H.; Jenkins, H. A.; Yu, H.-Z.; Clyburne, J. A. C. *Chem. Commun.* **2004**, 2432-2433. Copyright 2004 Royal Society of Chemistry.

The reactivity of the *m*-terphenyl SAM was demonstrated by the treatment of the monolayer with a THF solution of adenine (2.7 mM). Adenine forms hydrogen bonds with the carboxylate group on surface (Figure 4.3) and significantly changes the FTIR spectrum (Figure 4.4b). The most obvious change is the appearance of a band at 3275 cm^{-1} for the NH stretch. The peak with shoulders at 1466 cm^{-1} may be attributed to both C=C aromatic stretches (*m*-terphenyls) and imidazole ring stretches (adenine, at 1453 cm^{-1}). Another change upon binding of adenine is the shift of the carboxylate C=O stretch from 1671 to 1659 cm^{-1} and the C-O stretches from 1148 and 1092 cm^{-1} to 1144 and 1088 cm^{-1}, respectively. The clear decrease of the overall absorbance also indicates the formation of an additional layer of molecules on top of the SAMs of **24** on gold.

4.2.3 Surface characterization by contact angle measurement

Wetting measurements were further used to characterize the SAM of **24** on gold. This method (Figure 4.5) involves the measurement of the contact angle between a buffered water droplet and the surface.[270] At high pH, carboxyl-terminated surfaces become more hydrophilic due to the formation of the carboxylate anion and show decreased contact angles. Conversely, as the pH decreases, the protonated surface becomes more hydrophobic and contact angles increase.

Figure 4.5 **Schematic representation of contact angle measurements at high (left) and low (right) pH.**

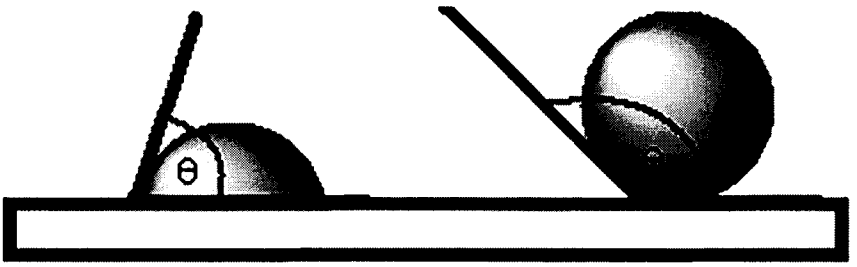

Figure 4.6 **Contact angle titration curve of *m*-terphenyl SAMs prepared from the adsorption of 24 on gold, measured using a nonreactive spreading protocol.**

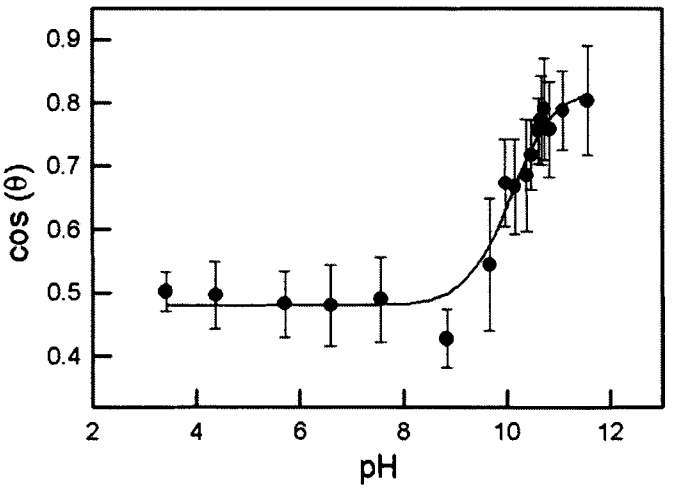

Reproduced with permission from Dickie, D. A.; Chan, A. Y. C.; Jalali, H.; Jenkins, H. A.; Yu, H.-Z.; Clyburne, J. A. C. *Chem. Commun.* **2004**, 2432-2433. Copyright 2004 Royal Society of Chemistry.

The plot of contact angle versus pH (Figure 4.6) represents a typical titration curve of surface carboxyl groups. The pK_a of the surface was evaluated by fitting the experimental data with the help of previously developed procedures.[270] To minimise errors associated with salt formation on the surface by different buffers and to ensure reproducibility, measurements were repeated on several spots on different samples. The pK_a of the SAM of the *m*-terphenyl **24** on gold was found to be 10.1±0.2, significantly higher than that of similar *m*-terphenyl carboxylic acids in solution (6.39).[263] It should be also noted that neither the protonated nor deprotonated forms of the surface are completely hydrophilic, which would be expected for a surface that was completely covered by carboxyl groups (e.g., 11-mercaptoundecanoic acid SAMs). This indicates that the surface density of carboxyl groups is relatively low, as desired, and that they are isolated by the hydrophobic terphenyl pockets.

4.3 Summary and conclusions

The new bifunctional thiol-carboxylate *m*-terphenyl molecule **24** was synthesized and used, in collaboration with Dr. Hogan Yu, to form a SAM on a gold substrate. The resultant SAM had a pK_a of 10.1 ± 0.2. Contact angle measurements showed that the use of the *m*-terphenyl backbone results in a surface with higher hydrophobicity than more traditional alkyl carboxylate surfaces. Finally, the well-isolated carboxyl groups were found to be amenable further reactions with biomolecules as shown by reaction with adenine.

4.4 Future work

The results obtained in this collaborative project could provide the basis for a number of new explorations. The present study used only spectroscopic techniques to characterize the SAM surface, but additional useful information such as the packing of the *m*-terphenyls on the surface could likely be obtained from scanning tunnelling microscopy[271] and other non-spectroscopic techniques.[272] Such techniques would also help confirm that **24** does indeed form a monolayer on gold, not a bilayer or other higher dimensionality aggregate.

Once a better understanding of the SAM surface features is available, it might be possible to exploit the isolated pocket-like environment to create DNA microarrays or "DNA chips" with optimized surface probe density for biological analysis.[273] Alternatively, the hydrogen-bonding capabilities of the ω-terminal carboxylic acid could be used as anchor points and nucleation sites for the self-assembly of electro-optic films[274] or epitaxial crystal growth.[275]

Another interesting investigation would be to reverse the location of the functional groups on the *m*-terphenyl molecules. Placing the thiol within the pocket, which would now be facing downward onto the surface, would result in a remarkably different environment for the carboxylic acid in the *para* position. It would retain similar spacing from neighbouring functional groups, but would no longer have any steric protection from the *m*-terphenyl. This would almost certainly lead to unusual reactivity of the carboxylic acid group towards other functionalized molecules.

Finally, the *m*-terphenyl thiol **24** should be tested for its ability to stabilize the formation of gold nanoparticles. Much research has been done to try to control the size

and shape of gold nanoparticles,[276] and it has long been known that the ratio of thiol stabilizer to metal can have a profound impact on the size of the resulting nanoparticles.[277] Since the steric demands of the *m*-terphenyl thiol **24** are so different from those of the alkylthiols typically used, they would likely give significantly different results. For example, they might be able to protect the gold surface while occupying fewer sites than alkylthiol stabilizers, leaving more metal atoms available for reaction with small molecules. It would also help overcome the problem of decreased chain-packing density as one gets further from the gold core,[278] since the core itself would always be protected. It may even be possible to use the *m*-terphenyl pocket to isolate and organize chromophores on the nanoparticles surface to produce photo-responsive organic-inorganic hybrid materials.[279]

4.5 Experimental

4-Bromomethyl-2,6-diphenylbenzoic acid (23): 4-Methyl-2,6-diphenylbenzoic acid **14** (2.00 g, 6.94 mmol) and *N*-bromosuccinimide (NBS) (1.36 g, 7.36 mmol) were suspended in 30 mL benzene. Benzoyl peroxide (0.17 g, 0.69 mmol) was added and the mixture was heated to reflux under nitrogen for 3.5 h. An additional portion of NBS (0.33 g, 1.85 mmol) was added and the reflux was continued for another 3 h. The reaction mixture was cooled to r.t. and the solvent was removed under vacuum. The residue was suspended in 20 mL hot H_2O and filtered to give a white powder. Yield = 0.78 g (31%), mp = 214-216 °C. ^{1}H NMR ($CDCl_3$, 499.770 MHz) δ 7.36-7.41 (m, 10H), 7.19 (s, 2H), 4.53 (s, 2H). $^{13}C\{^1H\}$ NMR ($CDCl_3$, 125.680 MHz) δ 173.0, 141.2, 140.7, 139.8, 139.5, 131.7, 129.7, 128.6, 128.1, 32.4. IR (nujol, cm^{-1}) ν 1698 (s), 1599 (w), 1494 (w), 1289 (m), 1277 (m), 1213 (w), 1146 (w), 1116 (m), 1075 (w), 1029 (w), 786

(m), 701 (s). HR-MS (*m/z*): [M^+] calculated for $C_{20}H_{15}BrO_2$, 366.0255; Found, 366.0250.

4-Mercaptomethyl-2,6-diphenylbenzoic acid (24): 4-Bromomethyl-2,6-diphenylbenzoic acid **23** (0.75 g, 2.04 mmol) and thiourea (0.17 g, 2.25 mmol) were suspended in 15 mL ethanol. The mixture was heated to reflux under nitrogen for 2.5 h. The solution was cooled to room temperature and a solution of sodium bicarbonate (0.45 g in 4.5 mL H_2O) was added dropwise to the reaction mixture. The mixture was again heated to reflux under nitrogen for 3 h, then cooled to r.t. and filtered. The solution was acidified with H_2SO_4 and cooled to -20 °C. A pale yellow powder was isolated by filtration. Yield = 0.56 g (86%), mp = 250 °C (dec). ^{1}H NMR (DMSO, 499.770 MHz) δ 7.35-7.44 (m, 10H), 7.18 (s, 2H), 3.81 (d, J = 8.1 Hz, 2H), 3.09 (t, J = 8.1 Hz, 1H). IR (nujol, cm^{-1}) ν 1673 (s), 1598 (m), 1576 (w), 1495 (w), 1295 (m), 1273 (m), 1180 (w), 1117 (w), 1089 (w), 1075 (w), 1045 (w), 1028 (w), 784 (w), 772 (w), 759 (w), 701 (s). HR-MS (*m/z*): [M^+] calculated for $C_{20}H_{16}O_2S$, 320.0871; Found, 320.0871.

5 NEW BIDENTATE *m*-TERPHENYL COMPOUNDS*

"In recent years there has been considerable and growing interest in the coordination chemistry of bulky bi- and tri-dentate ligands, in part because these ligands can be used to provide protective shields for catalytically active metal centres."[280] This statement by Gibson provided the motivation to see what other potentially bidentate functional groups besides carboxylates could be inserted into the pocket of *m*-terphenyl backbones to make new ligands with unusual properties. To narrow down the almost unlimited number of possible functional groups, we decided to concentrate on groups that were either *isoelectronic* or *isostructural* to carboxylic acids, namely hydroxylated Schiff bases, secondary amides, and boronic acids (Figure 5.1) with the goal of producing a catalytically active metal complex.

Figure 5.1 **Carboxylic acids (A) are isoelectronic with Schiff bases (B) and amides (C), and isostructural with boronic acids (D).**

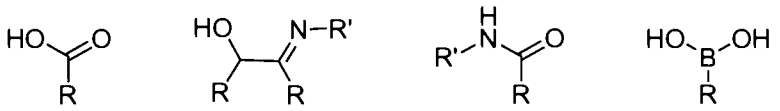

A **B** **C** **D**

5.1 Schiff bases, amides and boronic acids in coordination chemistry

Schiff bases are a special class of imines having the general formula Ar(H)C=NR. Originally, the term Schiff base was applied to all imines formed by the condensation

* Portions of this chapter are reproduced in part, with permission, from Dickie, D. A.; Jalali, H.; Samant, R. G.; Jennings, M. C.; Clyburne, J. A. C. *Can. J. Chem.*, **2004**, *82*, 1346-1352 (Copyright 2004 NRC Canada).

reaction of an aldehyde with a primary amine, but it has since been restricted to only those products derived from *aryl* aldehydes.[281] Perhaps the best-known Schiff base ligands are the family of tetradentate Salen molecules, so named because they are formed from salicylaldehyde.

Scheme 5.1 General synthesis of Salen molecules.

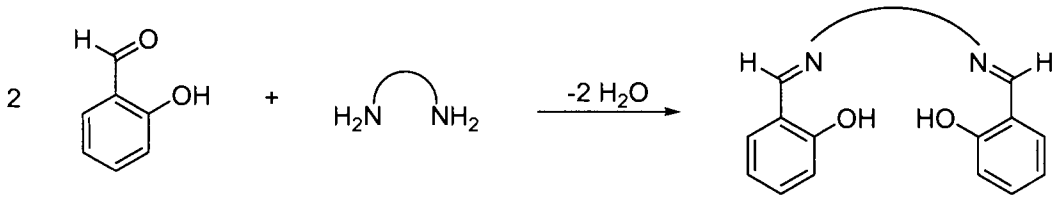

The coordination chemistry of Salen molecules and the saturated Salan-type ligands with main group elements has been extensively reviewed.[282] Their popularity is derived, in part, from the phenol that can act as an additional binding site along with the imino nitrogen. Thus, hydroxylated Schiff base ligands are, like carboxylates, versatile and potentially monoanionic. The ability of the nitrogen and oxygen heteroatoms to bind metals in a monodentate fashion, chelate the metal, or bridge multiple metal centres make these ligands very useful for varying metal coordination environments.[283]

Specific recent applications for Schiff bases complexes are remarkably diverse and run from biology[284] and medicine,[285] to materials science where they are components of oxygen selective membranes,[286] non-linear optical materials,[287] phosphorescent and luminescent compounds,[288] and single molecule magnets.[289] In addition to these applications, Schiff bases are commonly used as ligands in catalysts for a variety of processes including epoxidation,[290] cyclopropanation,[291] and transfer hydrogenation,[292] as well as both addition[293] and ring-opening[294] (ROP) polymerization. If the Schiff base is chiral, several of these catalytic reactions can be made enantioselective.[295]

Amides are less common than other N,O-ligands[296] perhaps because under certain conditions they are susceptible to transamination[297] or hydrolysis[298] reactions. Nevertheless, they have been used in catalytic applications, including hydroamination[185] and atom-transfer radical polymerization.[299] Sterically hindered amides, when bound to nickel, have been found to give high molecular weight poly(ethylene),[300] while amides bound to zinc through carbon, rather than one of the heteroatoms, are known as Reformatsky amides and have extensive uses in synthetic organic chemistry as carbon nucleophiles.[301] The metal-bridging capability of amides has been specifically exploited to design luminescent bimetallic platinum-thallium coordination networks.[302]

Boronic acids have perhaps the most diverse chemistry of the three ligand classes discussed in this chapter. Despite the fact that they are diprotic analogues of carboxylic acids, they are not often used as ligands. One notable exception is aluminium-boronic acid complexes that act as co-catalysts in various systems, particularly structurally characterized alternatives to the ubiquitous but notoriously undefined MAO co-catalyst.[303] On their own, boronic acids have recently been found to catalyze the formation of amides directly from carboxylic acids and amines,[304] but they are more often used as a substrate for a number of essential cross-coupling reactions.[305] They are also known for their potent biological activity,[306] and are found in many chemosensors, due to their ability to reversibly bind diol groups found in sugars.[307] This is due to their hydrogen-bonding characteristics, which is also why they are becoming popular synthons for crystal engineering.[308] Finally, boronic acids can be oxidized to phenols that may be difficult to make by other routes.[309]

5.2 *m*-Terphenyl Schiff base ligands

Recent work by Scott has demonstrated that one of the major limitations in the commercial use of metal-Schiff base catalysts, alkyl insertion into the imine bond, is reduced or eliminated if there is appropriate steric hindrance near the C=N bond.[310] What better way to shield this bond that to place it within the pocket of a *m*-terphenyl? The synthesis of the *m*-terphenyl Schiff base began with the preparation of a *m*-terphenyl aldehyde that could then undergo a condensation reaction with an appropriate amine. 2,4,6-Triphenylbenzaldehyde **25** is readily synthesized on a large scale with good yield (80%) according to a variation of literature procedures[311] by lithiation of 2,4,6-triphenylbromobenzene followed by addition of *N,N'*-dimethylformamide (Scheme 5.2). Both the ^{1}H and ^{13}C NMR spectra of **25** show characteristic aldehyde resonances. The aldehyde *H* signal is observed at 10.0 ppm in the ^{1}H NMR spectrum, while in the ^{13}C NMR spectrum, the aldehyde carbon signal appears at 193 ppm. IR spectroscopy provided further confirmation, with ν C=O at 1698 cm^{-1} and ν C-H at 2747 cm^{-1}.

Scheme 5.2 Synthesis of 2,4,6-triphenylbenzaldehyde 25.

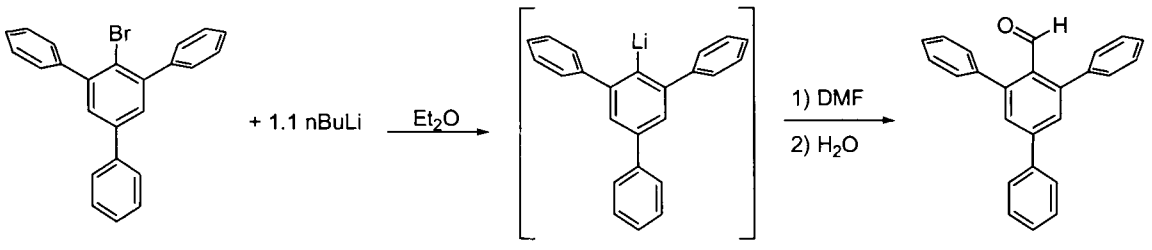

25

The *m*-terphenyl Schiff base ligand **26** was prepared by treatment of the aldehyde **25** with 2-aminophenol in ethanol solution to form *N*-(2',4',6'-triphenylbenzylidene)-2-iminophenol (TPIP – for **TriPhenylIminoPhenol**) **26** (Scheme 5.3). The product was

isolated in high yield (>90%) as a yellow crystalline compound. TPIP is a somewhat unusual Schiff base in that its pendant phenol comes from the amine moiety rather than the aldehyde fragment as in Salen-type molecules.[312]

Spectroscopic studies indicated the presence of the imine functionality with a peak at 8.59 ppm in the ^{1}H NMR spectrum as well as by a C=N stretch at 1625 cm^{-1} in the IR spectrum. These values are consistent with those reported by Yamamoto[313] for the related 2-(phenylmethylene)aminophenol (δ N*H* 8.68 ppm, ν C=N 1630 cm^{-1}). The alcohol group was observed as a sharp singlet at 5.49 ppm in the ^{1}H NMR spectrum and at 3419 cm^{-1} in the infrared. The value of the O-H stretch in **26** is significantly higher than that of Yamamoto[313] at 3130cm^{-1}. It is more comparable to molecules that feature *intramolecular* [O-H···π] interactions, such as 2,6-diphenylphenol with an O-H stretch of 3565 cm^{-1}.[314]

Scheme 5.3 Synthesis of TPIP 26 and TPAP 27.

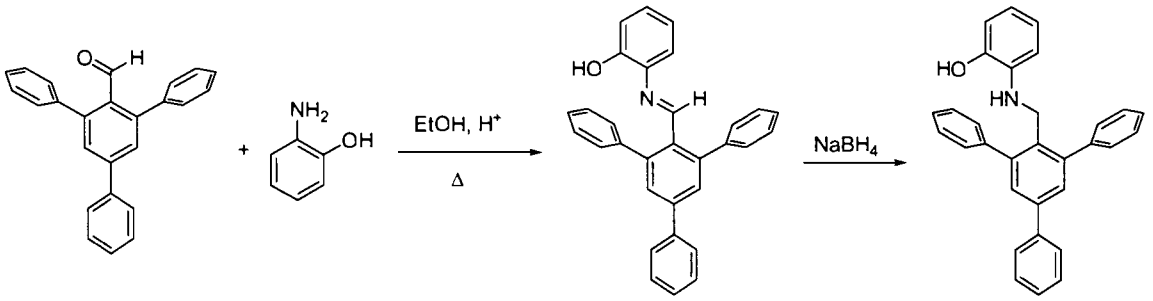

25 **26** **27**

The saturated version of TPIP, called TPAP for **Tri**Phenyl**Amino**Phenol, was also prepared. Reduction of the C=N double bond in TPIP **26** by the addition of $NaBH_4$ in ethanol solution gave TPAP **27** (Scheme 5.3). The ^{1}H NMR spectrum showed a peak for the methylene protons at 4.05 ppm. This is consistent with data presented by Endo[315] for

the related *N*-benzyl-2-aminophenol where the methylene resonance is observed at 4.37 ppm. In the IR spectrum of **27**, the N-H stretch appeared as a sharp peak at 3321 cm^{-1} while the O-H appeared as a weak signal at 3391 cm^{-1}.

X-ray crystallographic studies* were performed on both **26** (Figure 5.2) and **27** (Figure 5.3). As expected from the spectroscopic data, an [O-H···π] interaction is observed between the phenolic proton and the centroid of one phenyl ring [C(41)-C(46)] in **26**. This interaction was not present in the saturated version **27**. As would be expected when going from an imine to an amine, the $C_{terphenyl}$-N bond length increased from 1.222(4) Å in TPIP to 1.448(3) Å in TPAP. At the same time, the C_{phenol}-N bond shortened slightly from 1.427(4) Å to 1.394(3) Å, while the C-O bond lengths remained essentially unchanged.

Figure 5.2 **Structure of TPIP 26. Thermal ellipsoids are shown at 50% probability and all hydrogen atoms except the phenolic proton have been removed for clarity.**

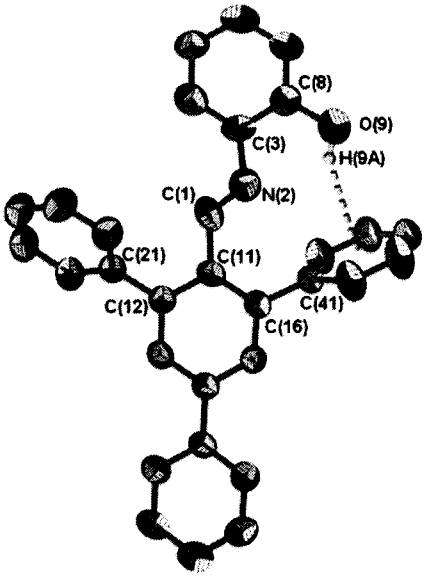

* Structures of **26** and **27** solved by Dr. Michael Jennings, University of Western Ontario.

Figure 5.3 Structure of TPAP 27. Thermal ellipsoids are shown at 50% probability and all hydrogen atoms except the phenolic and amino protons have been removed for clarity.

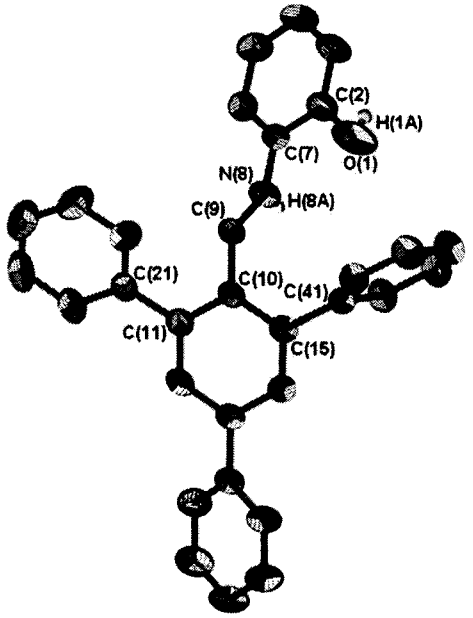

Reproduced with permission from Dickie, D. A.; Jalali, H.; Samant, R. G.; Jennings, M. C.; Clyburne, J. A. C. *Can. J. Chem.*, **2004**, *82*, 1346-1352. Copyright 2004 NRC Canada.

Table 5.1 Selected structural data for TPIP 26 and TPAP 27.

Bond lengths (Å)			
TPIP **26**		TPAP **27**	
N(2)-C(1)	1.222(4)	N(8)-C(9)	1.448(3)
N(2)-C(3)	1.427(4)	N(8)-C(7)	1.394(3)
O(9)-C(8)	1.393(5)	O(1)-C(2)	1.375(3)
Bond angles (°)			
C(1)-N(2)-C(3)	119.0(3)	C(7)-N(8)-C(9)	118.91(18)

5.3 Main group *m*-terphenyl Schiff base complexes

While Schiff bases are generally fairly robust ligands, there have been at least two reports of ligand decomposition in the presence of tin(II),[316] so to test whether this would occur with the new *m*-terphenyl Schiff base ligand TPIP **26**, it was treated with $Sn[N(SiMe_3)_2]_2$ in dichloromethane. The ^1H NMR spectrum of the orange-red product **28** showed a slight downfield shift of the imino C*H* proton to 8.91 ppm from 8.59 ppm in the free ligand. The $SiCH_3$ protons from the remaining bis(trimethylsilyl)amino ligand

appeared as a singlet at -0.12 ppm. The ^{119}Sn NMR spectrum showed a single sharp peak at -5.95 ppm.

Scheme 5.4 Synthesis of Sn·TPIP complex 28.

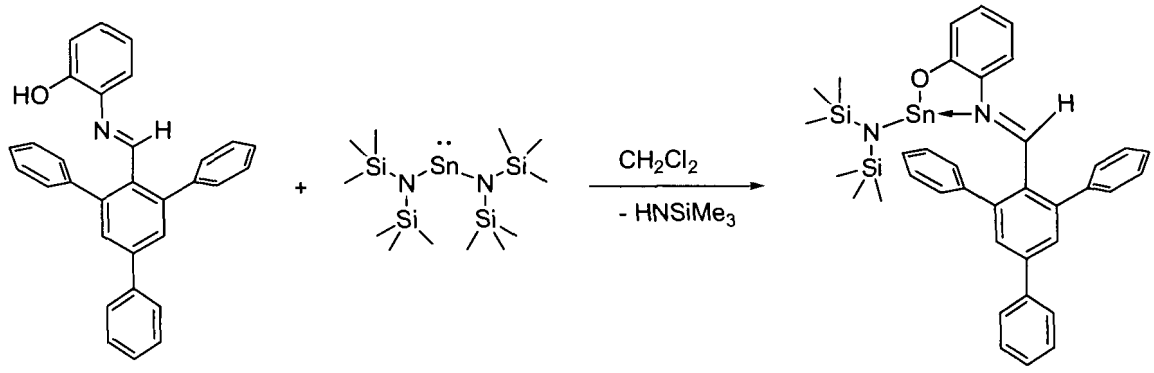

26 **28**

To confirm the proposed structure of **28**, X-ray crystallographic studies were performed.* The asymmetric unit (Figure 5.4) of the Sn·TPIP complex was found to contain two crystallographically distinct molecules of **28**, along with three molecules of CH_2Cl_2. As expected, the tin was chelated by the two heteroatoms of the TPIP ligand, forming a five-membered ring. In order to accommodate the tin fragment, the flanking phenyls of the TPIP ligand were twisted closer to co-planarity with the central ring (ca. 45 to 49°) than in **26** (ca. 61 and 72°).

*Structure solved by Diane Dickie, with the assistance of Dr. Gabriele Schatte, Saskatchewan Structural Science Centre.

Figure 5.4 **Structure of Sn·TPIP 28. Thermal ellipsoids are shown at 50% probability and hydrogen atoms and solvent molecules have been removed for clarity. Only one of two crystallographically independent molecules is shown.**

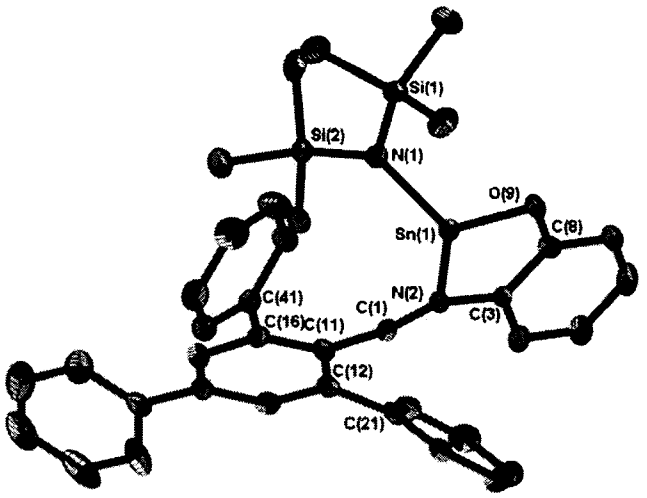

Table 5.2 **Selected structural data for Sn·TPIP 28.**

Bond lengths (Å)			
Sn(1)-N(1)	2.138(4)	Sn(2)-N(3)	2.137(4)
Sn(1)-N(2)	2.487(4)	Sn(2)-N(52)	2.499(4)
Sn(1)-O(9)	2.138(3)	Sn(2)-O(59)	2.156(3)
Sn(1)-O(9)*	2.647	Sn(2)-O(59)*	2.539(3)
N(1)-Si(1)	1.733(4)	N(3)-Si(3)	1.741(4)
N(1)-Si(2)	1.736(4)	N(3)-Si(4)	1.738(4)
N(2)-C(1)	1.275(6)	N(52)-C(51)	1.271(6)
N(2)-C(3)	1.424(6)	N(52)-C(53)	1.423(6)
O(9)-C(8)	1.355(5)	O(59)-C(58)	1.350(5)
Bond angles (°)			
N(1)-Sn(1)-N(2)	91.65(14)	N(3)-Sn(2)-N(52)	92.69(14)
N(1)-Sn(1)-O(9)	99.35(14)	N(3)-Sn(2)-O(59)	100.49(13)
N(2)-Sn(1)-O(9)	72.24(13)	N(52)-Sn(2)-O(59)	71.18(12)

Symmetry transformation used to generate equivalent atoms: * -x, -y+1, -z

There is a difference of more than 0.3 Å between the Sn-N dative and covalent bonds [2.487(4) vs 2.138(4) Å] in **28**. The C=N bond is slightly lengthened from 1.222(4) Å in the free ligand **26** to 1.275(6) or 1.271(6) in the complex **28**. Likewise, the C-O bond is slightly shorter, at 1.355(5) Å compared to 1.393(5) Å in **26**. Somewhat surprisingly, given the bulk of the ligands, each of the molecules formed an additional long Sn-O interaction of 2.642 and 2.539(3) Å in the Sn(1) and Sn(2) fragments,

respectively (Figure 5.5). In contrast to a recently reported copper(II) salicylaldimine complex in which the bulky substituents forced the metal to distort from square planar to pseudo-tetrahedral geometry,[317] the solid-state Sn_2O_2 dimer of **26** is perfectly flat and lies in the same plane as the N-Sn-O chelated ring, and the C3-C8 phenyl ring, giving rise to an extended 6-5-4-5-6 pentacyclic π-system.

Figure 5.5 Solid state dimer formed through Sn-O dative bonds in Sn·TPIP 28. Only one of two crystallographically independent molecules is shown.

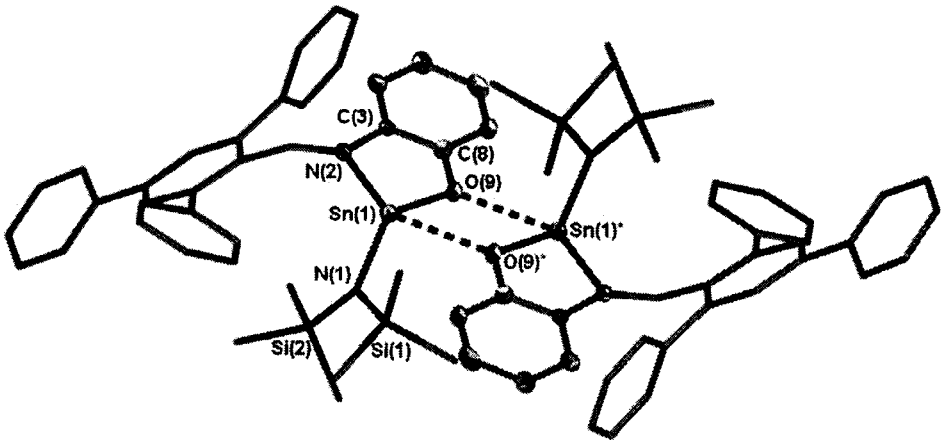

The *m*-terphenyl Schiff base ligand TPIP **26** also reacted with trimethylaluminium in toluene (Scheme 5.5) to give an orange solid **29**. Along with the expected signals from the TPIP ligand, the ^{1}H NMR spectrum indicated the presence of two different aluminium methyl environments with resonances observed at -1.31 and -0.89 ppm. These signals had relative integrated intensities of 6:9 and were assigned, respectively, to an N,O-chelated dimethylaluminium and an O-coordinated trimethylaluminium. This pattern was observed even if only one equivalent of trimethylaluminium was used, in which case a yellow powder was also formed which was not characterized due to its insolubility in

conventional solvents. Noticeably absent from the IR spectrum of **29** was the O-H stretch observed in the free ligand **26**.

Scheme 5.5 Synthesis of TPIP·$AlMe_2$·$AlMe_3$ 29.

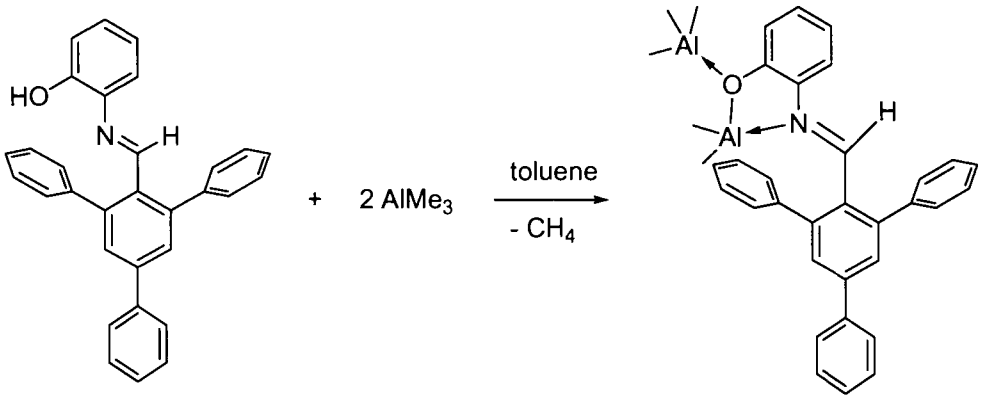

26 **29**

Figure 5.6 Complexes showing similar aluminium coordination to TPIP·$AlMe_2$·$AlMe_3$ 29.

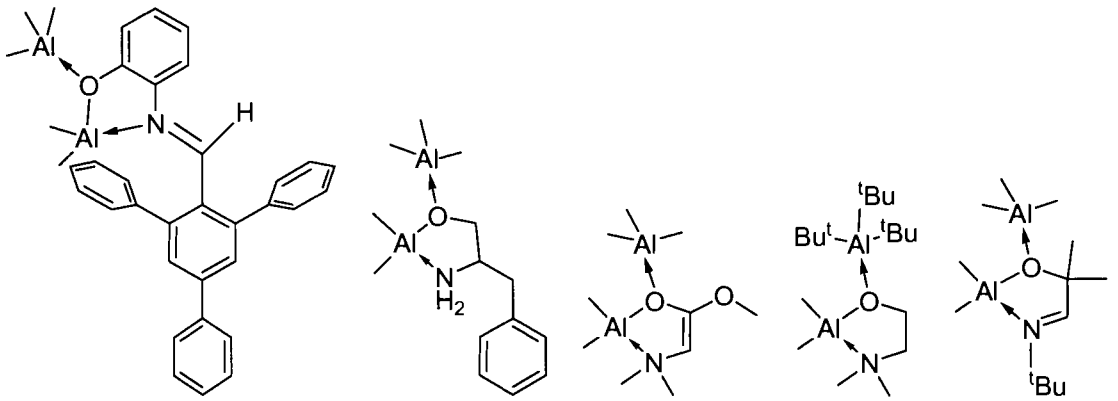

29 Ref. 318 Ref. 319 Ref. 320a Ref. 320b

The coordination pattern observed in **29**, while unexpected, is not unprecedented. Atwood, [312c,318] Barron[319] and van Koten[320] have reported similar five-membered N-Al-O heterocyclic chelates with a second trialkylaluminium datively

coordinated to the oxygen atom (Figure 5.6). X-ray crystallographic studies* confirmed the proposed formula of **29** as TPIP·$AlMe_2$·$AlMe_3$ (Figure 5.7). The Al-N and Al-O bond lengths of **29** are comparable to those of the complexes in Figure 5.6. The environment around each aluminium centre in **29** is that of a distorted tetrahedron, with bond angles ranging from 84.13°-120.30° in the chelated aluminium, Al(13), and 102.02°-115.47° for the other, Al(4). The large distortions in the chelated centre are likely due to the steric constraints imposed by the formation of a five-membered ring, as well as the presence of the bulky *m*-terphenyl fragment. Finally, as with Sn·TPIP **28**, the flanking phenyls are much less twisted (ca. 40 and 48°) relative to the central phenyl than in the free ligand **26**. The other structural parameters of the ligand are relatively unchanged upon complexation with aluminium.

Figure 5.7 **Structure of TPIP·$AlMe_2$·$AlMe_3$ 29. Thermal ellipsoids are shown at 50% probability and hydrogen atoms have been removed for clarity.**

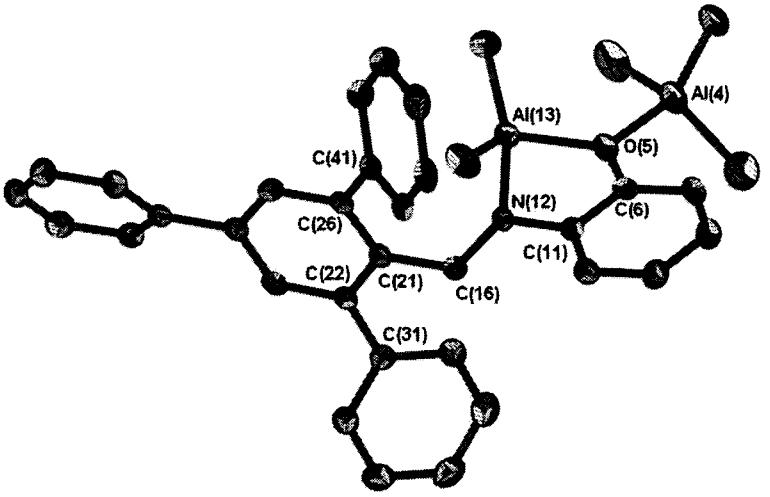

* Structure solved by Dr. Michael Jennings, University of Western Ontario.

Table 5.3 Selected structural data for TPIP·AlMe$_2$·AlMe$_3$ 29.

Bond lengths (Å)			
Al(4)-O(5)	1.9359(19)	O(5)-C(6)	1.386(3)
Al(13)-O(5)	1.8704(19)	N(12)-C(11)	1.430(3)
Al(13)-N(12)	2.013(2)	N(12)-C(16)	1.289(3)
Bond angles (°)			
O(5)-Al(13)-N(12)	84.13(8)	Al(13)-O(5)-Al(4)	123.50(9)

Finally, when the TPAP ligand **27**, which features an amine rather than an imine nitrogen, was combined with trimethylaluminium, the anticipated product TPAP·AlMe·AlMe$_3$ was not detected (Scheme 5.6). Instead, characterization by IR, ^{1}H and ^{13}C NMR spectroscopy indicated that the product was the mononuclear complex TPAP·AlMe$_2$ **30**. The IR spectrum showed a peak assigned to an N-H stretch at 3321 cm^{-1}. In the free ligand, this appears at 3291 cm^{-1}. The ^{1}H NMR spectrum also indicated that the amino hydrogen was still present, with then the N*H* signal appearing as a triplet at 3.08 ppm (J = 7 Hz), coupled to the signal for the methylene protons, a doublet at 4.01 ppm (J = 7 Hz). Also observed in the ^{1}H NMR spectrum was a sharp singlet at -1.35 ppm that was assigned to the six Al(C*H*$_3$)$_2$ hydrogens. Similarly, the signal at -8.1 ppm in the ^{13}C NMR spectrum was assigned to the two aluminium methyl carbons.

Scheme 5.6 Synthesis of TPAP·AlMe$_2$ 30.

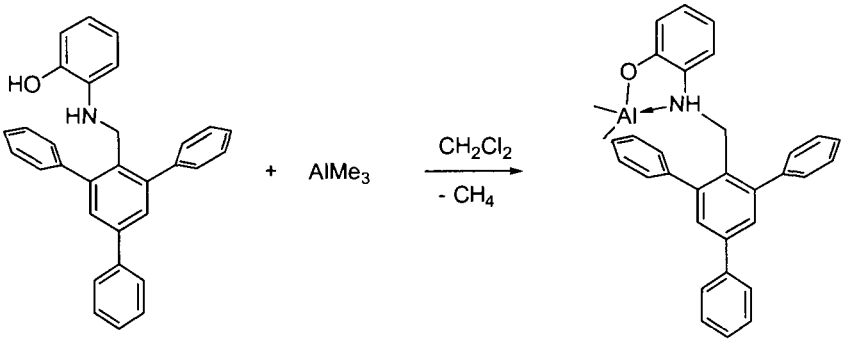

27 **30**

These spectroscopic observations, specifically the decreased frequency of ν_{N-H} in the IR spectrum and the N*H*-C*H* $^3J_{H-H}$ coupling constant in the ^{1}H NMR spectrum, are reminiscent of trialkylaluminum-dialkylamine adducts previously reported by Bradley,[321] and consistent with the suggested formula of **30**. Unfortunately, despite numerous attempts in various solvents and conditions, **30** did not form crystals suitable for X-ray crystallographic studies. Instead, elemental analysis was performed on samples of **30**, and the results agree more closely with the suggested structure of **30** than any of the other likely reaction products.

5.3.1 Ring-opening polymerization of ε-caprolactone

The aluminium complexes TPIP·$AlMe_2$·$AlMe_3$ **29** and TPAP·$AlMe_2$ **30** were tested as initiators in the ring-opening polymerization (ROP) of ε-caprolactone and propylene oxide. Addition of a 55-fold excess of ε-caprolactone to a toluene solution of **29** was found to give poly(caprolactone) upon methanol work-up. The identity of the polymer was confirmed by IR and ^{1}H NMR spectroscopy as well as matrix-assisted laser desorption ionization time-of-flight (MALDI-TOF) mass spectrometry. A THF solution of the polymer was subjected to gel-permeation chromatography* (GPC) to determine the molecular weight and polydispersity. It was found to have M_w = 10 964 and polydispersity of 1.50. Under similar conditions, the bulky alkylaluminium initiators described by Okuda[322] produced polymers with M_w in the range of 50 000 with polydispersities from 1.8-3.3.

* GPC analysis done by Marianne Rodgers and Ken Shi, Simon Fraser University.

In our hands, complex **30** was not an active ROP initiator for ε-caprolactone and neither **29** nor **30** were active towards propylene oxide. To exclude the possibility that free $AlMe_3$ was dissociating from **29** and acting as the initiator, analogous reactions using $AlMe_3$ instead of **29** were performed. No polymerization was observed.

Scheme 5.7 Ring-opening polymerization of ε-caprolactone (top) and propylene oxide (bottom).

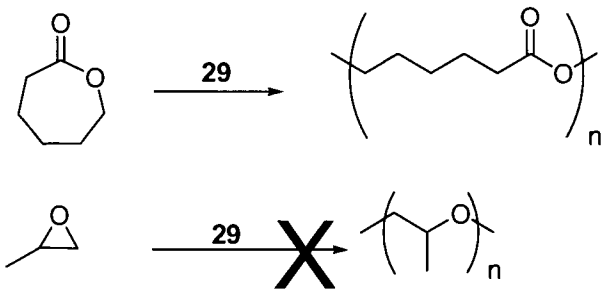

5.4 *m*-Terphenyl amides and boronic acids

To prepare a *m*-terphenyl amide, it was necessary to return to the very first ligand described in this thesis, the carboxylic acid 2,4,6-triphenylbenzoic acid **1**. The first step of the amide synthesis involved the conversion of **1** to an acid chloride by treatment with thionyl chloride in benzene at elevated temperature. The acid chloride was then combined with isopropylamine to give the *m*-terphenyl amide **31** (Scheme 5.8).

Scheme 5.8 Synthesis of the *m*-terphenyl amide 30.

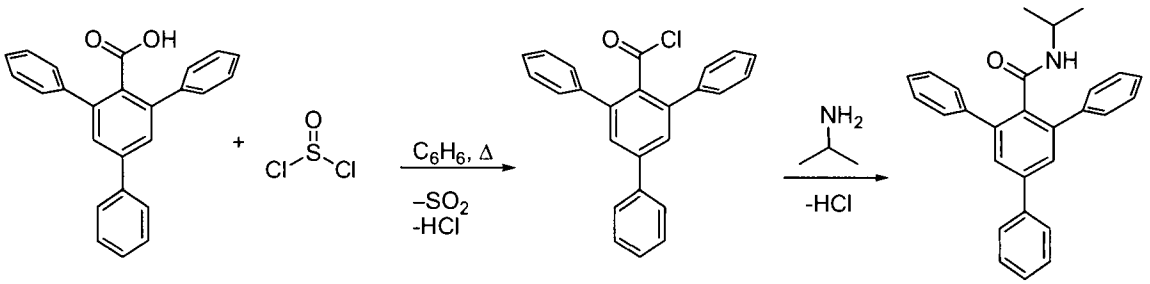

1 **31**

Despite several attempts in various conditions, crystals of **31** suitable for single crystal X-ray diffraction were not obtained, but the elemental analysis was consistent the proposed formula. The ^{1}H NMR spectrum confirmed the addition of the isopropyl fragment to the *m*-terphenyl. A sharp doublet of six hydrogens was observed at 0.73 ppm, and was coupled to the tertiary C*H* proton, a multiplet centred at 3.83 ppm. This multiplet was complicated by coupling to the N*H* proton, a doublet at 5.08 ppm.

In the aromatic region, the two hydrogens of the central phenyl ring appeared as a singlet at 7.59 ppm. The *para* and *meta* hydrogens of the three flanking phenyls, which should ideally appear as two triplets and two doublets of doublets, respectively, were not resolved. They were assigned to a multiplet centred at 7.43 ppm. The *ortho* protons were identified, and assigned to doublets at 7.64 ppm for the *para* phenyl ring and 7.53 ppm for the two *ortho* phenyls.

The IR spectrum of **31** showed signals due to both the N-H and C=O groups. As is typical for secondary amides in the solid state,[323] the N-H stretch appeared as multiple bands. The strongest was at 3252 cm^{-1}, with weaker absorptions at 3081 and 3058 cm^{-1}. For comparison, the corresponding signals in *N*-isopropylbenzamide appear at 3298 and 2971 cm^{-1}.[324] The amide I and II bands, due to the C=O stretch and N-H bend, respectively, were found at 1626 and 1552 cm^{-1}. Again, these absorptions are comparable to those of *N*-isopropylbenzamide at 1633 and 1536.[324]

Attempts were made to prepare a metal complex of **31** by reaction with trimethylaluminium. Preliminary results, based on ^{1}H NMR spectra, suggest that the ligand is decomposing. As was mentioned in Section 5.1, this is not totally unknown for amide ligands.[297,298] Additional studies are needed to determine exactly what the

decomposition products are, and whether this pathway can be avoided, if necessary, with different metals or reaction conditions.

Scheme 5.9 Synthesis of boronic acids 32 and 33.

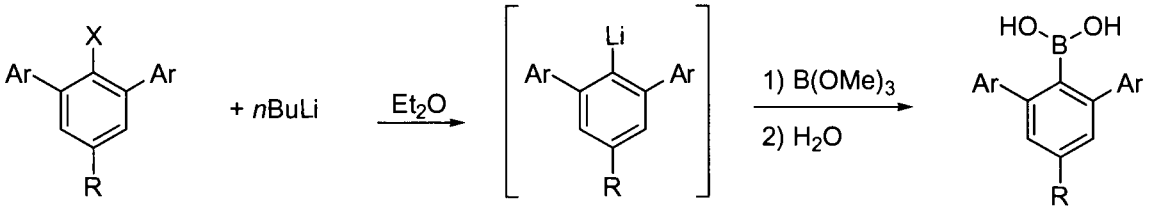

X = Br, Ar = Ph, R = Ph **32**
X = I, Ar = Mes, R = H **33**

The synthesis of the *m*-terphenyl boronic acids began in a similar manner to the synthesis of the carboxylic acids. Lithiation of either 2,4,6-triphenylbromobenzene or 2,6-bis(2,4,6-trimethylphenyl)iodobenzene in diethyl ether, followed by addition of trimethoxyborane and aqueous work gave the *m*-terphenyl boronic acids **32** and **33** respectively. Despite the lack of an unambiguous NMR handle like the isopropyl group of **31**, the ^{1}H NMR spectra of **32** and **33** were helpful for the characterization of the boronic acids. Most definitive was the appearance of a two-proton singlet at 4.11 or 4.06 ppm in the spectra of **32** and **33** respectively, assigned to the O*H* protons. The upfield shift of these protons relative to phenylboronic acid (4.61 ppm)[325] may be due to shielding by the aryls substituents.

As usual, the methyl protons of **33** were singlets, with the six *para*-methyl hydrogens at 2.33 ppm and the 12 *ortho*-methyl hydrogens at 2.02 ppm. The aromatic region of both **32** and **33** was remarkably well resolved in the ^{1}H NMR spectra, with all of the protons identified as distinct singlets, doublets or triplets, as appropriate. The ^{11}B

NMR spectra of **32** and **33** each showed a single sharp peak, at 31.37 ppm for **32** and 29.30 ppm for **33**. These values are comparable to other phenylboronic acids.[326]

Somewhat surprisingly, **32** and **33** showed different absorptions in the O-H region of the IR spectrum. In the triphenyl-substituted derivative **32**, there was a very strong O-H stretch at 3586 cm^{-1} and a broad absorption at 3280 cm^{-1}, while **33** showed instead four weak absorptions between 3668 and 3417 cm^{-1}. Since this region should be affected primarily by hydrogen bonding, attempts were made to grow crystals of both *m*-terphenyl boronic acids in order to see if they exhibited different coordination patterns. Unfortunately only **33** yielded crystals suitable for single crystal X-ray diffraction.

Figure 5.8 **Structure of 2,6-bis(2,4,6-trimethylphenyl)phenylboronic acid 33. Thermal ellipsoids are shown at 50% probability and hydrogen atoms, except OH protons, have been removed for clarity.**

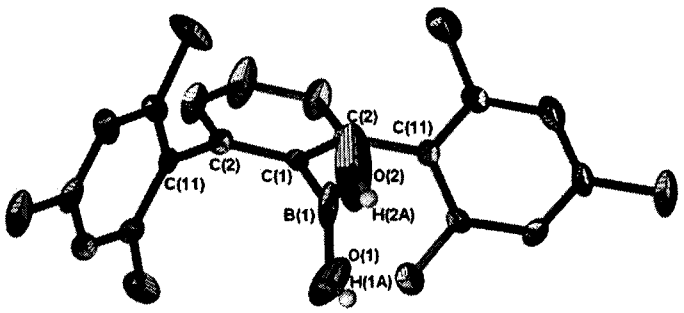

Figure 5.9 **[O-H···O] hydrogen bonds in 33, viewed along the crystallographic *a* axis.**

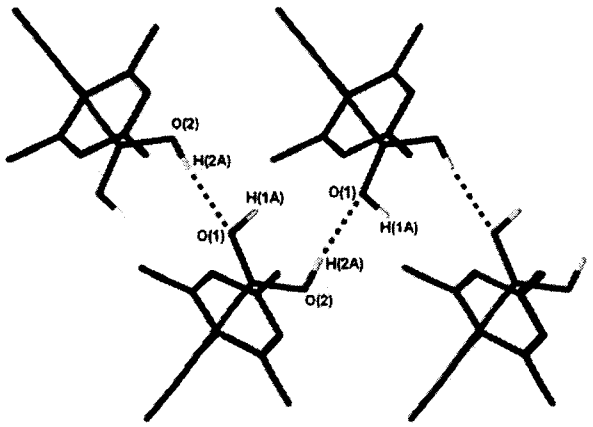

The X-ray crystallographic analysis* revealed that, as expected, there is intermolecular [O-H···O] hydrogen bonding in **33**, with O(2) as the donor and O(1) as the acceptor, forming a zigzag chain (Figure 5.9). In the absence of other hydrogen bond donor/acceptor groups, all other structurally characterized phenylboronic acids[112] form homodimers with eight-membered $B_2O_4H_2$ rings rather than infinite chains like **33**. Homodimerization was also observed in the two related *m*-terphenyl carboxylic acids **14** and **15H₂**. Since the carboxylic acids both feature smaller aryl substituents than **33** (phenyl vs mesityl), **32**, which also has the smaller phenyl substituents, may also form a homodimer, and that would explain the differences in the IR spectra of **32** and **33**.

Table 5.4 Selected structural data for 2,6-bis(2,4,6-trimethylphenyl)phenylboronic acid 33.

Bond lengths (Å)		Hydrogen bond lengths (Å)	
B(1)-O(1)	1.355(10)	H(2A)···O(1)#2	2.03
B(1)-O(2)	1.364(12)	O(2)···O(1)*	2.869(10)
B(1)-C(1)	1.569(9)		
Bond angles (°)		Hydrogen bond angles (°)	
O(1)-B(1)-O(2)	120.9(8)	O(2)-H(2A)···O(1)*	174.2

Symmetry transformations used to generate equivalent atoms: * -x, -y, z+1/2

Another difference between *m*-terphenyl boronic acid **33** and the carboxylic acids **14** and **15H₂** is the geometry of the functional groups. The boronic acid group was twisted exactly 90° perpendicular to the plane of the central phenyl ring, much more than the carboxylic acids **14** (65.3°) or **15H₂** (46.9 and 68.45°, pocket only). Again, this was found to be an unusual conformation among phenylboronic acids. Of the 47 structurally characterized phenyl boronic acids in the CSD,[112] only seven were twisted more than 30°

* Structure solved by Diane Dickie with the assistance of Dr. Gabriele Schatte, Saskatchewan Structural Science Centre.

relative to the phenyl ring, as measured by the [B-O-C-C] torsion angle, and only two were greater than 80°.

Presumably, the twist in **33** is due to intramolecular steric repulsion from the *ortho* aryl substituents. This supposition is only partially supported by the structural data. It is true that all but one[308a] of the seven molecules with twists greater than 30° have *ortho* substituents, and this one exception has an intermolecular Lewis acid-base interaction between the an imidazole nitrogen and the boron. On the other hand, four *ortho*-substituted derivatives are below that cut-off point, including 2,4-dimethoxyphenyl boronic acid[327] at only 2.7°. The only readily apparent distinguishing feature of the two examples with torsion angles above 80° is that they are the only examples with an *ortho* substituent (nitro[328] or acetyl[329]) that forms an intermolecular [O-H···O] hydrogen bond with the boronic acid group. The *ortho*-aryls of **33** are clearly incapable of forming [O-H···O] hydrogen bonds, so this observation does not help explain the unusual conformation of **33**.

5.5 Summary and conclusions

In this chapter, the synthesis and characterization of five new substituted *m*-terphenyl molecules were described. This included two Schiff base ligands derived from 2-aminophenol, TPIP **26** and TPAP **27**, an amide **31**, and two boronic acids **32** and **33**. All five were characterized spectroscopically and by elemental analysis. Additionally, the Schiff base ligands **26** and **27** and boronic acid **33** were crystallographically characterized.

TPIP **26** formed complexes with both tin and aluminium, giving **28** and **29** respectively. In both cases, the oxygen atom of the ligand formed a secondary dative interaction with the metal, in addition to the primary covalent bond formed from the protonolysis reactions. For the tin complex **28**, this secondary interaction was *inter*molecular, resulting in Sn_2O_2 dimers. In aluminium complex **29**, on the other hand, it was *intra*molecular, and the resulting complex had a formula of TPIP·$AlMe_2$·$AlMe_3$.

The activity of **29** as a ring-opening polymerization initiator was examined. Poly(caprolactone) with M_w = 10964 and polydispersity of 1.50 was produced, however the molecule was not active for the polymerization of propylene oxide. This is relatively poor compared to other alkylaluminium compounds featuring nitrogen and oxygen donors,[330] but it tells us that active metal sites can be incorporated into the bulky *m*-terphenyl pocket. The activity of **29** could likely be improved with further optimization of the reaction conditions. Complex **30**, formed by the reaction of TPAP **27** with $AlMe_3$, was also tested as a ROP initiator, but showed no activity. Somewhat surprisingly, only a single protonolysis reaction occurred during complex formation, at the oxygen atom. The nitrogen atom in **29** was left to donate a formal lone pair in a Lewis acid-base manner, just as it did in **28**, despite the reduction of the ligand from an imine. Characterization of **30** was based primarily on NMR spectroscopy, and it was formulated as TPAP·$AlMe_2$.

NMR and IR spectroscopy was also the primary means of identification for the *m*-terphenyl amide **31** and the boronic acid **32**. Both were based on the same 2,4,6-triphenylbenzene backbone as TPIP **26** and TPAP **27** and the carboxylic acid **1**. The second boronic acid, **33**, was based on the bulkier 2,6-bis(2,4,6-trimethylphenyl)benzene backbone. Crystallographic studies revealed that **33** has two unusual features. The first

was its hydrogen-bonding pattern of chains instead of dimers, and the second was the twist of the boronic acid group relative to the central phenyl ring of the molecule. Based on IR evidence, **32** does not form the same unusual hydrogen bonds, suggesting that steric hindrance from the flanking aryls may be behind the different features of **33**.

5.6 Future work

Most pressing among all the possible future directions for the work described in this chapter is the need to test the *m*-terphenyl amide **31** and boronic acids **32** and **33** as ligands for main group elements and/or transition metals. Unfortunately, this may not be as straightforward as it appears. Both amides and boronic acids have potential pitfalls of which one must be aware, but these should not prohibit their use as ligands.

In the case of the amides, the nature of the apparent decomposition products of **31** must be identified, as they could in fact be ligands that are more interesting. For example, under certain conditions Lin was able to take advantage of the non-innocent nature of his bulky amide ligands in the presence of trialkylaluminium and transform them to nacnac ligands.[331] Other metals should be tested with **31** to see if they cause the same (or different) decomposition, or form the desired amide complexes. Given the success of Schafer et al.[185,296] with titanium-amide complexes, this metal may be the best choice for initial testing of **31**.

For the boronic acids, it may be necessary to turn to salt metathesis reactions rather than the protonolysis reactions studied for most other systems in this thesis. That is because boronic acids are known to dehydrate under anhydrous conditions,[308] and such conditions are an absolute requirement for metal alkyls like $AlMe_3$ or $ZnEt_2$. Obviously,

both **32** and **33** need to be tested for their resistance to dehydration, as the flanking aryl groups of the *m*-terphenyl backbones may be large enough to prevent the formation of the standard boroxine (B_3O_3) dehydration products. Thermogravimetric analysis (TGA) would reveal the susceptibility of **32** and **33** to thermal dehydration, while NMR studies should be able to reveal solvent-related dehydration.

If the *m*-terphenyl boronic acids are readily dehydrated, and especially if they give something other than a boroxine, they could be investigated as building blocks for porous covalent-organic frameworks (COFs).[332] Related to the MOCNs discussed in Chapter 3, COFs rely on covalent bonds formed between boron and oxygen formed by dehydration of boronic acids in the presence of polyphenols. Initial studies would simply require reaction of **32** and/or **33** with simple phenols. Then, if these tests are successful, they should be treated with polyphenols. Final COF synthesis would require a new bifunctional *m*-terphenyl boronic acid similar to **15H$_2$**, but such a molecule should be readily available from the corresponding dihalide.

No matter what the results of the dehydration studies, it would be interesting to attempt to design a bifunctional *m*-terphenyl ligand like thiol **24** with a boronic acid in place of the carboxylic acid. Because boronic acids are known for their chemosensing abilities,[307] SAM formation by this hybrid ligand would allow isolation and immobilization of the boronic acid group within the *m*-terphenyl pocket. As with **24**, this would lead to more efficient use of the functional groups when sensing large biological analytes. The hydrophobic *m*-terphenyl pocket also may give different selectivity than unsubstituted boronic acids.

Gibson[333] has recently found that titanium complexes of ligands similar to both TPIP **26** and TPAP **27** are highly active catalysts for the co-polymerization of ethylene and 1-hexene, so that would be a good place to begin future work with these Schiff base ligands. Work by Nguyen[334] demonstrated that tin(II) Salen complexes were able to catalyze the formation of propylene carbonate from CO_2 and propylene oxide, although not as efficiently as the analogous tin(IV) complexes because of differences in Lewis acidity. Since **26** is bidentate rather than tetradentate like Salen, and the Sn·TPIP complex **28** demonstrates Lewis acidity through intermolecular dimerization with oxygen, it might overcome some of the problems found in Nguyen's compounds. Presumably, this reaction would proceed via CO_2 insertion into the Sn-amide bond as was described in Chapter 2, so the types of CO_2 insertion reactions proposed for **6-9** should also be tested for **28**.

For the more adventurous, it should be noted that alkylaminoethoxy ligands, which like **26** and **27** have a neutral nitrogen and anionic oxygen separated by a two-carbon bridge, have been used as auxiliary ligands for tin(II) to prepare isolable low-valent main group azides.[335] This project would be a risky use of Sn·TPIP **28**, however, since such azido compounds are often very explosive. A somewhat safer project would be to oxidize **28** to Sn(IV) and then test its biocidal and toxicological activity, following the example of Beltrán's antibacterial Schiff-base complexes.[336]

Based on the results from the ROP studies of the aluminium complexes **29** and **30**, they should both be tested as initiators for other types of polymerization reactions, as well as with different substrates for ROP. Many systems require cationic aluminium complexes rather than neutral ones like **29** and **30**, so it would be interesting to test

whether the difficulties reported by Gibson[280] in preparing stable cationic complexes from less bulky Schiff base systems are overcome with these molecules.

These aluminium complexes are also appealing for studies that are more fundamental. Barron[337] has shown that the type of ring-system formed by N,O-donor ligands upon reaction with trialkylaluminium is highly dependent on the rigidity of the ligand as well as the steric bulk of it and the alkyl groups. Both **29** and **30** feature five-membered O-Al-N rings, but it is easy to imagine that changing to bulkier alkyl groups on the aluminium or an extra carbon in the ligand bridge could result in very different structures, likely with different reactivity as well.

Finally, **29** could be tested to see if the presence of two aluminium centres in **29** makes it useful as a chelating Lewis acid for anion recognition.[338] The dative bond between the oxygen and the $AlMe_3$ fragment may not be strong enough to keep the metal in place when other anions are around, but if that were the case, it would still be informative to see how the oxygen compensates for the loss. Would it form a dimer analogous to Sn·TPIP **28**, or could a different metal be introduced leading to a hetero-bimetallic complex?

5.7 Experimental

5.7.1 Synthesis of ligands and precursors

2,4,6-Triphenylbenzaldehyde (25): Prepared according to a variation of literature procedure.[311] Under an inert atmosphere, *n*-BuLi (1.6 M in hexane, 36 mL, 57 mmol) was added dropwise to a suspension of 2,4,6-triphenylbromobenzene (20 g, 52 mmol) in ca. 200 mL anhydrous Et_2O. The reaction was stirred at r.t. for 3 h, then an

excess of DMF (17 mL) was added dropwise. After 2 h, the reaction was quenched with H_2O and extracted with Et_2O. The combined organic fractions were dried over $MgSO_4$, concentrated under vacuum and cooled -20 °C to give yellow crystals. Yield = 13.8 g (80%), mp 128-129 °C (lit 130-132 °C). ^1H NMR ($CDCl_3$, 400.137 MHz) δ 10.00 (s, 1H), 7.40-7.71 (m, 17H). $^{13}C\{^1H\}$ ($CDCl_3$, 100.624 MHz) δ 193.0, 145.2, 144.2, 139.8, 139.4, 131.6, 129.6, 129.1, 129.0, 128.5, 128.2, 127.7, 127.4. IR (nujol mull) ν 2747 (m), 1698 (s), 1590 (s), 1343 (s), 1198 (s), 892 (m), 764 (vs).

***N*-(2',4',6'-Triphenylbenzylidene)2-iminophenol (TPIP) (26):** 2,4,6,-Triphenylbenzaldehyde **25** (10.0 g, 29.9 mmol) and 2-aminophenol (3.7 g, 29.9 mmol) were suspended in ca. 200 ml of anhydrous EtOH and heated to reflux. Glacial acetic acid (5 mL) was added and heating continued for 3 h. Upon cooling r.t., bright yellow needle-like crystals formed. Yield = 11.5 g (90%), mp = 158 – 159 °C. ^1H NMR ($CDCl_3$, 400.137 MHz) δ 8.59 (s, 1H), 7.65 (s, 2H), 7.38-7.53 (m, 15H), 7.01-7.06 (m, 1H), 6.76-6.79 (m, 2H), 6.68-6.72 (m, 1H), 5.49 (s, 1H). $^{13}C\{^1H\}$ ($CDCl_3$, 100.624 MHz) δ 193.0, 129.5, 129.4, 129.0, 128.9, 128.4, 128.2, 128.0, 127.7, 127.4, 127.2, 119.7 (quaternary carbons not observed). IR (nujol mull) ν 3417(m), 1625 (m), 1584 (m), 1297, (m), 1249 (m), 1212 (m), 887 (m), 699 (s). Anal. Calcd. for $C_{31}H_{23}NO$: C, 87.50; H, 5.45; N, 3.29. Found: C, 87.42; H, 5.47; N, 3.41.

***N*-(2',4',6'-Triphenylbenzyl)-2-aminophenol (TPAP) (27):** TPIP **26** (4.05 g, 9.52 mmol) and sodium borohydride (0.90 g, 23.8 mmol) were suspended in ca. 200 mL of anhydrous EtOH. The mixture was heated to reflux over 1 hour and then allowed to cool to r.t. The reaction was quenched with H_2O and extracted with CH_2Cl_2. The combined organic fractions were washed with H_2O and a saturated $NaCl_{(aq)}$ and dried

over $MgSO_4$. The solvent was removed under vacuum to give a brown powder that was recrystallized from Et_2O. Yield = 2.54 g (62%), mp = 174-176 °C. ^1H NMR ($CDCl_3$, 400.137 MHz) δ 7.38-7.67 (m, 17H), 6.63 (s, 4H), 6.24 (s, 1H, N*H*), 5.06 (br s, 1H, O*H*), 4.06 (s, 2H, CH_2). $^{13}C\{^1H\}$ ($CDCl_3$, 125.680 MHz) δ 145.5, 144.0, 141.3, 140.1, 139.9, 135.6, 132.8, 129.1, 128.8, 128.3, 127.5, 127.4, 127.1, 120.9,119.5, 115.4, 114.2, 44.6. IR (nujol mull) ν 3391 (w), 3321 (m), 1595 (m), 1493 (m), 1480 (s), 1275 (m), 1251 (m), 886 (m), 702 (s). Anal. Calcd. for $C_{31}H_{25}NO$: C, 87.09; H, 5.89; N, 3.28. Found: C, 87.13; H, 5.97; N, 3.21.

2,4,6-Triphenylbenzyl-*N*-isopropylamide (31): Under an inert atmosphere, freshly distilled thionyl chloride (8.49 g, 71.3 mmol) was added dropwise to a suspension of 2,4,6-triphenylbenzoic acid (5.0 g, 14.3 mmol) in 40 mL benzene. The mixture was heated to reflux for 2 h, and then the volatiles were removed under vacuum to give the yellow acid chloride. The solid was dissolved in anhydrous CH_2Cl_2 and cooled to 0 °C. Isopropylamine (4.20 g, 71.3 mmol) was added dropwise to the cold solution and the mixture was allowed to warm to r.t. over 3 h. The reaction was quenched with H_2O and dilute (1 M) HCl, and then extracted with CH_2Cl_2. The combined organic fractions were dried over $MgSO_4$ and the solvent was removed under vacuum to give a pale yellow powder. Yield = 3.32 g (59%), mp = 199-203 °C. ^1H NMR ($CDCl_3$, 400.137 MHz) δ 7.64 (d, J = 7.5 Hz, 2H), 7.59 (s, 2H), 7.53 (d, 4H), 7.47-7.37 (m, 9H), 5.08 (d, J = 8.1Hz, 1H), 3.87-3.79 (m, 1H), 0.73 (d, J = 6.4 Hz, 6H). ^{13}C ($CDCl_3$, 125.680 MHz) δ 167.9, 141.9, 140.9, 140.7, 140.3, 135.2, 129.1, 128.9, 128.5, 128.1, 128.0, 127.8, 127.5, 41.5, 22.2. IR (nujol mull) ν 3252 (vs), 3081 (w), 3058 (w), 1698 (w), 1626 (vs), 1596 (m),

1552 (s), 1492 (m), 1298 (w), 1074 (w), 1029 (w), 891 (m), 811 (w), 776 (m), 758 (s), 697 (vs). Anal Calcd for $C_{28}H_{25}NO$: C, 85.90; H, 6.44. Found: C, 85.87; H, 6.23.

2,4,6-Triphenylphenylboronic acid (32): Under an inert atmosphere, *n*-BuLi (9.7 mL, 1.6 M in hexanes) was added to a suspension of 2,4,6-triphenylbromobenzene (5.00 g, 12.98 mmol) in 50 mL anhydrous Et_2O. After 2 h, the solution was cooled to -30 °C in a methanol/ice bath and $B(OMe)_3$ (1.62 g, 15.57 mmol) was added dropwise. The reaction was warmed to r.t. and stirred overnight. The reaction was quenched with H_2O and allowed to stir 4 h before being extracted with Et_2O. The combined organic fractions were dried over $MgSO_4$ and then the solvent was removed under vacuum to give a pale yellow solid. Yield = 1.29 g (27%) mp 356-357 °C. ^1H NMR ($CDCl_3$, 400.137 MHz) δ 7.67 (d, 2H, J = 7.1 Hz), 7.63 (s, 2H), 7.53 (d, J = 6.8 Hz, 4H), 7.45 (t, J = 6.8 Hz, 6H), 7.40 (t, J = 7.1 Hz, 3H), 4.11 (s, 2H, $B(O\mathit{H})_2$). $^{13}C\{^1H\}$ ($CDCl_3$, 125.679 MHz) δ 146.8, 143.2, 142.1, 129.1, 128.8, 127.8, 127.5, 127.1, 126.9. ^{11}B ($CDCl_3$, 128.370 MHz) δ 31.37. IR (nujol mull) ν 3586 (vs), 3280 (br), 3056 (w), 3057 (w), 1595 (s), 1575 (w), 1538 (w), 1492 (s), 1445 (s), 1396 (s), 1335 (vs), 1208 (w), 1193 (w), 1083 (m), 1041 (m), 1030 (m), 983 (w), 917 (w), 888 (s), 821 (m), 782 (m), 761 (s), 751 (s), 699 (vs). Anal Calcd for $C_{24}H_{19}BO_2$: C, 82.31; H, 5.47. Found: C, 82.62; H, 5.40.

2,6-bis(2,4,6-Trimethylphenyl)phenyl boronic acid (33): Prepared according to the same procedure as **32**, beginning with 2,6-bis(2,4,6-trimethylphenyl)iodobenzene (5.0 g, 14.1 mmol). Yield = 3.67 g (73%), mp = 268-270 °C. ^1H NMR ($CDCl_3$, 400.137 MHz) δ 7.53 (t, J = 7.5 Hz, 1H), 7.06 (d, J = 7.5 Hz, 2H), 6.99 (s, 4H), 4.06 (s, 2H), 2.33 (s, 6H), 2.02 (s, 12H). ^{13}C ($CDCl_3$, 125.679 MHz) δ 146.9, 139.4, 137.8, 135.9, 130.9

(d), 129.1 (d), 128.6 (d), 21.4 (q), 20.8 (q). ^{11}B ($CDCl_3$, 128.370 MHz) δ 29.30. IR (nujol mull) ν 3668 (w), 3652 (w), 3646 (w), 3539 (br), 3417 (w), 1729 (w), 1613 (m), 1584 (m), 1561 (m), 1360 (s), 1309 (vs), 1261 (m), 1150 (w), 1112 (m), 1094 (m), 1087 (m), 1048 (m), 1038 (m), 848 (s), 811 (m), 759 (s), 742 (m), 666 (w), 656 (w). Anal Calcd for $C_{24}H_{27}BO_2$: C, 80.46; H, 7.60. Found: C, 80.37; H, 7.49.

5.7.2 Synthesis of metal Schiff base complexes

Sn·TPIP (28): Under an inert atmosphere, a solution of $Sn[N(SiMe_3)_2]_2$ (1.14 g, 2.58 mmol) in 5 mL CH_2Cl_2 was added dropwise to a stirring solution of *N*-(2',4',6'-triphenylbenzylidene)2-iminophenol **26** (1.00 g, 2.35 mmol) in 15 mL CH_2Cl_2. After 3 h at r.t., the solution was concentrated under vacuum and then cooled to -30 °C. The next day, the solution was decanted from orange-red crystals. Yield = 1.27 g (77%), mp = 175-177 °C. ^1H NMR (CD_2Cl_2, 499.768 MHz) δ 8.91 (s, 1H), 7.73 (s, 2H), 7.70 (d, J = 7.6 Hz, 2H), 7.49-7.52 (m, 5H), 7.44 (m, 3H), 7.34-7.39 (m, 5H), 7.13 (t, J = 8.2 Hz, 1H), 7.08 (d, J = 8.1 Hz, 1H), 6.65 (d, J = 8.2 Hz, 1H), 6.53 (t, J = 8.1 Hz, 1H), -0.12 (s, 18 H). $^{13}C\{^1H\}$ (CD_2Cl_2, 125.680 MHz) δ 163.6, 158.2, 144.4, 139.9, 139.6, 134.1, 132.0, 131.3, 130.4, 129.2, 128.7, 128.5, 128.3, 127.5, 121.4, 116.7, 116.4, 109.9, 5.5. $^{119}Sn\{^1H\}$ (CD_2Cl_2, 223.867 MHz) δ -5.95. IR (nujol mull) ν 3061 (w), 1597 (m), 1582 (m), 1498 (m), 1474 (s), 1454 (s), 1398 (m), 1363 (m), 1301 (m), 1276 (m), 1250 (s), 1183 (w), 1149 (w), 1112 (w), 1080 (w), 1044 (w), 1030 (w), 923 (vs), 884 (m), 866 (s), 839 (m), 828 (s), 774 (m), 763 (m), 746 (m), 700 (m). Anal Calcd for $C_{37}H_{40}N_2OSi_2Sn$: C, 63.16; H, 5.73; N, 3.98. Found: C, 62.93; H, 6.02; N, 3.68.

TPIP·AlMe$_2$·AlMe$_3$ (29): Under an inert atmosphere, AlMe$_3$ (1.4 mL, 2.8 mmol, 2.0 M in toluene) was added dropwise to a solution of TPIP **26** (0.5 g, 1.18 mmol) in ca. 15 mL anhydrous toluene. Evolution of gas ceased after the halfway point of the addition. The solution was allowed to stir for 15 min and then the solvent was removed under vacuum. The resulting yellow powder was recrystallized by slow evaporation of a CH_2Cl_2 solution to give yellow crystals. Yield = 0.58 g (89%), mp = 276 °C (dec.). ^{1}H NMR (CD_2Cl_2, 400.137 MHz) δ 8.98 (s, 1H), 7.73-7.82 (m, 4H), 7.19-7.54 (m, 17H), -0.89 (s, 9H), -1.31 (s, 6H). $^{13}C\{^1H\}$ (CD_2Cl_2, 100.624 MHz) δ 143.7, 129.5, 138.8, 131.8, 130.3, 129.5, 129.4, 129.2, 128.9, 128.7, 127.7, 127.6, 120.8, 119.2, 117.5, 25.6, -7.2, -10.5. IR (nujol mull) ν 3058 (w), 3029 (w), 1596 (vs), 1575 (s), 1556 (m), 1485 (s). Anal. Calcd. for $C_{36}H_{37}Al_2NO$: C, 78.10; H, 6.74; N, 2.53. Found: C, 77.80; H, 6.70; N, 2.26.

TPAP·AlMe$_2$ (30): Under an inert atmosphere, AlMe$_3$ (0.32 mL, 0.64 mmol, 2.0 M in hexanes) was added dropwise to a solution of TPAP **27** (0.25 g, 0.58 mmol) in ca. 5 mL anhydrous CH_2Cl_2. Gas evolution was observed and the solution turned reddish brown. Slow evaporation of the solvent to gave a pale brown powder. Yield = 0.23 g, (82%), mp >260 °C. ^{1}H NMR (CD_2Cl_2, 400.137 MHz) δ 7.56 (s, 2H), 7.02-7.73 (m, 15H), 6.80 (d of d, J = 8 Hz, 1 Hz, 1H), 6.54 (t of d, J = 8 Hz, 1 Hz, 1H), 6.17 (d of d, J = 8 Hz, 1 Hz, 1H), 4.01 (d, J = 7 Hz, 2H), 3.08 (t, J = 8 Hz, 1H), -1.35 (s, 6H). $^{13}C\{^1H\}$ (CD_2Cl_2, 100.624 MHz) δ 154.1, 145.8, 142.5, 142.0, 141.7, 133.5, 133.1, 130.8, 130.7, 130.6, 129.9, 129.7, 129.6, 129.5, 128.9, 127.3, 120.7, 118.7, 50.6, -8.1,. IR (nujol mull) ν 3291 (w), 1595 (s), 1574 (m), 1564 (m), 1493 (s). Anal. Calcd. for $C_{33}H_{30}AlNO$: C,

81.96; H, 6.25; N, 2.90. Found: C, 80.57; H, 6.40; N, 2.65. (Reason for discrepancy not clear).

5.7.3 Polymerization reactions

ROP of ε-caprolactone: TPIP-$AlMe_2AlMe_3$ **29** (0.1 g, 0.2 mmol) was dissolved in 5 mL of warm anhydrous toluene. ε-Caprolactone (1.21 g, 0.011 mol) was added to the toluene solution. Over the course of one hour, the solution became noticeably more viscous. The reaction was quenched with ca. 50 mL of methanol and the resulting yellow powder was isolated by filtration. The solid poly(caprolactone) (0.48 g, 40%) was characterized by GPC as a THF solution.

6 MAIN GROUP AND TRANSITION METAL COMPLEXES OF *m*-TERPHENYL PHENOLS AND BENZYL ALCOHOLS

Alkoxides and aryloxides are among the most versatile ligands known, and have been placed on virtually every element of the periodic table.[339] It is not surprising, therefore, that one of the very first substituted *m*-terphenyls to be used as a ligand was 2,6-diphenylphenol, in a tungsten olefin metathesis complex.[65b] The structure and reactivity, including catalytic behaviour, of early transition metal complexes of this ligand have since been extensively explored by Rothwell[340] and others.[341] The search for new and improved catalysts has also motivated much of research into group 13 *m*-terphenyl phenol complexes,[342] based largely on the pioneering work by Yamamoto on aluminium tris(2,6-diphenylphenoxide) (Figure 6.1).[343]

Figure 6.1 Two of Yamamoto's "designer" catalysts, methylaluminium bis(2,6-di-t-butyl-4-methylphenoxide (left) and aluminium tris(2,6-diphenylphenoxide) (right).

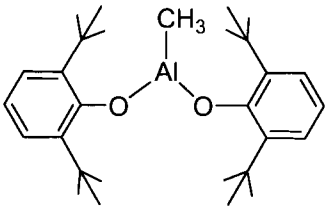

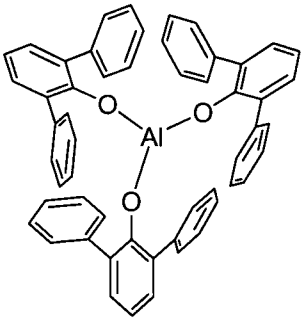

Yamamoto noticed early on that certain bulky aluminium aryloxide catalysts give different products in Claisen rearrangements than those obtained from other Lewis acids or by thermally induced processes.[344] He has since has developed a series of "designer"

Lewis acid catalysts (Figure 6.1) for diverse organic transformations of oxygen-containing substrates. These transformations include conjugate addition to α,β-unsaturated carbonyl compounds (used in the synthesis of terpenoids and taxol derivatives), *exo*-selective Diels-Alder additions (opposite to the typical *endo* preference), and stereoselective Claisen rearrangements.[345] One of these designer catalysts, methylaluminium bis(2,6-di-*t*-butyl-4-methylphenoxide), is capable of distinguishing between pairs of similar ethers, ketones and esters. Another catalyst, aluminium tris(2,6-diphenylphenoxide), is based on a *m*-terphenyl ligand and discriminates between pairs of aldehydes. The same *m*-terphenyl phenol is the basis for the biphenol ligand used by Yamamoto to prepare a polymeric aluminium tris(phenoxide) complex with solid-state catalytic behaviour similar to the analogous homogeneous catalysts.[346]

m-Terphenyl phenol complexes of tin and germanium have been less studied than the corresponding group 13 and transition metal complexes. Because most studies to date have been primarily structural[347,348,349] rather than reactivity surveys,[350] no catalytic behaviour has yet been identified for group 14 complexes. Instead, such compounds are most often promoted as potential single-source precursors for ceramic oxide materials. Metal alkoxides have long been used for this type of application; however, their exact structures are often unknown, as they have a tendency to form polymeric materials.[351] As has been emphasized throughout this thesis, the steric bulk of the ligand helps control the degree of aggregation in the complex.[352,353] *m*-Terphenyls are therefore ideally suited for model studies aimed at gaining an understanding of the factors influencing structure and reactivity. One example of the importance of understanding aggregation is the work of

Okuda, who found a marked difference in ring-opening polymerization of lactones depending on whether the aluminium aryloxide catalyst was monomeric or dimeric in solution.[322]

Closely related to phenols are benzyl alcohols. Although *m*-terphenyl derivatives have been known since at least 1960,[109] no metal complexes have been published to date. Studies on other 2,6-disubstituted benzyl alcohols are also quite limited compared to analogous phenols. Since the presence of the methylene group will both alter the basicity of the oxygen atom[354] and reduce the steric pressure at that site by distancing it from the flanking aryls,[355] a study of *m*-terphenyl benzyl alcohols as ligands for transition metals and main group elements could reveal unexpected behaviour.

6.1 Ligand synthesis

The targeted *m*-terphenyl phenol for this study was 2,6-bis(2,4,6-trimethylphenyl)phenol **34**, which had previously only been synthesized as a byproduct in the reaction of corresponding *m*-terphenyl copper complex with oxygen,[90] or through the palladium-catalyzed cross coupling of phenol with 2,4,6-trimethylbromobenzene.[356] Neither of these routes involved the *m*-terphenyl precursors that were readily available, so two alternatives were developed. One route involves the oxidation of boronic acids with Oxone®.[309] This reaction was tested with the *m*-terphenyl boronic acid **33** and proceeded smoothly to give the *m*-terphenyl phenol **34**. Boronic acid **33**, however, comes from 2,6-bis(2,4,6-triphenyl)iodobenzene, and recently Power[357] developed a synthesis of related *m*-terphenyl phenols directly from the halogenated starting material, so this shorter route was pursued. Lithiation followed by addition of excess nitrobenzene at -78

°C results in the immediate formation of the dark red solution that is quenched with methanol to give **34** upon aqueous work-up.

Scheme 6.1 Synthesis of 2,6-bis(2,4,6-trimethylphenyl)phenol 34.

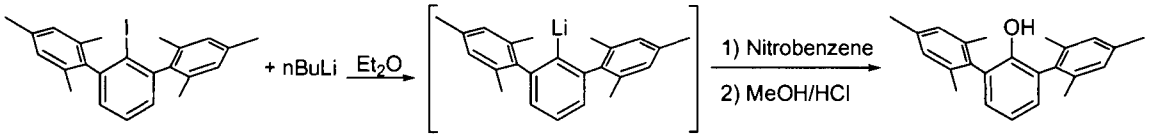

34

Figure 6.2 Known *m*-terphenyl phenols, from least to most bulky.

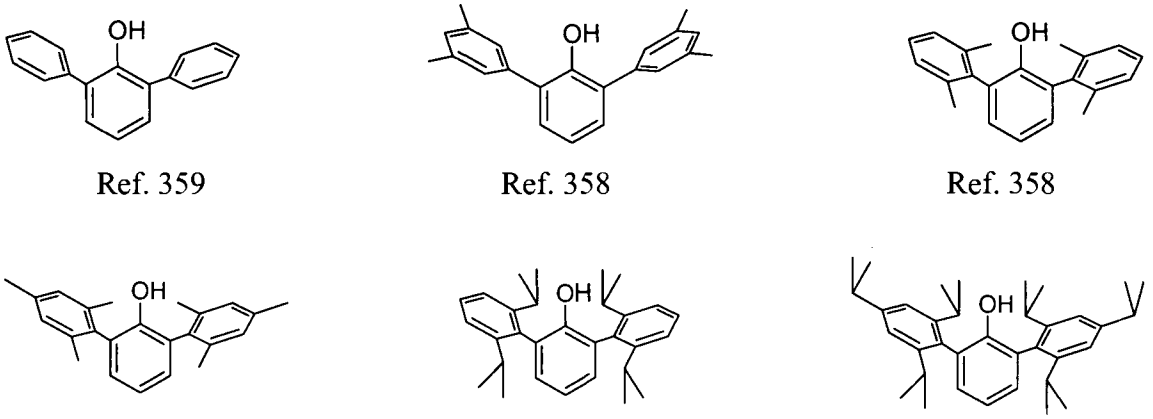

Ref. 359 Ref. 358 Ref. 358

34 Ref. 357 Ref. 357

In the ^{1}H NMR spectrum of **34**, the O*H* appears as a singlet at 4.53 ppm. The methyl groups are found, as usual, at 2.33 (*para*) and 2.06 (*ortho*) ppm. Additional evidence for the presence of the OH was provided by strong IR absorptions at 3486 and 3451 cm^{-1}. These stretches are comparable to those reported by Lüning[358] for 2,6-bis(2,6-dimethylphenyl)phenol, at 3482 and 3431 cm^{-1}. Four other previously published *m*-terphenyl phenols (Figure 6.2), namely 2,6-diphenylphenol,[359] 2,6-bis(3,5-dimethylphenyl)phenol,[358] 2,6-bis(2,6-diisopropylphenyl)phenol[357] and 2,6-bis(2,4,6-triisopropylphenyl)phenol,[357] each reported only a single OH stretch between 3520-3533

cm^{-1} in the IR spectrum. Since three of these five compounds had been crystallographically characterized, single crystal X-ray diffraction studies were performed on **34** to see if there was a difference in hydrogen bonding that could explain the differences in the IR spectra.

Figure 6.3 **Structure of 2,6-bis(2,4,6-trimethylphenyl)phenol 34. Thermal ellipsoids are shown at 50% probability and all hydrogens except phenolic protons have been removed for clarity.**

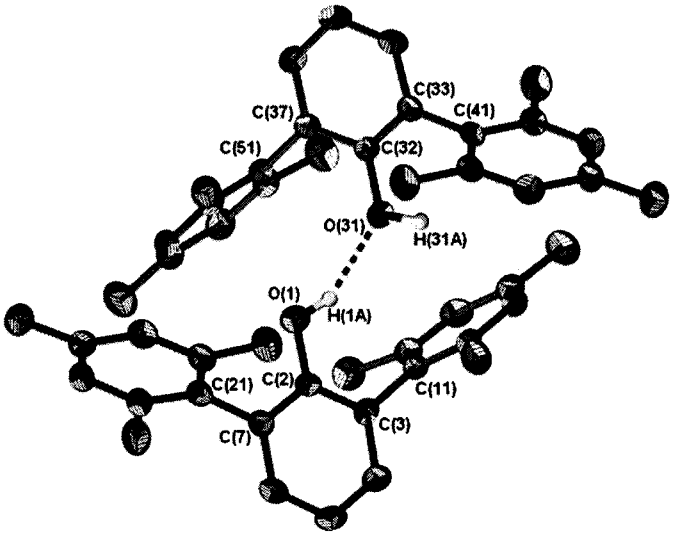

The crystallographic studies* revealed that in the solid state, **34** exists as two crystallographically distinct molecules (Figure 6.3). These molecules are connected by a weak[228] [O-H···O] hydrogen bond to form a dimer. This is in contrast to unsubstituted phenol (C_6H_5OH), which forms infinite hydrogen-bonded chains[360] with an average [O···O] distance of 2.67 Å, compared to 2.823(3) Å in **34**. It is also in contrast to all three previously structurally characterized *m*-terphenyl phenols, none of which exhibit [O-H···O] hydrogen bonds. Based on the IR evidence, it would appear that Lüning's 2,6-bis(2,6-dimethylphenyl)phenol follows the same pattern as **34**, while his 3,5-derivative is more similar to the others.[357,359]

* Structure solved by Dr. Michael Jennings, University of Western Ontario.

Table 6.1 Selected structural data for 2,6-bis(2,4,6-trimethylphenyl)phenol 34.

Bond lengths (Å)			
O(1)-C(2)	1.356(3)	H(1A)···O(31)	2.05
O(31)-C(32)	1.375(3)	O(1)···O(31)	2.823(3)
Bond angles (°)			
O(1)-C(2)-C(7)	116.7(2)	O(1)-C(2)-C(3)	121.7(2)
O(31)-C(32)-C(37)	116.3(2)	O(31)-C(32)-C(33)	121.0(2)
O(1)-H(1A)···O(31)	152.9		

Another feature that was found in each of the crystallographically characterized *m*-terphenyl phenols, including **34**, is an intramolecular [O-H···π] interaction. In the case of the extremely bulky 2,6-bis(2,4,6-triisopropylphenyl)phenol and 2,6-bis(2,6-diisopropylphenyl)phenol, steric hindrance hampers intermolecular interactions, but does not prevent intramolecular [O-H···π] interaction with a flanking aryl. This interaction occurs primarily through the *ipso* carbon atoms (H···C_{ipso} = 2.64 and 2.39 Å, respectively).[357] In fact, the restricted rotation caused by the presence of such bulky groups may even enhance the interaction by locking the aryls into place.

Restricted rotation is clearly not necessary though, since the crystal structure of the least hindered *m*-terphenyl, 2,6-diphenylphenol, also showed an [O-H···π] interaction of 2.43 Å.[359] The corresponding H···C_{ipso} distances in **34** are 2.41 and 2.47 Å [H(1A)···C(11) and H(31A)···C(41), respectively]. It is not immediately clear why 2,6-diphenylphenol does not also engage in [O-H···O] hydrogen bonds like **34**, but it may be that [C-H···π] interactions through the *para* hydrogen of the central phenyl provide more favourable packing interactions. Taken together, these examples illustrate how subtle changes in steric demands can have a large effect on intermolecular interactions.

To prepare the *m*-terphenyl benzyl alcohols, no direct synthesis from the halogenated starting materials was identified. Instead, the chosen route involved a sodium borohydride reduction of the corresponding aldehydes, a variation on the lithium

aluminium hydride reduction used by Lüning to prepare 2,6-bis(2,6-dimethylphenyl)benzyl alcohol[53] and 2,6-bis(2,6-diisopropylphenyl)benzyl alcohol.[358] One of the required aldehydes, 2,4,6-triphenylbenzaldedhyde **25** had already been made as a precursor of Schiff base **26** (see Chapter 5), and the second, 2,6-bis(2,4,6-trimethylphenyl)benzaldehyde **35** was prepared in an analogous manner by lithiation of 2,6-bis(2,4,6-trimethylphenyl)iodobenzene followed by addition of DMF.

The ^{1}H NMR spectrum of **35** showed a singlet at 9.65 ppm due to the aldehyde C*H*, and the corresponding peak in the ^{13}C NMR spectrum appeared at 192.4 ppm. These values compare very well to the chemical shifts of **25** at 10.00 ppm (^{1}H) and 193.0 (^{13}C), and the C*H* signal in the ^{1}H NMR spectrum also matches well with Lüning's 2,6-bis(2,6-diisopropylphenyl)benzaldehyde at 9.70 ppm.[358] The relevant absorptions in the IR spectrum are also quite similar, with aldehyde C-H stretch at 2743 cm^{-1} in **35** (2747 cm^{-1} in **25**), and the C=O stretch at 1702 cm^{-1} (1698 cm^{-1} in **25**).

Scheme 6.2 Synthesis of 2,4,6-triphenylbenzylalcohol 36 and 2,6-bis(2,4,6-trimethylphenyl)benzyl alcohol 37.

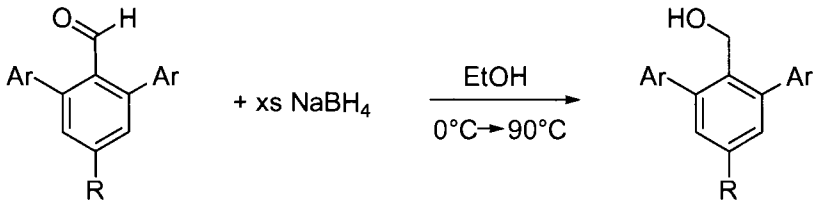

25 Ar = Ph, R = Ph
35 Ar = Mes, R = H

36 Ar = Ph, R = Ph
37 Ar = Mes, R = H

Addition of excess sodium borohydride to cold (0 °C) ethanol solutions of **25** or **35** followed by heating to reflux and aqueous work-up gave the *m*-terphenyl benzyl alcohols **36**[361] and **37** in good yields. The ^{1}H NMR spectra of **36** and **37** showed that the downfield aldehyde C*H* singlet had been replaced by peaks for the new methylene

protons. These protons appear as a doublet at 4.48 ppm in **36** or a broad unresolved peak at 3.94 ppm in **37**. Given that there was no clear coupling of the C*H*$_2$ protons in **37** to the O*H* proton, it is not surprising that no signal was observed for the alcohol in the ^{1}H NMR spectrum of **37**. In contrast, the ^{1}H NMR spectrum of **36** showed the O*H* triplet at 1.45 ppm.

The conversion of aldehydes **25** and **35** to alcohols was also evident in the IR spectra, with the complete disappearance of the C=O stretches and appearance of new O-H stretches. In **36**, the O-H appeared as two broad absorbances at 3428 and 3324 cm^{-1}. The corresponding stretches in the bulkier **37** appeared at 3563 and 3522 cm^{-1}. In contrast, only a single O-H stretch was reported by Lüning for the related benzyl alcohols 2,6-bis(2,6-dimethylphenyl)benzyl alcohol (3522 cm^{-1})[53] and 2,6-bis(2,6-diisopropylphenyl)benzyl alcohol (3569 cm^{-1}).[358]

Both of the *m*-terphenyl benzyl alcohols proved amenable to single-crystal formation, so X-ray crystallographic studies were performed on **36** and **37**.* Unlike most of the molecules described so far in this thesis, the benzyl alcohols each exhibited some disorder. In **36** (Figure 6.4), the disorder was in the twist of the *para* phenyl rings [C(21)-C(26) and C(71)-C(76)] of the two crystallographically distinct molecules relative to the central phenyl, while in **37** (Figure 6.5), the disorder was located around the benzyl alcohol group.

* Structure of **36** and **37** solved by Dr. Michael Jennings, University of Western Ontario.

Figure 6.4 **Structure of 2,4,6-triphenylbenzyl alcohol 36. Thermal ellipsoids are shown at 50% probability and all hydrogen atoms except the OH protons have been removed for clarity. Only one of the two crystallographically distinct molecules is shown, and only the major conformation of the disordered phenyl is shown, as isotropic spheres.**

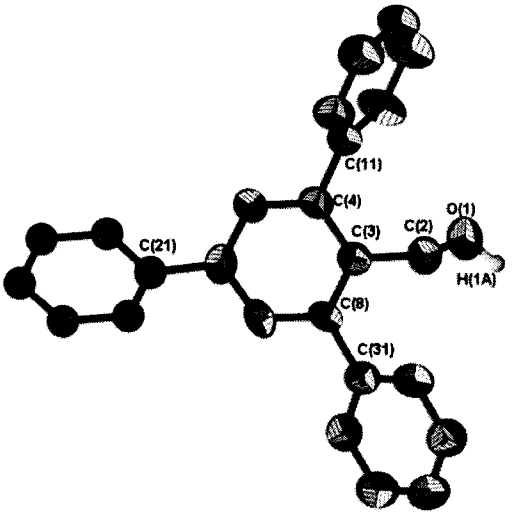

Figure 6.5 **Structure of 2,6-bis(2,4,6-trimethylphenyl)benzyl alcohol 37. Thermal ellipsoids are shown at 50% probability and all hydrogen atoms except the OH protons have been removed for clarity. For the disordered OHs, only the major conformation is shown.**

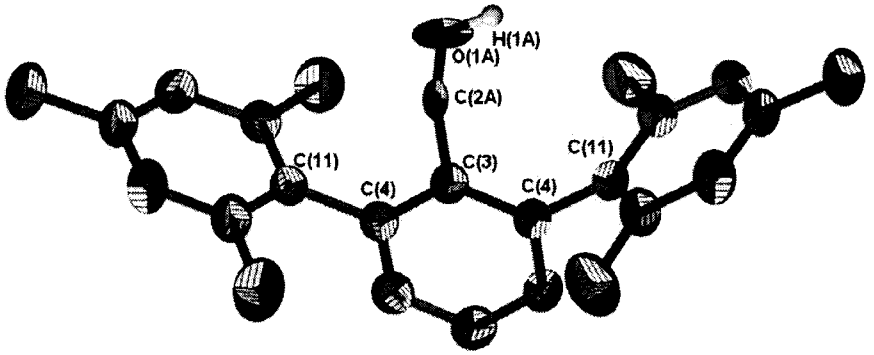

Table 6.2 **Selected structural parameters of 2,4,6-triphenylbenzylalcohol 36 and2,6-bis(2,4,6-trimethylphenyl)benzyl alcohol 37.**

Bond lengths (Å)			
36		**37**	
O(1)-C(2)	1.428(6)	O(1A)-C(2A)	1.193(10)
C(2)-C(3)	1.513(8)	C(2A)-C(3)	1.601(6)
Bond angles (°)			
O(1)-C(2)-C(3)	113.4(5)	O(1A)-C(2A)-C(3)	112.3(10)

The less hindered 2,4,6-triphenylbenzyl alcohol **36**, whose O*H* hydrogen atoms were located in the Fourier difference map, forms a solid-state tetramer (Figure 6.6) with

two distinct intermolecular [O-H···O] hydrogen bonds between O(1)···O(51) and O(51)···O(51)*. The third [O-H···O] hydrogen bond that would be expected between O(1)···O(1)* to complete the tetramer is not present due to the non-complementary positions of the H(1A) hydrogen atoms.

Figure 6.6 [O-H···O] hydrogen bonds in 2,4,6-triphenylbenzyl alcohol 36 form a solid-state tetramer.

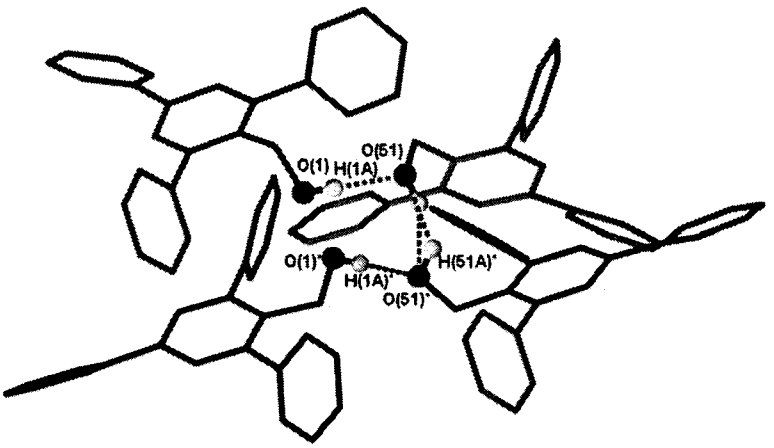

Unlike phenol (C_6H_5OH), benzyl alcohol ($C_6H_5CH_2OH$) is a liquid at room temperature and its crystal structure has not been reported. It is therefore not possible to compare and contrast with the hydrogen bonding structure of **36**. There is only one benzyl alcohol with a 2,6-substitution pattern that has been characterized as the free alcohol, and that is 2,4,6-tris(trifluoromethyl)benzyl alcohol.[362] It exists as a solid-state hexamer, in contrast to the tetrameric pattern observed in **36**. The average [O···O] distances are slightly shorter in $(F_3C)_3C_6H_2CH_2OH$ at 2.647 Å, compared to 2.752 Å in **36**. Given the disorder in **37**, it is not possible to unambiguously identify intermolecular [O-H···O] hydrogen bonds or intramolecular [O-H···π] interactions analogous to those seen in the *m*-terphenyl phenols including **34**. From the packing diagram, **37** does not appear to form solid-state tetramers like **36**.

Table 6.3 [O-H···O] hydrogen bond lengths and angles in 2,4,6-triphenylbenzyl alcohol 36.

Hydrogen bond lengths (Å)			
O(1)···O(51)	2.772	H(1A)···O(51)	1.933
O(51) ···O(51)*	2.808	H(51A)···O(51)*	2.160
O(1)···O(1)*	2.676		
Hydrogen bond angles (°)			
O(1)-H(1A)···O(51)	176.56	O(51)-H(51A)···O(51)*	133.90

6.2 Main group *m*-terphenyl phenol complexes

Despite the fact that the first Sn(II) and Ge(II) compounds found to exist as dicoordinate monomers in the solid state were based upon bulky phenol ligands,[116] structural data on bivalent group 14 alkoxy or aryloxy compounds remains relatively rare. Besides being interesting simply from a structural perspective, group 14 alkoxy or aryloxy complexes are being studied as catalysts[363] and as molecular precursors to superconductors and/or ceramic materials for applications including flat panel displays, gas sensors, solar cells and lithium battery anodes.[130d,348b,364] These elements, therefore, seemed an appropriate starting point for the exploration of the coordination chemistry of the *m*-terphenyl phenol **34**.

The protonolysis reaction of $Sn[N(SiMe_3)_2]_2$ with **34** in benzene gives the tin(II) *m*-terphenyl phenoxide **38** in good yield. No signal from the C*H*$_3$ groups of the silylamine ligand was observed ^{1}H NMR spectrum of **38**, indicating that both amido groups had been lost to give the tin(II) bis(phenoxide) complex. The disappearance of the O*H* signal in both the ^{1}H NMR and IR spectra also indicated the formation of **38**, but the most unambiguous evidence was provided by the peak at -344 ppm in the ^{119}Sn NMR spectrum. This value is slightly upfield of the signal at -289 ppm for the most closely related $Sn(OAr)_2$ compound in the literature, namely Power's bis(phenoxide) based on the *m*-terphenyl 2,6-bis(2,6-diisopropylphenyl)phenol.[349]

Scheme 6.3 Synthesis of $[Sn(OC_6H_3Mes_2)_2]$ 38.

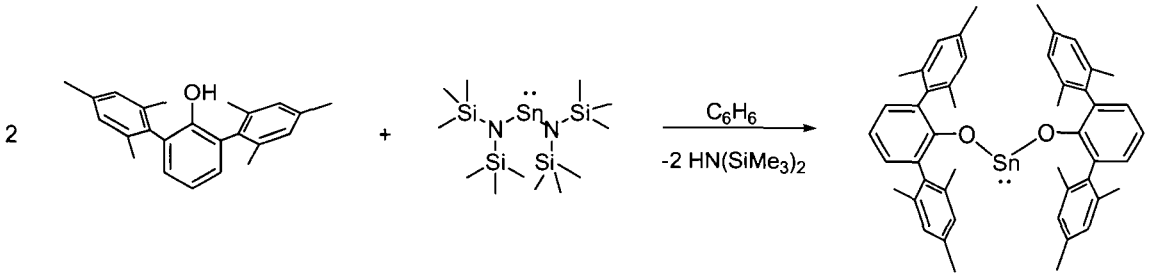

34 **38**

Final confirmation of the structure of **38** was provided by single crystal X-ray diffraction. The crystallographic studies* revealed that it does indeed exist as a monomer in the solid state (Figure 6.7). The geometry at tin is v-shaped, due to the stereochemically active lone pair. As in other few other known Sn(II) bis(aryloxides),[349,365] the O-Sn-O angle is quite acute, measuring only 87.32(11)°. The tin atom in **38** is not truly dicoordinate, however, as it has extensive Sn-π interactions resulting from being sandwiched between two flanking aryls of the *m*-terphenyl ligand. The Sn···centroid distances measure 2.942 and 2.980 Å for the C(111) and C(221) rings, respectively. Such interactions are not present in Power's bulkier *m*-terphenyl phenol complex, and if persistent in solution, would explain the relative upfield shift in the ^{119}Sn chemical shift of **38**.

* Structure solved by Diane Dickie.

Figure 6.7 **Structure of $[Sn(OC_6H_3Mes_2)_2]$ 38, showing Sn-π interactions. Thermal ellipsoids are shown at 50% probability and hydrogen atoms have been removed for clarity.**

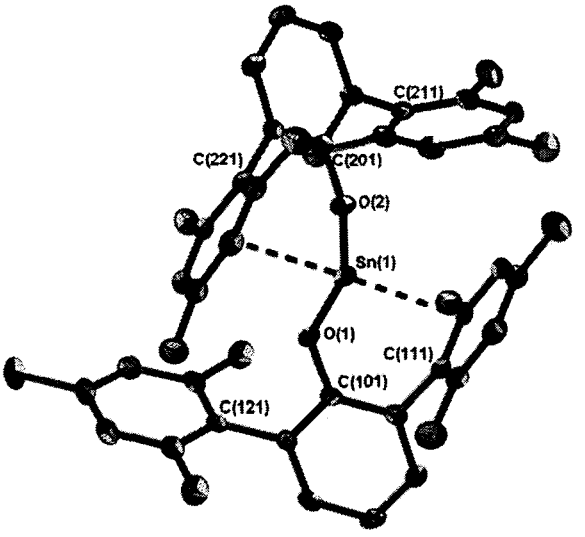

Table 6.4 **Selected structural data for $[Sn(OC_6H_3Mes_2)_2]$ 38.**

		Bond lengths (Å)	
Sn(1)-O(1)	2.039(3)	Sn(1)-O(2)	2.043(3)
O(1)-C(101)	1.343(5)	O(2)-C(201)	1.342(5)
		Bond angles (°)	
C(101)-O(1)-Sn(1)	127.7(2)	O(1)-Sn(1)-O(2)	87.32(11)
C(201)-O(2)-Sn(1)	125.7(2)		

The reaction in dichloromethane of $Ge[N(SiMe_3)_2]_2$ with the *m*-terphenyl phenol **34** gave a mixture of compounds, one of which was the mixed aryloxy-amido germanium complex **39**. This complex could be identified in the ^1H NMR spectrum of the crude reaction mixture as a singlet of 18 hydrogens at 0.00 ppm, and singlets at 2.18 and 2.42 ppm for the *ortho* and *para* methyls of the *m*-terphenyl ligand. Since $Sn[N(SiMe_3)_2]_2$ is known to react with dichloromethane solvent (see Chapter 2), it seemed possible that this could also be happening during the synthesis of **39**, so an attempt was made to repeat the synthesis in hexanes. Unfortunately, only traces of the mixed complex **39** were observed in the ^1H NMR spectrum. The major product was the germanium bis(aryloxide) **39a**. This assignment was based on similarities with the tin bis(aryloxide) **38**, namely the pronounced upfield shift of the *ortho* methyl protons to 1.79 ppm (1.82 ppm in **38**) and an

elevated melting point of 318 °C (321 °C in **38**). Elemental analysis was consistent with the proposed composition of **39a**.

Scheme 6.4 Synthesis of [$(Me_3Si)_2NGe(OC_6H_3Mes_2)$] 39.

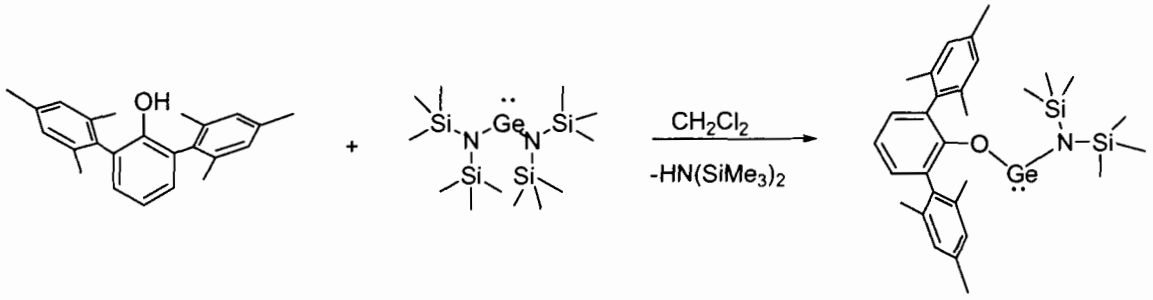

34 **39**

Scheme 6.5 Synthesis of [$Ge(OC_6H_3Mes_2)_2$] 39a.

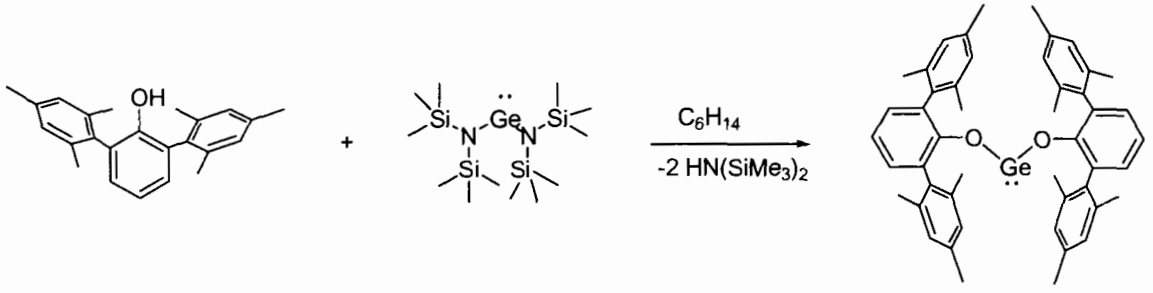

34 **39a**

Recrystallization of both **39** and **39a** from benzene was attempted, but only **39** yielded single crystals suitable for X-ray diffraction studies.* Compound **39** is the first structurally characterized mixed alkoxy-amido germanium(II) complex (Figure 6.8). The Ge-O bond length of 1.8414(16) Å is longer than those found in other dicoordinate non-calixarene Ge(II) compounds [1.814(2) to 1.8296(14) Å].[349,350,366] The opposite is true of the Ge-N bond, which, at 1.851(2) Å is shorter than in comparable compounds [1.855(2)

*Structure solved by Diane Dickie with the assistance of Dr. Hilary Jenkins, Saint Mary's University.

to 1.939(6) Å].[77,367] The germanium does not have any significant inter- or intramolecular interactions.

Figure 6.8 Structure of $[(Me_3Si)_2NGe(OC_6H_3Mes_2)]$ 39.

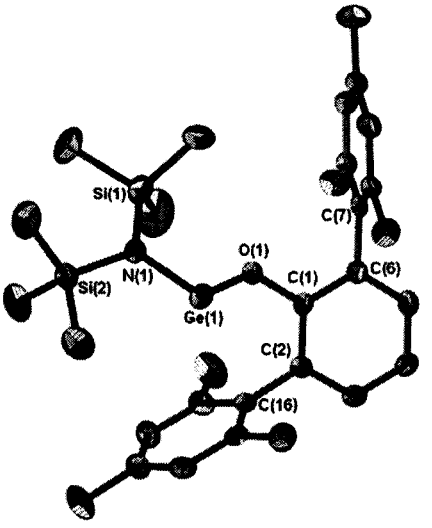

Table 6.5 Selected structural data for $[(Me_3Si)_2NGe(OC_6H_3Mes_2)]$ 39.

Bond lengths (Å)			
Ge(1)-N(1)	1.851(2)	Ge(1)-O(1)	1.8414(16)
Si(1)-N(1)	1.753(2)	C(1)-O(1)	1.366(3)
Si(2)-N(1)	1.750(2)		
Bond angles (°)			
O(1)-Ge(1)-N(1)	97.59(8)	Si(2)-N(1)-Si(1)	122.42(12)
Si(2)-N(1)-Ge(1)	114.71(11)	Si(1)-N(1)-Ge(1)	122.83(11)

As with the germanium complex **39**, the reaction of the *m*-terphenyl phenol **34** with $AlMe_3$ in dichloromethane leads to the substitution of only a single ligand to give the dialkylaluminium monophenoxide **40**. Evidence for this product is given by the ^1H NMR spectrum, which showed peaks at -1.26, 2.15 and 2.19 ppm with relative intensities of 6:12:6, due to the aluminium methyls, and *m*-terphenyl *ortho* and *para* methyl groups, respectively.

Scheme 6.6 Synthesis of $[Me_2Al(\mu\text{-}OC_6H_3Mes_2)]_2$ 40.

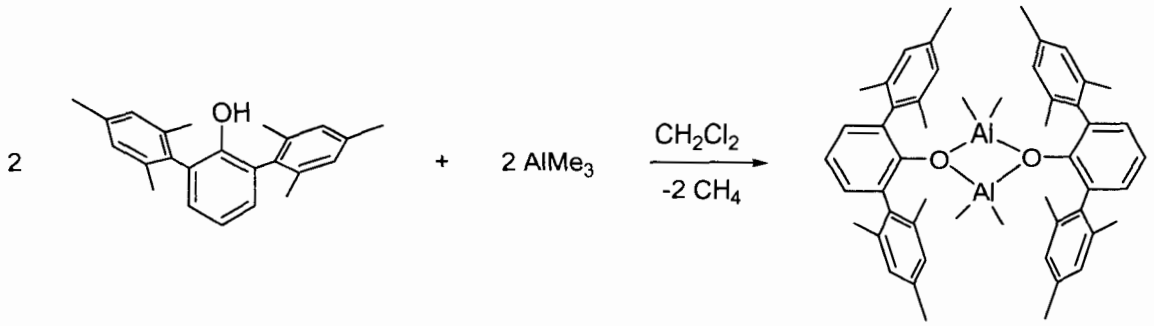

34 **40**

Figure 6.9 Structure of $[Me_2Al(\mu\text{-}OC_6H_3Mes_2)]_2$ 40. Thermal ellipsoids are shown at 50% probability, and hydrogen atoms and CH_2Cl_2 solvent have been removed for clarity.

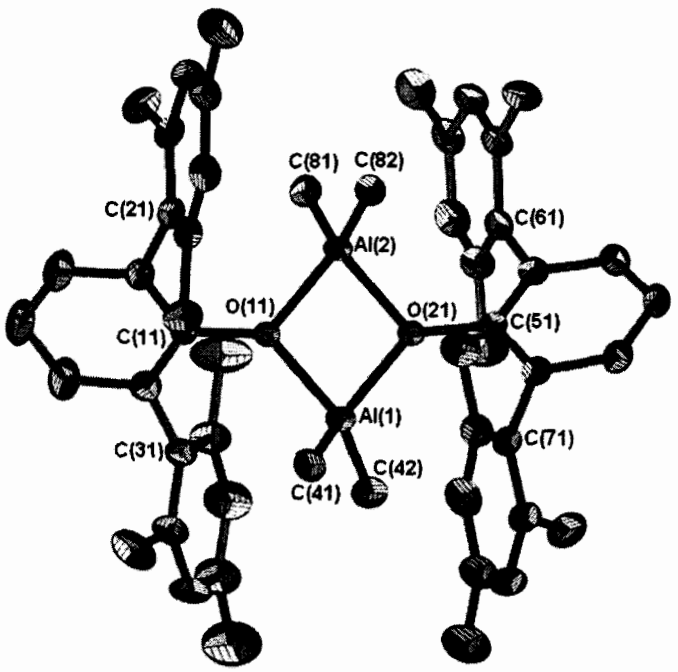

X-ray crystallographic studies* confirmed the formula proposed based on the ^1H NMR data, and showed that despite the bulk of the *m*-terphenyl, **40** exists in the solid state as an oxygen-bridged dimer (Figure 6.9). An identical motif was described by Rothwell for his less hindered 2,6-diphenylphenol aluminium complex[368] (Figure 6.10). In contrast, Power's bulkier 2,6-bis(2,4,6-triisopropylphenyl)phenol aluminium complex

* Structure solved by Dr. Gabriele Schatte, Saskatchewan Structural Sciences Centre.

can be isolated only as a base-stabilized monomeric ether solvate[349] (Figure 6.10). The Al-O bond lengths in **40** are very similar around the Al_2O_2 core, ranging from 1.8892(17) to 1.9044(18) Å, indicating equal Al-O interactions rather than distinct covalent and dative bonds. These values are longer than most Al-O bonds in tetracoordinate dialkylaluminium Al_2O_2 heterocycles, but still within the reported range [1.852(7) to 1.917(2) Å, mean = 1.880 Å].[368,369] The Al_2O_4 core of **40** is planar, as it is in most phenol-bridged aluminium dimers, unless constrained by linked ligands.[369c,e] The Al···Al distance of 2.8947(10) Å is, like the Al-O bonds, slightly above the average of 2.882 Å.

Figure 6.10 Rothwell's 2,6-diphenylphenol aluminium complex (left) and Power's 2,6-bis(2,4,6-triisopropylphenyl) phenol aluminium complex (right).

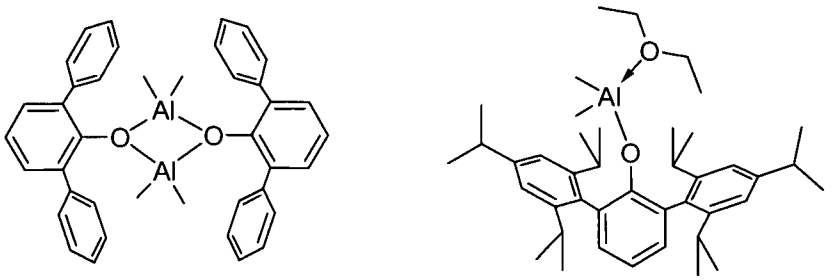

Table 6.6 Selected structural data for $[Me_2Al(\mu\text{-}OC_6H_3Mes_2)]_2$ 40.

Bond lengths (Å)			
Al(1)-O(21)	1.8892(17)	Al(2)-O(11)	1.8931(17)
Al(1)-O(11)	1.8979(18)	Al(2)-O(21)	1.9044(18)
Al(1)-C(41)	1.943(3)	Al(2)-C(81)	1.942(3)
Al(1)-C(42)	1.938(3)	Al(2)-C(82)	1.952(3)
O(11)-C(11)	1.402(3)	O(21)-C(51)	1.406(3)
Al···Al	2.8947(10)		
Bond angles (°)			
O(21)-Al(1)-O(11)	80.40(7)	O(11)-Al(2)-O(21)	80.14(7)
Al(2)-O(11)-Al(1)	99.56(8)	Al(1)-O(21)-Al(2)	99.47(8)
C(11)-O(11)-Al(2)	127.06(14)	C(51)-O(21)-Al(1)	134.17(15)
C(11)-O(11)-Al(1)	133.34(14)	C(51)-O(21)-Al(2)	125.17(14)

6.3 Transition metal *m*-terphenyl phenol and benzyl alcohol complexes

Of all the transition metals, titanium complexes are by far the most common for 2,6-diphenylphenol. Virtually all of these complexes feature two *m*-terphenyl phenol ligands on the titanium centre, and a few even accommodate three.[370] Only one complex is known with a single 2,6-diphenylphenol ligand, and it uses cyclopentadienyl as an ancillary ligand.[371] Would the increased bulk of **34** make it possible to isolate a titanium monophenoxide complex?

Addition of tetrakis(dimethylamino)titanium to a solution of **34** in dichloromethane resulted in the formation of an orange solid **41**. The ^{1}H NMR spectrum showed a 1:1 ratio between the N*Me*$_2$ ligand at 2.30 ppm and the *m*-terphenyl at 2.24 (*para*) and 2.11 (*ortho*) ppm. Given that titanium is tetravalent, that data suggested formation of a bis(phenoxide) complex with a formula of $(Me_2N)_2Ti(OC_6H_3Mes_2)_2$. This is formed even when only a single equivalent of the *m*-terphenyl phenol ligand is added.

Scheme 6.7 Synthesis of $[(Me_2N)_2Ti(OC_6H_3Mes_2)_2]$ 41.

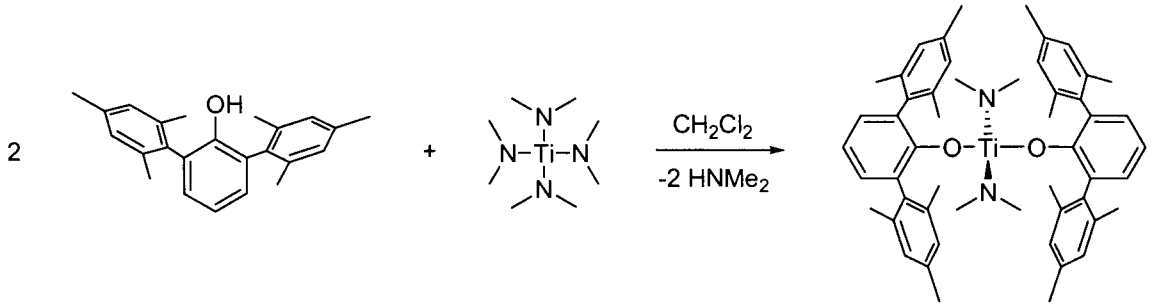

34 **41**

X-ray crystallographic studies of **41**[*] confirmed the proposed structure (Figure 6.11). The geometry at titanium is tetrahedral, with the greatest deviation in the O(11)-Ti(1)-O(21) angle [119.25.(5)°] and N(31)-Ti(1)-N(41) angle [102.88(6)°]. The Ti-O bonds are the same within experimental error, and are within the range of similar titanium complexes [1.786(2) - 1.862(5) Å].[372] The same is true for the two Ti-N bond lengths, for which literature values of similar compounds range from 1.854(7) to 1.897(5) Å.[372] The nature of the oxygen ligand appears to be the most important factor governing the coordination at titanium. All but one of the structurally characterized examples[112] of tetracoordinate titanium complexes with two oxygen donors and two nitrogen donors of any type $[(R_2N)_2Ti(OR)_2]$ were based on 2,6-disubstituted phenol ligands. The one exception featured a 2,6-disubstituted aniline instead.[373] It is not immediately clear if this is merely a coincidence or if the steric shielding of the *meta* substituents is chemically required.

Figure 6.11 Structure of $[(Me_2N)_2Ti(OC_6H_3Mes_2)_2]$ 41. Thermal ellipsoids are shown at 50% probability and hydrogen atoms have been removed for clarity.

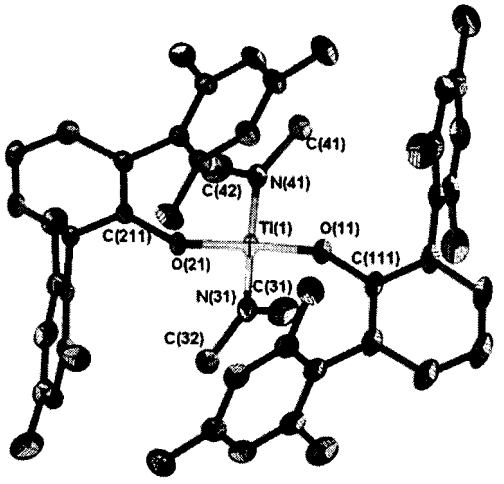

[*] Structure solved by Dr. Gabriele Schatte, Saskatchewan Structural Sciences Centre.

Table 6.7 Selected structural data for $[(Me_2N)_2Ti(OC_6H_3Mes_2)_2]$ 41.

Bond lengths (Å)			
Ti(1)-N(31)	1.8822(13)	N(31)-C(31)	1.451(2)
Ti(1)-N(41)	1.8763(13)	N(31)-C(32)	1.454(2)
Ti(1)-O(11)	1.8460(10)	N(41)-C(41)	1.446(2)
Ti(1)-O(21)	1.8495(10)	N(41)-C(42)	1.453(2)
O(11)-C(111)	1.3622(17)	O(21)-C(211)	1.3601(16)
Bond angles (°)			
O(11)-Ti(1)-O(21)	119.25(5)	N(31)-Ti(1)-N(41)	102.88(6)
O(11)-Ti(1)-N(41)	106.63(5)	O(11)-Ti(1)-N(31)	109.17(5)
O(21)-Ti(1)-N(31)	107.72(5)	O(21)-Ti(1)-N(41)	109.98(5)
C(111)-O(11)-Ti(1)	144.80(10)	C(211)-O(21)-Ti(1)	147.13(10)
C(31)-N(31)-C(32)	111.80(15)	C(41)-N(41)-C(42)	111.32(15)
C(31)-N(31)-Ti(1)	123.47(12)	C(41)-N(41)-Ti(1)	128.66(12)
C(32)-N(31)-Ti(1)	124.72(11)	C(42)-N(41)-Ti(1)	119.98(12)

The literature precedents for *m*-terphenyl phenol complexes of 2,6-diphenylphenol helped guide the choice of which metals would be appropriate for reaction with the bulkier 2,6-bis(2,4,6-trimethylphenyl)phenol **34**, but no such background existed for the related benzyl alcohols. Any of the metals previously reacted with the *m*-terphenyl phenols or carboxylic acids (Chapter 2) would therefore have given a novel product. The decision to treat 2,4,6-triphenylbenzyl alcohol **36** with diethyl zinc was based on the realization that the zinc compounds **4** and **22** had perhaps most clearly demonstrated the ability of *m*-terphenyl ligands to stabilize low-coordinate complexes. Complex **4** featured a tricoordinate zinc carboxylate molecule, while **22** contained tetracoordinate zinc in a 2-D network with labile ethanol coordination.

The equimolar reaction of **36** with $ZnEt_2$ proceeded readily in dichloromethane to give colourless crystals of **42**. The ^1H NMR data were in agreement with the reaction stoichiometry, with the diagnostic singlet for the *m*-terphenyl methylene protons at 4.91 ppm, slightly downfield from the corresponding doublet in the free ligand. The CH_2 and CH_3 protons of the remaining ethyl group were also readily identified as a quartet at 0.09

ppm and a triplet at 1.06 ppm. These values are similar to those reported for the zinc carboxylate complex **4**.

Scheme 6.8 Synthesis of $[EtZn(\mu\text{-}OCH_2C_6H_2Ph_3)]_2$ 42.

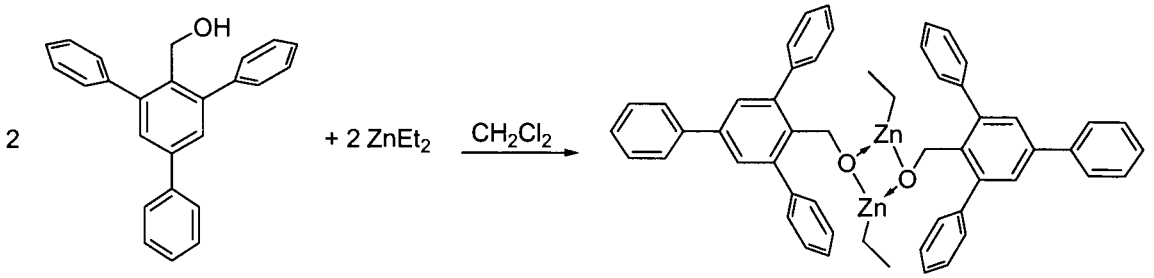

36 **42**

To determine whether **42** was a solid-state monomer like **39** or a dimer like **40**, X-ray crystallographic studies were performed.* Two crystallographically distinct oxygen bridged homodimers were found (Figure 6.12). The geometry at both the zinc atoms and the oxygen atoms is trigonal planar ($\Sigma\angle$ Zn = 360°; O = 356°). Unlike the zinc carboxylate **4**, there are no metal-π interactions. In **42**, the zinc···centroid distances measure 3.579 Å and 3.448 Å for Zn(1)···C(31-36) and Zn(2)···C(71-76) respectively, significantly longer than the sum of the van der Waals radii for zinc and benzene (1.39 + 1.77 = 3.16 Å).[115]

* Structure solved by Diane Dickie.

Figure 6.12 **Structure of $[EtZn(\mu\text{-}OCH_2C_6H_2Ph_3)]_2$ 42. Thermal ellipsoids are shown at 50% probability, and hydrogen atoms have been removed for clarity. Only one of the two crystallographically independent molecules is shown.**

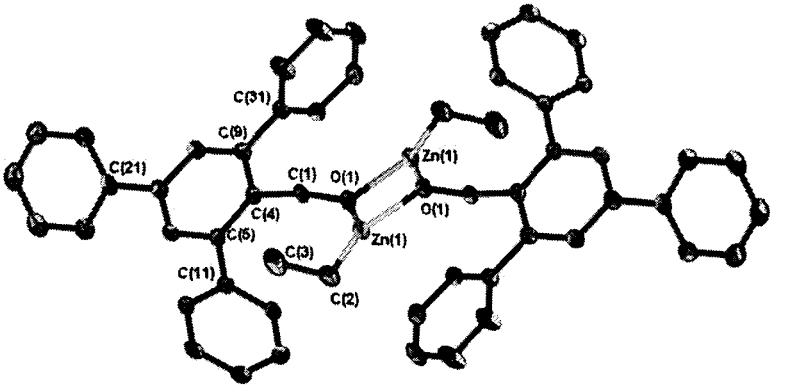

Table 6.8 **Selected structural data for $[EtZn(\mu\text{-}OCH_2C_6H_2Ph_3)]_2$ 42.**

Bond lengths (Å)			
Zn(1)-O(1)	1.9448(17)	Zn(2)-O(2)	1.9358(19)
Zn(1)-O(1)#1	1.9439(17)	Zn(2)-O(2)#2	1.9484(18)
Zn(1)-C(2)	1.944(3)	Zn(2)-C(42)	1.946(3)
O(1)-C(1)	1.427(3)	O(2)-C(41)	1.424(3)
Zn(1)···Zn(1)#1	2.9428(6)	Zn(2)···Zn(2)#2	2.9390(7)
Bond angles (°)			
O(1)#1-Zn(1)-O(1)	81.64(8)	O(2)-Zn(2)-O(2)#2	81.66(8)
O(1)#1-Zn(1)-C(2)	139.76(10)	O(2)-Zn(2)-C(42)	141.34(14)
C(2)-Zn(1)-O(1)	138.60(10)	C(42)-Zn(2)-O(2)#2	136.99(14)
C(1)-O(1)-Zn(1)#1	131.23(15)	C(41)-O(2)-Zn(2)	130.35(16)
C(1)-O(1)-Zn(1)	126.50(15)	C(41)-O(2)-Zn(2)#2	126.74(17)
Zn(1)#1-O(1)-Zn(1)	98.36(8)	Zn(2)-O(2)-Zn(2)#2	98.34(8)

Symmetry transformations used to generate equivalent atoms: #1 -x+1,-y+1,-z+1 #2 -x+1,-y+2,-z

Similar Zn_2O_2 heterocycles with *tricoordinate* zinc appear to be known only for bridging phenols, rather than bridging alcohols. The Zn-O bond lengths of **42** fall between 1.9358(19) to 1.9484(18) Å, within the range found for the related phenol complexes [1.911(1) to 2.021(4) Å].[374] Tolman recently published two *tetracoordinate* Zn-carbene complexes with bridging benzyl alcohol ligands,[375] and the Zn-O bond lengths and angles of 1.9198(15) to 2.0135(14) are quite comparable to both the phenolic examples and **42**, despite the difference in coordination number. The Zn···Zn separations in **42** [Zn(1)···Zn(1)#1 = 2.9428(6) Å; Zn(2)···Zn(2)#2 = 2.9390(7) Å] are within the

range of related literature compounds [2.894 to 3.0211(6)],[374,375] but significantly shorter than in the bridging carboxylate complex **4** at 3.5769(6) Å.

6.4 Summary and conclusions

The X-ray crystal structures of a *m*-terphenyl phenol and two *m*-terphenyl benzyl alcohols were described. The hydrogen bonding pattern observed in phenol **34**, intermolecular [O-H···O] dimerization, is very different from that observed in related *m*-terphenyl phenols. The steric demands of **34** are intermediate between those of previously characterized derivatives. This balance appears to be the key to the supramolecular interactions, as the same 2,4,6-trimethylphenyl substituent was used in the boronic acid **33** that also exhibited unprecedented [O-H···O] hydrogen bonds. Unfortunately, this analogy of different hydrogen bonding between phenyl and 2,4,6-trimethylphenyl derivatives could not be extended to the benzyl alcohols **36** and **37** due to disorder in the CH_2OH fragment of **37**.

Given the differences in the structures of the free ligands, it seemed possible that the main group and transition metal complexes of **34** would also have features not found in more and/or less bulky analogues. In the case of titanium complex **41** and aluminium complex **40**, this was not the case. Both molecules were essentially isostructural to known 2,6-diphenylphenol derivatives. The tin complex **38**, on the other hand, did show differences. The secondary metal-π interaction between the tin atom and flanking aryls of the *m*-terphenyl ligand in **38** provides increased thermal stability of nearly 100 °C relative to the bulkier 2,6-diisopropylphenylphenol derivatives in which that interaction is sterically hindered.

No such metal-π interactions were seen zinc complex **42**, the first structurally characterized *m*-terphenyl benzyl alcohol complex. This is in contrast to the zinc carboxylate **4**, in which the zinc was also bound by one carbon and two oxygen atoms, and may be due to the greater electron donating ability of the benzyl alcohol relative to carboxylate ligands, since the negative charge is localized on a single atom. The switch from phenol to benzyl alcohol appeared to have little effect on the structure of **42**, as its Zn_2O_2 core is a known motif for bridging phenols.

6.5 Future work

The solvent dependency of the reaction of $Ge[N(SiMe_3)_2]_2$ with the *m*-terphenyl phenol **34** needs to be explored in further detail to determine a reliable, reproducible synthesis of the mixed aryloxy/amido germylene **39**. Next most urgent is the synthesis of more complexes of the benzyl alcohols **36** and especially **37**. Diethylzinc should be the first metal tested with **37**, in order to compare and contrast it with the **42**. Both ligands should then be treated with each of the metals used in the study of phenol **34**, in order to probe the differences between the behaviour of benzyl alcohols and phenols. Aluminium and titanium have been the most studied in the literature for the related phenols, so they would be good starting points.

For the complexes that have already been made, several areas of future study are available. The zinc complex **42** should be treated with *N*-heterocyclic carbenes (NHCs) and/or the corresponding imidazolium salts to see if ring-opening polymerization catalysts related to those recently described by Tolman can be prepared.[375] Aluminium complex **40** should also be tested as a ring-opening polymerization catalyst, particularly

since recent studies have suggested that the active species in MAO-catalyst systems is in fact an Al-O-Al fragment,[376] which is present in **40**.

Of course, future research should by no means be limited only to the complexes already prepared. One option is to vary the metal-ligand stoichiometry for the combinations presented in this chapter. For example, although there was one previously known analogue of aluminium compound **40**, bis and tris(2,6-diphenylphenoxide) complexes are much more common, especially for catalytic applications. Attempts could be made to prepare 2:1 and or 3:1 complexes of **34** with aluminium to see if they display complementary reactivity. The same could be done with the benzyl alcohols **36** and **37**.

The second route is potentially more rewarding. Despite extensive studies of bulky phenols with early transition metals, the chemistry of late transition metals is essentially untouched. No *m*-terphenyl phenol complexes have been made with group seven or group 10 elements, and only a single example is known in groups eight[377] and nine.[378] Recent work by Fogg demonstrated that replacing halide ligands in ruthenium catalysts with aryloxides can lead to greatly improved activity, but if the sterics are not carefully controlled, decomposition by bridging is common.[379] Ligands like **34**, **36** and **37** could provide just the right balance.

A similar discrepancy exists in the main group elements. Tin(IV), germanium(IV) and especially aluminium(III) are very well studied for 2,6-diphenylphenol, but there is a combined total of only four complexes for all the remaining elements in groups 13-15.[357,380] The elements that may be most interesting to combine with **34**, **36**, and **37** are bismuth and silicon. Bulky phenols have been used as ligands on bismuth(III) to prepare model compounds of the active mixed-metal Bi-Mo

catalyst in the SOHIO process (oxidation/ammoxidation of propylene to acrolein or acrylonitrile, producing 5 000 000 tons/year in 2000).[381] Bismuth(III) aryloxides have also been studied as precursors to bismuth oxide catalysts, superconductors and ferroelectric materials.[382]

Reaction of the *m*-terphenyl phenol **34** and/or benzyl alcohols **36** and **37** with an appropriate silicon precursor could lead to new silylenes (R_2Si:). The silylenes are still the rarest of the divalent group 14 element,[383] and would be analogous to the germylene **39a** and stannylene **38**. The work of Barrau[384] on silanethiones (R_2Si=S) suggests that *m*-terphenyl phenol complexes might be precursors for that class of molecules as well as the elusive silanones (R_2Si=O).[184]

Finally, instead of looking at what others have done with smaller alkoxy and aryloxy ligands, inspiration for new pathways could be drawn from nitrogen-based derivatives. Lappert and Power recently used an amido ligand with steric demands similar to the *m*-terphenyls to prepare a "metalloid cluster" of 15 tin atoms $[Sn_9(Sn\{NRR'\})_6]$.[385] Could a similar structure be obtained from the oxygen-based ligands **34**, **36** or **37**?

6.6 Experimental

6.6.1 Synthesis of ligands and precursors

2,6-bis(2,4,6-Trimethylphenyl)phenol (34): Under an inert atmosphere, *n*-BuLi (2.8 mL, 4.5 mmol, 1.6 M in hexanes) was added dropwise to a suspension of 2,6-bis(2,4,6-trimethylphenyl)iodobenzene (1.32 g, 3.0 mmol) in 20 mL anhydrous Et_2O. After 2 h, the solution was cooled to -78 °C and freshly distilled nitrobenzene (1.5 mL,

15 mmol) was added dropwise. The bright red solution was allowed to stir for 5 min and then 20 mL of methanol was added slowly. After warming to r.t., 30 mL of H_2O was added and the organic layer was separated. The aqueous layer was acidified with 1 mL concentrated HCl and then extracted with Et_2O. The combined organic fractions were washed with water and saturated $NaCl_{(aq)}$ and then dried over $MgSO_4$. The solution was concentrated to ca. 10 mL and then passed through a plug of silica. After addition of ca. 10 mL pentane, the solution was left to evaporate slowly at room temperature overnight. The resultant pale brown solid was recrystallized to give colourless to pale blue crystals. Yield = 0.39 g (40%), mp = 145 °C. ^{1}H NMR ($CDCl_3$, 499.767 MHz,) δ 7.03 (m, 3H), 6.98 (s, 4H), 4.53 (s, 1H), 2.33 (s, 6H), 2.06 (s, 12H). $^{13}C\{^1H\}$ NMR ($CDCl_3$, 100.624 MHz) δ 137.5, 137.2, 135.9, 133.4, 129.6, 128.5, 128.1, 120.7, 21.2, 20.4. IR (nujol mull) ν 3486 (s), 3451 (s), 1611 (w), 1584 (w), 1573 (w), 1490 (m), 1320 (s), 1260 (m), 1221 (vs), 1170 (s), 1089 (m), 1071 (m), 1030 (w), 1008 (w), 848 (vs), 829 (s), 797 (s), 780 (w), 752 (vs), 740 (w), 715 (w). Anal Calcd for $C_{24}H_{26}O$: C, 87.23; H, 7.93. Found: C, 87.50; H, 8.04. HR-MS (*m/z*): [M^+] calculated for $C_{24}H_{26}O$, 330.198; Found: 330.198.

2,6-bis(2,4,6-Trimethylphenyl)benzaldehyde (35): Prepared according to the same procedure as **25**, beginning with 2,6-bis(2,4,6-trimethylphenyl)iodobenzene (15.0 g, 34.1 mmol). Yield = 8.13 g (76%), mp = 208-210 °C. ^{1}H NMR ($CDCl_3$, 499.767 MHz) δ 9.65 (s, 1H), 7.66 (t, J = 7.5 Hz, 1H), 7.17 (d, J = 7.5 Hz, 2H), 6.94 (s, 4H), 2.34 (s, 6H), 1.96 (s, 12H). $^{13}C\{^1H\}$NMR ($CDCl_3$, 100.624) δ 192.4, 143.8, 136.9, 136.4, 135.3, 133.4, 132.5, 129.9, 128.1, 21.1, 20.6. IR (nujol mull) ν 2743 (m), 1702 (vs), 1612 (s), 1574 (s), 1416 (m), 1396 (m), 1277 (m), 1195 (s), 1178 (m), 1105 (w), 1090 (w), 1034

(m), 1013 (m), 858 (s), 846 (s), 777 (w), 751 (m), 739 (m), 675 (m). Anal Calcd for $C_{25}H_{26}O$: C, 87.68; H, 7.65. Found: C, 87.41; H, 7.41.

2,4,6-Triphenylbenzylalcohol (36): A solution of 2,4,6-triphenylbenzaldehyde **24** (4.0 g, 12.0 mmol) in 50 mL 90% EtOH was cooled to 0 °C and $NaBH_4$ (0.5 g, 13.1 mmol) was added slowly in small portions. The reaction mixture was then heated to 120 °C for 30 min. Upon cooling to r.t., 30 mL H_2O was added and the mixture was acidified with 6 M HCl to pH 1-2. The reaction was extracted with Et_2O, then the organic layer was washed with saturated $NaCl_{(aq)}$ and dried over $MgSO_4$. The solution was concentrated under vacuum and then cooled to -20 °C to give colourless crystals. Yield = 3.0 g (75%), mp = 116-120 °C (lit. 128 °C).[109] ^1H NMR ($CDCl_3$, 499.767 MHz) δ 7.65 (d, J = 7.2 Hz, 2H), 7.54-7.56 (m, 6H), 7.40-7.49 (m, 10H), 7.35 (t, J = 7.2 Hz, 1H), 4.48 (d, J = 5.9 Hz, 2H), 1.45 (t, J = 5.9 Hz, 1H). IR (nujol mull) ν 3428 (br), 3324 (br), 1595 (m), 1565 (w), 1493 (m), 1455 (s), 1414 (m), 1198 (w), 1155 (w), 1087 (w), 1075 (m), 1030 (m), 992 (s), 886 (s), 772 (s), 760 (vs), 718 (w), 699 (vs).

2,6-bis(2,4,6-Trimethylphenyl)benzyl alcohol (37): Prepared according to the same procedure as **36**, beginning with 2,6-bis(2,4,6-trimethylphenyl)benzaldehyde **35** (0.25 g, 0.7 mmol). Yield = 0.19 g (75%), mp = 202 °C. ^1H NMR ($CDCl_3$, 499.767 MHz) δ 7.34 (t, J = 7.6 Hz, 1 H), 6.98 (d, J = 7.6 Hz, 2H), 6.88 (s, 4H), 3.94 (br, 2H), 2.26 (s, 6H), 1.93 (s, 12H). $^{13}C\{^1H\}$ NMR ($CDCl_3$, 125.677 MHz) δ 141.4, 137.4, 136.8, 135.9, 128.7, 128.5, 128.2, 128.1, 60.7, 21.1, 20.7. IR (nujol mull) ν 3563 (w), 3522 (w), 3050 (w), 2729 (w), 1611 (m), 1581 (w), 1573 (w), 1484 (m), 1261 (m), 1192 (w), 1171 (w), 1100 (m), 1013 (s), 975 (w), 959 (w), 940 (w), 846 (s), 803 (vs), 759 (m), 743 (w), 701 (w). Elemental analysis not obtained.

6.6.2 Synthesis of main group complexes

[Sn(OC$_6$H$_3$Mes$_2$)$_2$] (38): Under an inert atmosphere, a solution of Sn[N(SiMe$_3$)$_2$]$_2$ (0.33 g, 0.76 mmol) in 2 mL anhydrous benzene was added dropwise to a solution of 2,6-bis(2,4,6-trimethylphenyl)phenol **34** (0.50 g, 1.51 mmol) in 10 mL anhydrous benzene. The mixture was allowed to stir for 3 h at r.t. and then filtered. Slow evaporation of the solvent gave a yellow solid that was recrystallized from warm hexanes to give colourless crystals: Yield = 0.48 g (81%), mp = 321-322 °C. ^{1}H NMR (CD_2Cl_2, 499.767 MHz) δ 6.84 (d, J = 6.9 Hz, 2H), 6.79 (s, 4H), 6.73 (t, J = 6.9 Hz, 1H), 2.29 (s, 6H), 1.82 (s, 12H). ^{13}C NMR (100.624 MHz, C_6D_6) δ 157.8, 138.5, 137.8, 137.4, 129.7, 129.5, 129.2, 117.9, 21.1, 20.5. ^{119}Sn{^{1}H} (CD_2Cl_2, 223.867 MHz) δ -344.23. IR (nujol mull) ν 1610 (m), 1584 (m), 1412 (s), 1262 (m), 1246 (s), 1088 (w), 1072 (m), 1031 (br), 844 (vs), 798 (w), 787 (w), 752 (m), 739 (w), 649 (m). Anal Calcd for $C_{48}H_{50}O_2Sn$: C, 74.14; H, 6.48. Found: C, 74.03; H, 6.39.

[(Me$_3$Si)$_2$NGe(OC$_6$H$_3$Mes$_2$)] (39): Under an inert atmosphere, a solution of Ge[N(SiMe$_3$)$_2$]$_2$ (0.57 g, 1.45 mmol) in 2 mL CH_2Cl_2 was added dropwise to a solution of 2,6-bis(2,4,6-trimethylphenyl)phenol **34** (0.48 g, 1.45 mmol) in 5 mL anhydrous CH_2Cl_2. After 5 min, the solvent was removed under vacuum and the crude product was recrystallized from benzene. Mp = 84-86 °C. ^{1}H NMR (C_6D_6, 499.768 MHz) δ 7.62 (t, J = 7.5 Hz, 1H), 7.22 (d, J = 7.5 Hz, 2H), 7.03 (s, 4H), 2.42 (s, 6H), 2.18 (s, 12H), 0.00 (s, 18H). (This molecule was not isolated as an analytically pure compound).

[Ge(OC$_6$H$_3$Mes$_2$)$_2$] (39a): Under an inert atmosphere, a solution of Ge[N(SiMe$_3$)$_2$]$_2$ (0.24 g, 0.61 mmol) in 2 mL hexanes was added dropwise to a suspension of 2,6-bis(2,4,6-trimethylphenyl)phenol **34** (0.20 g, 0.61 mmol) in 5 mL

anhydrous hexanes. After 45 min, the solvent was decanted from a white precipitate. Yield = 0.16 g (72%), mp = 318-319 °C. ^{1}H NMR (CD_2Cl_2, 499.767 MHz) δ 6.81-6.88 (m, 3H), 6.75 (s, 4H), 2.29 (s, 6H), 1.79 (s, 12H). ^{13}C NMR (CD_2Cl_2, 125.678 MHz) δ 138.1, 136.2, 129.5, 129.2, 128.8, 128.5, 119.2, 21.0, 20.1. IR (nujol mull) ν 1610 (w), 1585 (w), 1484 (m), 1414 (s), 1260 (s), 1230 (vs), 1091 (m), 1071 (s), 1016 (m), 948 (w), 845 (vs), 799 (m), 754 (s), 739 (w), 728 (w), 670 (m), 659 (s), 609 (m). Anal Calcd for $C_{48}H_{50}GeO_2$: C, 78.81; H, 6.89. Found: C, 79.14; H, 7.08.

$[Me_2Al(\mu\text{-}OC_6H_3Mes_2)]_2$ (40): Under an inert atmosphere, $AlMe_3$ (1.01 mL, 2.0 M in hexanes) was added dropwise to a solution of 2,6-bis(2,4,6-trimethylphenyl)phenol **34** (0.56 g, 1.69 mmol) in 10 mL anhydrous CH_2Cl_2. After stirring for 5 min at r.t., the solution was concentrated under vacuum and then cooled to -30 °C. The next day, the solution was decanted from colourless crystals. Yield = 0.25 g (38 %), mp = 238-240 °C. ^{1}H NMR (C_6D_6, 499.767 MHz) δ 6.85 (s, 4H), 6.69 (t, J = 7 Hz, 1H), 6.59 (d, J = 7 Hz, 2H), 2.19 (s, 6H), 2.15 (s, 12H), -1.26 (s, 6H). ^{13}C NMR (C_6D_6, 125.680 MHz) δ 138.3, 137.9, 135.9, 133.1, 129.5, 129.3, 128.3, 21.9, 21.7. IR (nujol mull) ν 1610 (w), 1405 (m), 1261 (w), 1190 (m), 1182 (m), 1091 (m), 1032 (w), 848 (m), 825 (m), 803 (w), 774 (w), 758 (w), 701 (s), 635 (m). Anal Calcd for$C_{52}H_{62}Al_2O_2$, C, 80.80; H, 8.08. Found: C, 81.14; H, 8.18.

6.6.3 Synthesis of transition metal complexes

$[(Me_2N)_2Ti(OC_6H_3Mes_2)_2]$ (41): Under an inert atmosphere, a solution of $Ti(NMe_2)_4$ (0.26 g, 1.15 mmol) in 5 mL anhydrous CH_2Cl_2 was added dropwise to a solution of 2,6-bis(2,4,6-trimethylphenyl)phenol **34** (0.76 g, 2.30 mmol) in 10 mL

anhydrous CH_2Cl_2. The solution was allowed to stir for 10 min at r.t. and then cooled to -30 °C. After 3 hours, the solution was decanted from orange crystals. Yield = 0.59 g (64%), mp 180 °C (dec). ^{1}H NMR (C_6D_6, 400.137 MHz) δ 6.82-6.87 (m, 7H), 2.30 (s, 6H), 2.24 (s, 6H), 2.11 (s, 12H). ^{13}C NMR (C_6D_6, 100.624 MHz) δ 160.2, 137.3, 136.7, 135.6, 131.1, 130.5, 128.3, 120.2, 43.8, 21.0, 20.9. IR (nujol mull) ν 3279 (m), 1611 (m), 1580 (m), 1484 (m), 1413 (vs), 1345 (m), 1251 (vs), 1229 (vs), 1146 (m), 1083 (s), 1054 (m), 1029 (m), 1008 (m), 950 (s), 904 (m), 876 (vs), 849 (vs), 799 (m), 778 (m), 757 (vs), 741 (w), 691 (vs), 679 (s), 597 (s). Anal Calcd for $C_{52}H_{62}N_2O_2Ti$: C, 78.57; H, 7.86; N, 3.52. Found: C, 78.20; H, 7.83; N, 3.37.

[EtZn(μ-OCH$_2$C$_6$H$_2$Ph$_3$)]$_2$ (42): Under an inert atmosphere, $ZnEt_2$ (4.9 mL, 4.93 mmol, 1.0 M in hexanes) was added dropwise to a solution of 2,4,6-triphenylbenzylalcohol **36** (0.79 g, 2.35 mmol) in 15mL anhydrous CH_2Cl_2. The solution was allowed to stir overnight, and was then concentrated under vacuum and cooled to -30 °C. The next day, the solution was decanted from colourless crystals. Yield = 0.69 g (68%), mp = 163-165 °C. ^{1}H NMR (C_6D_6, 400.136 MHz) δ 7.54 (s, 2H), 7.14-7.44 (m, 15H), 4.91 (s, 2H), 1.06 (t, J = 8.1 Hz, 3 H), 0.09 (q, J = 8.1 Hz, 2H). ^{13}C{^{1}H} (CD_2Cl_2, 125.680 MHz) δ 144.3, 143.6, 141.8, 141.1, 139.5, 130.5, 130.2, 129.7, 129.6, 128.9, 128.5, 128.4, 64.1, 12.6, 0.00. IR (nujol mull) ν 3054 (m), 3029 (m), 2807 (w), 2721 (w), 1595 (m), 1574 (w), 1562 (w), 1493 (s), 1442 (m), 1430 (w), 1416 (w), 1396 (w), 1194 (w), 1178 (w), 1156 (w), 1077 (m), 1032 (vs), 1012 (m), 999 (m), 889 (m), 794 (m), 770 (s), 761 (vs), 704 (vs), 697 (s). Anal calcd for $C_{27}H_{24}OZn$: C, 75.44; H, 5.63. Found: C, 75.66; H, 5.58.

7 GLOBAL CONCLUSIONS

A recent editorial in a leading ACS publication stated that although "the goal of basic chemical research is to create and understand chemical materials and processes well enough to predict their properties," scientists are "generally unable to predict the impact of their latest results, much less whether the work will yield something useful to society. [...] The true outcome will depend on other scholars' thinking and on future research, and these complexities cannot be known ahead of time."[386] In light of that assertion, this chapter is designed to pull together the conclusions drawn from the work described in the previous chapters, to help bring into focus the contribution of this research to the knowledge of the greater chemical community.

In broad terms, I studied the influence of substituted *m*-terphenyl ligands on main group and transition metal complexes in order to better understand the impact of sterics on the coordination and reactivity at these metal centres. One of the specific goals of this project was to discover if it was possible to incorporate *m*-terphenyls into materials beyond simple molecules, to take advantage of their steric shielding in a new context. The metal-organic frameworks described in Chapter 3, especially the zinc complex **22**, demonstrated how *m*-terphenyls limit the coordination at metal atoms to well-defined two-dimensional arrays reminiscent of common clays. A different type of array was discussed in Chapter 4, namely the self-assembled monolayer of *m*-terphenyl thiols on gold. Although *m*-terphenyls have long been known to limit aggregation in molecular

complexes, using them in this way, to lower the number of active sites on a 2-D functionalized surface, has opened up a completely new field for these molecules.

Of course, the work on these extended structures was possible only because of the knowledge gained by studying discrete molecules as model compounds. The tri-coordinate zinc carboxylate **4**, described in Chapter 2, provided the most compelling evidence that *m*-terphenyls are capable of enforcing low coordination numbers at metal sites. The series of tin(II) carboxylates (**6-8**) with a common $Sn_2O_4C_2$ core, also described in Chapter 2 showed that the steric bulk of the ligand could be varied without affecting the coordination environment. Once a certain steric threshold is crossed, though, the differences are dramatic, as illustrated by the differences in the aluminium (**40**) and tin (**38**) phenol complexes of Chapter 6 with respect to the bulkier analogues recently reported by Power.[349]

Having control over the coordination environment is useful because it allows reactivity to be managed, and not simply blocked. Aluminium complex **29** (Chapter 5) was found to initiate the ring-opening polymerization of ε-caprolacton, thereby establishing that *m*-terphenyls can control the environment around a metal without completely shutting down the reactivity. This reactivity was an important contributing factor for the serendipitous discovery of the most unusual molecule in this thesis, the Sn_2N_2 heterocycle **9** (Chapter 2) whose bonding and electronic nature is still being studied.

APPENDIX 1: CRYSTALLOGRAPHIC DATA

Table A1: Crystallographic data for compounds in chapter 2.

Compound name (#)	$[Me_2Al(\mu\text{-}O_2C C_6H_2(Ph_3)]_2$ **(2)**	$[EtZn(\mu\text{-}O_2C C_6H_3Mes_2)]_2$ **(4)**	$[(Me_3Si)_2NSn(\mu\text{-}O_2CC_6H_2Ph_3)]_2$ **(6)**	$[(Me_3Si)_2NSn(\mu\text{-}O_2CC_6H_3Mes_2)]_2$ **(7)**
Formula	$C_{54}H_{46}Al_2O_4$	$C_{54}H_{60}O_4Zn_2$	$C_{64}H_{74}Cl_4N_2O_4Si_4Sn_2$	$C_{63}H_{88}Cl_2N_2O_4Si_4Sn_2$
FW	812.87	903.76	1426.79	1357.99
T, K	294(2)	150(2)	150(2)	173(2)
colour	colourless	colourless	colourless	colourless
size	0.58 x 0.48 x 0.15	0.68 x 0.41 x 0.34	0.125 x 0.20 x 0.225	0.25 x 0.25 x 0.25
cryst. syst.	triclinic	orthorhombic	triclinic	monoclinic
space group	P-1	Pbca	P-1	P2/c
a, Å	9.9702(2)	23.1334(4)	10.429(2)	17.2290(2)
b, Å	10.6813(2)	15.9039(2)	13.276(3)	19.5480(2)
c, Å	11.3952(2)	25.6396(4)	14.405(3)	20.4440(2)
α, deg	77.0130(10)	90	104.92(3)	90
β, deg	85.6730(10)	90	110.62(3)	95.4530(6)
γ, deg	74.0890(10)	90	101.70(3)	90
V, Å^3	1137.06(4)	9433.1(2)	1706.1(6)	6854.23(13)
Z	1	8	1	4
D_{calc}, Mg·m^{-3}	1.187	1.273	1.389	1.316
μ, mm^{-1}	0.109	1.061	1.004	0.920
R_1*	0.0433	0.0465	0.0348	0.0368
wR_2*	0.1128	0.0949	0.0737	0.0716
Data collect.	UWO	UWO	UWO	SSSC
Struct. sol.	Dr. M. Jennings	Dr. M. Jennings	D. Dickie	Dr. G. Schatte
CCDC no.	230826	266025	618667	618668

* $R_1 = [\Sigma||F_o|-|F_c||]/[\Sigma|F_o|]$ for $[F_o^2 > 2\sigma(F_o^2)]$; $wR_2 = \{[\Sigma w(F_o^2-F_c^2)^2]/[\Sigma w(F_o^2)^2]\}^{1/2}$

Table A1 (cont)

Compound name (#)	$[(Me_3Si)_2NSn(\mu\text{-}O_2CC_6H_2Mes_2Me)]_2$ **(8)**	$[(Mes_2C_6H_3CO_2)Sn(\mu\text{-}NSiMe_3)]_2$ **($9\cdot CH_2Cl_2$)**	$[(Mes_2C_6H_3CO_2)Sn(\mu\text{-}NSiMe_3)]_2$ **($9\cdot Et_2O$)**	$(CH_2Cl)(Cl)Sn[N(SiMe_3)_2]_2$ **(11)**
Formula	$C_{66}H_{94}Cl_4N_2O_4Si_4Sn_2$	$C_{29}H_{36}Cl_2NO_2SiSn$	$C_{60}H_{78}N_2O_5Si_2Sn_2$	$C_{13}H_{38}Cl_2N_2Si_4Sn$
FW	1470.97	648.29	1200.80	524.40
T, K	150(2)	223(2)	173(2)	173(2)
colour	colourless	colourless	colourless	colourless
size	0.125 x 0.30 x 0.40	0.2 x 0.45 x 0.45	0.20 x 0.20 x 0.25	0.15 x 0.20 x 0.20
cryst. syst.	triclinic	triclinic	triclinic	triclinic
space group	P-1	P-1	P-1	P-1
a, Å	11.8023(6)	10.5733(6)	10.8922(3)	8.55900(10)
b, Å	12.5695(9)	11.8229(6)	11.7957(3)	11.3010(2)
c, Å	14.2170(10)	13.8362(7)	12.3240(3)	14.9150(3)
α, deg	67.446(3)	67.2930(10)	77.2409(16)	105.9710(12)
β, deg	65.690(2)	79.9680(10)	75.5426(16)	96.8970(13)
γ, deg	76.473(3)	89.7190(10)	87.3334(17)	108.9690(14)
V, Å^3	1767.8(2)	1567.46(14)	1495.34(7)	1276.35(4)
Z	1	2	1	2
D_{calc}, Mg·m^{-3}	1.382	1.374	1.333	1.365
μ, mm^{-1}	0.971	1.048	0.922	1.397
R_1*	0.0635	0.0433	0.0427	0.0247
wR_2*	0.1723	0.1173	0.0920	0.0562
Data collect.	UWO	SMU	SSSC	SSSC
Struct. sol.	D. Dickie	D.Dickie/H. Jenkins	D.Dickie/G.Schatte	D.Dickie/G.Schatte
CCDC no.	618669	618670	618671	618666

* $R_1 = [\Sigma||F_o|-|F_c||]/[\Sigma|F_o|]$ for $[F_o^2 > 2\sigma(F_o^2)]$; $wR_2 = \{[\Sigma w(F_o^2-F_c^2)^2]/[\Sigma w(F_o^2)^2]\}^{1/2}$

Table A1 (cont)

Compound name (#)	$[(Mes_2C_6H_3CO_2)Si(NMe_2)_3]$ **(12)**	$[(Mes_2C_6H_3CO_2)Ti(NMe_2)_3]$ **(13)**	$[(Mes_2C_6H_3CO_2)_2Ti(NMe_2)_2]$ **(13a)**
Formula	$C_{31}H_{43}N_3O_2Si$	$C_{31}H_{43}N_3O_2Ti$	$C_{55}H_{64}Cl_2N_2O_4Ti$
FW	517.77	537.58	935.88
T, K	173(2)	295(2)	173(2)
colour	colourless	yellow	orange
size	0.25 x 0.25 x 0.20	0.3 x 0.3 x 0.3	0.10 x 0.15 x 0.20
cryst. syst.	triclinic	orthorhombic	monoclinic
space group	P-1	Pna2(1)	P2(1)/c
a, Å	8.6310(2)	23.3385(4)	22.6200(5)
b, Å	10.3890(3)	11.3985(3)	10.8510(10)
c, Å	18.1010(5)	12.0121(5)	24.4610(11)
α, deg	80.7600(9)	90	90
β, deg	78.8330(10)	90	121.716(3)
γ, deg	72.7830(13)	90	90
V, Å^3	1511.73(7)	3195.51(17)	5107.3(5)
Z	2	4	4
D_{calc}, Mg·m^{-3}	1.137	1.117	1.217
μ, mm^{-1}	0.108	0.296	0.318
R_1*	0.0691	0.0542	0.0627
wR_2*	0.1875	0.1423	0.1334
Data collect.	SSSC	SSSC	SSSC
Struct. sol.	Dr. G. Schatte	D. Dickie	D. Dickie
CCDC no.	618676	618678	618679

* $R_1 = [\Sigma||F_o|-|F_c||]/[\Sigma|F_o|]$ for $[F_o^2 > 2\sigma(F_o^2)]$; $wR_2 = \{[\Sigma w(F_o^2-F_c^2)^2]/[\Sigma w(F_o^2)^2]\}^{1/2}$

Table A2: Crystallographic data for compounds in chapter 3.

Compound name (#)	2,6-Diphenyl-1,4-dibenzoic acid **(15H$_2$)**	**15H$_2$**·4.4'Bipy **(16)**	**15**·Zn·(py)$_2$·MeOH **(17)**	**15**·Co·(py)$_2$·MeOH **(18)**
Formula	$C_{20}H_{14}O_4$	$C_{30}H_{22}N_2O_4$	$C_{31}H_{26}N_2O_5Zn$	$C_{31}H_{26}CoN_2O_5$
FW	318.31	474.50	571.91	565.47
T, K	173(2)	173(2)	173(2)	223(2)
colour	colourless	colourless	colourless	pink
size	0.10 x 0.10 x 0.20	0.20 x 0.25 x 0.25	0.05 x 0.13 x 0.13	0.04 x 0.28 x 0.34
cryst. syst.	tetragonal	monoclinic	monoclinic	monoclinic
space group	$P4_12_12$	$P2_1/c$	$P2_1/n$	$P2_1/n$
a, Å	13.5640(3)	10.4550(2)	10.6080(2)	10.640(1)
b, Å	13.5640(3)	13.3910(3)	14.9550(4)	15.018(2)
c, Å	17.0150(4)	19.0530(5)	16.4450(4)	16.425(2)
α, deg	90	90	90	90
β, deg	90	116.6730(8)	90.676(1)	90.703(2)
γ, deg	90	90	90	90
V, Å^3	3130.4(1)	2383.61(9)	2608.7(1)	2624.5(6)
Z	8	4	4	4
D_{calc}, Mg·m^{-3}	1.351	1.322	1.456	1.431
μ, mm^{-1}	0.094	0.089	0.987	0.699
R_1*	0.0396	0.0518	0.0463	0.0422
wR_2*	0.0808	0.1190	0.0946	0.0970
Data collect.	SMU	SSSC	SSSC	SMU
Struct. sol.	Dr. H. Jenkins	Dr. G. Schatte	Dr. G. Schatte	D. Dickie/H. Jenkins
CCDC no.	266027	279136	279137	279138

* $R_1 = [\Sigma||F_o|-|F_c||]/[\Sigma|F_o|]$ for $[F_o^2 > 2\sigma(F_o^2)]$; $wR_2 = \{[\Sigma w(F_o^2-F_c^2)^2]/[\Sigma w(F_o^2)^2]\}^{1/2}$

Table A2 (cont)

Compound name (#)	**(15H)$_2$**·Cu·(py)$_2$ **(19)**	**(15H)$_2$**·Cu·(py)$_4$·(H$_2$O)$_2$ **(20)**	**15**·Ag$_2$ **(21)**	**15**·Zn·(EtOH)$_2$ **(22)**
Formula	$C_{50}H_{36}CuN_2O_8$	$C_{120}H_{100}Cu_2N_8O_{20}$	$C_{20}H_{12}Ag_2O_4$	$C_{24}H_{24}O_6Zn$
FW	856.35	2101.18	532.04	473.80
T, K	173(2)	223(2)	150(2)	295(2)
colour	blue	blue	colourless	colourless
size	0.15 x 0.20 x 0.20	0.060x 0.25x 0.40	0.08 x 0.27x 0.47	0.20 x 0.22x 0.28
cryst. syst.	orthorhombic	triclinic	monoclinic	triclinic
space group	Pbca	P-1	C2/c	P-1
a, Å	17.2170(2)	9.3336(5	17.334(1)	11.1000(3)
b, Å	12.9640(3)	11.7460(6)	11.1485(9)	13.6800(6)
c, Å	18.7630(4)	24.569(1)	9.4161(5)	15.7170(6)
α, deg	90	76.949(1)	90	98.866(2)
β, deg	90	86.176(1)	114.154(4)	90.857(2)
γ, deg	90	79.1960(10)	90	95.610(2)
V, Å^3	4187.9(1)	2576.6(2)	1660.4(2)	2345.6(1)
Z	4	1	4	4
D_{calc}, Mg·m^{-3}	1.358	1.354	2.128	1.342
μ, mm^{-1}	0.580	0.489	2.382	1.082
R_1*	0.0426	0.0398	0.0330	0.0657
wR_2*	0.0954	0.0777	0.0833	0.1806
Data collect.	SSSC	SMU	UWO	UWO
Struct. sol.	Dr. G. Schatte	D. Dickie/H. Jenkins	Dr. M. Jennings	Dr. M. Jennings
CCDC no.	279139	279140	279141	266026

* $R_1 = [\Sigma||F_o|-|F_c||]/[\Sigma|F_o|]$ for $[F_o^2 > 2\sigma(F_o^2)]$; $wR_2 = \{[\Sigma w(F_o^2-F_c^2)^2]/[\Sigma w(F_o^2)^2]\}^{1/2}$

Table A3: Crystallographic data for compounds in chapters 4 and 5.

Compound name (#)	4-Methyl-2,6-diphenylbenzoic acid **(14)**	*N*-(2',4',6'-Triphenyl benzylidene)-2-iminophenol **(26)**	N-(2',4',6'-Triphenyl benzyl)-2-amino phenol **(27)**	Sn·TPIP **(28)**
Formula	$C_{20}H_{16}O_2$	$C_{31}H_{23}NO$	$C_{31}H_{25}NO$	$C_{153}H_{170}Cl_{10}N_8O_4Si_8Sn_4$
FW	288.33	425.50	427.52	3238.95
T, K	223(2)	297(2)	296(2)	173(2)
colour	colourless	yellow	orange-brown	orange
size	0.2 x 0.2 x 0.35	0.33 x 0.28 x 0.05	0.40 x 0.35 x 0.28	0.15 x 0.10 x 0.10
cryst. syst.	monoclinic	monoclinic	monoclinic	triclinic
space group	P2(1)/c	P2(1)/c	P2(1)/n	P-1
a, Å	9.4738(7)	17.4903(4)	12.4184(3)	13.8303(3)
b, Å	13.377(1)	5.7029(1)	10.6374(2)	15.9914(5)
c, Å	12.2980(9)	23.3492(6)	17.9932(5)	19.5290(5)
α, deg	90	90	90	104.669(2)
β, deg	104.107(1)	99.234(1)	101.353(1)	97.199(2)
γ, deg	90	90	90	108.549(2)
V, Å^3	1511.49(19)	2298.79(9)	2330.38(10)	3860.21(18)
Z	4	4	4	1
D_{calc}, Mg·m^{-3}	1.267	1.229	1.219	1.393
μ, mm^{-1}	0.081	0.074	0.073	0.929
R_1*	0.0625	0.0690	0.0526	0.0534
wR_2*	0.1176	0.1910	0.1413	0.1130
Data collect.	SMU	UWO	UWO	SSSC
Struct. sol.	Dr. H. Jenkins	Dr. M. Jennings	Dr. M. Jennings	D.Dickie/G. Schatte
CCDC no.	244469	244653	244652	618677

* $R_1 = [\Sigma||F_o|-|F_c||]/[\Sigma|F_o|]$ for $[F_o^2 > 2\sigma(F_o^2)]$; $wR_2 = \{[\Sigma w(F_o^2-F_c^2)^2]/[\Sigma w(F_o^2)^2]\}^{1/2}$

Table A3 (cont)

Compound name (#)	TPIP·$AlMe_2$·$AlMe_3$ **(29)**	2,6-Dimesityl phenylboronic acid **(33)**
Formula	$C_{36}H_{37}Al_2NO$	$C_{24}H_{27}BO_2$
FW	553.63	358.27
T, K	150(2)	173(2)
colour	orange	colourless
size	0.28 x 0.23 x 0.10	not recorded
cryst. syst.	triclinic	orthorhombic
space group	P-1	Cmc2(1)
a, Å	10.0605(2)	23.178(6)
b, Å	12.4185(4)	12.9810(4)
c, Å	13.8863(5)	6.7470(3)
α, deg	100.619(1)	90
β, deg	97.415(1)	90
γ, deg	110.549(2)	90
V, Å^3	1560.91(8)	2030.0(5)
Z	2	4
D_{calc}, Mg·m^{-3}	1.178	1.172
μ, mm^{-1}	0.121	0.072
R_1*	0.0529	0.0705
wR_2*	0.1201	0.1672
Data coll.	UWO	SSSC
Struct. sol.	Dr. M. Jennings	D. Dickie / G. Schatte
CCDC no.	244654	618675

* $R_1 = [\Sigma||F_o|-|F_c||]/[\Sigma|F_o|]$ for $[F_o^2 > 2\sigma(F_o^2)]$; $wR_2 = \{[\Sigma w(F_o^2-F_c^2)^2]/[\Sigma w(F_o^2)^2]\}^{1/2}$

Table A4: Crystallographic data for compounds in chapter 6.

Compound name (#)	2,6-Dimesitylphenol **(34)**	2,4,6-Triphenyl benzyl alcohol **(36)**	2,6-Dimesityl benzyl alcohol **(37)**	$[Sn(OC_6H_3Mes_2)_2]$ **(38)**
Formula	$C_{24}H_{26}O$	$C_{25}H_{20}O$	$C_{25}H_{28}O$	$C_{48}H_{50}O_2Sn$
FW	330.45	336.41	344.47	777.59
T, K	173(2)	200(2)	296(2)	173(2)
colour	colourless	colourless	colourless	colourless
size	0.20 x 0.15 x 0.15	0.35 x 0.08 x 0.03	0.56 x 0.16 x 0.15	0.10 x 0.08 x 0.08
cryst. syst.	triclinic	monoclinic	orthorhombic	triclinic
space group	P-1	P2/c	Pnma	P-1
a, Å	9.9380(2)	14.4768(3)	6.7390(2)	9.7264(2)
b, Å	11.5740(3)	17.9691(6)	23.7974(7)	11.6250(3)
c, Å	17.7140(6)	18.2367(6)	12.7734(3)	18.1089(3)
α, deg	105.4600(13)	90	90	107.0250(10)
β, deg	100.3660(15)	127.34(3)	90	90.2950(10)
γ, deg	94.5700(18)	90	90	90.8970(10)
V, Å^3	1914.14(9)	3771.72(19)	2048.48(10)	1957.49(7)
Z	4	8	4	2
D_{calc}, Mg·m^{-3}	1.147	1.185	1.117	1.319
μ, mm^{-1}	0.068	0.071	0.066	0.690
R_1*	0.0752	0.0876	0.0909	0.0402
wR_2*	0.2019	0.2272	0.2536	0.1206
Data coll.	SSSC	UWO	UWO	SSSC
Struct. sol.	Dr. M. Jennings	Dr. M. Jennings	Dr. M. Jennings	D. Dickie
CCDC no.	618683	618684	618682	618685

* $R_1 = [\Sigma||F_o|-|F_c||]/[\Sigma|F_o|]$ for $[F_o^2 > 2\sigma(F_o^2)]$; $wR_2 = \{[\Sigma w(F_o^2-F_c^2)^2]/[\Sigma w(F_o^2)^2]\}^{1/2}$

Table A4 (cont): Crystallographic data for compounds in chapter 6.

Compound name (#)	$[(Me_3Si)_2NGe(OC_6H_3Mes_2)]$ **(39)**	$[Me_2Al(\mu\text{-}OC_6H_3Mes_2)]_2$ **(40)**	$[(Me_2N)_2Ti(OC_6H_3Mes_2)_2]$ **(41)**	$[EtZn(\mu\text{-}OCH_2C_6H_2Ph_3)]_2$ **(42)**
Formula	$C_{30}H_{43}GeNOSi_2$	$C_{53}H_{64}Al_2Cl_2O_2$	$C_{52}H_{62}N_2O_2Ti$	$C_{27}H_{24}OZn$
FW	562.42	857.90	794.94	429.83
T, K	223(2)	173(2)	173(2)	173(2)
colour	pale yellow	colourless	orange	colourless
size	0.35 x 0.42 x 0.5	0.30 x 0.25 x 0.25	0.30 x 0.25 x 0.25	not recorded
cryst. syst.	orthorhombic	monoclinic	triclinic	triclinic
space group	P2(1)2(1)2(1)	$P2_1/c$	P-1	P-1
a, Å	11.6223(8)	17.5020(3)	10.96300(10)	10.1499(4)
b, Å	11.8066(8)	13.1600(3)	13.1040(2)	15.4439(5)
c, Å	23.2495(15)	22.3220(4)	16.5680(2)	15.4694(5)
α, deg	90	90	101.2510(5)	69.695(2)
β, deg	90	109.5440(11)	98.8800(5)	89.788(2)
γ, deg	90	90	99.5070(7)	71.263(2)
V, Å	3190.3(4)	4845.12(16)	2259.10(5)	2137.77(13)
Z	4	4	2	4
D_{calc}, Mg·m^{-3}	1.171	1.176	1.169	1.336
μ, mm^{-1}	1.056	0.209	0.230	1.163
R_1*	0.0280	0.0682	0.0444	0.0388
wR_2*	0.0698	0.1856	0.1051	0.0945
Data coll.	SMU	SSSC	SSSC	SSSC
Struct. sol.	D.Dickie/H. Jenkins	Dr. G. Schatte	Dr. G. Schatte	D. Dickie
CCDC no.	618681	618680	618686	618687

* $R_1 = [\Sigma||F_o|-|F_c||]/[\Sigma|F_o|]$ for $[F_o^2 > 2\sigma(F_o^2)]$; $wR_2 = \{[\Sigma w(F_o^2-F_c^2)^2]/[\Sigma w(F_o^2)^2]\}^{1/2}$

APPENDIX 2: ATOMIC COORDINATES

Atomic coordinates (x 10^4) and equivalent isotropic displacement parameters ($Å^2$x 10^3) for **2**. U(eq) is defined as one third of the trace of the orthogonalized U^{ij} tensor:

	x	y	z	U(eq)		x	y	z	U(eq)
O(1)	953(1)	1266(1)	-550(1)	59(1)	C(34)	-5485(2)	3494(2)	-507(2)	76(1)
C(2)	1325(2)	1196(2)	2043(2)	77(1)	C(35)	-5684(2)	3506(2)	697(2)	72(1)
C(3)	-1270(3)	3436(2)	286(2)	78(1)	C(36)	-5132(2)	2377(2)	1551(2)	54(1)
Al(4)	-37(1)	1681(1)	772(1)	42(1)	C(41)	-700(2)	-2956(2)	3102(1)	50(1)
O(5)	-1138(1)	557(1)	1227(1)	56(1)	C(42)	-485(2)	-4274(2)	3067(2)	82(1)
C(6)	-1459(1)	-500(1)	1246(1)	42(1)	C(43)	847(3)	-5117(2)	3121(3)	103(1)
C(7)	-2520(1)	-866(1)	2160(1)	39(1)	C(44)	1960(2)	-4661(3)	3218(2)	97(1)
C(8)	-3876(1)	-31(1)	2144(1)	39(1)	C(45)	1773(2)	-3356(3)	3271(2)	91(1)
C(9)	-4835(1)	-409(1)	3008(1)	42(1)	C(46)	442(2)	-2501(2)	3225(2)	68(1)
C(10)	-4493(1)	-1578(1)	3887(1)	42(1)	C(51)	-5563(2)	-1966(2)	4772(1)	46(1)
C(11)	-3136(2)	-2383(2)	3885(1)	47(1)	C(52)	-6725(2)	-1022(2)	5071(2)	59(1)
C(12)	-2142(1)	-2054(1)	3034(1)	43(1)	C(53)	-7734(2)	-1401(2)	5865(2)	74(1)
C(31)	-4372(1)	1211(1)	1208(1)	41(1)	C(54)	-7599(2)	-2718(2)	6377(2)	76(1)
C(32)	-4171(2)	1219(2)	-10(1)	50(1)	C(55)	-6456(2)	-3663(2)	6110(2)	70(1)
C(33)	-4728(2)	2364(2)	-863(2)	66(1)	C(56)	-5443(2)	-3297(2)	5307(1)	56(1)

Atomic coordinates (x 10^4) and equivalent isotropic displacement parameters ($Å^2$x 10^3) for **4**. U(eq) is defined as one third of the trace of the orthogonalized U^{ij} tensor:

	x	y	z	U(eq)		x	y	z	U(eq)
Zn(1)	1416(1)	5592(1)	1306(1)	35(1)	C(37)	861(2)	8589(2)	3250(1)	40(1)
Zn(2)	192(1)	6627(1)	1866(1)	33(1)	C(38)	-915(2)	6955(3)	3776(2)	70(2)
O(1)	1297(1)	5801(2)	2067(1)	30(1)	C(39)	952(2)	5436(2)	3455(1)	39(1)
C(2)	1269(2)	6495(2)	2309(1)	25(1)	C(41)	49(2)	8394(2)	1152(1)	30(1)
O(3)	884(1)	7044(2)	2224(1)	32(1)	C(42)	243(2)	8665(2)	1644(1)	30(1)
O(4)	1388(1)	6730(2)	1003(1)	31(1)	C(43)	-145(2)	8647(2)	2061(1)	34(1)
C(5)	889(2)	7014(2)	923(1)	29(1)	C(44)	-717(2)	8397(2)	2004(1)	33(1)
O(6)	438(1)	6691(2)	1116(1)	34(1)	C(45)	-897(2)	8148(2)	1514(1)	35(1)
C(7)	1396(2)	4450(3)	1029(2)	53(1)	C(46)	-523(2)	8135(2)	1088(1)	35(1)
C(8)	1015(3)	4289(3)	576(2)	85(2)	C(47)	850(2)	8984(3)	1721(1)	38(1)
C(9)	-533(2)	6058(3)	2027(2)	45(1)	C(48)	-1120(2)	8412(3)	2464(2)	48(1)
C(10)	-876(2)	5836(3)	1541(2)	55(1)	C(49)	-741(2)	7826(3)	561(1)	49(1)
C(11)	1706(2)	6696(2)	2722(1)	24(1)	C(51)	2506(2)	6177(2)	2130(1)	26(1)
C(12)	1516(2)	7013(2)	3203(1)	27(1)	C(52)	2646(2)	5320(2)	2118(1)	30(1)
C(13)	1930(2)	7254(2)	3573(1)	32(1)	C(53)	2815(2)	4963(2)	1652(1)	34(1)
C(14)	2508(2)	7159(2)	3473(1)	37(1)	C(54)	2850(2)	5425(2)	1195(1)	33(1)
C(15)	2692(2)	6805(2)	3007(1)	33(1)	C(55)	2712(2)	6278(2)	1216(1)	32(1)
C(16)	2297(2)	6567(2)	2628(1)	27(1)	C(56)	2547(2)	6664(2)	1681(1)	26(1)
C(21)	832(2)	7761(2)	567(1)	28(1)	C(57)	2601(2)	4782(2)	2609(1)	43(1)

C(22)	446(2)	8417(2)	689(1)	30(1)	C(58)	3034(2)	5028(3)	687(1)	47(1)
C(23)	430(2)	9121(3)	368(1)	37(1)	C(59)	2422(2)	7592(2)	1690(1)	33(1)
C(24)	761(2)	9169(3)	-75(1)	39(1)	C(61)	1540(2)	7098(2)	-79(1)	28(1)
C(25)	1120(2)	8514(2)	-206(1)	35(1)	C(62)	2144(2)	7182(2)	-90(1)	32(1)
C(26)	1169(2)	7801(2)	110(1)	29(1)	C(63)	2475(2)	6547(3)	-313(1)	36(1)
C(31)	891(2)	7017(2)	3350(1)	24(1)	C(64)	2231(2)	5837(3)	-532(1)	39(1)
C(32)	580(2)	7764(2)	3377(1)	30(1)	C(65)	1641(2)	5755(2)	-509(1)	40(1)
C(33)	-1(2)	7737(3)	3519(1)	39(1)	C(66)	1288(2)	6370(2)	-288(1)	33(1)
C(34)	-276(2)	6984(3)	3629(1)	40(1)	C(67)	2440(2)	7944(2)	133(1)	42(1)
C(35)	41(2)	6252(3)	3606(1)	37(1)	C(68)	2603(2)	5170(3)	-790(1)	59(1)
C(36)	622(2)	6252(2)	3463(1)	27(1)	C(69)	638(2)	6256(3)	-295(1)	45(1)

Atomic coordinates (x 10^4) and equivalent isotropic displacement parameters ($Å^2$x 10^3) for **6**. U(eq) is defined as one third of the trace of the orthogonalized U^{ij} tensor:

	x	y	z	U(eq)		x	y	z	U(eq)
Sn(1)	-169(1)	4053(1)	1024(1)	22(1)	C(21)	465(4)	6741(3)	4176(3)	33(1)
O(1)	1389(2)	5770(2)	1682(2)	25(1)	C(22)	-510(4)	5937(3)	4264(3)	39(1)
O(2)	-105(2)	3568(2)	-534(2)	25(1)	C(23)	-1813(4)	5309(3)	3415(3)	39(1)
N(1)	1513(3)	3456(2)	1619(2)	25(1)	C(24)	-2159(4)	5490(3)	2473(3)	35(1)
Si(1)	1469(1)	2994(1)	2632(1)	33(1)	C(25)	-1194(3)	6302(2)	2373(3)	28(1)
Si(2)	2738(1)	3303(1)	1086(1)	30(1)	C(30)	3267(3)	10856(2)	4755(2)	25(1)
C(1)	986(3)	6540(2)	1444(3)	21(1)	C(31)	2412(4)	11237(2)	5213(3)	32(1)
C(2)	1567(3)	7660(2)	2305(2)	21(1)	C(32)	2950(4)	12271(3)	6002(3)	42(1)
C(3)	1165(3)	7820(2)	3145(2)	22(1)	C(33)	4337(4)	12933(3)	6321(3)	44(1)
C(4)	1730(3)	8868(2)	3936(2)	24(1)	C(34)	5200(4)	12570(3)	5870(3)	41(1)
C(5)	2675(3)	9753(2)	3897(3)	23(1)	C(35)	4669(4)	11536(2)	5088(3)	35(1)
C(6)	3039(3)	9567(2)	3052(3)	24(1)	C(40)	-230(4)	3011(3)	2794(3)	41(1)
C(7)	2498(3)	8536(2)	2240(2)	22(1)	C(41)	1437(5)	1534(3)	2312(4)	59(1)
C(10)	2961(3)	8405(2)	1368(3)	23(1)	C(42)	2984(4)	3877(4)	3952(3)	65(1)
C(11)	2780(3)	9089(3)	778(3)	33(1)	C(50)	3336(3)	4491(2)	693(3)	31(1)
C(12)	3285(4)	9024(3)	5(3)	40(1)	C(51)	4448(4)	3278(3)	2088(3)	48(1)
C(13)	3983(4)	8270(3)	-193(3)	39(1)	C(52)	1991(4)	1988(3)	-89(3)	43(1)
C(14)	4148(3)	7571(3)	371(3)	37(1)	C(60)	6686(4)	-5(3)	2741(4)	60(1)
C(15)	3645(3)	7640(2)	1148(3)	29(1)	Cl(1)	8465(1)	54(1)	2980(1)	87(1)
C(20)	137(3)	6932(2)	3230(3)	24(1)	Cl(2)	6460(1)	1289(1)	2957(1)	67(1)

Atomic coordinates (x 10^4) and equivalent isotropic displacement parameters ($Å^2$x 10^3) for **7**. U(eq) is defined as one third of the trace of the orthogonalized U^{ij} tensor:

	x	y	z	U(eq)		x	y	z	U(eq)
Sn(1)	1937(1)	2504(1)	5844(1)	25.2(1)	C(43)	3624(2)	910(2)	7068.9(16)	59.4(14)
Sn(2)	2995(1)	2511(1)	3962(1)	25(1)	C(44)	1380(2)	1070(2)	7556.6(16)	61(14)
Si(41)	2846(5)	1044(4)	6372(4)	35.1(2)	C(45)	1183(2)	2571(2)	7240.6(15)	53(11)
Si(42)	1901(5)	1845(5)	7286(4)	39.9(3)	C(46)	2654(2)	2061(2)	7978.1(15)	66.9(15)
Si(81)	3226(5)	3416(4)	2672(4)	34.4(3)	C(51)	4169(2)	3567(1)	5693.3(12)	28.2(8)
Si(82)	1900(5)	3879(4)	3424(4)	34.4(3)	C(52)	4933(2)	3342(2)	5652.4(12)	33.4(9)
O(11)	1707(10)	1726(9)	5060(8)	27.7(6)	C(53)	5545(2)	3745(2)	5937.1(15)	46(10)
O(12)	1760(10)	2275(9)	4104(8)	28.4(5)	C(54)	5401(2)	4346(2)	6243.5(17)	58.6(12)
O(51)	3186(11)	2725(9)	5753(8)	31.2(6)	C(55)	4646(2)	4564(2)	6287.9(16)	51.8(11)

O(52)	3272(1)	3247(9)	4791(8)	31(6)	C(56)	4014(2)	4176(14)	6013(13)	345 (9)
N(41)	2262(1)	1738(11)	6529(10)	29(7)	C(57)	3494(14)	3146(12)	5390(12)	24(8)
N(81)	2668(13)	3321(11)	3329(9)	28(7)	C(61)	5111(2)	2676(2)	5339(14)	34(9)
C(11)	850(14)	1365(12)	4150(11)	21(7)	C(62)	5211(2)	2088(2)	5731(2)	45(11)
C(12)	1029(2)	886(12)	3680(11)	24(8)	C(63)	5401(2)	1475(2)	5432(2)	58(13)
C(13)	440(2)	459(13)	3406(12)	29(8)	C(64)	5485(2)	1433(2)	4770(2)	60(14)
C(14)	-308(2)	502(13)	3593(14)	32(9)	C(65)	5394(2)	2017(2)	4396(2)	52(11)
C(15)	-483(14)	981(13)	4055(13)	29(8)	C(66)	5214(2)	2643(2)	4670(14)	38(10)
C(16)	93(14)	1421(12)	4341(11)	23(7)	C(67)	5113(2)	2119(2)	6452(2)	62(14)
C(17)	1484(14)	1825(12)	4459(11)	22(7)	C(68)	5676(3)	751(2)	4465(3)	94(2)
C(21)	1835(2)	816(14)	3472(12)	30(8)	C(69)	5154(2)	3283(2)	4252(14)	47(11)
C(22)	2370(2)	386(2)	3827(2)	38(10)	C(71)	3197(2)	4408(14)	6061(13)	35(9)
C(23)	3123(2)	344(2)	3623(2)	57(13)	C(72)	2826(2)	4834(14)	5575(14)	42(10)
C(24)	3335(2)	684(2)	3079(2)	61(14)	C(73)	2057(2)	5029(2)	5614(2)	51(11)
C(25)	2785(2)	1070(2)	2722(2)	55(11)	C(74)	1638(2)	4814(2)	6119(2)	53(11)
C(26)	2038(2)	1158(2)	2911(13)	37(9)	C(75)	2013(2)	4406(2)	6600(2)	48(11)
C(27)	2145(2)	-27(2)	4399(2)	52(11)	C(76)	2790(2)	4200(2)	6589(14)	41(10)
C(28)	4168(2)	651(2)	2891(3)	100(2)	C(77)	3254(2)	5070(2)	5007(2)	57(14)
C(29)	1470(2)	1628(2)	2530(14)	53(11)	C(78)	794(2)	5018(2)	6144(2)	82(2)
C(31)	-127(14)	1962(13)	4806(12)	24(8)	C(79)	3183(2)	3767(2)	7132(2)	53(13)
C(32)	-316(2)	2620(13)	4566(12)	29(8)	C(81)	2629(2)	3507(2)	1866(14)	59(2)
C(33)	-537(2)	3115(14)	4999(14)	36(9)	C(82)	3896(2)	4168(2)	2756(2)	56(12)
C(34)	-596(2)	2980(2)	5657(14)	39(10)	C(83)	3881(2)	2658(2)	2600(2)	48(11)
C(35)	-423(2)	2323(2)	5878(13)	36(9)	C(84)	1041(2)	3688(2)	2825(14)	54(13)
C(36)	-179(2)	1812(14)	5472(12)	29(8)	C(85)	1558(2)	3868(2)	4264(13)	37(9)
C(37)	-310(2)	2785(2)	3851(13)	41(10)	C(86)	2183(2)	4788(2)	3270(2)	54(13)
C(38)	-850(2)	3528(2)	6110(2)	61(14)	Cl(91)	2689(6)	3068(6)	2.5(5)	77(4)
C(39)	20(2)	1107(2)	5739(14)	41(10)	Cl(92)	2485(6)	1817(6)	737(6)	84(4)
C(41)	2270(18)	230(2)	6277(2)	48(11)	C(91)	2514(2)	2189(2)	-43(2)	73(2)
C(42)	3359(2)	1134(14)	5611(14)	35(9)					

Atomic coordinates (x 10^4) and equivalent isotropic displacement parameters ($Å^2$x 10^3) for **8**. U(eq) is defined as one third of the trace of the orthogonalized U^{ij} tensor:

	x	y	z	U(eq)		x	y	z	U(eq)
Sn(1)	1576(1)	9356(1)	-1312(1)	27(1)	C(17)	5758(7)	6597(8)	-1446(7)	58(2)
Si(1)	2116(2)	8203(1)	-3164(1)	30(1)	C(18)	2787(7)	7392(7)	2003(7)	51(2)
Si(2)	-490(2)	9323(1)	-2379(1)	30(1)	C(20)	-2480(5)	7484(5)	2834(5)	30(1)
O(1)	256(4)	8220(3)	201(3)	30(1)	C(21)	-2927(6)	7561(5)	2020(5)	32(1)
O(2)	313(4)	10962(3)	-1493(3)	31(1)	C(22)	-3951(6)	8343(6)	1905(6)	38(1)
N(1)	991(5)	8912(4)	-2307(4)	28(1)	C(23)	-4580(6)	9006(5)	2590(6)	39(2)
C(1)	-61(5)	8177(5)	1173(5)	25(1)	C(24)	-4172(6)	8843(5)	3432(6)	36(1)
C(2)	-164(5)	6998(5)	2052(5)	26(1)	C(25)	-3132(6)	8116(5)	3556(5)	32(1)
C(3)	-1320(5)	6714(5)	2891(5)	28(1)	C(26)	-2362(7)	6773(6)	1341(6)	40(2)
C(4)	-1392(6)	5662(5)	3733(5)	30(1)	C(27)	-5655(7)	9881(7)	2422(7)	51(2)
C(5)	-344(6)	4879(5)	3765(5)	30(1)	C(28)	-2686(6)	8041(6)	4438(6)	39(2)

C(6)	782(6)	5164(5)	2908(5)	30(1)	C(31)	3702(6)	8215(6)	-3174(6)	39(2)
C(7)	893(6)	6206(5)	2034(5)	28(1)	C(32)	1865(7)	6643(6)	-2744(6)	43(2)
C(8)	-435(6)	3762(5)	4697(5)	36(1)	C(33)	2221(7)	8906(6)	-4617(5)	42(2)
C(10)	2126(5)	6381(5)	1113(5)	30(1)	C(41)	-510(6)	10742(6)	-3467(5)	36(1)
C(11)	2383(6)	5921(5)	283(5)	34(1)	C(42)	-1003(7)	8249(7)	-2723(7)	49(2)
C(12)	3559(7)	6006(6)	-528(5)	43(2)	C(43)	-1724(6)	9414(6)	-1061(5)	39(2)
C(13)	4488(6)	6535(6)	-556(6)	45(2)	C(101)	4900(10)	5310(20)	3850(20)	225(14)
C(14)	4206(6)	6990(6)	274(6)	44(2)	Cl(1)	4277(5)	4596(4)	3506(4)	143(2)
C(15)	3046(6)	6920(5)	1107(6)	37(1)	Cl(2)	4041(4)	6332(4)	4408(4)	125(1)
C(16)	1412(7)	5333(7)	284(6)	46(2)					

Atomic coordinates (x 10^4) and equivalent isotropic displacement parameters (Å^{2}x 10^3) for **9·CH_2Cl_2**. U(eq) is defined as one third of the trace of the orthogonalized U^{ij} tensor:

	x	y	z	U(eq)		x	y	z	U(eq)
Sn(1)	-68(1)	1268(1)	5292(1)	36(1)	C(14)	4352(5)	2335(5)	5798(4)	54(1)
Si(1)	1590(1)	-1150(1)	6654(1)	40(1)	C(15)	766(5)	3994(5)	7660(4)	56(1)
O(1)	1929(3)	1661(3)	4547(2)	39(1)	C(16)	2083(5)	5982(4)	3669(4)	54(1)
O(2)	935(3)	3246(3)	3630(2)	43(1)	C(17)	3160(4)	2687(4)	1768(3)	39(1)
N(1)	519(3)	-626(2)	5847(2)	23(1)	C(18)	2424(4)	3353(4)	1015(3)	44(1)
C(1)	3241(4)	3394(4)	3264(3)	34(1)	C(19)	1832(5)	2744(5)	513(4)	53(1)
C(2)	3848(4)	4049(4)	3737(3)	36(1)	C(20)	1928(5)	1511(5)	736(4)	55(1)
C(3)	5065(4)	4614(4)	3242(4)	48(1)	C(21)	2643(5)	863(5)	1505(4)	55(1)
C(4)	5667(4)	4538(5)	2301(4)	54(1)	C(22)	3268(5)	1426(4)	2018(4)	47(1)
C(5)	5055(4)	3910(5)	1834(4)	51(1)	C(23)	4077(6)	686(5)	2809(5)	68(2)
C(6)	3827(4)	3332(4)	2303(3)	39(1)	C(24)	1282(7)	876(7)	173(5)	79(2)
C(7)	1939(4)	2749(4)	3827(3)	33(1)	C(25)	2224(6)	4681(5)	777(4)	59(1)
C(8)	3151(4)	4114(4)	4753(3)	36(1)	C(102)	1638(6)	-104(5)	7362(5)	66(1)
C(9)	2260(4)	4998(4)	4714(3)	39(1)	C(103)	1104(5)	-2729(5)	7626(5)	65(1)
C(10)	1511(4)	4954(4)	5665(4)	43(1)	C(104)	3172(5)	-1149(6)	5837(4)	62(1)
C(11)	1640(4)	4066(4)	6643(3)	41(1)	Cl(1)	5005(2)	8323(2)	1364(2)	104(1)
C(12)	2571(4)	3235(4)	6664(3)	41(1)	Cl(3)	3247(3)	8020(3)	89(2)	124(1)
C(13)	3340(4)	3242(4)	5737(3)	38(1)	C(501)	4578(8)	7514(8)	663(6)	95(2)

Atomic coordinates (x 10^4) and equivalent isotropic displacement parameters (Å^{2}x 10^3) for **9·Et_2O**. U(eq) is defined as one third of the trace of the orthogonalized U^{ij} tensor:

	x	y	z	U(eq)		x	y	z	U(eq)
Si(1)	-1715(1)	9888(1)	3513(1)	33(1)	C(15)	1333(4)	12991(3)	970(4)	55(1)
Sn(1)	34(1)	8522(1)	5341(1)	27(1)	C(16)	4710(4)	10562(4)	2482(4)	54(1)
N(1)	-551(2)	9914(2)	4174(2)	16(1)	C(17)	3132(3)	5939(3)	4412(3)	32(1)
O(1)	1997(2)	8671(2)	4366(2)	31(1)	C(18)	2220(4)	5117(3)	4480(3)	37(1)
O(2)	958(2)	7695(2)	3544(2)	34(1)	C(19)	1534(4)	4531(3)	5557(3)	41(1)

C(1)	1966(3)	8058(2)	3630(3)	26(1)	C(20)	1731(4)	4749(3)	6566(3)	39(1)
C(2)	3222(3)	7760(3)	2906(3)	29(1)	C(21)	2668(4)	5538(3)	6478(3)	37(1)
C(3)	3828(3)	8544(3)	1899(3)	34(1)	C(22)	3389(3)	6136(3)	5417(3)	36(1)
C(4)	4983(4)	8227(4)	1259(3)	47(1)	C(23)	1965(4)	4866(4)	3410(3)	51(1)
C(5)	5527(4)	7173(4)	1619(4)	56(1)	C(24)	945(5)	4147(4)	7724(3)	55(1)
C(6)	4934(4)	6418(4)	2623(4)	49(1)	C(25)	4435(4)	6959(3)	5366(4)	49(1)
C(7)	3778(3)	6693(3)	3282(3)	35(1)	C(26)	-1958(4)	11406(3)	2791(4)	48(1)
C(8)	3239(3)	9699(3)	1579(3)	33(1)	C(27)	-3160(4)	9282(5)	4603(4)	65(1)
C(9)	2289(3)	9831(3)	968(3)	35(1)	C(28)	-1295(5)	8990(4)	2434(4)	61(1)
C(10)	1697(3)	10905(3)	770(3)	41(1)	C(41)	7604(14)	3918(9)	252(10)	87(3)
C(11)	2014(4)	11843(3)	1160(3)	42(1)	C(42)	6174(16)	3964(17)	470(20)	89(5)
C(12)	2984(4)	11705(3)	1723(3)	41(1)	O(43)	5740(20)	5033(18)	-150(20)	78(3)
C(13)	3609(3)	10659(3)	1923(3)	38(1)	C(44)	4370(30)	5120(30)	50(30)	80(5)
C(14)	1946(4)	8830(4)	528(4)	48(1)	C(45)	4117(19)	6200(20)	-790(20)	99(6)

Atomic coordinates (x 10^4) and equivalent isotropic displacement parameters (Å^{2}x 10^3) for **11**. U(eq) is defined as one third of the trace of the orthogonalized U^{ij} tensor:

	x	y	z	U(eq)		x	y	z	U(eq)
Sn(1)	6604(1)	4446(1)	6764(1)	20(1)	C(12)	3908(3)	-42(2)	6827(2)	42(1)
Cl(1)	4070(1)	4607(1)	6078(1)	33(1)	C(13)	2208(3)	1909(3)	6999(2)	50(1)
Cl(2)	8958(1)	3120(1)	5572(1)	44(1)	C(21)	8047(3)	1252(2)	7608(2)	37(1)
Si(1)	4026(1)	1531(1)	6603(1)	27(1)	C(22)	6687(4)	2690(3)	9159(2)	51(1)
Si(2)	7480(1)	2737(1)	8055(1)	25(1)	C(23)	9524(3)	4194(2)	8379(2)	44(1)
Si(3)	6737(1)	6718(1)	8694(1)	28(1)	C(31)	4760(3)	5322(3)	8612(2)	41(1)
Si(4)	9493(1)	7385(1)	7562(1)	28(1)	C(32)	8108(4)	7224(3)	9911(2)	50(1)
N(1)	5977(2)	2834(2)	7200(1)	21(1)	C(33)	6091(4)	8110(3)	8581(2)	46(1)
N(2)	7790(2)	6241(2)	7806(1)	25(1)	C(41)	11137(3)	6692(3)	7254(2)	44(1)
C(1)	7646(3)	4053(2)	5515(2)	30(1)	C(42)	10616(4)	8916(3)	8629(2)	51(1)
C(11)	3718(4)	1160(2)	5281(2)	41(1)	C(43)	8681(3)	7865(2)	6556(2)	37(1)

Atomic coordinates (x 10^4) and equivalent isotropic displacement parameters (Å^{2}x 10^3) for **12**. U(eq) is defined as one third of the trace of the orthogonalized U^{ij} tensor:

	x	y	z	U(eq)		x	y	z	U(eq)
Si(1)	-692(9)	3952(7)	8228.4(4)	23(2)	C(27)	4507(4)	2859(4)	7082.6(18)	38.1(11)
O(11)	415(2)	2574(19)	7784.6(11)	25.9(6)	C(28)	2940(4)	6837(3)	5123.2(19)	36.8(10)
O(12)	-933(3)	2726(2)	6818.8(12)	32.9(7)	C(29)	1517(4)	2507(3)	5008.7(17)	32.3(9)
N(41)	-2125(3)	3408(3)	8879.2(14)	33.1(8)	C(31)	106(3)	-548(3)	7675.1(17)	25.5(8)
N(51)	700(3)	4319(3)	8642.5(15)	33.5(8)	C(32)	-1284(4)	-550(3)	7383.7(17)	28.4(9)
N(61)	-1483(3)	5297(2)	7621.6(14)	32.2(8)	C(33)	-2629(4)	-807(3)	7886(2)	34.6(10)
C(11)	1638(3)	1041(3)	6872.8(15)	21.6(8)	C(34)	-2633(4)	-1047(3)	8668(2)	37.4(10)
C(12)	2966(3)	1300(3)	6353(15)	23.6(8)	C(35)	-1254(4)	-1026(3)	8936.5(18)	36.3(10)

C(13)	4246(4)	202(3)	6108.8(17)	29.2(9)	C(36)	126(4)	-779(3)	8461.3(17)	29.8(9)
C(14)	4204(4)	-1111(3)	6376.7(19)	34.6(9)	C(37)	-1339(4)	-284(3)	6543.7(18)	36.3(10)
C(15)	2876(4)	-1355(3)	6887.7(18)	32(9)	C(38)	-4100(5)	-1343(5)	9193(3)	59.4(16)
C(16)	1571(3)	-292(3)	7141.8(16)	24.6(8)	C(39)	1601(4)	-768(4)	8781(2)	42.8(11)
C(17)	214(3)	2211(3)	7138.8(15)	22.1(8)	C(41)	-3030(4)	2523(4)	8745(2)	47.6(12)
C(21)	2984(3)	2723(3)	6043.5(15)	23.2(8)	C(42)	-2923(6)	4161(5)	9527(2)	63.7(16)
C(22)	3705(3)	3472(3)	6390.8(16)	27.1(9)	C(51)	1745(5)	3266(4)	9105(2)	45.1(12)
C(23)	3687(4)	4786(3)	6076.4(17)	29.4(9)	C(52)	943(6)	5638(4)	8617(3)	59.2(16)
C(24)	2976(3)	5393(3)	5438.4(17)	29.2(9)	C(61)	-3181(5)	5696(4)	7517(3)	55.7(14)
C(25)	2290(4)	4625(3)	5096(16)	28.1(9)	C(62)	-414(5)	5759(3)	6972.4(19)	48.9(13)
C(26)	2278(3)	3304(3)	5388.2(16)	25.3(8)					

Atomic coordinates (x 10^4) and equivalent isotropic displacement parameters ($Å^2$x 10^3) for **13**. U(eq) is defined as one third of the trace of the orthogonalized U^{ij} tensor:

	x	y	z	U(eq)		x	y	z	U(eq)
Ti(1)	706(1)	9431(1)	5475(1)	52(1)	C(14)	2596(2)	10826(5)	7167(4)	73(1)
N(1)	1027(2)	8368(3)	6536(4)	79(1)	C(15)	3069(3)	7081(4)	5158(7)	110(2)
N(2)	-34(1)	9748(3)	5986(3)	72(1)	C(16)	2408(2)	10582(4)	2978(4)	76(1)
N(3)	596(2)	8388(4)	4291(4)	89(1)	C(17)	927(1)	13671(3)	5159(3)	45(1)
O(1)	1155(1)	10940(3)	6208(2)	70(1)	C(18)	615(2)	13739(3)	4182(3)	52(1)
O(2)	1138(1)	10679(3)	4446(2)	68(1)	C(19)	30(2)	13984(4)	4246(4)	61(1)
C(1)	1318(1)	11240(3)	5262(3)	42(1)	C(20)	-241(1)	14159(3)	5262(4)	61(1)
C(2)	1738(1)	12212(3)	5127(3)	41(1)	C(21)	81(2)	14110(3)	6209(4)	58(1)
C(3)	1555(1)	13380(3)	5101(3)	44(1)	C(22)	667(1)	13861(3)	6181(3)	48(1)
C(4)	1967(2)	14265(3)	4999(4)	55(1)	C(23)	1005(2)	13800(4)	7253(3)	64(1)
C(5)	2540(2)	13988(3)	4936(4)	61(1)	C(24)	-884(2)	14410(5)	5305(6)	98(2)
C(6)	2715(1)	12834(3)	4945(3)	55(1)	C(25)	890(2)	13558(5)	3054(4)	77(1)
C(7)	2321(1)	11932(3)	5046(3)	42(1)	C(26)	1230(3)	8741(7)	7601(5)	120(2)
C(8)	2509(1)	10675(3)	5073(3)	43(1)	C(27)	1114(4)	7093(6)	6388(8)	148(3)
C(9)	2558(1)	10048(3)	4084(3)	49(1)	C(28)	-369(3)	9333(7)	6935(7)	125(3)
C(10)	2737(2)	8883(4)	4132(4)	60(1)	C(29)	-323(2)	10640(6)	5351(7)	115(2)
C(11)	2872(2)	8340(3)	5131(4)	62(1)	C(30)	69(3)	7797(8)	3913(8)	151(3)
C(12)	2813(2)	8987(4)	6097(4)	60(1)	C(31)	1088(3)	7999(6)	3633(6)	116(2)
C(13)	2638(1)	10154(3)	6086(3)	47(1)					

Atomic coordinates (x 10^4) and equivalent isotropic displacement parameters ($Å^2$x 10^3) for **13a**. U(eq) is defined as one third of the trace of the orthogonalized U^{ij} tensor:

	x	y	z	U(eq)		x	y	z	U(eq)
Ti(1)	2880(1)	454(1)	343(1)	26(1)	C(28)	3207(3)	1903(6)	3062(2)	78(2)
Cl(1)	4121(1)	6474(2)	4090(1)	101(1)	C(29)	1394(2)	-251(4)	1051(2)	42(1)
Cl(2)	5033(1)	6867(2)	5443(1)	112(1)	C(31)	3001(2)	-1741(3)	690(2)	25(1)

O(1)	1743(1)	227(2)	-186(1)	29(1)	C(32)	3085(2)	-3062(3)	874(2)	25(1)
O(2)	2289(1)	1822(2)	416(1)	30(1)	C(33)	2805(2)	-3964(3)	391(2)	26(1)
O(3)	3129(1)	-1360(2)	266(1)	31(1)	C(34)	2854(2)	-5195(3)	569(2)	29(1)
O(4)	2797(1)	-958(2)	934(1)	30(1)	C(35)	3192(2)	-5538(4)	1209(2)	34(1)
N(1)	2883(2)	928(3)	-389(2)	41(1)	C(36)	3489(2)	-4637(4)	1684(2)	30(1)
N(2)	3722(2)	1039(3)	1032(2)	41(1)	C(37)	3440(2)	-3398(3)	1527(2)	28(1)
C(1)	1716(2)	1256(3)	42(2)	27(1)	C(41)	3778(2)	-2481(3)	2066(2)	27(1)
C(2)	1042(2)	1810(3)	-114(2)	26(1)	C(42)	3479(2)	-2222(4)	2428(2)	33(1)
C(3)	946(2)	2180(3)	387(2)	28(1)	C(43)	3838(2)	-1465(4)	2968(2)	40(1)
C(4)	306(2)	2643(4)	232(2)	34(1)	C(44)	4489(2)	-990(4)	3167(2)	37(1)
C(5)	-224(2)	2807(4)	-399(2)	36(1)	C(45)	4765(2)	-1231(4)	2790(2)	35(1)
C(6)	-116(2)	2481(4)	-889(2)	33(1)	C(46)	4424(2)	-1967(4)	2240(2)	31(1)
C(7)	506(2)	1970(3)	-759(2)	27(1)	C(47)	4758(2)	-2205(5)	1857(2)	47(1)
C(11)	590(2)	1649(4)	-1314(2)	28(1)	C(48)	4892(3)	-256(5)	3784(2)	57(1)
C(12)	337(2)	537(4)	-1639(2)	29(1)	C(49)	2781(2)	-2741(4)	2243(2)	46(1)
C(13)	381(2)	312(4)	-2177(2)	37(1)	C(51)	2420(2)	-3654(3)	-311(2)	25(1)
C(14)	661(2)	1166(4)	-2402(2)	37(1)	C(52)	1737(2)	-3201(3)	-617(2)	27(1)
C(15)	916(2)	2258(4)	-2065(2)	39(1)	C(53)	1391(2)	-2929(4)	-1268(2)	33(1)
C(16)	889(2)	2523(4)	-1521(2)	31(1)	C(54)	1701(2)	-3102(4)	-1626(2)	35(1)
C(17)	1165(2)	3737(4)	-1176(2)	46(1)	C(55)	2369(2)	-3564(4)	-1315(2)	36(1)
C(18)	694(3)	901(5)	-2991(2)	56(1)	C(56)	2736(2)	-3841(4)	-666(2)	29(1)
C(19)	24(2)	-410(4)	-1416(2)	40(1)	C(57)	3474(2)	-4323(4)	-347(2)	39(1)
C(21)	1517(2)	2083(4)	1080(2)	29(1)	C(58)	1310(2)	-2797(5)	-2333(2)	54(1)
C(22)	1728(2)	941(4)	1390(2)	34(1)	C(59)	1369(2)	-3013(4)	-260(2)	39(1)
C(23)	2268(2)	918(4)	2033(2)	44(1)	C(61)	3091(3)	2153(5)	-468(3)	75(2)
C(24)	2602(2)	1971(5)	2371(2)	48(1)	C(62)	2545(3)	219(5)	-991(2)	58(1)
C(25)	2376(2)	3087(4)	2054(2)	41(1)	C(63)	4372(2)	1234(6)	1050(3)	85(2)
C(26)	1834(2)	3174(4)	1416(2)	31(1)	C(64)	3800(3)	1228(4)	1658(2)	55(1)
C(27)	1610(2)	4412(4)	1094(2)	41(1)	C(71)	4265(3)	6195(5)	4842(3)	75(2)

Atomic coordinates (x 10^4) and equivalent isotropic displacement parameters ($Å^2$x 10^3) for **15H$_2$**. U(eq) is defined as one third of the trace of the orthogonalized U^{ij} tensor:

	x	y	z	U(eq)		x	y	z	U(eq)
O(1)	2175(9)	3334(10)	-5029(9)	41.7(5)	O(3)	4183(10)	6942(9)	-2333(9)	41.895)
O(2)	6660(9)	6096(9)	-4424(8)	35.5(4)	O(4)	6890(10)	2387(9)	-3013(8)	38.2(5)
C(1)	3067(12)	3067(12)	-5000	29.0(7)	C(13)	3933(12)	6067(12)	-2500	29.4(7)
C(2)	3842(13)	3842(13)	-5000	28.1(6)	C(14)	4712(12)	5287(12)	-2500	28.8(7)
C(3)	4829(13)	3582(13)	-5088(11)	30.6(6)	C(15)	5695(13)	5550(13)	-2429(11)	30.3(6)
C(4)	5568(13)	4300(13)	-5095(11)	28.5(6)	C(16)	6436(12)	4838(13)	-2454(11)	27.6(6)
C(5)	5291(12)	5291(12)	-5000	27.0(6)	C(17)	6163(12)	3837(12)	-2500	26.3(6)
C(6)	6072(12)	6072(12)	-5000	26.5(6)	C(18)	6944(12)	3056(12)	-2500	25.0(6)
C(7)	6616(13)	4003(13)	-5200(11)	29.4(6)	C(19)	7484(13)	5167(13)	-2480(12)	27.8(6)

C(8)	7226(15)	4460(15)	-5746(13)	38.8(7)	C(20)	8048(14)	4977(14)	-3142(12)	37.6(7)
C(9)	8206(16)	4180(17)	-5809(15)	52.0(8)	C(21)	9011(15)	5322(15)	-3185(15)	44.7(8)
C(10)	8586(16)	3455(18)	-5328(16)	53.6(9)	C(22)	9416(15)	5840(15)	-2573(14)	43.3(7)
C(11)	7987(15)	2999(16)	-4793(14)	45.3(7)	C(23)	8864(15)	6033(15)	-1916(13)	42.2(7)
C(12)	7003(14)	3260(14)	-4733(12)	35.4(7)	C(24)	7895(15)	5699(14)	-1868(12)	36.1(7)

Atomic coordinates (x 10^4) and equivalent isotropic displacement parameters ($Å^2$x 10^3) for **16**. U(eq) is defined as one third of the trace of the orthogonalized U^{ij} tensor:

	x	y	z	U(eq)		x	y	z	U(eq)
O(11)	9299(14)	1905(10)	2362(8)	38(4)	C(31)	6701(19)	3345(14)	1590(11)	32(6)
O(12)	9187(14)	2177(11)	3493(8)	41(5)	C(32)	6318(2)	3601(16)	815(12)	45(7)
O(13)	1906(14)	667(10)	1317(8)	39(4)	C(33)	6722(3)	4506(19)	629(14)	61(9)
O(14)	2004(14)	1474(12)	320(8)	45(5)	C(34)	7511(3)	5177(18)	1216(15)	63(10)
C(11)	7057(18)	1715(14)	2353(11)	30(6)	C(35)	7892(3)	4938(16)	1987(13)	50(8)
C(12)	6475(19)	859(14)	2525(11)	31(6)	C(36)	7491(2)	4030(15)	2177(12)	37(6)
C(13)	5004(19)	680(13)	2098(11)	31(6)	N(41)	9132(16)	4097(12)	5426(9)	34(5)
C(14)	4149(19)	1313(13)	1495(11)	30(6)	N(51)	1922(16)	2610(12)	3089(9)	36(5)
C(15)	4738(19)	2159(14)	1338(11)	31(6)	C(41)	8734(2)	3585(16)	4762(12)	38(7)
C(16)	6178(19)	2387(14)	1768(11)	30(6)	C(42)	7345(2)	3294(16)	4290(11)	36(6)
C(17)	8635(19)	1951(14)	2805(11)	31(6)	C(43)	6264(18)	3556(13)	4491(10)	29(6)
C(18)	2572(19)	1147(14)	986(11)	30(6)	C(44)	6678(19)	4089(15)	5183(12)	36(6)
C(21)	7385(19)	136(14)	3142(11)	35(6)	C(45)	8100(2)	4340(15)	5630(12)	38(6)
C(22)	7003(2)	-162(17)	3721(13)	49(8)	C(51)	2346(19)	2983(14)	3806(11)	33(6)
C(23)	7866(3)	-814(18)	4306(15)	59(9)	C(52)	3720(19)	3311(15)	4267(11)	32(6)
C(24)	9086(3)	-1202(18)	4313(16)	62(9)	C(53)	4752(18)	3251(13)	3994(11)	29(5)
C(25)	9449(3)	-937(2)	3730(18)	66(10)	C(54)	4289(2)	2879(17)	3239(12)	42(7)
C(26)	8615(2)	-272(17)	3151(14)	51(8)	C(55)	2894(2)	2576(18)	2813(13)	46(8)

Atomic coordinates (x 10^4) and equivalent isotropic displacement parameters ($Å^2$x 10^3) for **17**. U(eq) is defined as one third of the trace of the orthogonalized U^{ij} tensor:

	x	y	z	U(eq)		x	y	z	U(eq)
Zn(1)	2369(1)	906(1)	4153(1)	20(1)	C(25)	3624(3)	-675(2)	943(2)	34(1)
O(11)	3532(2)	1317(2)	3250(1)	22(1)	C(26)	3981(3)	207(2)	1024(2)	28(1)
O(12)	5498(2)	1152(2)	3747(1)	26(1)	C(31)	5702(3)	3248(2)	3314(2)	23(1)
O(13)	6939(2)	2814(2)	-239(1)	31(1)	C(32)	6796(3)	3733(2)	3482(2)	31(1)
O(14)	6293(2)	4085(2)	280(1)	31(1)	C(33)	6950(3)	4186(2)	4208(2)	37(1)
O(61)	4000(2)	786(2)	4962(1)	26(1)	C(34)	6019(4)	4158(2)	4778(2)	36(1)
N(41)	781(2)	1041(2)	3326(2)	23(1)	C(35)	4918(3)	3689(2)	4624(2)	33(1)
N(51)	2398(2)	-488(2)	4058(1)	22(1)	C(36)	4760(3)	3246(2)	3888(2)	27(1)
C(11)	5201(2)	1874(2)	2467(2)	18(1)	C(41)	-386(3)	962(3)	3605(2)	41(1)
C(12)	5202(3)	1420(2)	1714(2)	21(1)	C(42)	-1443(3)	1115(3)	3125(2)	48(1)
C(13)	5613(3)	1877(2)	1030(2)	24(1)	C(43)	-1298(3)	1331(3)	2324(2)	44(1)
C(14)	5982(3)	2763(2)	1062(2)	23(1)	C(44)	-106(3)	1397(3)	2024(2)	49(1)
C(15)	5964(3)	3199(2)	1810(2)	25(1)	C(45)	907(3)	1247(3)	2544(2)	34(1)
C(16)	5608(3)	2767(2)	2520(2)	21(1)	C(51)	2543(3)	-978(2)	4733(2)	26(1)
C(17)	4724(3)	1404(2)	3222(2)	20(1)	C(52)	2587(3)	-1902(2)	4724(2)	33(1)
C(18)	6419(3)	3248(2)	320(2)	26(1)	C(53)	2483(3)	-2336(2)	3992(2)	34(1)
C(21)	4819(3)	467(2)	1643(2)	21(1)	C(54)	2341(3)	-1840(2)	3286(2)	32(1)

C(22)	5282(3)	-187(2)	2166(2)	26(1)	C(55)	2300(3)	-926(2)	3348(2)	26(1)
C(23)	4922(3)	-1075(2)	2075(2)	33(1)	C(61)	4234(3)	1152(3)	5745(2)	36(1)
C(24)	4094(3)	-1320(2)	1460(2)	35(1)					

Atomic coordinates (x 10^4) and equivalent isotropic displacement parameters ($Å^2$x 10^3) for **18**. U(eq) is defined as one third of the trace of the orthogonalized U^{ij} tensor:

	x	y	z	U(eq)		x	y	z	U(eq)
C(1)	5273(3)	3606(2)	6771(2)	21(1)	C(101)	7458(3)	5967(2)	5283(2)	32(1)
C(2)	4797(2)	3131(2)	7520(2)	19(1)	C(102)	7428(3)	6885(2)	5305(2)	40(1)
C(3)	4397(2)	2246(2)	7469(2)	21(1)	C(103)	7531(3)	7305(2)	6039(2)	41(1)
C(4)	4040(3)	1808(2)	8175(2)	26(1)	C(104)	7651(3)	6798(2)	6743(2)	39(1)
C(5)	4022(3)	2234(2)	8923(2)	23(1)	C(105)	7677(3)	5893(2)	6673(2)	32(1)
C(6)	4384(3)	3122(2)	8962(2)	24(1)	C(201)	10362(3)	4041(3)	6379(2)	48(1)
C(7)	4789(2)	3575(2)	8278(2)	20(1)	C(202)	11416(3)	3900(3)	6857(2)	59(1)
C(8)	5181(3)	4526(2)	8359(2)	22(1)	C(203)	11279(3)	3680(3)	7646(2)	53(1)
C(9)	6026(3)	4778(2)	8963(2)	31(1)	C(204)	10094(3)	3594(3)	7933(2)	56(1)
C(10)	6372(3)	5658(2)	9052(2)	39(1)	C(205)	9083(3)	3736(3)	7423(2)	39(1)
C(11)	5884(3)	6301(2)	8553(2)	39(1)	C(301)	5766(3)	3855(3)	4247(2)	42(1)
C(12)	5041(3)	6059(2)	7947(2)	36(1)	O(1)	6461(2)	3697(1)	6744(1)	23(1)
C(13)	4692(3)	5183(2)	7851(2)	28(1)	O(2)	4497(2)	3855(1)	6248(1)	28(1)
C(14)	4314(3)	1756(2)	6673(2)	24(1)	O(3)	6009(2)	4199(2)	5037(1)	32(1)
C(15)	3236(3)	1280(2)	6501(2)	34(1)	O(4)	3079(2)	2189(1)	10238(1)	31(1)
C(16)	3076(3)	831(2)	5772(2)	44(1)	O(5)	3674(2)	918(1)	9706(1)	29(1)
C(17)	4003(3)	859(2)	5199(2)	39(1)	N(1)	7586(2)	5468(2)	5957(2)	27(1)
C(18)	5093(3)	1326(2)	5364(2)	37(1)	N(2)	9200(2)	3942(2)	6641(2)	27(1)
C(19)	5256(3)	1768(2)	6100(2)	29(1)	Co(1)	7616(1)	4078(1)	5814(1)	23(1)
C(20)	3585(3)	1749(2)	9669(2)	26(1)					

Atomic coordinates (x 10^4) and equivalent isotropic displacement parameters ($Å^2$x 10^3) for **19**. U(eq) is defined as one third of the trace of the orthogonalized U^{ij} tensor:

	x	y	z	U(eq)		x	y	z	U(eq)
Cu(1)	5000	5000	0	26.4(1)	C(23)	2333(2)	5640(3)	2262(17)	73.2(13)
O(11)	4724(8)	4202(11)	862(7)	29.6(4)	C(24)	1689(2)	5264(3)	1946(18)	79.2(15)
O(12)	3729(9)	3172(12)	566(7)	35.2(5)	C(25)	1695(18)	4259(3)	1664(17)	80.7(16)
O(13)	3798(9)	2199(13)	4262(8)	42.3(6)	C(26)	2369(16)	3665(2)	1719(14)	53.4(10)
O(14)	4937(8)	1418(12)	4085(8)	36(5)	C(31)	5439(13)	2051(16)	1389(11)	32.5(7)
N(41)	3903(10)	5444(14)	-153(9)	29.4(5)	C(32)	6228(14)	2146(18)	1512(13)	41.5(8)
C(11)	4253(12)	3078(15)	1733(10)	24.8(6)	C(33)	6764(16)	1834(2)	1000(17)	55.4(10)
C(12)	3692(12)	3370(15)	2234(10)	26.9(6)	C(34)	6510(2)	1430(2)	368(16)	64(11)
C(13)	3761(12)	3010(16)	2931(10)	29.5(6)	C(35)	5729(2)	1297(2)	242(15)	62.4(10)
C(14)	4362(12)	2363(16)	3130(10)	27.2(6)	C(36)	5194(16)	1604(2)	751(13)	48.4(9)
C(15)	4910(12)	2063(15)	2629(11)	27.9(6)	C(41)	3581(14)	5376(17)	-801(12)	35.3(7)
C(16)	4863(12)	2410(16)	1928(11)	27.2(6)	C(42)	2807(15)	5583(2)	-917(14)	46.7(9)
C(17)	4230(12)	3516(15)	982(10)	25.6(6)	C(43)	2354(15)	5907(2)	-359(16)	50.3(9)
C(18)	4408(12)	1950(16)	3873(11)	28.9(6)	C(44)	2681(14)	6011(19)	302(14)	43.8(8)
C(21)	3014(13)	4047(17)	2065(11)	33.7(7)	C(45)	3454(13)	5760(17)	387(12)	35.7(7)
C(22)	2994(17)	5049(19)	2329(15)	50.9(9)					

Atomic coordinates (x 10^4) and equivalent isotropic displacement parameters ($Å^2$x 10^3) for **20**. U(eq) is defined as one third of the trace of the orthogonalized U^{ij} tensor:

	x	y	z	U(eq)		x	y	z	U(eq)
Cu(1)	4901(1)	130(1)	2491(1)	39(1)	C(38)	6153(3)	-5527(2)	2985(1)	55(1)
C(1)	2053(3)	2613(2)	1013(1)	34(1)	C(39)	5644(3)	-5382(2)	3501(1)	57(1)
C(2)	1231(3)	2099(2)	707(1)	35(1)	C(40)	6326(3)	-4771(2)	3795(1)	51(1)
C(3)	-65(2)	2757(2)	471(1)	36(1)	C(101)	3403(3)	2294(2)	2865(1)	41(1)
C(4)	-565(2)	3899(2)	539(1)	33(1)	C(102)	2722(3)	2979(2)	3225(1)	51(1)
C(5)	250(2)	4407(2)	837(1)	35(1)	C(103)	2499(3)	2458(2)	3773(1)	51(1)
C(6)	1568(3)	3785(2)	1074(1)	34(1)	C(104)	2944(3)	1250(2)	3946(1)	45(1)
C(7)	3452(3)	1874(2)	1279(1)	36(1)	C(105)	3614(2)	615(2)	3563(1)	37(1)
C(8)	-2012(3)	4543(2)	313(1)	38(1)	C(201)	6978(3)	1577(2)	1873(1)	51(1)
C(9)	1641(3)	836(2)	650(1)	41(1)	C(202)	8142(4)	2179(3)	1785(1)	68(1)
C(10)	1168(4)	-38(3)	1028(2)	96(1)	C(203)	8855(3)	2280(3)	2230(2)	70(1)
C(11)	1512(4)	-1220(3)	975(2)	120(2)	C(204)	8389(3)	1805(2)	2756(1)	57(1)
C(12)	2300(4)	-1499(3)	529(2)	86(1)	C(205)	7237(3)	1215(2)	2815(1)	41(1)
C(13)	2784(5)	-640(3)	157(2)	117(2)	C(301)	7311(3)	-1471(2)	2047(1)	51(1)
C(14)	2474(4)	521(3)	220(1)	110(2)	C(302)	8025(3)	-2189(3)	1712(1)	62(1)
C(15)	2374(3)	4415(2)	1381(1)	38(1)	C(303)	7306(3)	-2372(2)	1279(1)	58(1)
C(16)	1634(3)	5030(2)	1766(1)	46(1)	C(304)	5893(3)	-1809(2)	1196(1)	50(1)
C(17)	2330(3)	5695(2)	2024(1)	57(1)	C(305)	5247(3)	-1083(2)	1545(1)	41(1)
C(18)	3777(4)	5765(2)	1899(1)	62(1)	C(401)	3650(3)	-2042(2)	2920(1)	39(1)
C(19)	4532(3)	5149(2)	1525(1)	59(1)	C(402)	2599(3)	-2720(2)	3112(1)	47(1)
C(20)	3835(3)	4482(2)	1265(1)	48(1)	C(403)	1162(3)	-2208(2)	3047(1)	51(1)
C(21)	7895(2)	-2563(2)	3964(1)	27(1)	C(404)	816(3)	-1032(2)	2786(1)	52(1)
C(22)	8375(2)	-3731(2)	3903(1)	28(1)	C(405)	1928(3)	-412(2)	2607(1)	45(1)
C(23)	9693(2)	-4357(2)	4130(1)	30(1)	O(1)	3378(2)	1443(1)	1793(1)	42(1)
C(24)	10539(2)	-3842(2)	4418(1)	29(1)	O(2)	4560(2)	1749(2)	966(1)	50(1)
C(25)	10057(2)	-2686(2)	4473(1)	31(1)	O(3)	-2772(2)	4107(2)	64(1)	56(1)
C(26)	8751(2)	-2024(2)	4249(1)	29(1)	O(4)	-2390(2)	5608(1)	422(1)	48(1)
C(27)	6474(3)	-1881(2)	3697(1)	30(1)	O(5)	6562(2)	-1213(1)	3227(1)	37(1)
C(28)	11967(3)	-4478(2)	4656(1)	32(1)	O(6)	5319(2)	-2047(1)	3973(1)	38(1)
C(29)	8344(2)	-762(2)	4304(1)	31(1)	O(7)	12679(2)	-4047(1)	4928(1)	47(1)
C(30)	6947(3)	-274(2)	4459(1)	38(1)	O(8)	12384(2)	-5538(1)	4548(1)	44(1)
C(31)	6629(3)	893(2)	4520(1)	47(1)	O(9)	5258(2)	6833(2)	35(1)	46(1)
C(32)	7676(3)	1591(2)	4431(1)	50(1)	O(10)	4715(2)	3293(2)	4994(1)	40(1)
C(33)	9067(3)	1114(2)	4283(1)	55(1)	N(1)	3854(2)	1119(2)	3029(1)	33(1)
C(34)	9396(3)	-46(2)	4218(1)	45(1)	N(2)	6530(2)	1087(2)	2383(1)	34(1)
C(35)	7551(2)	-4322(2)	3577(1)	30(1)	N(3)	5932(2)	-908(2)	1968(1)	36(1)
C(36)	8038(3)	-4469(3)	3060(1)	68(1)	N(4)	3334(2)	-894(2)	2670(1)	33(1)
C(37)	7329(4)	-5054(3)	2760(1)	83(1)					

Atomic coordinates (x 10^4) and equivalent isotropic displacement parameters ($Å^2$x 10^3) for **21**. U(eq) is defined as one third of the trace of the orthogonalized U^{ij} tensor:

	x	y	z	U(eq)		x	y	z	U(eq)
Ag	4872(1)	8566(1)	895(1)	32(1)	O(8)	5159(2)	513(3)	1466(4)	26(1)
O(1)	4545(2)	6734(3)	1236(4)	28(1)	C(11)	3680(3)	2383(4)	-54(5)	26(1)
C(2)	5000	6216(6)	2500	23(1)	C(12)	3272(3)	1362(5)	185(6)	33(1)

C(3)	5000	4882(6)	2500	22(1)	C(13)	2619(4)	828(6)	-1051(7)	45(2)
C(4)	4401(3)	4245(4)	1264(5)	23(1)	C(14)	2328(4)	1323(6)	-2526(7)	55(2)
C(5)	4384(3)	2996(4)	1256(5)	21(1)	C(15)	2716(4)	2320(6)	-2772(7)	51(2)
C(6)	5000	2383(6)	2500	19(1)	C(16)	3400(3)	2838(5)	-1557(5)	33(1)
C(7)	5000	1032(6)	2500	22(1)					

Atomic coordinates (x 10^4) and equivalent isotropic displacement parameters ($Å^2$x 10^3) for **22**. U(eq) is defined as one third of the trace of the orthogonalized U^{ij} tensor:

	x	y	z	U(eq)		x	y	z	U(eq)
Zn(1)	847(1)	-1009(1)	14688(1)	48(1)	C(48)	1305(5)	2452(4)	12220(3)	46(1)
Zn(2)	4590(1)	3738(1)	10408(1)	53(1)	C(49)	798(5)	1934(4)	12844(3)	48(1)
O(11)	271(4)	-2187(3)	13839(3)	66(1)	C(50)	3141(5)	3077(5)	11465(4)	51(1)
O(12)	-1216(4)	-1238(3)	13976(3)	72(1)	O(51)	3632(3)	2629(3)	10812(2)	58(1)
C(13)	-781(6)	-2001(5)	13638(4)	55(2)	O(52)	3154(4)	3977(3)	11635(3)	66(1)
C(14)	-1512(5)	-2725(4)	12957(4)	52(1)	C(53)	546(3)	2997(3)	11705(2)	53(1)
C(15)	-2279(5)	-3512(4)	13192(4)	54(1)	C(54)	486(4)	2774(3)	10811(2)	72(2)
C(16)	-3001(5)	-4124(4)	12560(4)	51(1)	C(55)	-194(4)	3312(4)	10335(2)	86(2)
C(17)	-2980(4)	-3985(4)	11710(3)	47(1)	C(56)	-814(4)	4074(4)	10753(3)	93(3)
C(18)	-2252(5)	-3192(4)	11485(4)	50(1)	C(57)	-754(4)	4297(3)	11647(3)	92(3)
C(19)	-1511(5)	-2544(4)	12100(4)	50(1)	C(58)	-74(4)	3758(3)	12123(2)	72(2)
C(20)	-3720(5)	-4675(5)	11034(4)	52(1)	C(61)	4592(2)	1868(3)	12404(3)	54(2)
O(21)	-4309(3)	-5420(3)	11259(2)	64(1)	C(62)	5072(4)	962(3)	12204(3)	76(2)
O(22)	-3689(3)	-4516(3)	10265(2)	58(1)	C(63)	6301(4)	940(3)	12055(3)	104(3)
C(23)	-2357(4)	-3719(4)	14099(2)	65(2)	C(64)	7050(3)	1824(4)	12105(3)	91(2)
C(24)	-3475(4)	-3748(4)	14486(3)	90(2)	C(65)	6570(3)	2730(3)	12305(3)	82(2)
C(25)	-3568(6)	-3948(5)	15325(3)	120(3)	C(66)	5341(3)	2752(3)	12454(3)	61(2)
C(26)	-2543(7)	-4119(4)	15776(2)	123(4)	O(201)	2489(4)	-1309(4)	15065(3)	76(1)
C(27)	-1425(6)	-4090(4)	15389(3)	127(4)	C(202)	2777(12)	-2028(10)	15541(8)	167(5)
C(28)	-1332(4)	-3890(4)	14551(3)	89(2)	C(203)	2290(14)	-2952(12)	15283(11)	228(7)
C(31)	-764(4)	-1686(3)	11821(3)	59(2)	O(301)	5609(4)	3054(4)	9528(3)	89(1)
C(32)	-1318(4)	-1075(4)	11339(3)	79(2)	C(302)	6328(13)	2245(10)	9707(10)	194(6)
C(33)	-635(6)	-293(3)	11048(3)	109(3)	C(303)	5616(13)	1386(12)	9547(10)	211(6)
C(34)	602(6)	-122(3)	11239(3)	115(4)	O(401)	3258(8)	327(7)	16083(5)	163(3)
C(35)	1155(4)	-733(4)	11721(3)	101(3)	C(402)	4182(15)	928(13)	15780(12)	243(8)
C(36)	472(4)	-1515(4)	12012(3)	77(2)	C(403)	4773(17)	1409(15)	16602(12)	264(9)
O(41)	1461(3)	108(3)	14154(2)	56(1)	O(501)	7203(9)	4145(7)	8755(6)	97(3)
O(42)	-108(3)	1036(3)	14206(2)	56(1)	C(502)	7940(15)	3835(14)	8147(11)	137(6)
C(43)	908(5)	793(4)	13933(3)	47(1)	C(503)	7040(30)	3540(30)	7443(11)	208(13)
C(44)	1479(5)	1373(4)	13292(3)	43(1)	O(601)	6550(10)	3985(9)	8352(7)	69(3)
C(45)	2704(5)	1348(4)	13128(3)	49(1)	C(602)	6690(30)	3910(100)	7464(17)	520(90)
C(46)	3252(4)	1879(4)	12531(3)	46(1)	C(603)	8050(20)	3931(19)	7339(16)	111(7)
C(47)	2540(5)	2433(4)	12075(3)	45(1)					

Atomic coordinates (x 10^4) and equivalent isotropic displacement parameters ($Å^2$x 10^3) for **14**. U(eq) is defined as one third of the trace of the orthogonalized U^{ij} tensor:

	x	y	z	U(eq)		x	y	z	U(eq)
O(1)	896(1)	410(1)	1376(1)	41(1)	C(12)	1955(2)	-1701(2)	2322(2)	45(1)
C(1)	1914(2)	157(1)	927(1)	32(1)	C(13)	1052(2)	-2285(2)	2802(2)	55(1)

O(2)	1714(2)	-167(1)	-62(1)	45(1)	C(14)	1189(3)	-2266(2)	3935(2)	57(1)
C(2)	3462(2)	215(1)	1596(1)	30(1)	C(15)	2234(3)	-1676(2)	4603(2)	59(1)
C(3)	4421(2)	857(1)	1225(1)	32(1)	C(16)	3117(3)	-1083(2)	4132(2)	49(1)
C(4)	5904(2)	785(2)	1719(2)	38(1)	C(21)	3864(2)	1640(1)	364(1)	33(1)
C(5)	6453(2)	110(2)	2574(2)	40(1)	C(22)	4529(2)	1809(2)	-508(2)	44(1)
C(6)	5469(2)	-457(2)	2990(2)	39(1)	C(23)	4018(3)	2557(2)	-1291(2)	53(1)
C(7)	3974(2)	-427(1)	2515(1)	33(1)	C(24)	2856(3)	3135(2)	-1213(2)	52(1)
C(8)	8072(2)	-33(2)	3019(2)	59(1)	C(25)	2187(2)	2983(2)	-352(2)	46(1)
C(11)	2992(2)	-1079(1)	2986(2)	35(1)	C(26)	2693(2)	2243(1)	440(2)	38(1)

Atomic coordinates (x 10^4) and equivalent isotropic displacement parameters ($Å^2$x 10^3) for **26**. U(eq) is defined as one third of the trace of the orthogonalized U^{ij} tensor:

	x	y	z	U(eq)		x	y	z	U(eq)
C(1)	2527(2)	-2428(7)	1111(2)	76(1)	C(23)	4(2)	-3974(8)	1481(2)	94(1)
N(2)	2968(2)	-2440(6)	754(1)	80(1)	C(24)	-230(2)	-3880(9)	897(2)	101(1)
C(3)	2954(2)	-4386(6)	368(1)	71(1)	C(25)	153(2)	-2518(9)	556(2)	104(1)
C(4)	2361(2)	-6049(7)	224(2)	82(1)	C(26)	807(2)	-1253(8)	806(2)	88(1)
C(5)	2443(2)	-7838(7)	-154(2)	86(1)	C(31)	2201(2)	4795(5)	2810(1)	58(1)
C(6)	3117(3)	-7986(7)	-392(2)	89(1)	C(32)	1627(2)	4507(6)	3154(1)	69(1)
C(7)	3692(2)	-6362(7)	-263(2)	86(1)	C(33)	1542(2)	6130(7)	3579(2)	79(1)
C(8)	3606(2)	-4564(7)	105(2)	78(1)	C(34)	2024(2)	8018(7)	3677(2)	79(1)
O(9)	4215(2)	-2976(6)	228(2)	121(1)	C(35)	2591(2)	8307(6)	3342(2)	77(1)
C(11)	2475(2)	-421(6)	1522(1)	60(1)	C(36)	2679(2)	6739(6)	2910(1)	67(1)
C(12)	1743(2)	25(6)	1674(1)	62(1)	C(41)	3926(2)	440(6)	1675(1)	58(1)
C(13)	1665(2)	1736(6)	2080(1)	62(1)	C(42)	4324(2)	-1537(7)	1881(2)	79(1)
C(14)	2289(2)	3041(5)	2353(1)	57(1)	C(43)	5065(2)	-1983(8)	1790(2)	86(1)
C(15)	3005(2)	2597(5)	2188(1)	59(1)	C(44)	5420(2)	-441(8)	1482(2)	84(1)
C(16)	3117(2)	908(5)	1783(1)	57(1)	C(45)	5048(2)	1553(9)	1269(2)	107(2)
C(21)	1051(2)	-1315(6)	1401(1)	67(1)	C(46)	4303(2)	2006(8)	1377(2)	91(1)
C(22)	638(2)	-2668(7)	1736(2)	80(1)					

Atomic coordinates (x 10^4) and equivalent isotropic displacement parameters ($Å^2$x 10^3) for **27**. U(eq) is defined as one third of the trace of the orthogonalized U^{ij} tensor:

	x	y	z	U(eq)		x	y	z	U(eq)
O(1)	9105(2)	407(2)	277(2)	119(1)	C(23)	4421(2)	3390(2)	-296(1)	81(1)
C(2)	9189(2)	1646(2)	498(2)	65(1)	C(24)	3607(2)	4106(1)	-67(1)	94(1)
C(3)	10059(2)	2384(3)	412(2)	76(1)	C(25)	3164(1)	3723(2)	548(1)	93(1)
C(4)	10098(3)	3614(3)	635(2)	81(1)	C(26)	3533(1)	2625(2)	934(1)	72(1)
C(5)	9282(2)	4088(3)	954(2)	80(1)	C(31)	3612(1)	-2252(1)	1805(1)	52(1)
C(6)	8395(2)	3349(2)	1040(2)	60(1)	C(32)	2657(1)	-2465(2)	1271(1)	66(1)
C(7)	8325(2)	2122(2)	799(1)	49(1)	C(33)	1918(1)	-3381(2)	1401(1)	78(1)
N(8)	7440(2)	1338(2)	839(1)	56(1)	C(34)	2133(1)	-4084(2)	2065(1)	81(1)
C(9)	6737(2)	1643(2)	1368(1)	50(1)	C(35)	3088(2)	-3872(2)	2599(1)	77(1)
C(10)	5920(2)	604(2)	1423(1)	46(1)	C(36)	3828(1)	-2956(2)	2469(1)	64(1)
C(11)	4793(2)	763(2)	1145(1)	48(1)	C(41)	7495(1)	-829(1)	2013(1)	50(1)
C(12)	4063(2)	-164(2)	1278(1)	52(1)	C(42)	8183(1)	-209(1)	2602(1)	61(1)
C(13)	4413(2)	-1268(2)	1666(1)	49(1)	C(43)	9296(1)	-496(2)	2774(1)	75(1)
C(14)	5539(2)	-1433(2)	1906(1)	51(1)	C(44)	9722(1)	-1403(2)	2356(1)	81(1)
C(15)	6291(2)	-530(2)	1790(1)	48(1)	C(45)	9034(1)	-2023(2)	1767(1)	78(1)

C(21)	4347(1)	1910(1)	705(1)	52(1)	C(46)	7921(1)	-1736(2)	1595(1)	65(1)
C(22)	4790(1)	2292(2)	91(1)	65(1)					

Atomic coordinates (x 10^4) and equivalent isotropic displacement parameters ($Å^2$x 10^3) for **28**. U(eq) is defined as one third of the trace of the orthogonalized U^{ij} tensor:

	x	y	z	U(eq)		x	y	z	U(eq)
Sn(1)	4504(1)	3614(1)	4748(1)	22(1)	N(52)	-82(3)	3021(3)	595(2)	20(1)
Si(1)	3406(1)	4170(1)	6201(1)	28(1)	C(51)	198(3)	2368(3)	691(2)	20(1)
Si(2)	2172(1)	2506(1)	4904(1)	25(1)	C(53)	-421(3)	3544(3)	1154(2)	19(1)
O(9)	5657(2)	4872(2)	5482(2)	24(1)	C(54)	-759(4)	3235(4)	1718(3)	26(1)
N(1)	3348(3)	3394(3)	5382(2)	24(1)	C(55)	-1093(4)	3783(4)	2241(3)	29(1)
N(2)	5677(3)	3188(3)	5554(2)	20(1)	C(56)	-1116(4)	4618(4)	2186(3)	28(1)
C(1)	5526(3)	2448(3)	5729(3)	21(1)	C(57)	-803(4)	4916(4)	1619(3)	24(1)
C(3)	6558(3)	4004(3)	5951(2)	19(1)	C(58)	-456(3)	4385(3)	1091(2)	18(1)
C(4)	7452(3)	3987(4)	6358(3)	27(1)	C(61)	375(4)	1687(3)	106(2)	22(1)
C(5)	8271(4)	4804(4)	6734(3)	31(1)	C(62)	-379(4)	1207(3)	-552(3)	22(1)
C(6)	8209(4)	5650(4)	6706(3)	33(1)	C(63)	-187(3)	569(4)	-1091(3)	23(1)
C(7)	7344(4)	5671(4)	6281(3)	26(1)	C(64)	708(3)	338(3)	-998(2)	21(1)
C(8)	6505(3)	4841(4)	5890(2)	23(1)	C(65)	1422(4)	785(4)	-326(3)	24(1)
C(11)	4763(3)	1528(3)	5276(2)	22(1)	C(66)	1279(3)	1457(3)	223(3)	21(1)
C(12)	4704(4)	1199(4)	4527(2)	23(1)	C(71)	-1444(3)	1258(3)	-670(3)	22(1)
C(13)	3960(4)	340(4)	4117(3)	25(1)	C(72)	-1932(4)	1276(4)	-1329(3)	29(1)
C(14)	3291(4)	-241(4)	4422(3)	24(1)	C(73)	-2969(4)	1218(4)	-1449(3)	38(1)
C(15)	3411(4)	72(4)	5185(3)	26(1)	C(74)	-3521(4)	1133(5)	-919(3)	41(2)
C(16)	4124(3)	940(4)	5601(3)	23(1)	C(75)	-2031(4)	1164(4)	-136(3)	26(1)
C(21)	5457(4)	1698(4)	4145(3)	27(1)	C(76)	-3064(4)	1105(4)	-264(3)	34(1)
C(22)	6532(4)	2035(4)	4427(3)	30(1)	C(81)	860(4)	-375(4)	-1583(2)	23(1)
C(23)	7228(5)	2430(5)	4044(4)	44(2)	C(82)	1857(4)	-367(4)	-1641(3)	31(1)
C(24)	6856(5)	2472(4)	3369(4)	47(2)	C(83)	1986(4)	-1025(4)	-2207(3)	35(1)
C(25)	5792(5)	2134(5)	3081(3)	43(2)	C(84)	1136(4)	-1678(4)	-2732(3)	35(1)
C(26)	5104(4)	1748(4)	3473(3)	33(1)	C(85)	139(4)	-1705(4)	-2679(3)	30(1)
C(31)	2477(4)	-1144(4)	3966(3)	27(1)	C(86)	9(4)	-1057(4)	-2112(3)	27(1)
C(32)	2591(5)	-1623(4)	3289(3)	41(2)	C(91)	2064(3)	1909(3)	921(2)	21(1)
C(33)	1810(6)	-2430(5)	2844(3)	56(2)	C(92)	2450(4)	1365(4)	1251(3)	27(1)
C(34)	911(5)	-2804(5)	3073(4)	55(2)	C(93)	3143(4)	1763(4)	1918(3)	37(1)
C(35)	807(5)	-2367(5)	3745(4)	62(2)	C(94)	3470(4)	2706(5)	2264(3)	41(2)
C(36)	1575(4)	-1532(5)	4186(4)	49(2)	C(95)	3115(4)	3256(4)	1945(3)	36(1)
C(41)	4180(3)	1226(4)	6404(2)	23(1)	C(96)	2408(4)	2859(4)	1275(3)	29(1)
C(42)	4147(4)	2084(4)	6762(3)	30(1)	C(301)	3256(4)	3184(4)	-390(3)	36(1)
C(43)	4170(4)	2322(4)	7499(3)	40(2)	C(302)	3229(4)	4648(4)	-1095(3)	34(1)
C(44)	4250(5)	1732(5)	7884(3)	42(2)	C(303)	1396(4)	2825(4)	-1506(3)	36(1)
C(45)	4269(4)	865(4)	7531(3)	36(1)	C(401)	3977(4)	5254(4)	912(3)	41(2)
C(46)	4227(4)	616(4)	6790(3)	30(1)	C(402)	2140(4)	5357(4)	1508(3)	40(2)
C(101)	4688(4)	4626(4)	6874(3)	41(2)	C(403)	2785(5)	6336(4)	402(4)	46(2)
C(102)	2430(4)	3626(5)	6701(3)	38(1)	Cl(1)	110(2)	728(2)	6842(1)	95(1)
C(103)	3128(5)	5191(4)	6073(4)	47(2)	Cl(2)	1063(2)	-441(2)	6020(1)	70(1)
C(201)	1716(4)	1591(4)	5354(3)	35(1)	C(500)	1251(6)	478(6)	6794(4)	65(2)
C(202)	2266(4)	1848(4)	3982(3)	32(1)	Cl(3)	410(4)	5450(6)	5760(3)	64(2)
C(203)	1086(4)	2949(4)	4750(3)	34(1)	Cl(4)	-390(8)	4803(12)	4203(4)	187(7)

Sn(2)	156(1)	3792(1)	-369(1)	19(1)	C(600)	706(8)	5325(13)	4906(4)	72(5)
Si(3)	2396(1)	3770(1)	-716(1)	25(1)	Cl(5)	6199(2)	2754(2)	1310(1)	81(1)
Si(4)	2620(1)	5249(1)	647(1)	28(1)	Cl(6)	4458(2)	1314(2)	193(2)	117(1)
O(59)	-158(2)	4683(2)	536(2)	20(1)	C(700)	5001(5)	2479(6)	723(4)	69(2)
N(3)	1824(3)	4261(3)	-59(2)	22(1)					

Atomic coordinates (x 10^4) and equivalent isotropic displacement parameters ($Å^2$x 10^3) for **29**. U(eq) is defined as one third of the trace of the orthogonalized U^{ij} tensor:

	x	y	z	U(eq)		x	y	z	U(eq)
C(1)	8368(3)	12879(3)	5220(2)	43(1)	C(25)	3494(3)	5633(2)	1077(2)	29(1)
C(2)	6312(4)	12530(3)	3061(3)	61(1)	C(26)	4890(3)	6401(2)	1593(2)	27(1)
C(3)	9873(4)	13551(3)	3291(3)	57(1)	C(31)	6402(3)	7544(2)	-577(2)	28(1)
Al(4)	8179(1)	12579(1)	3751(1)	38(1)	C(32)	7337(3)	8730(3)	-228(2)	35(1)
O(5)	8002(2)	10957(2)	3284(1)	31(1)	C(33)	8254(3)	9283(3)	-807(2)	43(1)
C(6)	9130(3)	10584(2)	3490(2)	26(1)	C(34)	8266(3)	8671(3)	-1735(2)	46(1)
C(7)	10426(3)	11286(3)	4155(2)	33(1)	C(35)	7318(3)	7497(3)	-2102(2)	42(1)
C(8)	11496(3)	10835(3)	4309(2)	34(1)	C(36)	6397(3)	6942(3)	-1533(2)	32(1)
C(9)	11273(3)	9693(3)	3819(2)	35(1)	C(41)	5381(3)	6363(2)	2639(2)	28(1)
C(10)	9973(3)	8985(2)	3163(2)	31(1)	C(42)	4511(3)	6370(3)	3342(2)	35(1)
C(11)	8912(3)	9439(2)	2988(2)	26(1)	C(43)	4945(3)	6267(3)	4299(2)	42(1)
N(12)	7500(2)	8784(2)	2362(2)	25(1)	C(44)	6231(3)	6126(3)	4560(2)	42(1)
Al(13)	6237(1)	9697(1)	2664(1)	31(1)	C(45)	7095(3)	6089(2)	3869(2)	38(1)
C(14)	5193(3)	9320(3)	3710(2)	44(1)	C(46)	6673(3)	6205(2)	2918(2)	31(1)
C(15)	5241(4)	9779(3)	1404(2)	49(1)	C(51)	1552(3)	4599(2)	-480(2)	30(1)
C(16)	7297(3)	7911(2)	1618(2)	27(1)	C(52)	876(3)	4697(3)	-1382(2)	34(1)
C(21)	5840(3)	7078(2)	1064(2)	26(1)	C(53)	-484(3)	3871(3)	-1893(2)	41(1)
C(22)	5411(3)	6906(2)	23(2)	26(1)	C(54)	-1200(3)	2942(3)	-1498(2)	43(1)
C(23)	4011(3)	6107(2)	-455(2)	28(1)	C(55)	-572(3)	2833(3)	-603(2)	41(1)
C(24)	3030(3)	5471(2)	53(2)	28(1)	C(56)	808(3)	3652(2)	-96(2)	35(1)

Atomic coordinates (x 10^4) and equivalent isotropic displacement parameters ($Å^2$x 10^3) for **33**. U(eq) is defined as one third of the trace of the orthogonalized U^{ij} tensor:

	x	y	z	U(eq)		x	y	z	U(eq)
B(1)	0	1355(6)	9557(14)	48(2)	C(12)	1368(2)	1532(3)	7272(6)	31(1)
O(1)	0	396(3)	8764(15)	111(3)	C(13)	1889(2)	1165(3)	8044(7)	37(1)
O(2)	0	1495(8)	11561(10)	125(4)	C(14)	2139(2)	1578(3)	9727(7)	33(1)
C(1)	0	2319(4)	8153(8)	22(1)	C(15)	1862(2)	2392(4)	10628(7)	41(1)
C(2)	524(2)	2750(3)	7521(6)	27(1)	C(16)	1341(2)	2779(3)	9932(6)	36(1)
C(3)	517(2)	3592(3)	6236(9)	53(2)	C(17)	1057(2)	3685(5)	10948(10)	82(2)
C(4)	0	4009(6)	5589(16)	73(3)	C(18)	2703(2)	1177(4)	10535(9)	52(1)
C(11)	1087(1)	2340(3)	8253(6)	25(1)	C(19)	1125(2)	1072(4)	5379(9)	56(1)

Atomic coordinates (x 10^4) and equivalent isotropic displacement parameters ($Å^2$x 10^3) for **34**. U(eq) is defined as one third of the trace of the orthogonalized U^{ij} tensor:

	x	y	z	U(eq)		x	y	z	U(eq)
O(1)	5306(2)	791(2)	2760(1)	55(1)	O(31)	4632(2)	2860(2)	2296(1)	46(1)
C(2)	4569(3)	102(2)	3095(2)	34(1)	C(32)	5316(3)	3365(2)	1827(2)	33(1)
C(3)	3409(3)	472(2)	3387(2)	35(1)	C(33)	4610(3)	3544(2)	1127(2)	34(1)
C(4)	2691(3)	-287(3)	3708(2)	43(1)	C(34)	5378(3)	4085(2)	692(2)	41(1)

C(5)	3108(3)	-1393(3)	3737(2)	49(1)	C(35)	6783(3)	4416(3)	949(2)	47(1)
C(6)	4255(3)	-1741(3)	3445(2)	43(1)	C(36)	7454(3)	4191(3)	1636(2)	42(1)
C(7)	5008(3)	-1000(2)	3121(2)	36(1)	C(37)	6739(3)	3658(2)	2089(2)	34(1)
C(11)	2960(3)	1664(2)	3345(2)	34(1)	C(41)	3093(3)	3175(2)	830(2)	34(1)
C(12)	1948(3)	1708(2)	2692(2)	38(1)	C(42)	2575(3)	1958(2)	440(2)	39(1)
C(13)	1529(3)	2815(3)	2661(2)	43(1)	C(43)	1160(3)	1640(3)	136(2)	45(1)
C(14)	2067(3)	3876(3)	3270(2)	48(1)	C(44)	242(3)	2494(3)	211(2)	42(1)
C(15)	3078(3)	3810(3)	3900(2)	47(1)	C(45)	789(3)	3690(3)	608(2)	45(1)
C(16)	3561(3)	2729(3)	3947(2)	40(1)	C(46)	2182(3)	4045(2)	913(2)	39(1)
C(17)	1334(3)	583(3)	2029(2)	52(1)	C(47)	3531(3)	998(3)	333(2)	54(1)
C(18)	1531(4)	5053(3)	3243(3)	68(1)	C(48)	-1282(3)	2133(3)	-128(2)	55(1)
C(19)	4726(3)	2708(3)	4615(2)	53(1)	C(49)	2733(3)	5365(3)	1332(2)	55(1)
C(21)	6247(3)	-1384(2)	2800(2)	37(1)	C(51)	7468(3)	3387(2)	2821(2)	36(1)
C(22)	7490(3)	-1340(2)	3327(2)	40(1)	C(52)	7634(3)	4231(3)	3573(2)	40(1)
C(23)	8611(3)	-1766(3)	3017(2)	43(1)	C(53)	8368(3)	3970(3)	4245(2)	46(1)
C(24)	8529(3)	-2230(2)	2201(2)	42(1)	C(54)	8917(3)	2894(3)	4189(2)	46(1)
C(25)	7296(3)	-2231(2)	1687(2)	43(1)	C(55)	8706(3)	2059(3)	3437(2)	45(1)
C(26)	6152(3)	-1808(2)	1969(2)	39(1)	C(56)	7991(3)	2284(2)	2749(2)	39(1)
C(27)	7645(3)	-820(3)	4223(2)	57(1)	C(57)	7006(4)	5394(3)	3660(2)	56(1)
C(28)	9733(3)	-2729(3)	1881(2)	55(1)	C(58)	9715(4)	2609(4)	4909(2)	67(1)
C(29)	4849(3)	-1783(3)	1391(2)	51(1)	C(59)	7771(3)	1342(3)	1948(2)	50(1)

Atomic coordinates (x 10^4) and equivalent isotropic displacement parameters ($Å^2$x 10^3) for **36**. U(eq) is defined as one third of the trace of the orthogonalized U^{ij} tensor:

	x	y	z	U(eq)		x	y	z	U(eq)
O(1)	507(5)	-8(2)	-1596(3)	90(2)	O(51)	-10106(5)	1496(2)	-6784(3)	95(2)
C(2)	465(6)	321(3)	-903(4)	72(2)	C(52)	-9712(7)	1861(3)	-5950(4)	80(2)
C(3)	-190(6)	1051(3)	-1198(4)	58(2)	C(53)	-9173(8)	2604(4)	-5833(4)	72(2)
C(4)	407(6)	1722(4)	-1036(4)	63(2)	C(54)	-7963(8)	2674(4)	-5351(4)	78(2)
C(5)	-163(7)	2400(4)	-1241(4)	70(2)	C(55)	-7490(7)	3383(5)	-5238(5)	91(2)
C(6)	-1329(8)	2432(4)	-1606(4)	70(2)	C(56)	-8185(10)	4013(4)	-5612(6)	94(3)
C(7)	-1903(6)	1761(4)	-1762(4)	69(2)	C(57)	-9378(8)	3934(4)	-6071(5)	95(2)
C(8)	-1372(6)	1076(3)	-1593(4)	58(2)	C(58)	-9891(8)	3243(4)	-6194(4)	79(2)
C(11)	1659(3)	1728(2)	-649(3)	66(2)	C(61)	-7141(5)	2031(3)	-4956(4)	81(2)
C(12)	1995(5)	1503(3)	-1185(3)	96(2)	C(62)	-7326(4)	1411(4)	-5486(3)	88(2)
C(13)	3163(6)	1502(3)	-814(4)	108(3)	C(63)	-6528(6)	831(3)	-5102(5)	99(2)
C(14)	3996(4)	1727(3)	92(5)	101(2)	C(64)	-5545(5)	870(4)	-4187(5)	113(3)
C(15)	3660(4)	1953(2)	628(3)	101(3)	C(65)	-5360(4)	1489(5)	-3657(3)	121(3)
C(16)	2492(5)	1953(2)	257(3)	86(2)	C(66)	-6158(6)	2070(3)	-4042(4)	105(3)
C(21)	-2016(6)	3134(3)	-1838(5)	95(6)	C(71)	-7786(10)	4816(5)	-5549(7)	123(8)
C(22)	-1455(5)	3768(4)	-1311(4)	95(3)	C(72)	-6677(10)	5004(5)	-4779(6)	129(5)
C(23)	-2064(7)	4432(3)	-1534(4)	125(4)	C(73)	-6216(8)	5698(6)	-4728(6)	141(6)
C(24)	-3233(7)	4463(3)	-2284(5)	145(5)	C(74)	-6865(10)	6203(5)	-5447(7)	137(6)
C(25)	-3794(5)	3830(5)	-2812(4)	132(4)	C(75)	-7975(9)	6014(5)	-6217(6)	124(5)
C(26)	-3186(6)	3166(3)	-2589(4)	99(3)	C(76)	-8436(8)	5321(6)	-6268(6)	119(5)
C(21b)	-1840(2)	3200(11)	-1855(14)	43(13)	C(71)	-7484(16)	4711(7)	-5462(8)	75(7)
C(22b)	-1430(2)	3752(17)	-2122(18)	125(14)	C(72)	-6368(16)	4718(8)	-5215(10)	150(9)
C(23b)	-1930(3)	4455(14)	-2359(18)	180(20)	C(73)	-5808(12)	5391(11)	-5073(11)	177(11)
C(24b)	-2850(2)	4605(11)	-2328(14)	64(9)	C(74)	-6365(15)	6057(8)	-5178(10)	102(7)

C(25b)	-3260(2)	4053(15)	-2062(17)	149(18)	C(75)	-7482(15)	6050(7)	-5425(10)	123(7)
C(26b)	-2760(3)	3351(12)	-1825(17)	114(13)	C(76)	-8041(11)	5377(9)	-5567(9)	132(8)
C(31)	-2089(4)	392(2)	-1823(3)	66(2)	C(81)	-11161(5)	3210(3)	-6683(4)	81(2)
C(32)	-2699(4)	309(2)	-1465(3)	73(2)	C(82)	-11630(8)	3475(3)	-6256(3)	109(3)
C(33)	-3382(4)	-318(3)	-1680(3)	92(2)	C(83)	-12826(8)	3473(3)	-6729(6)	125(3)
C(34)	-3454(4)	-863(2)	-2254(3)	85(2)	C(84)	-13554(5)	3206(4)	-7628(6)	132(3)
C(35)	-2844(4)	-780(2)	-2613(3)	85(2)	C(85)	-13085(7)	2940(3)	-8054(3)	141(4)
C(36)	-2161(4)	-153(3)	-2397(3)	79(2)	C(86)	-11889(7)	2942(3)	-7582(4)	116(3)

Atomic coordinates (x 10^4) and equivalent isotropic displacement parameters (Å^{2}x 10^3) for **37**. U(eq) is defined as one third of the trace of the orthogonalized U^{ij} tensor:

	x	y	z	U(eq)		x	y	z	U(eq)
O(1A)	810(20)	7500	2997(9)	84(5)	C(12)	-784(6)	6187(1)	4033(3)	59(1)
C(2A)	1779(12)	7500	3779(4)	68(2)	C(13)	-268(7)	5660(2)	3646(3)	67(1)
O(1B)	3109(13)	7500	3869(6)	112(4)	C(14)	1390(7)	5373(2)	4006(3)	65(1)
C(2B)	1779(12)	7500	3779(4)	68(2)	C(15)	2521(6)	5626(2)	4767(4)	72(1)
C(3)	434(7)	7500	4812(3)	52(1)	C(16)	2048(6)	6148(1)	5183(3)	62(1)
C(4)	-190(5)	6992(1)	5266(2)	50(1)	C(17)	-2616(8)	6472(2)	3614(4)	94(2)
C(5)	-1379(6)	7002(2)	6149(3)	59(1)	C(18)	1887(9)	4797(2)	3591(4)	89(2)
C(6)	-1976(9)	7500	6591(4)	66(2)	C(19)	3313(8)	6398(2)	6038(4)	98(2)
C(11)	383(5)	6435(1)	4809(2)	50(1)					

Atomic coordinates (x 10^4) and equivalent isotropic displacement parameters (Å^{2}x 10^3) for **38**. U(eq) is defined as one third of the trace of the orthogonalized U^{ij} tensor:

	x	y	z	U(eq)		x	y	z	U(eq)
Sn(1)	6156(1)	7243(1)	1850(1)	26(1)	C(129)	7868(5)	4788(4)	3791(3)	40(1)
O(1)	6087(3)	7364(3)	2995(2)	31(1)	C(201)	6888(4)	9793(3)	1868(2)	24(1)
O(2)	6120(3)	9079(2)	2172(2)	29(1)	C(202)	8220(4)	9471(3)	1590(2)	24(1)
C(101)	5259(4)	6748(3)	3342(2)	23(1)	C(203)	8980(4)	10255(4)	1293(2)	32(1)
C(102)	5720(4)	6574(3)	4036(2)	23(1)	C(204)	8446(4)	11340(4)	1269(3)	36(1)
C(103)	4824(4)	5994(4)	4423(2)	27(1)	C(205)	7142(4)	11657(4)	1548(2)	32(1)
C(104)	3549(4)	5576(4)	4134(2)	32(1)	C(206)	6340(4)	10901(3)	1847(2)	25(1)
C(105)	3109(4)	5726(4)	3442(2)	29(1)	C(211)	4946(4)	11270(3)	2165(2)	24(1)
C(106)	3955(4)	6317(3)	3040(2)	25(1)	C(212)	3808(4)	11186(3)	1674(2)	27(1)
C(111)	3518(4)	6456(4)	2274(2)	26(1)	C(213)	2536(4)	11582(4)	1987(2)	29(1)
C(112)	3588(4)	5465(4)	1607(2)	31(1)	C(214)	2359(4)	12061(4)	2775(2)	30(1)
C(113)	3297(5)	5642(4)	892(2)	37(1)	C(215)	3493(4)	12125(4)	3261(2)	30(1)
C(114)	2945(5)	6746(5)	821(3)	39(1)	C(216)	4769(4)	11724(3)	2967(2)	28(1)
C(115)	2865(4)	7713(4)	1484(3)	34(1)	C(217)	5963(5)	11765(4)	3514(2)	38(1)
C(116)	3138(4)	7588(4)	2217(2)	28(1)	C(218)	980(5)	12527(5)	3101(3)	42(1)
C(117)	3024(5)	8655(4)	2924(3)	37(1)	C(219)	3948(5)	10651(5)	807(2)	39(1)
C(118)	2679(6)	6922(6)	33(3)	61(2)	C(221)	8793(4)	8305(4)	1629(2)	24(1)
C(119)	4050(6)	4262(4)	1646(3)	44(1)	C(222)	9098(4)	8135(3)	2356(2)	24(1)
C(121)	7141(4)	6949(3)	4336(2)	22(1)	C(223)	9463(4)	6998(4)	2389(2)	28(1)
C(122)	8171(4)	6089(4)	4221(2)	27(1)	C(224)	9563(4)	6026(4)	1730(2)	30(1)
C(123)	9502(4)	6444(4)	4495(2)	31(1)	C(225)	9338(4)	6227(4)	1017(2)	32(1)
C(124)	9827(4)	7627(4)	4884(2)	29(1)	C(226)	8952(4)	7337(4)	952(2)	28(1)
C(125)	8787(4)	8469(4)	4996(2)	29(1)	C(227)	8604(5)	7475(4)	165(2)	41(1)

C(126)	7462(4)	8163(4)	4731(2)	26(1)	C(228)	9916(5)	4794(4)	1785(3)	42(1)
C(127)	6378(5)	9100(4)	4851(3)	36(1)	C(229)	9016(5)	9156(4)	3090(2)	34(1)
C(128)	11269(5)	8007(5)	5176(3)	45(1)					

Atomic coordinates (x 10^4) and equivalent isotropic displacement parameters ($Å^2$x 10^3) for **39**. U(eq) is defined as one third of the trace of the orthogonalized U^{ij} tensor:

	x	y	z	U(eq)		x	y	z	U(eq)
C(1)	2632(2)	9756(2)	1727(1)	29(1)	C(19)	2504(3)	5938(2)	2815(1)	42(1)
C(2)	2527(2)	9441(2)	2313(1)	32(1)	C(20)	3515(2)	6484(2)	2695(1)	42(1)
C(3)	2430(3)	10304(2)	2718(1)	44(1)	C(21)	3547(2)	7624(2)	2540(1)	38(1)
C(4)	2432(3)	11425(2)	2564(1)	45(1)	C(22)	4693(3)	8201(3)	2441(2)	63(1)
C(5)	2514(2)	11719(2)	1987(1)	40(1)	C(23)	2484(3)	4702(2)	2997(2)	67(1)
C(6)	2608(2)	10897(2)	1566(1)	30(1)	C(24)	345(3)	8304(3)	2575(1)	56(1)
C(7)	2648(2)	11210(2)	940(1)	31(1)	C(101)	4620(5)	6400(3)	-128(2)	115(2)
C(8)	1626(2)	11281(2)	628(1)	33(1)	C(102)	5184(3)	7888(4)	852(2)	105(2)
C(9)	1687(3)	11512(2)	37(1)	40(1)	C(103)	3413(4)	8630(3)	-46(2)	86(1)
C(10)	2704(3)	11676(2)	-240(1)	40(1)	C(201)	1332(3)	5055(3)	1272(2)	77(1)
C(11)	3715(2)	11627(2)	80(1)	38(1)	C(202)	2224(4)	4776(3)	86(1)	80(1)
C(12)	3711(2)	11395(2)	667(1)	33(1)	C(203)	3853(3)	4631(3)	1118(2)	78(1)
C(13)	4818(2)	11331(3)	997(1)	47(1)	Si(1)	3983(1)	7435(1)	393(1)	64(1)
C(14)	2744(3)	11893(3)	-884(1)	59(1)	Si(2)	2590(1)	5378(1)	803(1)	46(1)
C(15)	477(2)	11117(3)	918(1)	46(1)	O(1)	2800(1)	8952(1)	1312(1)	37(1)
C(16)	2517(2)	8229(2)	2489(1)	33(1)	N(1)	2854(2)	6837(2)	790(1)	40(1)
C(17)	1468(2)	7693(2)	2616(1)	36(1)	Ge(1)	1880(1)	7688(1)	1248(1)	38(1)
C(18)	1481(2)	6549(2)	2781(1)	42(1)					

Atomic coordinates (x 10^4) and equivalent isotropic displacement parameters ($Å^2$x 10^3) for **40**. U(eq) is defined as one third of the trace of the orthogonalized U^{ij} tensor:

	x	y	z	U(eq)		x	y	z	U(eq)
Al(1)	2033(1)	1302(1)	4806(1)	32(1)	C(52)	3635(2)	2022(2)	3819(1)	30(1)
Al(2)	3360(1)	2740(1)	5197(1)	29(1)	C(53)	4063(2)	1626(2)	3442(1)	34(1)
O(11)	2415(1)	2392(1)	5386(1)	26(1)	C(54)	4163(2)	596(2)	3388(1)	37(1)
O(21)	2919(1)	1729(1)	4565(1)	27(1)	C(55)	3799(2)	-59(2)	3692(1)	36(1)
C(11)	2115(2)	2875(2)	5821(1)	28(1)	C(56)	3353(2)	292(2)	4065(1)	30(1)
C(12)	2646(2)	3153(2)	6426(1)	33(1)	C(61)	3549(2)	3157(2)	3798(1)	32(1)
C(13)	2340(2)	3668(3)	6843(2)	52(1)	C(62)	2797(2)	3601(2)	3463(1)	38(1)
C(14)	1528(2)	3888(3)	6686(2)	66(1)	C(63)	2746(2)	4658(2)	3398(1)	43(1)
C(15)	1014(2)	3598(3)	6098(2)	56(1)	C(64)	3412(2)	5286(2)	3647(1)	41(1)
C(16)	1280(2)	3085(2)	5656(1)	36(1)	C(65)	4153(2)	4834(2)	3957(1)	39(1)
C(21)	3548(2)	2971(2)	6691(1)	32(1)	C(66)	4238(2)	3782(2)	4038(1)	35(1)
C(22)	3850(2)	2014(2)	6939(1)	34(1)	C(67)	2050(2)	2973(3)	3160(2)	56(1)
C(23)	4676(2)	1907(2)	7269(1)	37(1)	C(68)	3328(2)	6431(2)	3603(2)	54(1)
C(24)	5214(2)	2709(2)	7364(1)	40(1)	C(69)	5072(2)	3360(2)	4374(2)	43(1)
C(25)	4906(2)	3646(2)	7119(1)	39(1)	C(71)	2931(2)	-538(2)	4296(1)	33(1)
C(26)	4081(2)	3804(2)	6795(1)	34(1)	C(72)	2225(2)	-957(2)	3864(2)	41(1)
C(27)	3296(2)	1121(2)	6898(2)	47(1)	C(73)	1891(2)	-1820(2)	4040(2)	50(1)
C(28)	6104(2)	2579(3)	7745(2)	58(1)	C(74)	2258(2)	-2303(2)	4613(2)	51(1)
C(29)	3793(2)	4876(2)	6622(1)	47(1)	C(75)	2963(2)	-1894(2)	5026(2)	45(1)
C(31)	611(2)	2839(2)	5047(1)	34(1)	C(76)	3310(2)	-1012(2)	4882(1)	36(1)

C(32)	433(2)	3512(2)	4532(2)	45(1)	C(77)	1856(2)	-543(3)	3196(2)	55(1)
C(33)	-277(2)	3398(3)	4023(2)	58(1)	C(78)	1908(3)	-3280(3)	4772(2)	76(1)
C(34)	-824(2)	2639(3)	4004(2)	62(1)	C(79)	4080(2)	-601(2)	5344(2)	45(1)
C(35)	-640(2)	1971(3)	4503(2)	56(1)	C(81)	3227(2)	4195(2)	5056(2)	42(1)
C(36)	67(2)	2059(2)	5035(2)	42(1)	C(82)	4431(2)	2174(2)	5640(1)	41(1)
C(37)	992(2)	4377(3)	4531(2)	75(1)	C(9)	572(4)	6307(7)	2393(4)	154(3)
C(38)	-1627(3)	2566(5)	3464(2)	107(2)	Cl(1A)	31(2)	7247(5)	2667(2)	156(2)
C(39)	192(2)	1354(3)	5592(2)	62(1)	Cl(2A)	367(2)	5153(5)	2731(3)	165(2)
C(41)	2070(2)	169(2)	5373(2)	47(1)	Cl(2B)	706(6)	5021(6)	2097(4)	342(7)
C(42)	1096(2)	1343(3)	4036(2)	52(1)	Cl(1B)	238(9)	6278(11)	2893(4)	345(7)
C(51)	3302(1)	1343(2)	4151(1)	28(1)					

Atomic coordinates (x 10^4) and equivalent isotropic displacement parameters ($Å^2$x 10^3) for **41**. U(eq) is defined as one third of the trace of the orthogonalized U^{ij} tensor:

	x	y	z	U(eq)		x	y	z	U(eq)
Ti(1)	2758(2)	83423(2)	2813(2)	23(1)	C(112)	1877(16)	11218(13)	2856(11)	35(5)
O(11)	1991(10)	9382(8)	2473(7)	27(3)	C(113)	1163(19)	11975(14)	3092(14)	49(6)
O(21)	2314(10)	6971(8)	2164(6)	25(3)	C(114)	-69(2)	11685(17)	3172(16)	60(8)
N(31)	2528(13)	8285(10)	3907(8)	30(4)	C(115)	-623(18)	10623(16)	3006(14)	50(7)
N(41)	4501(12)	8840(10)	2961(8)	29(4)	C(116)	3199(16)	11612(12)	2783(10)	32(5)
C(11)	-2109(15)	6631(14)	2158(11)	36(5)	C(117)	3513(19)	11606(14)	1994(11)	41(6)
C(12)	-2947(18)	5543(16)	1931(13)	48(6)	C(118)	2534(2)	11125(19)	1204(13)	59(8)
C(13)	-1652(15)	7085(14)	1546(10)	35(5)	C(119)	4733(2)	12050(15)	1943(14)	49(7)
C(14)	-923(15)	8107(14)	1731(10)	33(5)	C(120)	5653(2)	12497(15)	2650(15)	51(7)
C(15)	-494(18)	8575(15)	1037(11)	42(6)	C(121)	6984(2)	12937(2)	2572(2)	78(12)
C(16)	-631(14)	8697(13)	2565(10)	31(5)	C(122)	5327(19)	12515(14)	3425(14)	47(6)
C(17)	-1074(15)	8248(14)	3196(10)	36(5)	C(123)	4112(17)	12087(13)	3511(11)	37(5)
C(18)	-805(2)	8857(18)	4099(12)	51(7)	C(124)	3800(2)	12143(17)	4369(12)	52(7)
C(19)	-1798(16)	7225(15)	2979(11)	38(6)	C(210)	2774(14)	5232(11)	2082(9)	25(4)
C(21)	1889(2)	4689(15)	4416(11)	42(6)	C(211)	2708(13)	6127(11)	1740(9)	23(4)
C(22)	1584(3)	4371(2)	5204(15)	69(1)	C(212)	3036(15)	6140(12)	954(9)	27(4)
C(23)	3121(18)	4995(15)	4335(10)	40(6)	C(213)	3431(18)	5263(14)	531(10)	37(5)
C(24)	3432(16)	5209(13)	3591(10)	31(5)	C(214)	3495(19)	4378(14)	861(11)	41(6)
C(25)	4798(17)	5460(16)	3521(12)	42(6)	C(215)	3168(17)	4369(12)	1630(10)	34(5)
C(26)	2454(15)	5136(11)	2912(9)	25(4)	C(216)	2959(15)	7052(12)	537(9)	27(4)
C(27)	1199(15)	4858(12)	2990(10)	30(5)	C(217)	1796(15)	7139(13)	99(10)	31(5)
C(28)	136(17)	4773(17)	2272(11)	46(6)	C(218)	616(17)	6368(15)	94(12)	42(6)
C(29)	940(17)	4634(13)	3743(12)	37(5)	C(219)	1759(15)	7915(14)	-368(10)	35(5)
C(31)	3195(2)	9084(17)	4648(12)	51(7)	C(220)	2840(17)	8606(13)	-405(10)	35(5)
C(32)	1693(2)	7436(15)	4118(12)	44(6)	C(221)	2781(2)	9419(16)	-937(12)	47(6)
C(41)	5164(2)	9700(16)	2666(16)	55(8)	C(222)	3979(16)	8517(13)	46(10)	34(5)
C(42)	5372(18)	8366(18)	3452(13)	50(7)	C(223)	4066(15)	7746(13)	513(9)	30(4)
C(110)	44(16)	9828(13)	2766(11)	35(5)	C(224)	5333(16)	7638(15)	955(11)	39(5)
C(111)	1311(15)	10135(12)	2701(10)	30(5)					

Atomic coordinates (x 10^4) and equivalent isotropic displacement parameters ($Å^2$x 10^3) for **42**. U(eq) is defined as one third of the trace of the orthogonalized U^{ij} tensor:

	x	y	z	U(eq)		x	y	z	U(eq)
Zn(1)	3610(1)	5462(1)	4449(1)	30(1)	C(35)	1144(3)	5786(3)	6496(2)	52(1)
Zn(2)	4085(1)	9445(1)	438(1)	42(1)	C(36)	2150(3)	6163(2)	6654(2)	46(1)
O(1)	4944(2)	5825(1)	5025(1)	29(1)	C(41)	3803(3)	11358(2)	719(2)	34(1)
O(2)	4276(2)	10708(1)	230(1)	34(1)	C(42)	2934(5)	8660(3)	1018(3)	70(1)
C(1)	4646(3)	6677(2)	5262(2)	27(1)	C(43)	3068(6)	8251(4)	2035(3)	88(2)
C(2)	1779(3)	6088(2)	3714(2)	38(1)	C(44)	3526(3)	10832(2)	1688(2)	29(1)
C(3)	1682(3)	5985(2)	2772(2)	50(1)	C(45)	2179(3)	11034(2)	1970(2)	29(1)
C(4)	5280(3)	6449(2)	6237(2)	26(1)	C(46)	2001(3)	10534(2)	2883(2)	29(1)
C(5)	6392(3)	6757(2)	6409(2)	26(1)	C(47)	3120(3)	9831(2)	3532(2)	29(1)
C(6)	6783(3)	6643(2)	7321(2)	28(1)	C(48)	4453(3)	9621(2)	3239(2)	31(1)
C(7)	6139(3)	6225(2)	8064(2)	29(1)	C(49)	4665(3)	10106(2)	2339(2)	31(1)
C(8)	5093(3)	5877(2)	7893(2)	30(1)	C(51)	898(3)	11773(2)	1334(2)	32(1)
C(9)	4673(3)	5982(2)	6996(2)	28(1)	C(52)	558(3)	11753(2)	474(2)	39(1)
C(11)	7158(3)	7215(2)	5662(2)	25(1)	C(53)	-642(3)	12449(2)	-104(2)	48(1)
C(12)	7639(3)	6814(2)	4986(2)	29(1)	C(54)	-1514(3)	13166(3)	169(2)	53(1)
C(13)	8358(3)	7240(2)	4307(2)	33(1)	C(55)	-1208(3)	13191(2)	1028(2)	49(1)
C(14)	8631(3)	8074(2)	4280(2)	34(1)	C(56)	-15(3)	12496(2)	1611(2)	39(1)
C(15)	8178(3)	8474(2)	4944(2)	31(1)	C(61)	2892(3)	9361(2)	4507(2)	27(1)
C(16)	7457(3)	8045(2)	5635(2)	28(1)	C(62)	1663(3)	9158(2)	4730(2)	30(1)
C(21)	6559(3)	6139(2)	9023(2)	30(1)	C(63)	1428(3)	8791(2)	5648(2)	35(1)
C(22)	5572(3)	6248(2)	9637(2)	37(1)	C(64)	2407(3)	8620(2)	6362(2)	36(1)
C(23)	5961(4)	6187(2)	10524(2)	43(1)	C(65)	3646(3)	8801(2)	6152(2)	34(1)
C(24)	7340(4)	6014(2)	10807(2)	43(1)	C(66)	3884(3)	9160(2)	5235(2)	30(1)
C(25)	8327(3)	5916(2)	10201(2)	40(1)	C(71)	6124(3)	9817(2)	2073(2)	39(1)
C(26)	7946(3)	5973(2)	9318(2)	35(1)	C(72)	6877(4)	10455(3)	1853(2)	58(1)
C(31)	3560(3)	5581(2)	6858(2)	29(1)	C(73)	8229(4)	10156(5)	1614(3)	81(2)
C(32)	3926(3)	4611(2)	6923(2)	32(1)	C(74)	8816(4)	9228(5)	1582(3)	87(2)
C(33)	2900(3)	4247(2)	6755(2)	39(1)	C(75)	8085(4)	8590(4)	1798(2)	74(1)
C(34)	1522(3)	4836(2)	6539(2)	44(1)	C(76)	6748(3)	8882(3)	2050(2)	51(1)

REFERENCE LIST

[1] Cowley, A. H. *J. Organomet. Chem.* **2004**, *689*, 3866-3872.

[2] Oxford English Dictionary, Online Edition. http://dictionary.oed.com (accessed Aug 2006).

[3] (a) Cowley, A. H.; Geerts, R. L.; Nunn, C. M. *J. Am. Chem. Soc.* **1987**, *109*, 6523-6524; (b) Atwood, D. A.; Contreras, L.; Cowley, A. H.; Jones, R. A.; Mardones, M. A. *Organometallics*, **1993**, *12*, 17-18; (c) Cowley, A. H.; Gabbaï, F. P.; Isom, H. S.; Decken, A. *J. Organomet. Chem.* **1995**, *500*, 81-88.

[4] Lewis acid stabilization has recently been reported. See: Vidovic, D.; Moore, J. A.; Jones, J. N.; Cowley, A. H. *J. Am. Chem. Soc.* **2005**, *127*, 4566-4567;

[5] (a) Arduengo, A. J., III.; Dias, H. V. R.; Harlow, R. L.; Kline, M. *J. Am. Chem. Soc.* **1992**, *114*, 5530-5534; (b) Dixon, D. A.; Arduengo, A. J., III. *J. Phys. Chem.* **1991**, *95*, 4180-4182; (c) Izod, K.; McFarlane, W.; Tyson, B. V.; Carr, I.; Clegg, W.; Harrington, R. W. *Organometallics*, **2006**, *25*, 1135-1143.

[6] Burford, N.; Clyburne, J. A. C.; Chan, M. S. W. *Inorg. Chem.* **1997,** *36,* 3204-3206; and references therein.

[7] Laing, M. *J. Chem. Ed.* **2001**, *78*, 1400-1405.

[8] Power, P. P. *J. Organomet. Chem.* **2004**, *689*, 3904.

[9] Sailaja, S.; Swarnabala, G.; Rajasekharan, M. V. *Acta Crystallogr., Sect. C*, **2001**, *C57*, 1162-1165.

[10] (a) Dasgupta, T. P.; Aquart, D. V. Metal-NO complexes: Structures, Syntheses, Properties and NO-releasing Mechanisms. In *Nitric Oxide Donors: For Pharmaceutical and Biological Applications*; Wang, P. G., Cai, T. B., Taniguchi, N., Eds; Wiley-VCH: New York, 2005; pp 109-129; (b) Praneeth, V. K. K.; Näther, C.; Peters, G.; Lehnert, N. *Inorg. Chem.* **2006**, *45*, 2795-2811.

[11] Burck, S.; Daniels, J.; Gans-Eichler, T.; Gudat, D.; Nättinen, K.; Nieger, M. *Z. Anorg. Allg. Chem.* **2005**, *631*, 1403-1412.

[12] Chaumonnot, A.; Donnadieu, B.; Sabo-Etienne, S.; Chaudret, B.; Buron, C.; Bertrand, G.; Metivier, P. *Organometallics*, **2001**, *20*, 5614-5618; and references therein.

[13] Winter, A. M.; Eichele, K.; Mack, H.-G.; Kaska, W. C.; Mayer, H. A. *Organometallics*, **2005**, *24*, 1837-1844.

[14] Quin, L. D. A Guide to Organophosphorus Chemistry; Wiley & Sons: Toronto, 2000; Chapter 3.

[15] (a) Christmann, U.; Vilar, R. *Angew. Chem. Int. Ed.* **2005**, *44*, 366-374; (b) Miura, M. *Angew. Chem. Int. Ed.* **2004**, *43*, 2201-2203.

[16] Hansen, L. M.; Marynick, D. S. *Organometallics*, **1989**, *8*, 2173-2179.

[17] (a) Grubbs, R. H. *Tetrahedron*, **2004**, *60*, 7117-7140; (b) Strieter, E. R.; Blackmond, D. G.; Buchwald, S. L. *J. Am. Chem. Soc.* **2003**, *125*, 13978-13980; (c) Clarke, M. L.; Heydt, M. *Organometallics*, **2005**, *24*, 6475-6478.

[18] (a) Möhring, P. C.; Coville, N. J. *Coord. Chem. Rev.* **2006**, *250*, 18-35; (b) Smith, J. M.; Pelly, S. C.; Coville, N. J. *J. Organomet. Chem.* **1996**, *525*, 159-166; (c) Coville, N. J.; du Plooy, K. E.; Pickl, W. *Coord. Chem. Rev.* **1992**, *116*, 1-267.

[19] Boeré, R. T.; Zhang, Y. *J. Organomet. Chem.* **2005**, *690*, 2651-2657.

[20] (a) Tolman, C. A. *J. Am. Chem. Soc.* **1970**, *92*, 2956-2965; (b) Tolman, C. A. *Chem. Rev.* **1977**, 77, 313-348.

[21] (a) Smith, J. M.; Taverner, B. C.; Coville, N. J. *J. Organomet. Chem.* **1997**, *530*, 131-140. (b) Ferguson, G.; Roberts, P. J.; Alyea, E. C.; Khan, M. *Inorg. Chem.* **1978**, *17*, 2965-2967.

[22] Kim, W.-K.; Fevola, M. J.; Liable-Sands, L. M.; Rheingold, A. L.; Theopold, K. H. *Organometallics*, **1998**, *17*, 4541-4543.

[23] Bourget-Merle, L.; Lappert, M. F.; Severn, J. R. *Chem. Rev.* **2002**, *102*, 3031-3065.

[24] (a) Pineda, L. W.; Jancik, V.; Starke, K.; Oswald, R. B.; Roesky, H. W. *Angew. Chem. Int. Ed.* **2006**, *45*, 2602-2605; (b) Hill, M. S.; Hitchcock, P. B.; Pongtavornpinyo, R. *Science*, **2006**, *311*, 1904-1907.

[25] (a) Hamaki, H.; Takeda, N.; Tokitoh, N. *Organometallics*, **2006**, *25*, 2457-2464; (b) Bai, G.; Wei, P.; Stephan, D. W. *Organometallics*, **2006**, *25*, 2649-2655.

[26] (a) York, J. T.; Young, V. G., Jr.; Tolman, W. B. *Inorg. Chem.* **2006**, *45*, 4191-4198; (b) Bai, G.; Wei, P.; Das, A. K.; Stephan, D. W. *Dalton Trans.* **2006**, 1141-1146.

[27] (a) Yao, Y.; Xue, M.; Luo, Y.; Zhang, Z.; Jiao, R.; Zhang, Y.; Shen, Q.; Wong, W.; Yu, K.; Sun, J. *J. Organomet. Chem.* **2003**, *678*, 108-116; (b) Yao, Y; Zhang, Z.; Peng, H.; Zhang, Y.; Shen, Q.; Lin, J. *Inorg. Chem.* **2006**, *45*, 2175-2183.

[28] Wright, R. J.; Power, P. P.; Scott, B. L.; Kiplinger, J. L. *Organometallics*, **2004**, *23*, 4801-4803.

[29] Carbenes are also known to bind "abnormally" through the alkeneic carbon, rather than the carbeneic carbon. For examples, see: (a) Kovacevic, A.; Gründemann, S.; Miecznikowski, J. R.; Clot, E.; Eisenstein, O.; Crabtree, R. H. *Chem. Commun.* **2002**, 2580-2581; (b) Gründemann, S.; Kovacevic, A.; Albrecht, M.; Faller, J. W.; Crabtree, R. H. *J. Am. Chem. Soc.* **2002**, *124*, 10473-10481; (c) Hu, X.; Castro-Rodriguez, I.; Meyer, K. *J. Am. Chem. Soc.* **2003**, *125*, 12237-12245; (d) Lebel, H.; Janes, M. K.; Charette, A. B.; Nolan, S. P. *J. Am. Chem. Soc.* **2004**, *126*, 5046-5047; (e) Chianese, A. R.; Kovacevic, A.; Zeglis, B. M.; Faller, J. W.;

Crabtree, R. H. *Organometallics*, **2004**, *23*, 2461-2468; (f) Graham, T. W.; Udachin, K. A.; Carty, A. J. *Chem. Commun.* **2006**, 2699-2701.

[30] (a) Herrmann, W. A. *Angew. Chem. Int. Ed.* **2002**, *41*, 1290-1309; (b) Crabtree, R. H. *J. Organomet. Chem.* **2005**, *690*, 5451-5457.

[31] (a) Gallivan, J. P.; Jordan, J. P.; Grubbs, R. H. *Tetrahedron Lett.* **2005**, *46*, 2577-2580. (b) Straub, B. F. *Angew. Chem. Int. Ed.* **2005**, *44*, 5974-5978.

[32] (a) Dorta, R.; Stevens, E. D.; Scott, N. M.; Costabile, C.; Cavallo, L.; Hoff, C. D.; Nolan, S. P. *J. Am. Chem. Soc.* **2005**, *127*, 2485-2495; (b) Hillier, A. C.; Sommer, W. J.; Yong, B. S.; Petersen, J. L.; Cavallo, L.; Nolan, S. P. *Organometallics*, **2003**, *22*, 4322-4326.

[33] Du, C.-J. F.; Hart, H.; Ng, K.-K. D. *J. Org. Chem.* **1986**, *51*, 3162-3165.

[34] Schiemenz, B.; Power, P. P. *Organometallics*, **1996**, *15*, 958-964.

[35] Saednya, A.; Hart, H. *Synthesis*, **1996**, 1455-1457.

[36] (a) Hino, S.; Olmstead, M. M.; Fettinger, J. C.; Power, P. P. *J. Organomet. Chem.* **2005**, *690*, 1638-1644; (b) Wright, R. J.; Steiner, J.; Beaini, S.; Power, P. P. *Inorg. Chim. Acta*, **2006**, *359*, 1939-1946; (c) Gupta, H. K.; Reginato, N.; Ogini, F. O.; Brydges, S.; McGlinchey, M. J. *Can. J. Chem.* **2002**, *80*, 1546-1554.

[37] (a) Elmorsy, S. S.; Pelter, A.; Smith, K. *Tetrahedron Lett.* **1991**, *32*, 4175-4176; (b) Kotha, S.; Kashinath, D.; Lahiri, K.; Sunoj, R. B. *Eur. J. Org. Chem.* **2004**, 4003-4013; (c) Li, Z.; Sun, W.-H.; Jin, X.; Shao, C. *Synlett*, **2001**, 1947-1949.

[38] (a) Kohler, E. P.; Blanchard, L. W., Jr. *J. Am. Chem. Soc.* **1935**, *57*, 367-371; (b) Shafig, Y. F. E-d.; Taylor, R. *J. Chem. Soc., Perkin Trans. 2*, **1978**, 1263-1267.

[39] Liu, J.-K. *Chem. Rev.* **2006**, *106*, 2209-2223.

[40] Srinivasan, K.; Rajakumar, P. *Synthesis* **2005**, 2772-2776.

[41] Camacho, D. H.; Salo, E. V.; Guan, Z. *Org. Lett.* **2004**, *6*, 865-868.

[42] Rajakumar, P.; Swaroop, M. G. *Tetrahedron Lett.* **2004**, *45*, 6165-6167.

[43] Rajakumar, P.; Senthilkumar, B.; Srinivasan, K. *Aust. J. Chem.* **2006**, *59*, 75-77.

[44] Shen, D.; Diele, S.; Pelzl, G.; Wirth, I.; Tschierske, C. *J. Mater. Chem.* **1999**, *9*, 661-672.

[45] (a) Rajakumar, P.; Ganesan, K. *Tetrahedron: Asymmetry*, **2005**, *16*, 2295-2298; (b) Rajakumar, P.; Srinivasan, K.; Periyasami, G. *J. Chem. Res.* **2005**, 135-137.

[46] Rajakumar, P.; Srinivasan, K. *Tetrahedron*, **2004**, *60*, 10285-10291

[47] Rajakumar, P.; Ganesan, K.; Jayavelu, S.; Murugesan, K. *Synthesis*, **2006**, 528-532.

[48] Rajakumar, P.; Ganesan, K. *Synlett*, **2004**, 2236-2238.

[49] Goto, K.; Yamamoto, G.; Tan, B.; Okazaki, R. *Tetrahedron Lett.* **2001**, *42*, 4875-4877.

[50] Riddle, J. A.; Bollinger, J. C.; Lee, D. *Angew. Chem. Int. Ed.* **2005**, *44*, 6689-6693.

[51] Toyota, S.; Yanagihara, T.; Yoshida, Y.; Goichi, M. *Bull. Chem. Soc. Jpn.* **2005**, *78,* 1351-1353.

[52] Gudimetla, V. B.; Rheingold, A. L.; Payton, J. L.; Peng, H.-L.; Simpson, M. C.; Protasiewicz, J. D. *Inorg. Chem.* **2006**, *45*, 4895-4901.

[53] Lüning, U.; Baumgartner, H.; Manthey, C.; Meynhardt, B. *J. Org. Chem.* **1996**, *61*, 7922-7926.

[54] Karastatiris, P.; Mikroyannidis, J. A.; Spiliopoulos, I. K.; Fakis, M.; Persephonis, P. *J. Polym. Sci., Part A: Polym. Chem.* **2004**, *42*, 2214-2224.

[55] Smith, R. C.; Protasiewicz, J. D. *Eur. J. Inorg. Chem.* **2004**, 998-1006.

[56] Smith, R. C.; Protasiewicz, J. D. *J. Am. Chem. Soc.* **2004**, *126*, 2268-2269.

[57] Dutan, C.; Shah, S.; Smith, R. C.; Choua, S.; Berclaz, T.; Geoffroy, M.; Protasiewicz, J. D. *Inorg. Chem.* **2003**, *42*, 6241-6251.

[58] (a) Twamley, B.; Haubrich, S. T.; Power, P. P. *Adv. Organomet. Chem.* **1999**, *44*, 1-65; (b) Clyburne, J. A. C.; McMullen, N. *Coord. Chem. Rev.* **2000**, *210*, 73-99.

[59] Matsumoto, K.; Hatano, K.; Umezawa, N.; Higuchi, T. *Synthesis*, **2004**, 2181-2185.

[60] Smith, R. C.; Protasiewicz, J. D. *Organometallics*, **2004**, *23*, 4215-4222.

[61] (a) Ohzu, Y.; Goto, K.; Sato, H.; Kawashima, T. *J. Organomet. Chem.* **2005**, *690*, 4175-4183; (b) Niyomura, O.; Tokunaga, M.; Obora, Y.; Iwasawa, T.; Tsuji, Y. *Angew. Chem. Int. Ed.* **2003**, *42*, 1287-1289.

[62] Goto, K.; Shimo, I.; Kawashima, T. *Bull. Chem. Soc. Jpn.* **2003,** *76*, 2389–2394.

[63] (a) Schrock, R. R. *Acc. Chem. Res.* **2005**, *38*, 955-962; (b) Schrock, R. R. *Phil. Trans. R. Soc. A*, **2005**, *363*, 959-969; (c) Yandulov, D. V.; Schrock, R. R. *Can. J. Chem.* **2005**, *83*, 341-357; (d) Ritleng, V.; Yandulov, D. V.; Weare, W. W.; Schrock, R. R.; Hock, A. S.; Davis, W. M. *J. Am. Chem. Soc.* **2004**, *126*, 6150-6163.

[64] (a) Maekawa, M.; Suenaga, Y.; Kuroda-Sowa, T.; Munakata, M. *Inorg. Chim. Acta*, **2004,** *357*, 331-338; (b) Masuhara, N.; Kamigaki, Y.; Nakashima, S.; Okuda, T. *Polyhedron*, **2005**, *24*, 1798-1802.

[65] (a) Bishop, P. T.; Dilworth, J. R.; Zubieta, J. A. *J. Chem. Soc., Chem. Commun.* **1985**, 257-259; (b) Quignard, F.; Leconte, M.; Basset, J.-M. *J. Chem. Soc., Chem. Commun.* **1985**, 1816-1817.

[66] Lingnau, R.; Strähle, J. *Angew. Chem. Int. Ed. Engl.* **1988**, *27*, 436.

[67] Haaland, A.; Rypdal, K.; Verne, H. P.; Scherer, W.; Thiel, W. R. *Angew. Chem. Int. Ed. Engl.* **1994**, *33*, 2443-2445.

[68] Hope, H.; Pestana, D. C.; Power, P. P *Angew. Chem. Int. Ed. Engl.* **1991**, *30*, 691-693.

[69] Borman, S. *Chem. Eng. News* **2005**, *83* (51), 15-20.

[70] Nguyen, T.; Sutton, A. D.; Brynda, M.; Fettinger, J. C.; Long, G. J.; Power, P. P. *Science*, **2005**, *310*, 844-847.

[71] Cotton, F. A.; Curtis, N. F.; Harris, C. B.; Johnson, B. F. G.; Lippard, S. J.; Mague, J. T.; Robinson, W. R.; Wood, J. S. *Science*, **1964**, *145*, 1305-1307.

[72] (a) Brynda, M.; Gagliardi, L.; Widmark, P.-O.; Power, P. P.; Roos, B. O. *Angew. Chem. Int. Ed.* **2006**, *45*, 3804-3807; (b) Frenking, G. *Science*, **2005**, *310*, 796-797; (c) Radius, U.; Breher, F. *Angew. Chem. Int. Ed.* **2006**, *45*, 3006-3010; (d) Landis, C. R.; Weinhold, F. *J. Am. Chem. Soc.* **2006**, *128*, 7335-7345.

[73] Norman, N. C. *Polyhedron*, **1993**, *12*, 2431-2446.

[74] (a) Power, P. P. *Chem. Rev.* **1999**, *99*, 3463-3503; (b) Jutzi, P. *Angew. Chem. Int. Ed.* **2000**, *39*, 3797-3800. (c) Escudie, J.; Ranaivonjatovo, H. *Adv. Organomet. Chem.* **1999**, *44*, 113-174.

[75] Filippou, A. C.; Philippopoulos, A. I.; Schnakenburg, G. *Organometallics*, **2003**, *22*, 3339-3341; and references therein.

[76] (a) Power, P. P. *Chem. Commun.* **2003**, 2091-2101; (b) Pu, L.; Phillips, A. D.; Richards, A. F.; Stender, M.; Simons, R. S.; Olmstead, M. M.; Power, P. P. *J. Am. Chem. Soc.* **2003**, *125*, 11626-11636.

[77] Cui, C.; Olmstead, M. M.; Fettinger, J. C.; Spikes, G. H.; Power, P. P. *J. Am. Chem. Soc.* **2005**, *127*, 17530-17541; and references therein.

[78] Spikes, G. H.; Fettinger, J. C.; Power, P. P. *J. Am.Chem. Soc.* **2005**, *127*, 12232-12233.

[79] Pettinari, C.; Marchetti, F.; Martini, D. Metal Complexes as Hydrogenation Catalysts. In *Comprehensive Coordination Chemistry II: From Biology to Nanotechnology*; McCleverty, J. A., Meyer, T. J., Ward, M. D., Eds.; Elsevier: New York, 2004; Vol. 9, pp 75-139.

[80] Hino, S.; Brynda, M.; Phillips, A. D.; Power, P. P. *Angew. Chem. Int. Ed.* **2004**, *43*, 2655-2658.

[81] Haubrich, S. T.; Power, P. P. *J. Am. Chem. Soc.* **1998**, *120*, 2202-2203.

[82] Niemeyer, M.; Power, P. P. *Angew. Chem. Int. Ed.* **1998**, *37*, 1277-1279.

[83] Hardman, N. J.; Wright, R. J.; Phillips, A. D.; Power, P. P. *J. Am. Chem. Soc.* **2003**, *125*, 2667-2679.

[84] Eichler, B. E.; Hardman, N. J.; Power, P. P. *Angew. Chem. Int. Ed.* **2000**, *39*, 383-385.

[85] Young, J. D.; Khan, M. A.; Wehmschulte, R. J. *Organometallics*, **2004**, *23*, 1965-1967.

[86] Wehmschulte, R. J.; Steele, J. M.; Young, J. D.; Khan, M. A. *J. Am. Chem. Soc.* **2003**, *125*, 1470-1471.

[87] Steffey, B. D.; Chamberlain, L. R.; Chesnut, R. W.; Chebi, D. E.; Fanwick, P. E.; Rothwell, I. P. *Organometallics*, **1989**, *8*, 1419-1423.

[88] Vilardo, J. S.; Lockwood, M. A.; Hanson, L. G.; Clark, J. R.; Parkin, B. C.; Fanwick, P. E.; Rothwell, I. P. *J. Chem. Soc., Dalton Trans.* **1997**, 3353-3362.

[89] Diaz, A. A.; Young, J. D.; Khan, M. A.; Wehmschulte, R. J. *Inorg. Chem.* **2006**, *45*, 5568-5575.

[90] There are exceptions to monodentate coordination. For example: Niemeyer, M. *Organometallics*, **1998**, *17*, 4649-4656.

[91] (a) Deacon, G. B.; Phillips, R. J. *Coord. Chem. Rev.* **1980**, *33*, 227-250; (b) Robert, V.; Lemercier, G. *J. Am. Chem. Soc.* **2006**, *128*, 1183-1187.

[92] (a) Rardin, R. L.; Bino, A.; Poganiuch, P.; Tolman, W. B.; Liu, S.; Lippard, S. J. *Angew. Chem. Int. Ed. Engl.* **1990**, *29*, 812-814; (b) Rardin, R. L.; Tolman, W. B.; Lippard, S. J. *New. J. Chem.* **1991**, *15*, 417-430.

[93] (a) Lee, D.; Lippard, S. J. *J. Am. Chem. Soc.* **1998**, *120*, 12153-12154; (b) Hagadorn, J. R.; Que, L., Jr.; Tolman, W. B. *J. Am. Chem. Soc.* **1998**, *120*, 13531-13532.

[94] He, C.; Mishina, Y. *Curr. Op. Chem. Biol.* **2004**, *8*, 201-208.

[95] (a) Tshuva, E. Y.; Lippard, S. J. *Chem. Rev.* **2004**, *104*, 987-1012; and references therein; (b) Yoon, S.; Lippard, S. J. *J. Am. Chem. Soc.* **2004**, *126*, 2666-2667; (c) Lee, D.; Lippard, S. J. Nonheme Di-iron Enzymes. In *Comprehensive Coordination Chemistry II: From Biology to Nanotechnology*; McCleverty, J. A., Meyer, T. J., Que, L., Jr., Tolman, W. B., Eds.; Elsevier: New York, 2004; Vol. 8, pp 309-342. (d) Carson, E. C.; Lippard, S. J. *Inorg. Chem.* **2006**, *45*, 828-836.

[96] (a) Hagadorn, J. R.; Zahn, T. I.; Que, L., Jr.; Tolman, W. B. *Dalton Trans.* **2003**, 1790-1794; (b) Chavez, F. A.; Que, L., Jr.; Tolman, W. B. *Chem. Commun.* **2001**, 111-112.

[97] Mukhopadhyay, S.; Gandhi, B. A.; Kirk, M. L.; Armstrong, W. H. *Inorg. Chem.* **2003**, *42*, 8171-8180.

[98] Ives, C.; Fillis, E. L.; Hagadorn, J. R. *Dalton Trans.* **2003**, 527-531.

[99] Asanuma, T.; Shiomura, T.; Uchikawa, N.; Sasaki, T.; Inoue, T. (Mitsui Toatsu Chemicals Inc.). EP 0 419 677 A1, 1990.

[100] For reviews of amidine coordination chemistry, see: (a) Barker, J.; Kilner, M. *Coord. Chem. Rev.* **1994**, *133*, 219-300; (b) Edelmann, F. T. *Coord. Chem. Rev.* **1994**, *137*, 403-481.

[101] Schmidt, J. A. R.; Arnold, J. *Organometallics*, **2002**, *21*, 2306-2313.

[102] (a) Abeysekera, D.; Robertson, K. N.; Cameron, T. S.; Clyburne, J. A. C. *Organometallics*, **2001**, *20*, 5532-5536; (b) Jenkins, H. A.; Abeysekera, D.; Dickie, D. A.; Clyburne, J. A. C. *J. Chem. Soc., Dalton Trans.* **2002**, 3919-3922.

[103] (a) Schmidt, J. A. R.; Arnold, J. *Chem. Commun.* **1999**, 2149-2150; (b) Schmidt, J. A. R.; Arnold, J. *J. Chem. Soc., Dalton Trans.* **2002**, 3454-3461.

[104] (a) Dagorne, S.; Jordan, R. F.; Young, V. G., Jr. *Organometallics*, **1999**, *18*, 4619-4623; (b) Zhou, Y.; Richeson, D. S. *Inorg. Chem.* **1996**, *35*, 2448-2451; (c) Zhou, Y.; Richeson, D. S. *Inorg. Chem.* **1997**, *36*, 501-504.

[105] *m*-Terphenyls have recently been used as nitrogen substituents for isoelectronic triazenido ligands. Hauber, S.-O.; Niemeyer, M. *Inorg. Chem.* **2005**, *44*, 8644-8646.

[106] Talarico, G.; Budzelaar, P. H. M. *Organometallics*, **2000**, *19*, 5691-5695.

[107] (a) Redshaw, C.; Elsegood, M. R. J. *Chem. Commun.* **2001**, 2016-2017; (b) Lewiński, J.; Zachara, J.; Justyniak, I. *Inorg. Chem.* **1998**, *37*, 2575-2577.

[108] Mehrotra, R. C.; Rai, A. K. *Polyhedron*, **1991**, *10*, 1967-1994; and references therein.

[109] Greber, G.; Egle, G. *Makromol. Chem.* **1960**, *40*, 1-15.

[110] Al-Wassil, A.-A. I.; Hitchcock, P. B.; Sarisaban, S.; Smith, J. D.; Wilson, C. L. *J. Chem. Soc., Dalton Trans.* **1985**, 1929-1934.

[111] (a) Bethley, C. E.; Aitken, C. L.; Harlan, C. J.; Koide, Y.; Bott, S. G.; Barron, A.R. *Organometallics*, **1997**, *16*, 329-341; (b) Branch, C. S.; Lewinski, J.; Justyniak, I.; Bott, S. G.; Lipkowski, J.; Barron, A. R. *J. Chem. Soc., Dalton Trans.* **2001**, 1253-1258; (c) Fischbach, A.; Perdih, F.; Herdtweck, E.; Anwander, R. *Organometallics*, **2006**, *25*, 1626-1642.

[112] CSD version 5.27 (November 2005 + 2 updates) See: Allen, F. H. *Acta. Cryst., Sect. B,* **2002**, *58*, 380-388.

[113] Archibald, S. J. Zinc. In *Comprehensive Coordination Chemistry II: From Biology to Nanotechnology*; McCleverty, J. A., Meyer, T. J., Fenton, D. E., Eds.; Elsevier: New York, 2004; Vol. 6, pp 1147-1251.

[114] Chinn, M. S.; Chen, J. *Inorg. Chem.* **1995**, *34*, 6080-6084; and references therein.

[115] Stępień, M.; Latos-Grażyński, L. *Inorg. Chem.* **2003**, *42*, 6183-6193; and references therein.

[116] Çetinkaya, B.; Gümrükçü, I.; Lappert, M. F.; Atwood, J. L.; Rogers, R. D.; Zaworotko, M. J. *J. Am. Chem. Soc.* **1980**, *102*, 2088-2089.

[117] Arduengo, A. J., III; Harlow, R. L.; Kline, M. *J. Am. Chem. Soc.* **1991**, *113*, 361-363.

[118] (a) Donaldson, J. D.; Jelen, A. *J. Chem. Soc. A*, **1968**, 1448-1450; (b) Donaldson, J. D.; Jelen, A. *J. Chem. Soc. A*, **1968**, 2244-2248; (c) Parr, J. Germanium, Tin, and Lead. In *Comprehensive Coordination Chemistry II: From Biology to Nanotechnology*; McCleverty, J. A., Meyer, T. J., Parkin, G. F. R., Eds.; Elsevier: New York, 2004; Vol. 3, pp 545-608.

[119] Wu, J.; Yu, T.-L.; Chen, C.-T.; Lin, C.-C. *Coord. Chem. Rev.* **2006**, *250*, 602-626.

[120] Hamilton, D. G.; Hawkins, C. M. (General Electric). EP 0 644 223 A2, 1994.

[121] Deacon, P. R.; Mahon, M. F.; Molloy, K. C.; Waterfield, P. C. *J. Chem. Soc., Dalton Trans.* **1997**, 3705-3712.

[122] (a) Neto, J. L.; de Lima, G. M.; Porto, A. O.; Ardisson, J. D.; Doriguetto, A. C.; Ellena, J. *J. Mol. Struct.* **2006**, *782*, 110-115; (b) Dewan, J. C.; Silver, J.; Andrews, R. H.; Donaldson, J. D.; Laughlin, D. R. *J. Chem. Soc., Dalton Trans.* **1977**, 368-371; (c) Harrison, P. G.; Thornton, E. W. *J. Chem. Soc., Dalton Trans.* **1978**, 1274-1278; (d) Donaldson, J. D.; Grimes, S. M.; Nicolaides, A.; Smith, P. J. *Polyhedron*, **1985**, *4*, 391-394; (e) Jelen, A.; Lindqvist, O. *Acta Chem. Scand.* **1969**, *23*, 3071-3080.

[123] (a) Arifin, Z.; Filmore, E. J.; Donaldson, J. D.; Grimes, S. M. *J. Chem. Soc., Dalton Trans.* **1984**, 1965-1968; (b) Donaldson, J. D.; Donoghue, M. T.; Smith, C. H. *Acta Crystallogr., Sect. B*, **1976**, *32*, 2098-2101; (c) Natarajan, S. *J. Solid State Chem.* **1998**, *139*, 200-203; (d) Ayyappan, S.; Cheetham, A. K.; Natarajan, S.; Rao, C. N. R. *Chem. Mater.* **1998**, *10*, 3746-3755; (e) Natarajan, S.; Vaidhyanathan, R.; Rao, C. N. R.; Ayyappan, S.; Cheetham, A. K. *Chem. Mater.* **1999**, *11*, 1633-1639; (f) Adair, B.; Natarajan, S.; Cheetham, A. K. *J. Mater. Chem.* **1998**, *8*, 1477-1479; (g) Stock, N.; Stucky, G. D.; Cheetham, A. K. *Chem. Commun.* **2000**, 2277-2278; (h) Salami, T. O.; Marouchkin, K.; Zavilij, P. Y.; Oliver, S. R. J. *Chem. Mater.* **2002**, *14*, 4851-4857; (i) Christie, A. D.; Howie, R. A.; Moser, W. *Inorg. Chim. Acta*, **1979**, *36*, L447-448; (j) Gleizes, A.; Galy, J. *J. Solid State Chem.* **1979**, *30*, 23-33.

[124] (a) Dewan, J. C.; Silver, J.; Donaldson, J. D.; Thomas, M. J. K. *J. Chem. Soc., Dalton Trans.* **1977**, 2319-2322; (b) Clark, S. J.; Donaldson, J. D.; Dewan, J. C.; Silver, J. *Acta Crystallogr., Sect. B*, **1979**, *35*, 2550-2553; (c) van Remoortere, F. P.; Flynn, J. J.; Boer, F. P.; North, P. P. *Inorg. Chem.* **1971**, *10*, 1511-1518; (d) Dewan, J. C. *Acta Crystallogr., Sect. B*, **1980**, *36*, 1935-1937; (e) Clark, A. M.; Rickard, C. E. F.; Roper, W. R.; Woodman, T. J.; Wright, L. J. *Organometallics*, **2000**, *19*, 1766-1774; (f) Donaldson, J. D.; Grimes, S. M.; Calogero, S.; Russo, U.; Valle, G.; Smith, P. J. *Inorg. Chim. Acta*, **1984**, *84*, 173-177.

[125] (a) Prabusankar, G.; Murugavel, R. *Organometallics*, **2004**, *23*, 5644-5647; and references therein; (b) Yang, S.-Y.; Xie, Z.-X.; Ng, S. W. *Acta Crystallogr., Sect. C*, **2004**, *60*, m123-m125; (c) Faggiani, R.; Johnson, J. P.; Brown, I. D.; Birchall, T. *Acta Crystallogr., Sect. B*, **1978**, *34*, 3742-3743; (d) Dietzel, S.; Jurkschat, K.; Tzschach, A.; Zschunke, A. *Z. Anorg. Allg. Chem.* **1986**, *537*, 163-168.

[126] (a) Wrackmeyer, B. Germanium, Tin and Lead NMR. In *Encyclopedia of Nuclear Magnetic Resonance*; Grant, D. M., Harris, R. K., Eds.; Wiley & Sons: New York, 1996; Vol. 4, pp. 2206-2215; (b) Wrackmeyer, B. Applications of ^{119}Sn NMR Parameters. In *Annual Reports on NMR Spectroscopy*; Webb, G. A., Ed.; Academic Press: New York, 1999; Vol. 38, pp. 203-264.

[127] Eichler, B. E.; Phillips, B. L.; Power, P. P.; Augustine, M. P. *Inorg. Chem.* **2000**, *39*, 5450-5453.

[128] Harrison, P. G. Compounds of tin: general trends. In *Chemistry of Tin, 2nd Edition*; Smith, P. J., Ed.; Chapman & Hall: New York, 1998; pp 10-61.

[129] Ruhlandt-Senge, K.; Bartlett, R. A.; Olmstead, M. M.; Power, P. P. *Angew. Chem. Int. Ed. Engl.* **1993**, *32*, 425-427; and references therein.

[130] (a) Foley, S. R.; Zhou, Y.; Yap, G. P. A.; Richeson, D. *Inorg. Chem.* **2000**, *39*, 924-929; (b) Hitchcock, P. B.; Hu, J.; Lappert, M. F.; Severn, J. R. *Dalton Trans.* **2004**, 4193-4201; (c) Hitchcock, P. B.; Lappert, M. F.; Lawless, G. A.; de Lima, G. M.; Pierssens, L. J.-M. *J. Organomet. Chem.* **2000**, *601*, 142-146; (d) Boyle, T. J.; Segall, J. M.; Alam, T. M.; Rodriguez, M. A.; Santana, J. M. *J. Am. Chem.*

Soc. **2002**, *124*, 6904-6913; (e) McGeary, M. J.; Folting, K.; Caulton, K. G. *Inorg. Chem.* **1989**, *28*, 4051-4053.

[131] (a) Bandoli, G.; Clemente, D. A.; Panattoni, C. *J. Chem. Soc. D.* **1971**, 311-312; (b) Faggiani, R.; Johnson, J. P.; Brown, I. D.; Birchall, T. *Acta Crystallogr., Sect. B*, **1978**, *34*, 3742-3743; (c) Faggiani, R.; Johnson, J. P.; Brown, I. D.; Birchall, T. *Acta Crystallogr., Sect. B*, **1979**, *35*, 1227-1229; (d) Birchall, T.; Johnson, J. P. *Can. J. Chem.* **1982**, *60*, 934-938; (e) Adams, S.; Dräger, M.; Mathiasch, B. *J. Organomet. Chem.* **1987**, *326*, 173-186.

[132] (a) Chen, E. Y.-X.; Marks, T. J. *Chem. Rev.* **2000**, *100*, 1391-1434; (b) Klosin, J.; Roof, G. R.; Chen, E. Y.-X.; Abboud, K. A. *Organometallics*, **2000**, *19*, 4684-4686; (c) Walker, D. A.; Woodman, T. J.; Schormann, M.; Hughes, D. L.; Bochmann, M. *Organometallics*, **2003**, *22*, 797-803.

[133] Kemp, R. A.; Chen, L.; Guzei, I.; Rheingold, A. L. *J. Organomet. Chem.* **2000**, *596*, 70-76.

[134] Bergquist, C.; Bridgewater, B. M.; Harlan, C. J.; Norton, J. R.; Friesner, R. A.; Parkin, G. *J. Am. Chem. Soc.* **2000**, *122*, 10581-10590.

[135] Doerrer, L. H.; Green, M. L. H. *J. Chem. Soc., Dalton Trans.* **1999**, 4325-4329.

[136] Neculai, D.; Roesky, H. W.; Neculai, A. M.; Magull, J.; Walfort, B.; Stalke, D. *Angew. Chem. Int. Ed.* **2002**, *41*, 4294-4296.

[137] Cox, H.; Hitchcock, P. B.; Lappert, M. F.; Pierssens, L. J.-M. *Angew. Chem. Int. Ed.* **2004**, *43*, 4500-4504.

[138] Forster, E. L. *Monatsh. Chem.* **1954**, *85*, 1104-1109.

[139] Sekiguchi, A.; Matsuo, T.; Watanabe, H. *J. Am. Chem. Soc.* **2000**, *122*, 5652-5653.

[140] Niecke, E.; Fuchs, A.; Baumeister, F.; Nieger, M.; Schoeller, W. W. *Angew. Chem. Int. Ed. Engl.* **1995**, *34*, 555-557.

[141] (a) Schoeller, W. W.; Begemann, C.; Niecke, E.; Gudat, D. *J. Phys. Chem. A*, **2001**, *105*, 10731-10738; (b) Schmidt, O.; Fuchs, A.; Gudat, D.; Nieger, M.; Hoffbauer, W.; Niecke, E.; Schoeller, W. W. *Angew. Chem. Int. Ed. Engl.* **1998**, *37*, 949-952.

[142] (a) Scheschkewitz, D.; Amii, H.; Gornitzka, H.; Schoeller, W. W.; Bourissou, D.; Bertrand, G. *Angew. Chem. Int. Ed.* **2004**, *43*, 585-587; (b) Abe, M.; Adam, W.; Borden, W. T.; Hattori, M.; Hrovat, D. A.; Nojima, M.; Nozaki, K.; Wirz, J. *J. Am. Chem. Soc.* **2004**, *126*, 574-582.

[143] Scheschkewitz, D.; Amii, H.; Gornitzka, H.; Schoeller, W. W.; Bourissou, D.; Bertrand, G. *Science*, **2002**, *295*, 1880-1881.

[144] Sugiyama, H.; Ito, S.; Yoshifuji, M. *Angew. Chem. Int. Ed.* **2003**, *42*, 3802-3804.

[145] Seierstad, M.; Kinsinger, C. R.; Cramer, C. J. *Angew. Chem. Int. Ed.* **2002**, *41*, 3894-3896.

[146] Jung, Y.; Head-Gordon, M. *ChemPhysChem*, **2003**, *4*, 522-525.

[147] (a) Wentrup, C. *Science*, **2002**, *295*, 1846-1847; (b) Jung, Y.; Head-Gordon, M. *J. Phys. Chem. A*, **2003**, *107*, 7475-7481.

[148] (a) Cheng, M.-J.; Hu, C.-H. *Mol. Phys.* **2003**, *101*, 1319-1323; (b) Abe, M.; Ishihara, C.; Nojima, M. *J. Org. Chem.* **2003**, *68*, 1618-1621.

[149] Tuononen, H. M.; Suontamo, R.; Valkonen, J.; Laitinen, R. S. *J. Phys. Chem. A*, **2004**, *108*, 5670-5677.

[150] (a) Schoeller, W. W.; Rozhenko, A.; Bourissou, D.; Bertrand, G. *Chem. Eur. J.* **2003**, *9*, 3611-3617; (b) Amii, H.; Vranicar, L.; Gornitzka, H.; Bourissou, D.; Bertrand, G. *J. Am. Chem. Soc.* **2004**, *126*, 1344-1345.

[151] Cui, C.; Brynda, M.; Olmstead, M. M.; Power, P. P. *J. Am. Chem. Soc.* **2004**, *126*, 6510-6511.

[152] (a) Jung, Y.; Brynda, M.; Power, P. P.; Head-Gordon, M. *J. Am. Chem. Soc.* **2006**, *128*, 7185-7192; (b) Sodt, A.; Beran, G. J. O.; Jung, Y.; Austin, B.; Head-Gordon, M. *J. Chem. Theory Comput.* **2006**, *2*, 300-305.

[153] *Gaussian 98* (Revision A.11.3), Frisch, M. J.; Trucks, G. W.; Schlegel, H. B.; Scuseria, G. E.; Robb, M. A.; Cheeseman, J. R.; Zakrzewski, V. G.; Montgomery, J. A.; Stratmann, R. E.; Burant, J. C.; Dapprich, S.; Millam, J. M.; Daniels, A. D.; Kudin, K. N.; Strain, M. C.; Farkas, O.; Tomasi, J.; Barone, V.; Cossi, M.; Cammi, R.; Mennucci, B.; Pomelli, C.; Adamo, C.; Clifford, S.; Ochterski, J.; Petersson, G. A.; Ayala, P. Y.; Cui, Q.; Morokuma, K.; Malick, D. K.; Rabuck, A. D.; Raghavachari, K.; Foresman, J. B.; Cioslowski, J.; Ortiz, J. V.; Stefanov, B. B.; Liu, G.; Liashenko, A.; Piskorz, P.; Komaromi, I.; Gomperts, R.; Martin, R. L.; Fox, D. J.; Keith, T.; Al-Laham, M. A.; Peng, C. Y.; Nanayakkara, A.; Gonzalez, C.; Challacombe, M.; Gill, P. M. W.; Johnson, B. G.; Chen, W.; Wong, M. W.; Andres, J. L.; Head-Gordon, M.; Replogle, E. S.; Pople, J. A. Gaussian, Inc., Pittsburgh, PA, **1998**.

[154] Lappert, M. F.; Misra, M. C.; Onyszchuk, M.; Rowe, R. S.; Power, P. P.; Slade, M. J. *J. Organomet. Chem.* **1987**, *330*, 31-46.

[155] Braunschweig, H.; Chorley, R. W.; Hitchcock, P. B.; Lappert, M. F. *J. Chem. Soc., Chem. Commun.* **1992**, 1311-1313.

[156] (a) Veith, M.; Agustin, D.; Huch, V. *J. Organomet. Chem.* **2002**, *646*, 138-145; (b) Bokii, N. G.; Struchkov, Y. T.; Prokofiev, A. K. *J. Struct. Chem.* **1972**, *13*, 619-623.

[157] Kano, N.; Nakagawa, N.; Shinozaki, Y.; Kawashima, T.; Sato, Y.; Naruse, Y.; Inagaki, S. *Organometallics*, **2005**, *24*, 2823-2826.

[158] Farren, C.; FitzGerald, S.; Bryce, M. R.; Beeby, A.; Batsanov, A. S. *J. Chem. Soc., Perkin Trans. 2*, **2002**, 59-66.

[159] (a) Willeke, R.; Tacke, R.; *Z. Anorg. Allg. Chem.* **2001**, *627*, 1537-1541; (b) Tacke, R.; Heermann, J.; Pülm, M.; Richter, l. *Organometallics*, **1998**, *17*, 1663-1668.

[160] Chen, L.; Xie, Q.; Sun, L.; Wang, H. *J. Organomet. Chem.* **2003**, *678*, 90-94.

[161] (a) Ovchinnikov, Y. E.; Macharashvili, A. A.; Struchkov, Y. T.; Shipov, A. G.; Baukov, Y. I. *J. Struct. Chem.* **1994**, *35*, 91-100; (b) Wagler, J.; Böhme, U.; Brendler, E.; Thomas, B.; Goutal, S.; Mayr, H.; Kempf, B.; Remennikov, G. Y.; Roewer, G. *Inorg. Chim. Acta*, **2005**, *358*, 4270-4286.

[162] (a) Gallasch, D. P.; Tiekink, E. R. T.; Rendina, L. M. *Organometallics*, **2001**, *20*, 3373-3382; (b) Shah, S. A. A.; Dorn, H.; Gindl, J.; Noltemeyer, M.; Schmidt, H.-G.; Roesky, H. W. *J. Organomet. Chem.* **1998**, *550*, 1-6; (c) Gibson, V. C.; Redshaw, C.; Clegg, W.; Elsegood, M. R. J. *J. Chem. Soc., Dalton Trans.* **1997**, 3207-3212.

[163] (a) Uppal, R.; Incarvito, C. D.; Lakshmi, K. V.; Valentine, A. M. *Inorg. Chem.* **2006**, *45*, 1795-1804; (b) Collins, J. M.; Uppal, R.; Incarvito, C. D.; Valentine, A. M. *Inorg. Chem.* **2005**, *44*, 3431-3440; (c) Kefalas, E. T.; Panagiotidis, P.; Raptopoulou, C. P.; Terzis, A.; Mavromoustakos, T.; Salifoglou, A. *Inorg. Chem.* **2005**, *44*, 2596-2605; (d) Dakanali, M.; Kefalas, E. T.; Raptopoulou, C. P.; Terzis, A.; Voyiatzis, G.; Kyrikou, I.; Mavromoustakos, T.; Salifoglou, A. *Inorg. Chem.* **2003**, *42*, 4632-4639.

[164] Papiernik, R.; Hubert-Pfalzgraf, L. G.; Vaissermann, J.; Goncalves, M. C. H. B. *J. Chem. Soc., Dalton Trans.* **1998**, 2285-2287.

[165] Kemmitt, T.; Al-Salim, N. I.; Gainsford, G. J.; Bubendorfer, A.; Waterland, M. *Inorg. Chem.* **2004**, *43*, 6300-6306; and references therein.

[166] Dunuwila, D. D.; Torgerson, B. A.; Chang, C. K.; Berglund, K. A. *Anal. Chem.* **1994**, *66*, 2739-2744.

[167] Hill, R. H.; Roman, P. J, Jr.; Suh, S.; Zhang, X. Titanium carbonate films for use in semiconductor processing. U. S. Patent 2003 0190820 A1, October 9, 2003.

[168] (a) Mijatovic, I.; Kickelbick, G.; Puchberger, M.; Schubert, U. *New J. Chem.* **2003**, *27*, 3-5; (b) Bashall, A.; Brown, D. A.; McPartlin, M.; Wallbridge, M. G. H. *J. Chem. Soc., Dalton Trans.* **1992**, 2529-2530.

[169] Barrow, H.; Brown, D. A.; Alcock, N. W.; Clase, H. J.; Wallbridge, M. G. H. *J. Chem. Soc., Chem. Commun.* **1995**, 1231-1232.

[170] (a) Kilgore, U. J.; Basuli, F.; Huffman, J. C.; Mindiola, D. J. *Inorg. Chem.* **2006**, *45*, 487-489; (b) Aleksandrov, G. G.; Struchkov, Y. T. *J. Struct. Chem.* **1971**, *12*, 605-612.

[171] (a) Clauss, A. W.; Wilson, S. R.; Buchanan, R. M.; Pierpont, C. G.; Hendrickson, D. N. *Inorg. Chem.* **1983**, *22*, 628-636; (b) Tarkhova, T. N.; Gladkikh, E. A.; Grishin, I. A.; Lineva, A. N.; Khalmanov, V. V. *J. Struct. Chem.* **1976**, *17*, 896-901.

[172] Stewart, P. J.; Blake, A. J.; Mountford, P. *J. Organomet. Chem.* **1998**, *564*, 209-214.

[173] Stewart, P. J.; Blake, A. J.; Mountford, P. *Inorg. Chem.* **1997**, *36*, 3616-3622.

[174] Hamura, S.; Oda, T.; Shimizu, Y.; Matsubara, K.; Nagashima, H. *J. Chem. Soc., Dalton Trans.* **2002**, 1521-1527.

[175] Sheldrick, G. M. *J. Fluorine Chem.* **1975**, *4*, 415-421.

[176] Radzewich, C. E.; Coles, M. P.; Jordan, R. F. *J. Am. Chem. Soc.* **1998**, *120*, 9384-9385.

[177] (a) Cheng, M.; Moore, D. R.; Reczek, J. J.; Chamberlain, B. M.; Lobkovsky, E. B.; Coates, G. W. *J. Am. Chem. Soc.* **2001**, *123*, 8738-8749; (b) Cheng, M.; Lobkovsky, E. B.; Coates, G. W. *J. Am. Chem. Soc.* **1998**, *120*, 11018-11019.

[178] Walker, D. A.; Woodman, T. J.; Hughes, D. L.; Bochmann, M. *Organometallics*, **2001**, *20*, 3772-3776.

[179] Ye, B.-H.; Li, X.-Y.; Williams, I. D.; Chen, X.-M. *Inorg. Chem.* **2002**, *41*, 6426-6431; and references therein.

[180] (a) Chang, C.-C.; Srinivas, B.; Wu, M.-L.; Chiang, W.-H.; Chiang, M. Y.; Hsiung, C.-S. *Organometallics*, **1995**, *14*, 5150-5159; (b) Dell'Amico, D. B; Calderazzo, F.; Labella, L.; Marchetti, F.; Pampaloni, G. *Chem. Rev.* **2003**, *103*, 3857-3897; (c) Tang, Y.; Zakharov, L. N.; Rheingold, A. L.; Kemp, R. A. *Organometallics*, **2004**, *23*, 4788-4791; (d) Tang, Y.; Kassel, W. S.; Zakharov, L. N.; Rheingold, A. L.; Kemp, R. A. *Inorg. Chem.* **2005**, *44*, 359-364.

[181] (a) Sita, L. R.; Babcock, J. R.; Xi, R. *J. Am. Chem. Soc.* **1996**, *118*, 10912-10913; (b) Xi, R.; Sita, L. R. *Inorg. Chim. Acta*, **1998**, *270*, 118-122.

[182] Tang, Y.; Felix, A. M.; Zakharov, L. N.; Rheingold, A. L.; Kemp, R. A. *Inorg. Chem.* **2004**, *43*, 7239-7242.

[183] (a) Jutzi, P.; Mix, A.; Rummel, B.; Schoeller, W. W.; Neumann, B.; Stammler, H.-G. *Science*, **2004**, *305*, 849-851; (b) Kim, K.-C.; Reed, C. A.; Elliott, D. W.; Mueller, L. J.; Tham, F.; Lin, L.; Lambert, J. B. *Science*, **2002**, *297*, 825-827.

[184] (a) Cypryk, M.; Chojnowski, J. *J. Organomet. Chem.* **2002**, *642*, 163-170; (b) Sakaki, S.; Takayama, T.; Sugimoto, M. *Organometallics*, **2001**, *20*, 3896-3905.

[185] Li, C.; Thomson, R. K.; Gillon, B.; Patrick, B. O.; Schafer, L. L. *Chem. Commun.*, **2003**, 2462-2463.

[186] Mendiratta, A.; Cummins, C. C.; Cotton, F. A.; Ibragimov, S. A.; Murillo, C. A.; Villagrán, D. *Inorg. Chem.* **2006**, *45*, 4328-4330.

[187] (a) Barbour, L. J. *J. Supramol. Chem.* **2001**, *1*, 189-191; (b) Atwood, J. L.; Barbour, L. J. *Cryst. Growth Des.* **2003**, *3*, 3-8.

[188] Nonius, B. V. Kappa CCD Software. Nonius BV, Delft, TheNetherlands, 1999.

[189] Otwinowski, Z.; Minor, W. Processing of X-ray Diffraction Data Collected in Oscillation Mode, Methods in Enzymology. In *Macromolecular Crystallography, Part A*; Carter, C. W., Sweet, R. M., Eds.; Academic Press: London, 1997; Vol.276, pp 307-326

[190] Sheldrick, G. M. *SHELXTL NT V6.12*; *Program Library for Structure Solution and Molecular Graphics*; Bruker AXS, Inc.: Madison, WI, 2000.

[191] Altomare, A.; Cascarano, G.; Giacovazzo, C.; Guagliardi, A.; Moliterni, A. G. G.; Burla, M. C.; Polidori, G.; Camalli, M.; Spagna, R. *J. Appl. Crystallogr.* **1999**, *32*, 115-119.

[192] Sheldrick, G. M. *SHELXL97-2, Program for the Solution of Crystal Structures;* University of Göttingen, Göttingen, Germany, 1997.

[193] The lithium salt of this ligand has been known since 1998, but the free acid has not been reported. See reference 93(b).

[194] (a) Beckmann, J.; Costantino, F.; Dakternieks, D.; Duthie, A.; Ienco, A.; Midollini, S.; Mitchell, C.; Orlandini, A.; Sorace, L. *Inorg. Chem.* **2005**, *44*, 9416-9423. (b) Bauer, S.; Müller, H.; Bein, T.; Stock, N. *Inorg. Chem.* **2005**, *44*, 9464-9470. (c) Clearfield, A.; Wang, Z. *J. Chem. Soc., Dalton Trans.* **2002**, 2937-2947.

[195] Li, F.-F.; Ma, J.-F.; Song, S.-Y.; Yang, J.; Liu, Y.-Y.; Su, Z.-M. *Inorg. Chem.* **2005**, *44*, 9374-9383.

[196] Janiak, C. *Dalton Trans.* **2003**, 2781-2804.

[197] (a) Zang, S.; Su, Y.; Li, Y.; Ni, Z.; Meng, Q. *Inorg. Chem.* **2006**, *45,* 174-180. (b) Fletcher, A. J.; Thomas, K. M.; Rosseinsky, M. J. *J. Solid State Chem.* **2005,** *178,* 2491-2510. (c) Du, M.; Cai, H.; Zhao, X.-J. *Inorg. Chim. Acta*, **2005,** *358,* 4034–4038. (d) Uemura, K.; Matsuda, R.; Kitagawa, S. *J. Solid State Chem.* **2005,** *178,* 2420–2429. (e) Mao, H.; Zhang, C.; Li, G.; Zhang, H.; Hou, H.; Li, L.; Wu, Q.; Zhu, Y.; Wang, E. *Dalton Trans.* **2004**, 3918-3925. (f) Kitaura, R.; Seki, K.; Akiyama, G.; Kitagawa, S. *Angew. Chem. Int. Ed.* **2003,** *42,* 428-431.

[198] Barnett, S. A.; Champness, N. R. *Coord. Chem. Rev.* **2003,** *246,* 145-168.

[199] Ding, B.-B.; Weng, Y.-Q.; Mao, Z.-W.; Lam, C.-K.; Chen, X.-M.; Ye, B.-H. *Inorg. Chem.* **2005,** *44,* 8836-8845.

[200] (a) Rao, C. N. R.; Natarajan, S.; Vaidhyanathan, R. *Angew. Chem. Int. Ed.* **2004**, *43*, 1466-1496. (b) Kitagawa, S.; Kitaura, R.; Noro, S. *Angew. Chem. Int. Ed.* **2004**, *43*, 2334-2375. (c) Yaghi, O. M.; O'Keeffe, M.; Ockwig, N. W.; Chae, H. K.; Eddaoudi, M.; Kim, J. *Nature* **2003**, *423*, 705-714.

[201] Matsuda, R.; Kitaura, R.; Kitagawa, S.; Kubota, Y.; Belosludov, R. V.; Kobayashi, T. C.; Sakamoto, H.; Chiba, T.; Takata, M.; Kawazoe, Y.; Mita, Y. *Nature* **2005**, *436*, 238-241.

[202] Li, H.; Eddaoudi, M.; Groy, T. L.; Yaghi, O. M. *J. Am. Chem. Soc.* **1998**, *120*, 8571-8572.

[203] Li, H.; Eddaoudi, M.; O'Keeffe, M.; Yaghi, O. M. *Nature* **1999**, *402*, 276-279.

[204] (a) Eddaoudi, M.; Kim, J.; Rosi, N.; Vodak, D.; Wachter, J.; O'Keeffe, M.; Yaghi, O. M. *Science* **2002**, *295*, 469-472. (b) Sudik, A. C.; Millward, A. R.; Ockwig, N. W.; Côté, A. P.; Kim, J.; Yaghi, O. M. *J. Am. Chem. Soc.* **2005**, *127*, 7110-7118.

[205] (a) Rowsell, J. L. C.; Millward, A. R.; Park, K. S.; Yaghi, O. M. *J. Am. Chem. Soc.* **2004**, *126*, 5666-5667. (b) Zhao, X.; Xiao, B.; Fletcher, A. J.; Thomas, K. M.;

Bradshaw, D.; Rosseinsky, M. J. *Science*, **2004**, *306*, 1012-1015. (c) Rowsell, J. L. C.; Yaghi, O. M. *Angew. Chem. Int. Ed.* **2005**, *44*, 4670-4679. (d) Chen, B.; Ockwig, N. W.; Millward, A. R.; Contreras, D. S.; Yaghi, O. M. *Angew. Chem. Int. Ed.* **2005**, *44*, 4745-4749; (e) Li, Y.; Yang, R. T. *J. Am. Chem. Soc.* **2006**, *128*, 8136-8137.

[206] (a) Rowsell, J. L. C.; Eckert, J.; Yaghi, O. M. *J. Am. Chem. Soc.* **2005**, *127*, 14904-14910. (b) Spencer, E. C.; Howard, J. A. K.; McIntyre, G. J.; Rowsell, J. L. C.; Yaghi, O. M. *Chem. Commun.* **2006**, 278-280.

[207] (a) Yaghi, O. M.; Davis, C. E.; Li, G.; Li, H. *J. Am. Chem. Soc.* **1997**, *119*, 2861-2868; (b) Zeng, M.-H.; Feng, X.-L.; Chen, X.-M. *Dalton Trans.* **2004**, 2217-2223. (c) Chae, H. K.; Siberio-Pérez, D. Y.; Kim, J.; Go, Y.; Eddaoudi, M.; Matzger, A. J.; O'Keeffe, M.; Yaghi, O. M. *Nature*, **2004**, *427*, 523-527. (d) Braga, D.; Curzi, M.; Johansson, A.; Polito, M.; Rubini, K.; Grepioni, F. *Angew. Chem. Int. Ed.* **2006**, *45*, 142-146.

[208] Pan, L.; Olson, D. H.; Ciemnolonski, L. R.; Heddy, R.; Li, J. *Angew. Chem. Int. Ed.* **2006**, *45*, 616-619.

[209] Daiguebonne, C.; Kerbellec, N.; Bernot, K.; Gérault, Y.; Deluzet, A.; Guillou, O. *Inorg. Chem.* **2006**, *45*, 5399-5406.

[210] Barbour, L. J. *Chem. Commun.* **2006**, 1163-1168.

[211] (a) Wu, C.-D.; Hu, A.; Zhang, L.; Lin, W. *J. Am. Chem. Soc.* **2005**, *127*, 8940-8941. (b) Fujita, M.; Kwon, Y. J.; Washizu, S.; Ogura, K. *J. Am. Chem. Soc.* **1994**, *116*, 1151-1152. (c) Kesanli, B.; Lin, W. *Coord. Chem. Rev.* **2003**, *246*, 305-326.

[212] Uemura, T.; Kitaura, R.; Ohta, Y.; Nagaoka, M.; Kitagawa, S. *Angew. Chem. Int. Ed.* **2006**, *45*, 4112-4116.

[213] Cho, S.-H.; Ma, B.; Nguyen, S. T.; Hupp, J. T.; Albrecht-Schmitt, T. E. *Chem. Commun.* **2006**, 2563-2565.

[214] Decurtins, S. *Phil. Trans. R. Soc. Lond. A*, **1999**, *357*, 3025-3040.

[215] (a) Li, X.-J.; Wang, X.-Y.; Gao, S.; Cao, R. *Inorg. Chem.* **2006**, *45*, 1508-1516; (b) Lu, J.; Yu, J.-H.; Chen, X.-Y.; Cheng, P.; Zhang, X.; Xu, J.-Q. *Inorg. Chem.* **2005**, *44*, 5978-5980; (c) Tynan, E.; Jensen, P.; Kelly, N. R.; Kruger, P. E.; Lees, A. C.; Moubaraki, B.; Murray, K. S. *Dalton Trans.* **2004**, 3440-3447.

[216] (a) Lo, S. M.-F.; Chui, S. S.-Y.; Shek, L.-Y.; Lin, Z.; Zhang, X. X.; Wen, G.-H.; Williams, I. D. *J. Am. Chem. Soc.* **2000**, *122*, 6293-6294; (b) Tran, D. T.; Fan, X.; Brennan, D. P.; Zavalij, P. Y.; Oliver, S. R. J. *Inorg. Chem.* **2005**, *44*, 6192-6196; (c) Del Sesto, R. E.; Deakin, L.; Miller, J. S. *Synth. Met.* **2001**, *122*, 543-546; (d) Moulton, B.; Lu, J.; Hajndl, R.; Hariharan, S.; Zaworotko, M. J. *Angew. Chem. Int. Ed.* **2002**, *41*, 2821-2824; (e) Cao, R.; Shi, Q.; Sun, D.; Hong, M.; Bi, W.; Zhao, Y. *Inorg. Chem.* **2002**, *41*, 6161-6168.

[217] Lu, T.-B.; Xiang, H.; Luck, R. L.; Mao, Z.-W.; Chen, X.-M.; Ji, L.-N. *Inorg. Chim. Acta*, **2003**, *355*, 229-241.

[218] Hong, C. S.; Yoon, J. H.; You, Y. S. *Inorg. Chim. Acta*, **2005**, *358*, 3341-3346.

[219] Sanselme, M.; Grenèche, J. M.; Riou-Cavellec, M.; Férey, G. *Chem. Commun.* **2002**, 2172-2173.

[220] Ye, Q.; Song, Y.-M.; Wang, G.-X.; Chen, K.; Fu, D.-W.; Chan, P. W. H.; Zhu, J.-S.; Huang, S. D.; Xiong, R.-G. *J. Am. Chem. Soc.* **2006**, *128*, 6554-6555.

[221] (a) Wang, Y.-T.; Fan, H.-H.; Wang, H.-Z.; Chen, X.-M. *Inorg. Chem.* **2005**, *44*, 4148-4150; (b) Han, L.; Hong, M.; Wang, R.; Luo, J.; Lin, Z.; Yuan, D. *Chem. Commun.* **2003**, 2580-2581; (c) Evans, O. R.; Lin, W. *Acc. Chem. Res.* **2002**, *35*, 511-522.

[222] (a) Zhao, B.; Chen, X. Y.; Cheng, P.; Liao, D.-Z.; Yan, S.-P.; Jiang, Z.-H. *J. Am. Chem. Soc.* **2004,** *126*, 15394-15395; (b) Lee, E. Y.; Jang, S. Y.; Suh, M. P. *J. Am. Chem. Soc.* **2005**, *127*, 6374-6381; (c) Zheng, S.-L.; Tong, M.-L.; Tan, S.-D.; Wang, Y.; Shi, J.-X.; Tong, Y.-X.; Lee, H. K.; Chen, X.-M. *Organometallics*, **2001**, *20*, 5319-5325; (d) Zhang, J.; Chen, Y.-B.; Chen, S.-M.; Li, Z.-J.; Cheng, J.-K.; Yao, Y.-G. *Inorg. Chem.* **2006**, *45*, 3161-3163.

[223] Ma, A.-Q.; Zhu, L.-G. *Trans. Met. Chem.* **2004**, *29*, 329-331.

[224] Li, H.; Davis, C. E.; Groy, T. L.; Kelley, D. G.; Yaghi, O. M. *J. Am. Chem. Soc.* **1998,** *120,* 2186-2187.

[225] Wright, R. S.; Vinod, T. K. *Tetrahedron Lett.* **2003,** *44,* 7129-7132.

[226] 2,6-Dimethylterephthalic acid has been known for more than 50 years (Dvoretzky, I.; Richter, G. H. *J. Org. Chem.* **1953**, *18,* 615-619), however it has never been structurally characterized. The only structurally characterized example with this substitution pattern is 1,2,3,5-benzenetetracarboxylic acid (Barrio, C.; García-Granda, S.; Gómez-Beltrán, F. *Acta Crystallogr., Sect. C*, **1993**, *49,* 253-257).

[227] This synthesis is based on the oxidation of toluene to benzoic acid in: Schoffstall, A. M; Gaddis, B. A.; Druelinger, M. L. Microscale and Miniscale Organic Chemistry Laboratory Experiments, 2nd Edition; McGraw-Hill: Toronto, 2004.

[228] Gilli, P.; Bertolasi, V.; Ferretti, V.; Gilli, G. *J. Am. Chem. Soc.* **1994**, *116*, 909-915.

[229] (a) Kaduk, J. A.; Golab, J. T. *Acta Crystallogr., Sect. B*, **1999**, *55*, 85-94. (b) Kaduk, J. A. *Acta Crystallogr., Sect. B*, **2000**, *56*, 474-485.

[230] Eddaoudi, M.; Kim, J.; O'Keeffe, M.; Yaghi, O. M. *J. Am. Chem. Soc.* **2002**, *124*, 376-377

[231] Śledź, M.; Janczak, J.; Kubiak, R. *J. Mol. Struct.* **2001**, *595*, 77-82; and references therein.

[232] Jorgensen, W. L.; Severance, D. L. *J. Am. Chem. Soc.* **1990**, *112*, 4768-4774.

[233] (a) Meiners, C.; Valiyaveettil, S.; Enkelmann, V.; Müllen, K. *J. Mater. Chem.* **1997**, *7*, 2367-2374. (b) Cowan, J. A.; Howard, J. A. K.; McIntyre, G. J.; Lo, S. M.-F.; Williams, I. D. *Acta Crystallogr., Sect. B*, **2003**, *59*, 794-801.

[234] (a) Chatterjee, S.; Pedireddi, V. R.; Rao, C. N. R. *Tet. Lett.* **1998**, *39*, 2843-2846. (b) Lough, A. J.; Wheatley, P. S.; Ferguson, G.; Glidewell, C. *Acta Crystallogr., Sect. B*, **2000**, *56*, 261-272.

[235] The term co-crystal is discouraged by some, but remains popular in the literature. (a) Desiraju, G. R. *CrystEngComm*, **2003**, *5*, 466-467; (b) Dunitz, J. D. *CrystEngComm*, **2003**, *5*, 506.

[236] (a) Desiraju, G. R. *Chem. Commun.* **2005**, 2995-3001; (b) Steiner, T. *Angew. Chem. Int. Ed.* **2002**, *41*, 48-76.

[237] Biradha, K.; Dennis, D.; MacKinnon, V. A.; Sharma, C. V. K.; Zaworotko, M. J. *J. Am. Chem. Soc.* **1998**, *120*, 11894-11903.

[238] Karanović, L.; Poleti, D.; Rogan, J.; Bogdanović, G. A.; Spasojević-de Biré, A. *Acta Crystallogr., Sect. C*, **2002**, *58*, m275-m279.

[239] Bourne, S. A.; Mondal, A.; Zaworotko, M. J. *Cryst. Eng.* **2001**, *4*, 25-36.

[240] (a) Wen, Y.-H.; Cheng, J.-K.; Feng, Y.-L.; Zhang, J.; Li, Z.-J.; Yao, Y.-G. *Inorg. Chim. Acta*, **2005**, *358*, 3347-3354; (b) Zou, R.-Q.; Bu, X.-H.; Du, M.; Sui, Y.-X. *J. Mol. Struct.* **2004**, *707*, 11-15; (c) Ma, A.-Q.; Xu, D.-J.; Zhu, L.-G. *Acta Crystallogr., Sect. E*, **2003**, *59*, m579-m581.

[241] (a) Shorrock, C. J.; Xue, B.-Y.; Kim, P. B.; Batchelor, R. J.; Patrick, B. O.; Leznoff, D. B. *Inorg. Chem.* **2002**, *41*, 6743-6753; (b) Braga, D.; Curzi, M.; Grepioni, F.; Polito, M. *Chem. Commun.* **2005**, 2915-2917; (c) Sun, D.; Cao, R.; Bi, W.; Weng, J.; Hong, M.; Liang, Y. *Inorg. Chim. Acta*, **2004**, *357*, 991-1001; (d) Riley, P. J.; Reid, J. L.; Côté, A. P.; Shimizu, G. K. H. *Can. J. Chem.* **2002**, *80*, 1584-1591.

[242] Schematic of grid generated with OLEX, version 2.55. See: Dolomanov, O. V; Blake, A. J.; Champness, N. R.; Schröder, M. *J. Appl. Crystallogr.* **2003**, *36*, 1283-1284.

[243] Hoffman, R. *Sci. Am.* **1993**, *268* (2), 66-73.

[244] Nuzzo, R. G.; Allara, D. L. *J. Am. Chem. Soc.* **1983**, *105*, 4481-4483.

[245] (a) Ulman, A. *Chem. Rev.* **1996**, *96*, 1533-1554; (b)Ferretti, S.; Paynter, S.; Russell, D. A.; Sapsford, K. E.; Richardson, D. J. *Trends Anal. Chem.* **2000**, *19*, 530-540.

[246] Vericat, C.; Vela, M. E.; Salvarezza, R. C. *Phys. Chem. Chem. Phys.* **2005**, *7*, 3258-3268.

[247] Briseno, A. L.; Aizenberg, J.; Han, Y.-J.; Penkala, R. A.; Moon, H.; Lovinger, A. J.; Kloc, C.; Bao, Z. *J. Am. Chem. Soc.* **2005**, *127*, 12164-12165.

[248] Flink, S.; van Veggel, F. C. J. M.; Reinhoudt, D. N. *Sensors Update*, **2001**, *8*, 3-19.

[249] Ma, H.; Wells, M.; Beebe, T. P., Jr.; Chilkoti, A. *Adv. Funct. Mater.* **2006**, *16*, 640-648.

[250] Ozoemena, K. I.; Nyokong, T. *Electrochim. Acta*, **2006**, *51*, 2669-2677.

[251] (a) Chi, Y. S.; Choi, I. S. *Adv. Funct. Mater.* **2006**, *16*, 1031-1036; (b) Zhang, F.; Cho, S. S.; Yang, S. H.; Seo, S. S.; Cha, G. S.; Nam, H. *Electroanalysis*, **2006**, *18*, 217-222.

[252] (a) Patel, N.; Davies, M. C.; Hartshorne, M.; Heaton, R. J.; Roberts, C. J.; Tendler, S. J. B.; Williams, P. M. *Langmuir*, **1997**, *13*, 6485-6490; (b) Yoo, S.-K.; Yoon, M.; Park, U. J.; Han, H. S.; Kim, J. H.; Hwang, H. J. *Exp. Mol. Med.* **1999**, *31*, 122-125; (c) Campbell, G. A.; Mutharasan, R. *Anal. Chem.* **2006**, *78*, 2328-2334; (d) Ostuni, E.; Yan, L.; Whitesides, G. M. *Colloids Surf., B*, **1999**, *15*, 3-30.

[253] Kisailus, D.; Truong, Q.; Amemiya, Y.; Weaver, J. C.; Morse, D. E. *Proc. Natl. Acad. Sci. U.S.A.* **2006**, *103*, 5652-5657.

[254] Willey, T. M.; Vance, A. L.; van Buuren, T.; Bostedt, C.; Nelson, A. J.; Terminello, L. J.; Fadley, C. S. *Langmuir*, **2004**, *20*, 2746-2752.

[255] Sabatani, E.; Cohen-Boulakia, J.; Bruening, M.; Rubinstein, I. *Langmuir*, **1993**, *9*, 2974-2981.

[256] Ishida, T.; Mizutani, W.; Azehara, H.; Miyake, K.; Aya, Y.; Sasaki, S.; Tokumoto, H. *Surf. Sci.* **2002**, *514*, 187-193.

[257] Arnold, R.; Azzam, W.; Terfort, A.; Wöll, C. *Langmuir*, **2002**, *18*, 3980-3992.

[258] Lüssem, B.; Müller-Meskamp, L.; Karthäuser, S.; Waser, R.; Homberger, M.; Simon, U. *Langmuir*, **2006**, *22*, 3021-3027.

[259] Choi, E. J.; Foster, M. D.; Daly, S.; Tilton, R.; Przybycien, T.; Majkrzak, C. F.; Witte, P.; Menzel, H. *Langmuir*, **2003**, *19*, 5464-5474.

[260] Fuxen, C.; Azzam, W.; Arnold, R.; Witte, G.; Terfort, A.; Wöll, C. *Langmuir*, **2001**, *17*, 3689-3695.

[261] Lahann, J.; Mitragotri, S.; Tran, T.-N.; Kaido, H.; Sundaram, J.; Choi, I. S.; Hoffer, S.; Somorjai, G. A.; Langer, R. *Science*, **2003**, *299*, 371-374.

[262] Liu, Y.; Mu, L.; Liu, B.; Zhang, S.; Yang, P.; Kong, J. *Chem. Commun.* **2004**, 1194-1195.

[263] (a) Chen, C.-T.; Siegel, J. S. *J. Am. Chem. Soc.* **1994**, *116*, 5959-5960; (b) Chen, C.-T.; Chadha, R.; Siegel, J. S.; Hardcastle, K. *Tetrahedron Lett.* **1995**, *36*, 8403-8406.

[264] Dynarowicz-Łątka, P.; Kita, K.; Milart, P.; Dhanabalan, A.; Cavalli, A.; Oliveira, O. N., Jr. *J. Colloid Interface Sci.* **2001**, *239*, 145-157.

[265] García, F.; García, J. M.; García-Acosta, B.; Martínez-Máñez, R.; Sancenón, F.; Soto, J. *Chem. Commun.* **2005**, 2790-2792.

[266] Tuleen, D. L.; Hess, B. A., Jr. *J. Chem. Educ.* **1971**, *48*, 476-477.

[267] Brown, T. M.; Carruthers, W.; Pellatt, M. G. *J. Chem. Soc., Perkin Trans. I*, **1982**, 483-487.

[268] Himmel, H.-J.; Terfort, A.; Wöll, C. *J. Am. Chem. Soc.* **1998**, *120*, 12069-12074.

[269] Yu, H.-Z.; Ye, S.; Zhang, H.-L.; Uosaki, K.; Liu, Z.-F. *Langmuir*, **2000**, *16*, 6948-6954; and references therein.

[270] (a) Creager, S. E.; Clarke, J. *Langmuir*, **1994**, *10*, 3675-3683; (b) Liu, Y.-J.; Navasero, N. M.; Yu, H.-Z. *Langmuir*, **2004**, *20*, 4039-4050; and references therein.

[271] Dameron, A. A.; Charles, L. F.; Weiss, P. S. *J. Am. Chem. Soc.* **2005**, *127*, 8697-8704.

[272] Smith, R. K.; Lewis, P. A.; Weiss, P. S. *Prog. Surf. Sci.* **2004**, *75*, 1-68.

[273] (a) Pirrung, M. C. *Angew. Chem. Int. Ed.* **2002**, *41*, 1276-1289; (b) Mack, N. H.; Dong, R.; Nuzzo, R. G. *J. Am. Chem. Soc.* **2006**, *128*, 7871-7881.

[274] Zhu, P.; Kang, H.; Facchetti, A.; Evmenenko, G.; Dutta, P.; Marks, T. J. *J. Am. Chem. Soc.* **2003**, *125*, 11496-11497.

[275] Travaille, A. M.; Kaptijn, L.; Verwer, P.; Hulsken, B.; Elemans, J. A. A. W.; Nolte, R. J. M.; van Kempen, H. *J. Am. Chem. Soc.* **2003**, *125*, 11571-11577.

[276] (a) Sau, T. K.; Murphy, C. J. *J. Am. Chem. Soc.* **2004**, *126*, 8648-8649; (b) Hiramatsu, H.; Osterloh, F. E. *Chem. Mater.* **2004**, *16*, 2509-2511; (c) Hostetler, M. J.; Wingate, J. E.; Zhong, C.-J.; Harris, J. E.; Vachet, R. W.; Clark, M. R.; Londono, J. D.; Green, S. J.; Stokes, J. J.; Wignall, G. D.; Glish, G. L.; Porter, M. D.; Evans, N. D.; Murray, R. W. *Langmuir*, **1998**, *14*, 17-30.

[277] (a) Brust, M.; Walker, M.; Bethell, D.; Schiffrin, D. J.; Whyman, R. *J. Chem. Soc., Chem. Commun.* **1994**, 801-802; (b) Leff, D. V.; Ohara, P. C.; Heath, J. R.; Gelbart, W. M. *J. Phys. Chem.* **1995**, *99*, 7036-7041.

[278] (a) Templeton, A. C.; Hostetler, M. J.; Kraft, C. T.; Murray, R. W. *J. Am. Chem. Soc.* **1998**, *120*, 1906-1911; (b) Shenhar, R.; Rotello, V. M. *Acc. Chem. Res.* **2003**, *36*, 549-561.

[279] Thomas, K. G.; Kamat, P. V. *Acc. Chem. Res.* **2003**, *36*, 888-898.

[280] Cameron, P. A.; Gibson, V. C.; Redshaw, C.; Segal, J. A.; White, A. J. P.; Williams, D. J. *J. Chem. Soc., Dalton Trans.* **2002**, 415-422.

[281] (a) Sprung, M. M. *Chem. Rev.* **1940**, *26*, 297-338; (b) Layer, R. W. *Chem. Rev.* **1963**, *63*, 489-510.

[282] (a) Atwood, D. A.; Harvey, M. J. *Chem. Rev.* **2001**, *101*, 37-52; (b) Atwood, D. A. *Coord. Chem. Rev.* **1997**, *165*, 267-296.

[283] Lewiński, J.; Zachara, J.; Kopeć, T. *Inorg. Chem. Commun.* **1998**, *1*, 182-184.

[284] (a) Schenkl, S.; van Mourik, F.; van der Zwan, G.; Haacke, S.; Chergui, M. *Science*, **2005**, *309*, 917-920; (b) Masgrau, L.; Roujeinikova, A.; Johannissen, L. O.; Hothi, P.; Basran, J.; Ranaghan, K. E.; Mulholland, A. J.; Sutcliffe, M. J.; Scrutton, N. S.; Leys, D. *Science*, **2006**, *312*, 237-241; (c) Sharif, S.; Denisov, G. S.; Toney, M. D.; Limbach, H.-H. *J. Am. Chem. Soc.* **2006**, *128*, 3375-3387.

[285] Sharma, V.; Piwnica-Worms, D. *Chem. Rev.* **1999**, *99*, 2545-2560.

[286] Kuraoka, K.; Chujo, Y.; Yazawa, T. *Chem. Commun.* **2000**, 2477-2478.

[287] (a) Evans, C.; Luneau, D. *J. Chem. Soc., Dalton Trans.* **2002**, 83-86; (b) Costes, J. P.; Lamère, J. F.; Lepetit, C.; Lacroix, P. G.; Dahan, F.; Nakatani, K. *Inorg. Chem.* **2005**, *44*, 1973-1982.

[288] (a) Che, C.-M.; Chan, S.-C.; Xiang, H.-F.; Chan, M. C. W.; Liu, Y.; Wang, Y. *Chem. Commun.* **2004**, 1484-1485; (b) Wong, W.-K.; Yang, X.; Jones, R. A.; Rivers, J. H.; Lynch, V.; Lo, W.-K.; Xiao, D.; Oye, M. M.; Holmes, A. L. *Inorg. Chem.* **2006**, *45*, 4340-4345.

[289] (a) Miyasaka, H.; Clérac, R.; Wernsdorfer, W.; Lecren, L.; Bonhomme, C.; Sugiura, K.-I.; Yamashita, M. *Angew. Chem. Int. Ed.* **2004**, *43*, 2801-2805; (b) Lu, Z.; Yuan, M.; Pan, F.; Gao, S.; Zhang, D.; Zhu, D. *Inorg. Chem.* **2006**, *45*, 3538-3548.

[290] Matsumoto, K.; Sawada, Y.; Saito, B.; Sakai, K.; Katsuki, T. *Angew. Chem. Int. Ed.* **2005**, *44*, 4935-4939.

[291] (a) Zhang, J.; Liang, J.-L.; Sun, X.-R.; Zhou, H.-B.; Zhu, N.-Y.; Zhou, Z.-Y.;Chan, P. W. H.; Che, C.-M. *Inorg. Chem.* **2005**, *44*, 3942-3954; (b) Li, G.-Y.; Zhang, J.; Chan, P. W. H.; Xu, Z.-J.; Zhu, N.; Che, C.-M. *Organometallics*, **2006**, *25*, 1676-1688.

[292] Venkatachalam, G.; Ramesh, R. *Inorg. Chem. Commun.* **2006**, *9*, 703-707.

[293] Zhang, D.; Jin, G.-X.; Weng, L.-H.; Wang, F. *Organometallics*, **2004**, *23*, 3270-3275.

[294] Gregson, C. K. A.; Blackmore, I. J.; Gibson, V. C.; Long, N. J.; Marshall, E. L.; White, A. J. P. *Dalton Trans.* **2006**, 3134-3140.

[295] (a) Jarvo, E. R.; Lawerence, B. M.; Jacobsen, E. N. *Angew. Chem. Int. Ed.* **2005**, *44*, 6043-6046; (b) Gennari, C.; Piarulli, U. *Chem. Rev.* **2003**, *103*, 3071-3100.

[296] (a) Thomson, R. K.; Zahariev, F. E.; Zhang, Z.; Patrick, B. O.; Wang, Y. A.; Schafer, L. L. *Inorg. Chem.* **2005**, *44*, 8680-8689; (b) Thomson, R. K.; Patrick, B. O.; Schafer, L. L. *Can. J. Chem.* **2005**, *83*, 1037-1042.

[297] Hoerter, J. M.; Otte, K. M.; Gellman, S. H.; Stahl, S. S. *J. Am. Chem. Soc.* **2006**, *128*, 5177-5183.

[298] Greenberg, A. The amide linkage as a ligand: Its properties and the role of distortion. In *The Amide Linkage: Structural Significance in Chemistry, Biochemistry and Materials Science*; Greenberg, A.; Breneman, C. M.; Liebman, J. F., Eds.; Wiley & Sons: New York, 2000; pp 47-83.

[299] Patten, T. E.; Troeltzsch, C.; Olmstead, M. M. *Inorg. Chem.* **2005**, *44*, 9197-9206.

[300] Kwon, H. Y.; Lee, S. Y.; Lee, B. Y.; Shin, D. M.; Chung, Y. K. *Dalton Trans.* **2004**, 921-928.

[301] Hlavinka, M. L.; Hagadorn, J. R. *Organometallics*, **2005**, *24*, 4116-4118; and references therein.

[302] Chen, W.; Liu, F.; Xu, D.; Matsumoto, K.; Kishi, S.; Kato, M. *Inorg. Chem.* **2006**, *45*, 5552-5560.

[303] (a) Richter, B.; Meetsma, A.; Hessen, B.; Teuben, J. H. *Angew. Chem. Int. Ed.* **2002**, *41*, 2166-2169; (b) Richter, B.; Meetsma, A.; Hessen, B.; Teuben, J. H. *Chem. Commun.* **2001**, 1286-1287.

[304] Arnold, K.; Davies, B.; Giles, R. L.; Grosjean, C.; Smith, G. E.; Whiting, A. *Adv. Synth. Catal.* **2006**, *348*, 813-820.

[305] (a) Strouse, J. J.; Ješelnik, M.; Arterburn, J. B. *Acta Chim. Slov.* **2005**, *52*, 187-199; (b) Kumagai, N.; Muncipinto, G.; Schreiber, S. L. *Angew. Chem. Int. Ed.* **2006**, *45*, 3635-3638; (c) Miyaura, N. *J. Organomet. Chem.* **2002**, *653*, 54-57; (d) Miyaura, N. *Topics Curr. Chem.* **2002**, *219*, 11-59.

[306] (a) Bachovchin, W. W.; Lai, H.-S.; O'Connell, D. P. Lipase inhibitors. WO 2006/053250 A2, May 18, 2006. (b) Irving, A. M.; Vogels, C. M; Nikolcheva, L. G.; Edwards, J. P.; He, X.-F.; Hamilton, M. G.; Baerlocher, M. O.; Baerlocher, F. J.; Decken, A.; Westcott, S. A. *New J. Chem.* **2003**, *27*, 1419-1424; and references therein.

[307] (a) Gamsey, S.; Baxter, N. A.; Sharrett, Z.; Cordes, D. B.; Olmstead, M. M.; Wessling, R. A.; Singaram, B. *Tetrahedron*, **2006**, *62*, 6321-6331; (b) Liu, S.; Bakovic, L.; Chen, A. *J. Electroanal. Chem.* **2006**, *591*, 210-216; (c) Cordes, D. B; Gamsey, S.; Singaram, B. *Angew. Chem. Int. Ed.* **2006**, *45*, 3829-3832; (d) Zhao, J.; Davidson, M. G.; Mahon, M. F.; Kociok-Köhn, G.; James, T. D. *J. Am. Chem. Soc.* **2004**, *126*, 16179-16186.

[308] (a) Aakeröy, C. B; Desper, J.; Levin, B. *CrystEngComm*, **2005**, *7*, 102-107; (b) Rodríguez-Cuamatzi, P.; Arillo-Flores, O. I.; Bernal-Uruchurtu, M. I.; Höpfl, H. *Cryst. Growth Des.* **2005**, *5*, 167-175.

[309] Webb, K. S.; Levy, D. *Tetrahedron Lett.* **1995**, *36*, 5117-5118.

[310] Knight, P. D.; Clarke, A. J.; Kimberley, B. S.; Jackson, R. A.; Scott, P. *Chem. Commun.* **2002**, 352-353.

[311] Suslick, K. S.; Fox, M. M. *J. Am. Chem. Soc.* **1983**, *105*, 3507-3510.

[312] (a) Norman, D. W.; Edwards, J. P.; Vogels, C. M.; Decken, A.; Westcott, S. A. *Can. J. Chem.* **2002**, *80*, 31-40; (b) Briggs, M. S. J.; Fossey, J. S.; Richards, C. J.; Scott, B.; Whateley, J. *Tetrahedron Lett.* **2002**, *43*, 5169-5171.

[313] Saito, S.; Hatanaka, K.; Yamamoto, H. *Tetrahedron*, **2001**, *57*, 875-887.

[314] Ueji, S.; Ueda, N.; Kinugasa, T. *J. Chem. Soc., Perkin Trans. 2*, **1976**, 178-180.

[315] Endo, Y.; Shudo, K.; Okamoto, T. *Synthesis*, **1983**, 471-472.

[316] (a) Nimitsiriwat, N.; Marshall, E. L.; Gibson, V. C.; Elsegood, M. R. J.; Dale, S. H. *J. Am. Chem. Soc.* **2004**, *126*, 13598-13599; (b) Parr, J.; Ross, A. T.; Slawin, A. M. Z. *Inorg. Chem. Commun.* **1998**, *1*, 159-160.

[317] Carlini, C.; Giaiacopi, S.; Marchetti, F.; Pinzino, C.; Galletti, A. M. R.; Sbrana, G. *Organometallics*, **2006**, *25*, 3659-3664.

[318] Atwood, D. A.; Gabbaï, F. P.; Lu, J.; Remington, M. P.; Rutherford, D.; Sibi, M. P. *Organometallics*, **1996**, *15*, 2308-2313.

[319] McMahon, C. N.; Bott, S. G.; Barron, A. R. *J. Chem. Soc., Dalton Trans.* **1998**, 3301-3304.

[320] (a) van der Steen, F. H.; van Mier, G. P. M.; Spek, A. L.; Kroon, J.; van Koten, G. *J. Am. Chem. Soc.* **1991**, *113*, 5742-5750; (b) van Vliet, M. R. P.; van Koten, G.; Rotteveel, M. A.; Schrap, M.; Vrieze, K.; Kojić-Prodić, B.; Spek, A. L.; Duisenberg, A. J. M. *Organometallics*, **1986**, *5*, 1389-1394.

[321] Bradley, D. C.; Coumbarides, G.; Harding, I. S.; Hawkes, G. E.; Maia, I. A.; Motevalli, M. *J. Chem. Soc., Dalton Trans.* **1999**, 3553-3558.

[322] Taden, I.; Kang, H.-C.; Massa, W.; Spaniol, T. P.; Okuda, J. *Eur. J. Inorg. Chem.* **2000**, 441-445.

[323] Silverstein, R. M.; Webster, F. X. *Spectrometric Identification of Organic Compounds, 6th Ed.;* John Wiley & Sons: New York, 1998; Chapter 3.

[324] Murphy, J. A.; Roome, S. J. *J. Chem. Soc., Perkin Trans 1*, **1995**, 1349-1358.

[325] Tokunaga, Y.; Ueno, H.; Shimomura, Y.; Seo, T. *Heterocycles*, **2002**, *57*, 787-790.

[326] Nöth, H.; Wrackmeyer, B. In *Nuclear Magnetic Resonance Spectroscopy of Boron Compounds*; Diehl, P., Fluck, E., Kosfeld, R., Eds.; NMR Basic Principles and Progress 14; Springer-Verlag: New York, 1978.

[327] Yang, Y.; Escobedo, J. O.; Wong, A.; Schowalter, C. M.; Touchy, M. C.; Jiao, L.; Crowe, W. E.; Fronczek, F. R.; Strongin, R. M. *J. Org. Chem.* **2005**, *70*, 6907-6912.

[328] Soundararajan, S.; Duesler, E. N.; Hageman, J. H. *Acta Crystallogr., Sect. C*, **1993**, *49*, 690-693.

[329] Ganguly, A.; Meyers, C. Y.; Robinson, P. D. *Acta Crystallogr., Sect. E*, **2003**, *59*, o759-o761.

[330] Baugh, L. S.; Sissano, J. A. *J. Polym. Sci., Part A: Polym. Chem.* **2002**, *40*, 1633-1651.

[331] Huang, Y.-L.; Huang, B.-H.; Ko, B.-T.; Lin, C.-C. *J. Chem. Soc., Dalton Trans.* **2001**, 1359-1365.

[332] Côté, A. P.; Benin, A. I.; Ockwig, N. W.; O'Keeffe, M.; Matzger, A. J.; Yaghi, O. M. *Science*, **2005**, *310*, 1166-1170.

[333] Oakes, D. C. H.; Gibson, V. C.; White, A. J. P.; Williams, D. J. *Inorg. Chem.* **2006**, *45*, 3476-3477.

[334] Jing, H.; Edulji, S. K.; Gibbs, J. M.; Stern, C. L.; Zhou, H.; Nguyen, S. T. *Inorg. Chem.* **2004**, *43*, 4315-4327.

[335] Khrustalev, V. N.; Portnyagin, I. A.; Zemlyansky, N. N.; Borisova, I. V.; Ustynyuk, Y. A.; Antipin, M. Y. *J. Organomet. Chem.* **2005**, *690*, 1056-1062.

[336] Zamudio-Rivera, L. S.; George-Tellez, R.; López-Mendoza, G.; Morales-Pacheco, A.; Flores, E.; Höpfl, H.; Barba, V.; Fernández, F. J.; Cabirol, N.; Beltrán, H. I. *Inorg. Chem.* **2005**, *44*, 5370-5378.

[337] Francis, J. A.; Bott, S. G.; Barron, A. R. *J. Chem. Soc., Dalton Trans.* **1998**, 3305-3310.

[338] Uhl, W.; Hannemann, F. *J. Organomet. Chem.* **1999**, *579*, 18-23.

[339] Horley, G. A.; Mahon, M. F.; Molloy, K. C.; Venter, M. M.; Haycock, P. W.; Myers, C. P. *Inorg. Chem.* **2002**, *41*, 1652-1657.

[340] (a) Fenwick, A. E.; Phomphrai, K.; Thorn, M. G.; Vilardo, J. S.; Trefun, C. A.; Hanna, B.; Fanwick, P. E.; Rothwell, I. P. *Organometallics*, **2004**, *23*, 2146-2156; (b) Schweiger, S. W.; Salberg, M. M.; Pulvirenti, A. L.; Freeman, E. E.; Fanwick, P. E.; Rothwell, I. P. *J. Chem. Soc., Dalton Trans.* **2001**, 2020-2031; (c) Lentz, M. R.; Vilardo, J. S.; Lockwood, M. A.; Fanwick, P. E.; Rothwell, I. P. *Organometallics*, **2004**, *23*, 329-343; and references therein.

[341] (a) Dilworth, J. R.; Hanich, J.; Krestel, M.; Beck, J.; Strähle, J. *J. Organomet. Chem.* **1986**, *315*, C9-C12; (b) Quignard, F.; Leconte, M.; Basset, J.-M.; Hsu, L.-Y.; Alexander, J. J.; Shore, S. G. *Inorg. Chem.* **1987**, *26*, 4272-4277; (c) Darensbourg, D. J.; Mueller, B. L.; Bischoff, C. J.; Chojnacki, S. S.; Reibenspies, J. H. *Inorg. Chem.* **1991**, *30*, 2418-2424; (d) Minhas, R. K.; Edema, J. J. H.; Gambarotta, S.; Meetsma, A. *J. Am. Chem. Soc.* **1993**, *115*, 6710-6717; (e) O'Donoghue, M. B.; Schrock, R. R.; LaPointe, A. M.; Davis, W. M. *Organometallics*, **1996**, *15*, 1334-1336; (f) Hascall, T.; Baik, M.-H.; Bridgewater, B. M.; Shin, J. H.; Churchill, D. G.; Friesner, R. A.; Parkin, G. *Chem. Commun.* **2002**, 2644-2645.

[342] (a) Johansson, A.; Håkansson, M. *Chem. Eur. J.* **2005**, *11*, 5238-5248; (b) Ooi, T.; Kondo, Y.; Maruoka, K. *Angew. Chem. Int. Ed.* **1998**, *37*, 3039-3041; (c) Clegg, W.; Elsegood, M. R. J.; Snaith, R.; Wheatley, A. E. H. *Acta Crystallogr., Sect. E*, **2003**, *59*, m225-227.

[343] (a) Ito, H.; Nagahara, T.; Ishihara, K.; Saito, S.; Yamamoto, H. *Angew. Chem. Int. Ed.* **2004**, *43*, 994-997; (b) Saito, S.; Nagahara, T.; Shiozawa, M.; Nakadai, M.; Yamamoto, H. *J. Am. Chem. Soc.* **2003**, *125*, 6200-6210; (c), Maruoka, K.; Imoto, H.; Saito, S.; Yamamoto, H. *J. Am. Chem. Soc.* **1994**, *116*, 4131-4132.

[344] Maruoka, K.; Sato, J.; Banno, H.; Yamamoto, H. *Tetrahedron Lett.* **1990**, *31*, 377-380.

[345] (a) Saito, S.; Yamamoto, H. *Chem. Commun.* **1997**, 1585-1592; (b) Saito, S.; Shiozawa, M.; Nagahara, T.; Nakadai, M.; Yamamoto, H. *J. Am. Chem. Soc.* **2000**, *122*, 7847-7848; (c) Yamamoto, H.; Saito, S. *Pure Appl. Chem.* **1999**, *71*, 239-245.

[346] Saito, S.; Murase, M.; Yamamoto, H. *Synlett*, **1999**, 57-58.

[347] (a) Smith, G. D.; Fanwick, P. E.; Rothwell, I. P. *Inorg. Chem.* **1989**, *28*, 618-620; (b) Smith, G. D.; Fanwick, P. E.; Rothwell, I. P. *J. Am. Chem. Soc.* **1989**, *111*, 750-

751; (c) Smith, G. D.; Visciglio, V. M.; Fanwick, P. E.; Rothwell, I. P. *Organometallics*, **1992**, *11*, 1064-1071.

[348] (a) Weinert, C. S.; Fanwick, P. E.; Rothwell, I. P. *Acta Crystallogr., Sect. E*, **2002**, *58*, m718-720; (b) Weinert, C. S.; Fanwick, P. E.; Rothwell, I. P. *Dalton Trans.* **2003**, 1795-1802; (c) Smith, G. D.; Fanwick, P. E.; Rothwell, I. P. *Inorg. Chem.* **1990**, *29*, 3221-3226.

[349] Stanciu, C.; Richards, A. F.; Stender, M.; Olmstead, M. M.; Power, P. P. *Polyhedron*, **2006**, *25*, 477-483.

[350] Weinert, C. S.; Fenwick, A. E.; Fanwick, P. E.; Rothwell, I. P. *Dalton Trans.* **2003**, 532-539.

[351] (a) Boyle, T. J.; Andrews, N. L.; Rodriguez, M. A.; Campana, C.; Yiu, T. *Inorg. Chem.* **2003**, *42*, 5357-5366; (b) Boyle, T. J.; Pedrotty, D. M.; Alam, T. M.; Vick, S. C.; Rodriguez, M. A. *Inorg. Chem.* **2000**, *39*, 5133-5146.

[352] (a) Schulz, S.; Roesky, H. W.; Noltemeyer, M.; Schmidt, H.-G. *J. Chem. Soc., Dalton Trans.* **1995**, 177-180; (b) Campbell, J. P.; Gladfelter, W. L. *Inorg. Chem.* **1997**, *36*, 4094-4098; (c) Liu, Y.-C.; Ko, B.-T.; Huang, B.-H.; Lin, C.-C. *Organometallics,* **2002**, *21*, 2066-2069.

[353] (a) Weinert, C. S.; Fanwick, P. E.; Rothwell, I. P. *Inorg. Chem.* **2003**, *42*, 6089-6094; (b) Hanna, T. A.; Ghosh, A. K.; Ibarra, C.; Mendez-Rojas, M. A.; Rheingold, A. L.; Watson, W. H. *Inorg. Chem.* **2004**, *43*, 1511-1516; (c) Wilkerson, M. P.; Burns, C. J.; Morris, D. E.; Paine, R. T.; Scott, B. L. *Inorg. Chem.* **2002**, *41*, 3110-3120.

[354] Lin, C.-H.; Ko, B.-T.; Wang, F.-C.; Lin, C.-C.; Kuo, C.-Y. *J. Organomet. Chem.* **1999**, *575*, 67-75.

[355] Çetinkaya, B.; Hitchcock, P. B.; Jasim, H. A.; Lappert, M. F.; Williams, H. D. *Polyhedron*, **1990**, *9*, 239-243.

[356] Bedford, R. B.; Limmert, M. E. *J. Org. Chem.* **2003**, *68*, 8669-8682.

[357] Stanciu, C.; Olmstead, M. M.; Phillips, A. D.; Stender, M.; Power, P. P. *Eur. J. Inorg. Chem.* **2003**, 3495-3500.

[358] Abbass, M.; Kühl, C.; Manthey, C.; Müller, A.; Lüning, U. *Collect. Czech. Chem. Commun.* **2004**, *69*, 1325-1344.

[359] Nakatsu, K.; Yoshioka, H.; Kunimoto, K.; Kinugasa, T.; Ueji, S. *Acta Crystallogr., Sect. B*, **1978**, *34*, 2357-2359.

[360] Zavodnik, V. E.; Belskii, V. K.; Zorkii, P. M. *J. Struct. Chem.* **1987**, *28*, 793-795.

[361] Previously synthesized by $LiAlH_4$ reduction of the corresponding methyl ester. See ref. 109.

[362] Edelmann, F. T.; Poremba, P.; Bohnen, F. M.; Herbst-Irmer, R. *Z. Anorg. Allg. Chem.* **2004**, *630*, 1671-1676.

[363] Kowalski, A.; Duda, A.; Penczek, S. *Macromolecules*, **2000**, *33*, 689-695.

[364] Boyle, T. J.; Ward, T. L.; De'Angeli, S. M.; Xu, H.; Hammetter, W. F. *Chem. Mater.* **2003**, *15*, 765-775.

[365] (a) Barnhart, D. M.; Clark, D. L.; Watkin, J. G. *Acta Crystallogr., Sect. C*, **1994**, *50*, 702-704; (b) McBurnett, B. G.; Cowley, A. H. *Chem. Commun.* **1999**, 17-18.

[366] Weinert, C. S.; Fanwick, P. E.; Rothwell, I. P. *J. Chem. Soc., Dalton Trans.* **2002**, 2948-2950.

[367] (a) Chorley, R. W.; Hitchcock, P. B.; Lappert, M. F.; Leung, W.-P.; Power, P. P.; Olmstead, M. M. *Inorg. Chim. Acta*, **1992**, *198*, 203-209; (b) Braunschweig, H.; Hitchcock, P. B.; Lappert, M. F.; Pierssens, L. J.-M. *Angew .Chem. Int. Ed. Engl.* **1994**, *33*, 1156-1158; (c) Veith, M.; Rammo, A. *Z. Anorg. Allg. Chem.* **2001**, *627*, 662-668; (d) Meller, A.; Ossig, G.; Maringgele, W.; Noltemeyer, M.; Stalke, D.; Herbst-Irmer, R.; Freitag, S.; Sheldrick, G. M. *Z. Naturforsch., B: Chem.Sci.* **1992**, *47*, 162-170.

[368] Son, A. J. R.; Thorn, M. G.; Fanwick, P. E.; Rothwell, I. P. *Organometallics*, **2003**, *22*, 2318-2324.

[369] (a) Kumar, R.; Sierra, M. L.; de Mel, V. S. J.; Oliver J. P. *Organometallics*, **1990**, *9*, 484-489; (b) Hendershot, D. G.; Kumar, R.; Barber, M.; Oliver, J. P. *Organometallics*, **1991**, *10*, 1917-1922; (c) Saied, O.; Simard, M; Wuest, J. D. *Organometallics*, **1996**, *15*, 2345-2349; (d) Aitken, C. L.; Barron, A. R. *J. Chem. Crystallogr.* **1996**, *26*, 293-295; (e) Saied, O.; Simard, M.; Wuest, J. D. *Inorg. Chem.* **1998**, *37*, 2620-2625; (f) Firth, A. V.; Stewart, J. C.; Hoskin, A. J.; Stephan, D. W. *J. Organomet. Chem.* **1999**, *591*, 185-193; (g) Giesbrecht, G. R.; Gordon, J. C.; Brady, J. T.; Clark, D. L.; Keogh, D. W.; Michalczyk, R.; Scott, B. L.; Watkin, J. G. *Eur. J. Inorg. Chem.* **2002**, 723-731; (h) Vertrees, T. W.; Hoben, G.; Kobylivker, A. N.; Edwards, C. L.; Bott, S. G.; Barron, A. R. *J. Chem. Crystallogr.* **2005**, *35*, 313-316.

[370] (a) Chesnut, R. W.; Durfee, L. D.; Fanwick, P. E.; Rothwell, I. P.; Folting, K.; Huffman, J. C. *Polyhedron*, **1987**, *6*, 2019-2026; (b) Thorn, M. G.; Etheridge, Z. C.; Fanwick, P. E.; Rothwell, I. P. *J. Organomet. Chem.* **1999**, *591*, 148-162; (c) Sato, A.; Hattori, A.; Ishihara, K.; Saito, S.; Yamamoto, H. *Chem. Lett.* **2003**, *32*, 1006-1007.

[371] Sturla, S. J.; Buchwald, S. L. *Organometallics*, **2002**, *21*, 739-748.

[372] (a) Jones, R. A.; Hefner, J. G.; Wright, T. C. *Polyhedron*, **1984**, *3*, 1121-1124; (b) Visciglio, V. M.; Fanwick, P. E.; Rothwell, I. P. *Inorg. Chim. Acta*, **1993**, *211*, 203-209; (c) Visciglio, V. M.; Fanwick, P. E.; Rothwell, I. P. *Acta Crystallogr., Sect. C*, **1994**, *50*, 896-898; (d) Zambrano, C. H.; Profilet, R. D.; Hill, J. E.; Fanwick, P. E.; Rothwell, I. P. *Polyhedron*, **1993**, *12*, 689-708.

[373] Scholz, J.; Kahlert, S.; Görls, H. *Organometallics*, **2004**, *23*, 1594-1603.

[374] (a) Olmstead, M. M.; Power, P. P.; Shoner, S. C. *J. Am. Chem. Soc.* **1991**, *113*, 3379-3385; (b) Chisholm, M. H.; Gallucci, J. C.; Yin, H.; Zhen, H. *Inorg. Chem.* **2005**, *44*, 4777-4785; (c) Parvez, M.; BergStresser, G. L.; Richey, H. G., Jr. *Acta*

Crystallogr., Sect. C. **1992**, *48*, 641-644; (d) Boyle, T. J.; Bunge, S. D.; Andrews, N. L.; Matzen, L. E.; Sieg, K.; Rodriguez, M. A.; Headley, T. J. *Chem. Mater.* **2004**, *16*, 3279-3288; (e) Cole, S. C.; Coles, M. P.; Hitchcock, P. B. *Organometallics*, **2004**, *23*, 5159-5168.

[375] Jensen, T. R.; Schaller, C. P.; Hillmyer, M. A.; Tolman, W. B. *J. Organomet. Chem.* **2005**, *690*, 5881-5891.

[376] Florjańczyk, Z.; Plichta, A.; Sobczak, M. *Polymer*, **2006**, *47*, 1081-1090.

[377] Darensbourg, D. J.; Ortiz, C. G.; Billodeaux, D. R. *Inorg. Chim. Acta*, **2004**, *357*, 2143-2149.

[378] Chebi, D. E.; Fanwick, P. E.; Rothwell, I. P. *Polyhedron*, **1990**, *9*, 969-974.

[379] (a) Conrad, J. C.; Amoroso, D.; Czechura, P.; Yap, G. P. A.; Fogg, D. E. *Organometallics*, **2003**, *22*, 3634-3636; (b) Snelgrove, J. L.; Conrad, J. C.; Yap, G. P. A.; Fogg, D. E. *Inorg. Chim. Acta*, **2003**, *345*, 268-278; (c) Snelgrove, J. L.; Conrad, J. C.; Eelman, M. D.; Moriarty, M. M.; Yap, G. P. A.; Fogg, D. E. *Organometallics*, **2005**, *24*, 103-109.

[380] (a) Webster, M.; Browning, D. J.; Corker, J. M. *Acta Crystallogr., Sect. C*, **1996**, *52*, 2439-2441; (b) van Zandt, W.; Huffman, J. C.; Stewart, J. L. *Main Group Met. Chem.* **1998**, *21*, 237-240; (c) Jaques, D.; Clark, J. R.; Chebi, D. E.; Fanwick, P. E.; Rothwell, I. P. *Acta Crystallogr., Sect. C*, **1994,** *50*, 898-899.

[381] (a) Hanna, T. A. *Coord. Chem. Rev.* **2004**, *248*, 429-440; (b) Hanna, T. A.; Rieger, A. L.; Rieger, P. H.; Wang, X. *Inorg. Chem.* **2002**, *41*, 3590-3592.

[382] Hodge, P.; James, S. C.; Norman, N. C.; Orpen, A. G. *J. Chem. Soc., Dalton Trans.* **1998**, 4049-4054; and references therein.

[383] Li, W.; Hill, N. J.; Tomasik, A. C.; Bikzhanova, G.; West, R. *Organometallics*, **2006**, *25*, 3802-3805; and references therein.

[384] Akkari-El Ahdab, A.; Rima, G.; Gornitzka, H.; Barrau, J. *J. Organomet. Chem.* **2002**, *658*, 94-105.

[385] Brynda, M.; Herber, R.; Hitchcock, P. B.; Lappert, M. F.; Nowik, I.; Power, P. P.; Protchenko, A. V.; Růžička, A.; Steiner, J. *Angew. Chem. Int. Ed.* **2006**, *45*, 4333-4337.

[386] Murray, R. W. *Anal. Chem.* **2006**, *78*, 3475.